


For Reference

NOT TO BE TAKEN FROM THIS ROOM

Ex libris
UNIVERSITATIS
ALBERTAENSIS





Digitized by the Internet Archive
in 2023 with funding from
University of Alberta Library

https://archive.org/details/Reid1972_0

THE UNIVERSITY OF ALBERTA

UNIVERSITY OF ALBERTA

FACULTY OF GRADUATE STUDIES AND RESEARCH

A PALAEOMAGNETIC STUDY AT 1800 MILLION YEARS IN CANADA

by



ALAN B. REID

A THESIS

SUBMITTED TO THE FACULTY OF GRADUATE STUDIES AND RESEARCH
IN PARTIAL FULFILLMENT OF THE REQUIREMENTS FOR THE DEGREE
OF DOCTOR OF PHILOSOPHY

DEPARTMENT OF PHYSICS

EDMONTON, ALBERTA

FALL, 1972

Thesis
72F-89D

UNIVERSITY OF ALBERTA
FACULTY OF GRADUATE STUDIES AND RESEARCH

The undersigned certify that they have read, and recommend to the Faculty of Graduate Studies and Research for acceptance, a thesis entitled A PALAEOMAGNETIC STUDY AT 1800 MILLION YEARS IN CANADA, submitted by ALAN B. REID in partial fulfillment of the requirements for the degree of Doctor of Philosophy.

ABSTRACT

Palaeomagnetic studies have been made of three sequences of red sediments in western Canada. The first two, the Cambrian Arctomys and Mount Clark Formations, yielded no useful palaeomagnetic results. The third was a detailed study of the red shales of the Kahochella Group, Great Slave Supergroup, sampled on Keith Island (111.9°W , 62.1°N) in the East Arm of Great Slave Lake. The Seton Formation within this group has a Rb/Sr whole rock isochron age of 1873 ± 13 m.y. The stratigraphic relationship of the sampling sites is known and the time duration represented by the between-site spacing has been estimated by use of a sedimentation rate analogy. The total time span represented by the sampling is about 60 m.y.

Alternating field and thermal demagnetization have revealed a stable remanence. Comprehensive magnetic and petrographic studies suggest that the stable remanence is primarily a CRM residing in the primary haematite pigment. The existence of a remagnetized post-folding component at least partially removed by thermal treatment has been demonstrated. The direction of the remagnetized component suggests that it was acquired soon after folding.

The known time relationship between sites has been exploited to obtain a reversal time scale and apparent polar wander path for the time represented by the sampling. Reversal rates vary from 0.4 to 1.1 reversals per million years. The dispersion of the palaeomagnetic field on two time scales has been estimated. Values of the circular standard deviation of 10.4° and 16.9° have been obtained for time scales of 0.6 and 25 m.y. respectively. It is thought that some polar wander may be included in the longer time scale.

The mean direction of magnetization for the main sampling sequence within the Kahochella Group is $D = 134.5^{\circ}$, $I = 45.5^{\circ}$ ($k = 21$, $N = 21$ sites, $\alpha_{95} = 7^{\circ}$). This implies a palaeomagnetic pole at 72.2°W and 6.2°N ($dp = 5.8^{\circ}$, $dm = 9.1^{\circ}$). The palaeolatitude implied by this result is 27° which is consistent with the observed palaeolatitude spectrum of redbeds.

The palaeomagnetic pole for the Kahochella Group has been used to modify the Precambrian apparent polar wander path established by published results.

ACKNOWLEDGEMENTS

I would like to acknowledge help given me by many people in the course of this study. The staff of the Physics and Geology Departments at the University of Alberta have provided considerable material help and encouragement. In particular my supervisor, Dr. E. W. McMurry, has been of great assistance. Dr. D. I. Gough provided supervision during the early stages of the project, for which I am grateful. Dr. M. E. Evans has provided a valuable stimulus by means of many discussions.

I would like to thank Drs. J. D. Aitken, H. A. K. Charlesworth, S. E. Haggerty, P. F. Hoffman, R. D. Morton and D. K. Norris for their aid in matters geological.

Mrs. E. Vincze performed many of the A.F. demagnetizations, for which I am grateful. Mr. D. Tomlinson operated the Electron Microprobe analyser. I would like to thank him for his indispensable help.

I was accompanied on various field trips by Mr. E. Popke, Dr. E. W. McMurry and Dr. M. E. Evans, without whom the collection of samples would have been a great deal more difficult.

Mrs. L. Cech and Mrs. M. Csaszar have done the typing and draughting of this thesis. I would like to thank

them for their cooperation under the pressure of a deadline.

Finally, I would like to express my sincere thanks to my wife, Christine, for her understanding and help during the last four years. This thesis is dedicated to her.

TABLE OF CONTENTS

	Page
CHAPTER 1. INTRODUCTION	
1.1 Principles of Palaeomagnetism	1
1.1.1 The geomagnetic field	1
1.1.2 Rock magnetism	5
1.1.3 Remanence mechanisms in rocks	15
1.2 Laboratory Techniques	23
1.3 Analysis of Data	25
1.4 The Importance of Precambrian Palaeomagnetic Results	31
CHAPTER 2. LABORATORY INSTRUMENTATION	
2.1 Spinner Magnetometers	34
2.2 Alternating Field Demagnetizer	37
2.3 Magnetically Shielded Room. Testing	38
2.4 Furnace for Palaeomagnetic Samples	40
CHAPTER 3. PALAEOMAGNETISM OF THE CAMBRIAN MOUNT CLARK AND ARCTOMYS FORMATIONS	
3.1 Objectives of the Studies	43
3.2 Mount Clark Formation	44
3.2.1 Geological setting and sampling	44
3.2.2 Natural remanence and A.F. demagnetiza- tion	49

	Page
3.2.3 Discussion	53
3.3 The Arctomys Formation, Southern Rocky Mountains	57
3.3.1 Geological setting and sampling	57
3.3.2 Natural remanence and A.F. demagnetization	59
3.3.3 Discussion	61
CHAPTER 4. NATURAL REMANENCE OF THE PRECAMBRIAN KAHOCELLA GROUP, GREAT SLAVE SUPERGROUP	
4.1 Introduction	62
4.1.1 Summary	62
4.1.2 Objectives of the study	62
4.2 Geologic Setting and Sampling	63
4.3 Natural Remanence and Demagnetization	77
4.3.1 Natural remanent magnetization	77
4.3.2 Alternating field demagnetization	79
4.3.3 Thermal demagnetization	90
4.4 Discussion	103
CHAPTER 5. ORIGIN OF THE MAGNETIZATION OF THE KAHOCELLA GROUP	
5.1 Introduction	104
5.2 Remanence Removed by Partial Demagnetization	105

	Page
5.3 Coercivity and Blocking Temperature Spectra	109
5.3.1 Alternating field demagnetization curves	110
5.3.2 Blocking temperature spectra	111
5.3.3 Intensities and reversals	116
5.4 Isothermal Remanence	118
5.5 Observations Using the Ore Microscope	127
5.5.1 Qualitative observations	128
5.5.2 Size distribution of ore grains	131
5.5.3 Ore grain reflectivities	134
5.5.4 Colour of rock samples	136
5.6 Electron Microprobe Analysis of Ore Grains	136
5.7 Discussion. Primary and Secondary Remanence	146
5.8 Discussion. Interpretation of the Palaeomagnetism	153
CHAPTER 6. VARIATION WITH TIME OF THE PALAEOMAGNETIC FIELD AT ca 1800 M.Y.	
6.1 Introduction	156
6.2 Time Resolution of Sampling	156
6.3 Reversal Rate Estimates	161
6.4 Secular Variation, Dipole Wobble and Apparent Polar Wander	165

Page

6.4.1	Calculation of between-site scatter	167
6.4.2	Apparent polar wander and dipole wobble	172
6.5	A Palaeomagnetic Pole for the Kahochella Group	174
CHAPTER 7. ANALYSIS OF PRECAMBRIAN RESULTS FOR NORTH AMERICA		
7.1	Acceptance Criteria	181
7.2	Dating Problems	182
7.3	The Precambrian Polar Wander Path for North America	183
7.4	Comparison With Other Palaeoblocks	186
BIBLIOGRAPHY OF PALAEOMAGNETIC RESULTS FROM PRECAMBRIAN ROCKS OF NORTH AMERICA		195
BIBLIOGRAPHY		202
APPENDIX 1.	DETAILED RESULTS OF PALAEO-MAGNETIC MEASUREMENTS	A1
APPENDIX 2.	LABORATORY INSTRUMENTATION	A3
APPENDIX 3.	USEFUL CONVERSIONS BETWEEN SI UNITS AND EMU	A6
APPENDIX 4.	STRIKES AND DIPS AT EACH SAMPLING SITE	A8

LIST OF TABLES

Table		Page
1.1a	Variation of relaxation time with temperature for haematite grains with average size of 0.4 μm .	14
1.1b	The effect of thermal agitation on DRM in haematite as a function of grain size.	22
3.2.1a	The Cambrian stratigraphic succession in the McConnell Range.	48
3.2.2a	Mount Clark Formation. Within-site statistics on NRMs.	50
4.2a	Precambrian time-scale for the Canadian Shield.	64
4.2b	Table of formations within the Great Slave Supergroup.	68
4.3.2a	A.F. demagnetization of Kahochella and Pethei Groups. Site level statistics.	84
4.3.2b	A.F. demagnetization of Kahochella and Pethei Groups. Section level statistics.	89
4.3.3a	Thermal demagnetization of Kahochella and Pethei Groups. Site level statistics.	98
4.3.3b	Thermal demagnetization of Kahochella and Pethei Groups. Section level statistics.	101
5.2a	Vector removed by demagnetization between 550°C and 600°C.	106
5.4a	Coercivity spectrum analysis using IRM data.	122

Table		Page
5.5.4a	Colour classification of rock samples.	137
5.6a	Electron microprobe ore grain analyses.	140
5.7a	Various magnetic parameters.	150
6.4.1a	Two-tier analysis of Variance, C section.	168
6.4.1b	Two-tier analysis of Variance, E section.	169
6.5a	Palaeomagnetic poles for the Great Slave Supergroup.	175
7.3a	Precambrian Pole positions relative to North America.	187

LIST OF FIGURES

Figure		Page
3.2.1a	The geographic location of sampling areas.	45
3.2.1b	Location of sampling sections, Mount Clark Formation.	46
3.2.2a	NRM site mean directions, Mount Clark Formation.	52
3.2.2b	A.F. cleaning of Mount Clark Formation.	54
3.3.1a	Sampling area, Arctomys Formation.	58
3.3.2a	A.F. cleaning of Arctomys Formation.	60
4.2a	The remnants of the Coronation Geosyncline.	66
4.2b	Palaeocurrent directions in the G.S.S.	71
4.2c	Sampling area, Great Slave Supergroup.	72
4.2d	Stratigraphic arrangement of sites in the Great Slave Supergroup.	73
4.2e	Sampling sites, Keith Island.	74
4.3.1a	The unstable NRM of the Kahochella Group.	78
4.3.2a-f	A.F. cleaning of the Kahochella Group.	80
4.3.2g	Site mean directions after A.F. cleaning.	87
4.3.3a-f	Thermal cleaning of the Kahochella Group.	92
4.3.3g	Stratigraphic interpretation of the mixed polarity at site CQ.	95

Figure		Page
4.3.3h	Site mean directions after thermal cleaning.	97
5.2a	Removal of a secondary magnetization from rocks of the C section.	108
5.3.2a	Demagnetization intensity curves.	112
5.3.2b	Demagnetization intensity curves for the F section.	114
5.3.2c	Thermal cleaning of specimens already A.F. treated.	115
5.3.3a	Intensity histograms.	117
5.3.3b	Intensity histograms for the B section.	119
5.4a	Correlation of hard with soft remanence.	125
5.5.2a	Size distribution of opaque grains.	132
5.5.2b	Correlation of opaque content with soft remanence.	133
5.5.3a	Ore grain reflectivities.	135
6.2a	Contemporary sedimentation rates.	158
6.2b	Depositional history of the Coronation Geosyncline.	160
6.3a	Polarity time scale for the C section.	163
6.3b	Polarity time scale for sections B and C.	166
6.4.2a	Polar wander within the Kahochella Group.	173
6.5a	Poles for the Kahochella Group.	176
6.5b	Site poles for the B normal sites.	178
7.3a	The Precambrian polar wander curve for North America.	184

LIST OF PLATES

Plate		Page
2.4a	Rock magnetic furnace and sample holder.	11
3.2.3a	Photomicrograph of material from the Mount Clark Formation.	55
4.2a	Red shales of the Vatschella Group exposed along the shores of the Great Slave Lake on Vatter Island.	75
5.5.1a	Photomicrographs of polished sections from the Vatschella Group.	114
5.6a	Electron Microprobe and optical photographs of material from site 81.	142
5.6b	Electron Microprobe and optical photographs of material from site 82.	144
5.6c	Electron Microprobe and optical photographs of lava from site 83.	146

Statement Concerning Conventions Employed in this Thesis

1. Units

The units employed in this thesis are S.I. units, formerly known as "Rationalized MKS units - Sommerfeld proposal". Electromagnetic units are included in parentheses where it is thought that this will help readers more familiar with these units. A conversion table may be found in Appendix 3.

2. Projections

All diagrams employing a projection are drawn using the azimuthal equal area or Schmidt projection. Direction plots display the north-seeking end of the magnetic vector on the upper hemisphere with open symbols and the lower hemisphere with closed symbols.

1. INTRODUCTION

1.1 Principles of Palaeomagnetism

1.1.1 The geomagnetic field

The earth possesses a magnetic field of strength $25\text{--}50 \text{ A.m}^{-1}$ ($0.3 - 0.6$ Oersted) at the surface. Its variation over the surface of the earth is approximately that of a short dipole located at the centre of the earth and making an angle of $11\frac{1}{2}^\circ$ with the rotation axis. Higher order terms in a spherical harmonic expansion of the surface field are of somewhat lower amplitude. They are collectively referred to as "non-dipole components".

The field also exhibits variation in time. Observatory records display periods varying from milliseconds to the entire time over which observations are available. The shorter periods are considered to be associated with extraterrestrial sources such as the sun, various phenomena in the upper atmosphere and the activities of man. Periods beyond that of the 11 year sunspot cycle are ascribed to electric currents circulating within the liquid core of the earth in a "self-exciting dynamo" (Jacobs, 1963), which is also thought to give rise to the steady field.

The studies of Archaeomagnetism and Palaeomagnetism are directed towards the observation of geomagnetic

phenomena on greater time scales than those accessible from observatory records. The polarity, direction and intensity of the field are all under study as functions of time and space. The recording instruments employed in these studies, are the only ones available to us, namely rocks, some of which display a primary remanence, or magnetic memory of the field in which they were formed.

The results have wide application, as in the production of palaeolatitudes of interest to palaeontologists, the generation of geographic reconstructions important in the study of tectonics and in the testing of theories of core formation and changes in the radius of the earth (Irving, 1964). More localized applications include studies of ore genesis (Symons, 1967) and geologic correlation (Fahrig & Jones, 1969; Du Bois, 1959).

Palaeomagnetic investigations have also yielded considerable information about the longer period variations of the geomagnetic field (Cox & Doell, 1964). Variations with periods extending from 11 years to several thousand years (secular variation) are ascribed by Bullard (1948) to eddies in the outer layers of the core.

The main dipole appears to have better stability than this. Palaeointensity results reviewed by Smith (1970) suggest a sinusoidal variation of dipole moment from 4 to

$12 \times 10^{22} \text{ A.m}^2$ ($4\text{--}12 \times 10^{25} \text{ emu}$) with period about 10^4 years. This is known as dipole oscillation. Directional changes (dipole wobble) appear to have a similar time scale. Hide (1967) and Hide & Stewartson (1972) suggest on theoretical grounds that the secular variation may be due to hydro-magnetic waves in the core and have time scales of $10^5 - 10^6$ years. The time scale beyond 10^6 years is the domain of apparent polar wander.

An analysis of the latitude dependence of scatter in palaeomagnetic results by Brock (1971) has yielded a good fit to a model which allows secular variation, dipole oscillations and dipole wobble (Cox, 1970). The first two effects cannot be separated by Cox's model because reduced dipole moment is equivalent to increased secular variation in its effects on palaeomagnetic scatter. Brock's results for the pre-Tertiary suggest angular standard deviations of 17.2° and 1.8° at the equator for secular variation (plus dipole oscillation) and dipole wobble respectively. The value for dipole wobble is considerably lower than that obtained from studies of Quaternary dipole wobble in the Pacific (Doell, 1969; Doell & Cox, 1972) where secular variation is anomalously low, allowing direct observation of dipole wobble. However, for most of geologic time, Brock's results suggest that dipole wobble has been small.

A time average of the geomagnetic field at a location over a period of greater than 10^4 years may thus be expected to yield the same field direction as an axial geocentric dipole. This is borne out for the last 30 m.y. by the grouping of palaeomagnetically determined poles around the rotation pole (Irving, 1964). Palaeolatitude spectra of some climatic indicators (Briden & Irving, 1964; Irving, 1964) are also in agreement with the hypothesis of an axial dipole field, but would not be sensitive to small deviations of the magnetic axis from the rotation axis.

The geomagnetic field also undergoes reversals of polarity at irregular intervals. The mean reversal rate for the last 3.5 m.y. (Cox et al., 1968) is based on radiometric dating and gives a mean rate of 5 reversals per million years. Extrapolation using oceanic magnetic anomalies (Heirtzler et al., 1968) suggests that the reversal rate was 3-4 per million years as far back as 40 m.y. Between 40 and the limit of observations at 75 m.y. it appears to have been lower (1-2 per million years).

Throughout this period the probabilities of observing normal or reversed polarities were about equal. A compilation of this probability function for the Phanerozoic by McElhinny (1971) shows variations with high probability of observing reversed polarity in the Permian and high probability of observing normal polarity in the Cretaceous. This behaviour

is rooted in the core and its determination through time can be expected to tell us something about the development of the core, intimately linked with the thermal history of the earth.

The present study has yielded estimates of reversal rate and the probability of observing reversed polarity at 1800 m.y.

1.1.2 Rock magnetism

All crystalline materials display magnetic properties. They may conveniently be divided into three groups. Those which become weakly magnetized in opposition to an applied field (i.e. show negative susceptibility) are known as diamagnetics. Those which become weakly magnetized in the same direction as an applied field (i.e. show positive susceptibility) are known as paramagnetics. Those which show large, field dependent, positive susceptibility and remain magnetized when the exciting field is removed are loosely termed ferromagnetics because iron with some of its compounds is the most outstanding natural example of the phenomenon.

Diamagnetism results from the precession of atomic electron orbits about the applied field. This constitutes an effective loop current whose magnetic moment is in oppo-

sition to the applied field. Diamagnetism is displayed by all materials, but the effects are masked when paramagnetism is also present. Paramagnetism is displayed by atoms possessing unpaired electron spins. These constitute moments which tend to be aligned by the applied field, opposed by randomizing thermal forces. Paramagnetics are unimportant in palaeomagnetism because they display no permanent magnetization.

Ferromagnetism results from "exchange interactions" whereby contiguous groups or domains of atoms become magnetically aligned. The interaction may be such as to produce oppositely magnetized but interpenetrating sublattices. If the sublattices have equal magnetizations, no net moment results and the material behaves like a paramagnetic. This is known as antiferromagnetism. It is displayed, at least to first order, by haematite, an iron oxide common in sedimentary rocks. If the sublattices do not have equal magnetizations, a net moment results, and the material behaves like a ferromagnetic, but with magnetization less than would otherwise be expected. This is known as ferrimagnetism, and is displayed by magnetite, a mineral found in many igneous rocks.

The domain configuration of ferro-, antiferro- and ferrimagnetics results because it leads to a reduction in

the total internal energy of the crystal. Six energy terms may be recognized (Stacey, 1963).

(i). Exchange energy. This is minimized by the formation of a uniformly magnetized lattice or set of sublattices as described above.

(ii). Magnetocrystalline anisotropy energy. Many crystals are more easily magnetized along particular crystallographic directions. Such magnetization is therefore energetically favoured.

(iii). Domain wall energy. In the boundary between domains magnetized along different easy directions, spins will be oriented in hard directions, increasing magnetocrystalline anisotropy energy. Exchange energy in the wall is reduced if the change in direction is distributed over a number of atoms to minimize the angle between adjacent spins. The domain wall energy is thus a tradeoff between terms (i) and (ii) above, and is not a fundamental quantity.

(iv). Magnetostrictive strain energy. The crystal lattice may be subjected to strain either from lattice defects or from particular domain configurations. It is frequently anisotropic. A reduction in strain energy is accomplished by magnetization along directions favoured by the anisotropy. They may not be the same directions as the magnetocrystalline easy directions. (In haematite the magnetocrystalline easy

directions are in the basal plane, The strain anisotropy easy directions are along the triad axis - Dunlop, 1971.)

(v). Magnetostatic energy. Some domain patterns give rise to a magnetic field external to the crystal, and a consequent "demagnetizing field" inside the crystal in opposition to the magnetization. This increases the potential energy of the aligned electron spins. The term will be a maximum for a uniformly magnetized grain. It will be a minimum for a closed domain configuration, but this involves expenditure of energy against all the four previous terms. Different grain sizes and shapes will lead to different domain configurations as the relative importance of various terms changes.

(vi). Energy due to an ambient field. A domain magnetized at a non-zero angle to the ambient field will have energy on this account. The existence of an ambient field therefore alters the energy balance and the domain pattern. The change may be reversible or irreversible. The irreversible changes are responsible for the remanence or magnetic memory exploited by studies of palaeomagnetism.

It will be appreciated that the magnetocrystalline and other anisotropies ensure that individual grains will not be magnetized along the ambient field direction except at saturation. A random distribution of such grains is,

however, isotropic in bulk. Bulk anisotropy of remanence is seldom appreciable except in ores (Hargraves, 1959) and metamorphic rocks.

Of particular interest to palaeomagnetism is the case where a grain has diameter of the order of the domain wall thickness or less. The grain will then contain only one domain and its magnetization will be the saturation magnetization of the material. Such grains frequently have higher coercivities than multidomain grains because a change in magnetization cannot be accomplished by the relatively easy mechanism of domain wall movement. An anisotropy energy must usually be overcome, and this may be large. The lower size limit for single domain grains is reached when thermal fluctuations are of the same order as the energy barriers between adjacent easy directions in the crystal. Thus the probability dP that thermal fluctuations will overcome an energy barrier E in time dt is given by Stacey (1963) as

$$dP = A \exp\left(\frac{-E}{kT}\right) dt \dots \dots (1.1)$$

If the energy barrier is provided by an anisotropy with energy per unit volume K , then

$$E = vK$$

where v is the grain volume.

A time constant τ may be defined for an assemblage of grains of similar size, which gives the time for the bulk magnetization to drop to $1/e$ of its initial value in the absence of an ambient field. Consideration of eqn. 1.1 above and others, yields

$$\tau = C \exp\left(\frac{vK}{kT}\right) \dots \dots \dots (1.2)$$

Neel (1955) argues that C is of the order of 10^{-9} sec. Stacey (1963) arrives at a similar figure by other means. The exact value is unimportant, because the expression for τ is dominated by the exponential.

For values of v or T such that τ is small on the experimental time scale, the remanence follows the ambient field for arbitrarily small values of the field, but still displays a field dependent susceptibility. The grain assemblage is then said to be superparamagnetic. For a given v , τ is strongly dependent on T . The temperature for $\tau = 100$ secs is called the blocking temperature for the particular grain size. Similarly the volume for $\tau = 100$ secs at room temperature is known as the blocking volume.

Most of the minerals of interest in palaeomagnetism have compositions located within the ternary system $\text{TiO}_2\text{-FeO-Fe}_2\text{O}_3$. Others of occasional interest include

goethite (α FeOOH) and Pyrrhotite (FeS).

Magnetite, of particular interest in dealing with igneous rocks, has a saturation magnetization of $4\mu_B$ (Bohr magnetons) per molecule or $92 \text{ A.m.}^2\text{Kg}^{-1}$ (92 emu/gm). The ferrimagnetic sublattices of magnetite are so arranged that there are twice as many iron atoms in the B sublattice as in the A. All the A sites and half the B sites are occupied by trivalent Fe^{3+} ions with moment $5\mu_B$ per ion. These therefore cancel. The remaining B sites are occupied by Fe^{2+} ions with moment $4\mu_B$ per ion which provide the externally measurable magnetization.

The magnetic properties of haematite are of particular interest. A high proportion of all the palaeomagnetic results to date are from redbeds whose main magnetic constituent is haematite. Since it is nominally antiferromagnetic, it should show no net magnetization. However, a small parasitic magnetization in the basal plane exists. Dzyaloshinski (Stacey, 1963) and Moriya (1960) have suggested that this is due to a spin interaction which cants the spins out of perfect antiparallelism, giving rise to the basal spontaneous magnetization of about $0.01\mu_B$ per molecule or $0.2 - 0.4 \text{ A.m.}^2\text{Kg}^{-1}$ ($0.2 - 0.4 \text{ emu/gm}$). Although the spin canted magnetization is thought to give rise to the high coercivity fraction of the remanence, at least in fine grained haematite

(Dunlop, 1971), there is evidence for a strain sensitive lattice defect moment along the triad axis (Porath, 1968).

Large haematite crystals exhibit a transition (the Morin transition - Stacey, 1963) at about -25°C below which the spin canted moment disappears, leaving only a magnetization along the triad axis. It is suppressed in grains smaller than $.03\mu\text{m}$ (Dunlop, 1971). Haematite shows another transition at 675°C which has been interpreted (Neel, 1955) as the Neel point, i.e. the temperature at which antiferromagnetic ordering disappears. There is some controversy over the behaviour of haematite, particularly at high temperatures. There appears to be another transition at 725°C , and Al-Khafaji and Vincenz (1971) report a ferrimagnetic Curie point in haematite at 725°C . They prefer the Neel (1955) theory of a lattice defect moment giving rise to "pseudo-ferrimagnetism" with coincident Curie and Neel points at 725°C . Smith & Fuller (1967) demonstrate the survival of a defect moment from below the Morin transition to 725°C , together with a soft spin canted moment existing between the Morin transition and 675°C . Their experiments appear to have been on single crystals, but this is not clear from their paper. Dunlop (1971) has shown that the ratio of saturation remanence to saturation magnetization in fine grained haematite is greater than 0.5, as would be

expected for an anisotropy with 6 easy directions in a plane (i.e. the spin canted moment). He reports that the lattice defect moment in such fine grained material is soft and is reduced or removed by annealing. The possibility of a dominant strain sensitive moment in haematite is disturbing, because rocks are frequently subjected to strain in the course of their history. However, both alternating field and thermal demagnetization appear to discriminate against it in fine grained haematite (Dunlop, 1971).

The coercivity of a mineral is a function of its anisotropy energy K and saturation magnetization J_s . It also depends on the symmetry of the anisotropy easy directions. For the spin canted moment of haematite it is deduced by Dunlop (1971) to be

$$H_c = \frac{4.76 K}{\mu_0 J_s} \dots \dots (1.3)$$

where μ_0 is the permeability of free space, $4\pi \times 10^{-7}$ H/m. K and J_s are both functions of temperature and grain size (Dunlop, 1971; Banerjee, 1971a), rather than constants, as has been frequently assumed in relaxation calculations (Creer, 1961; Chamalaun, 1964; Strangway et al., 1968). Dunlop (1971) gives the temperature dependence of H_c and σ_s (the magnetization per unit mass) for grains in the size range .2 - .7 μm ,

so that the temperature dependence of K may be deduced. Insertion of these values of K into eqn. 1.2 gives the variation in relaxation time with temperature shown in Table 1.1a.

Table 1.1a Variation of Relaxation Time with Temperature
For Haematite Grains With Average Size of $0.4 \mu\text{m}$

T ($^{\circ}\text{C}$)	σ_s ($\text{A.m}^2/\text{Kg}$)	H_c (A/m)	K (j/m^3)	$\frac{vK}{kT}$	τ
500	.20	8×10^4	22	69	10^{21} secs
530	.185	4×10^4	10	31	2×10^4 secs
550	.18	3.2×10^4	8	23	13 secs
600	.15	1.6×10^4	3.2	9	10^{-5} secs

The result of taking the temperature dependence of K into account is to make relaxation time an even more sharply varying function of T than has hitherto been thought. A range of 50°C takes this grain size from the very stable relaxation time of 4×10^{13} years to the boundary of the superparamagnetic state.

The superparamagnetic size limit for haematite at room temperature was recently found experimentally by Banerjee (1971b) to be $.0275\mu\text{m}$ or 27.5 nm. This is also a strong function of temperature, since it is believed that K for haematite drops to 0 for the size range $.029 - .06\mu\text{m}$ at least over the temperature range $100-300^{\circ}\text{C}$ (Banerjee, 1971a and pers. comm.). This has a profound effect on interpretation of remanence mechanisms in ultrafine haematite. Banerjee has also deduced the critical size for single domain to multidomain transition to be $15\mu\text{m}$ from data of Chevallier & Mathieu (Banerjee, 1971b). Thus between $15\mu\text{m}$ and 27.5 nm ($.0275\mu\text{m}$) haematite is expected to form stable single domains at room temperature. This covers the size range most commonly observed in red shales and silts. Thus the possibility of multidomain behaviour with its attendant complications need not be considered here.

1.1.3 Remanence mechanisms in rocks

There are a number of mechanisms whereby rocks may acquire a natural remanent magnetization (NRM).

(i). Thermo-remanent magnetization (TRM). An assemblage of ferromagnetic grains in a typical igneous melt will be above its Curie point, and will therefore behave paramagnetically. As the intruded or extruded melt cools and solidifies the grains will become magnetically locked

into the direction of the ambient field at their individual blocking temperatures. In sedimentary rocks this mechanism is only of importance where they have been strongly heated, such as at the margin of an intrusion.

(ii). Chemical (or crystallization) remanent magnetization (CRM). A magnetic mineral phase in a rock may be formed by low temperature crystallization. Thus haematite may be formed by dehydration of goethite during lithification. As the haematite crystal grows, its volume will pass the blocking volume and it will become magnetically locked in the direction of the ambient field. This mechanism is considered to be of great importance in the magnetization of red sediments (Creer, 1962; Collinson, 1969).

A number of natural chemical systems may produce the magnetic minerals (mainly haematite) observed in sedimentary rocks. Minerals of interest include ferrous bicarbonate- $\text{Fe}(\text{HCO}_3)_2$, siderite- FeCO_3 , goethite- αFeOOH , magnetite- Fe_3O_4 , maghemite- $\gamma\text{Fe}_2\text{O}_3$ and haematite- $\alpha\text{Fe}_2\text{O}_3$.

Ferrous bicarbonate can be transported by water in solution, amorphous FeOOH as a colloid and the oxides in suspension. The bicarbonate will precipitate as the carbonate in the absence of CO_2 and then may break down to form either maghemite or haematite (Deer, Howie & Zussman, 1966). Amorphous FeOOH may crystallize as goethite or dehydrate directly to

haematite. Goethite itself could acquire a CRM since it is, like haematite, an antiferromagnetic with a stable parasitic remanence (Strangway et al., 1968). It is likely to dehydrate to haematite during lithification.

Maghemite is ferrimagnetic, with spontaneous magnetization similar to magnetite, but it inverts to haematite on heating to between 200 and 700°C, depending on the history of the sample (Deer, Howie & Zussman, 1966). Exchange interaction between the two minerals has been reported. Porath (1968) found that haematite produced isothermally from maghemite acquired a CRM in the ambient field direction, but at 90% completion of the reaction, exchange interaction between the two minerals occurred, locking the remaining maghemite to the CRM direction, and producing a strong remanence. Porath argues that this implies the haematite remanence is along the triad axis rather than in the basal plane, because otherwise spin interaction should magnetize the maghemite at right angles to the CRM. Hedley (1968) reports a self reversal during a similar experiment, presumably also due to exchange interaction.

Magnetite occurs as a detrital mineral in many sediments and will oxidize to haematite in suitable conditions, perhaps via maghemite. Porath (1968) points out that magnetite and maghemite both have inverse spinel structures,

so that if maghemite participates in exchange interaction with haematite, magnetite might also do so. This has not been reported. The possibility of exchange interactions during CRM formation complicates the interpretation of haematite CRM where residual maghemite is present.

Any of the above oxidations, dehydrations and inversions could lead to the growth of haematite grains in isothermal conditions, making a CRM possible.

For palaeomagnetic purposes the main problem associated with CRM is the time of acquisition. It could in principle extend from the time of deposition to the present. However most of the processes described above should be activated during lithification. Roy (1972) has shown by a series of acid leaching experiments that the remanence of the Hopewell group consists of a detrital remanence (see below) followed by a CRM in the haematite pigment which is distributed in time and spans at least one field reversal. The system became closed in a period of less than 35 m.y. as demonstrated by a fold test (Graham, 1949). This places a tentative upper limit on the time lag between deposition and the acquisition of a CRM.

(iii). Viscous remanent magnetization (VRM). If a range of sizes of magnetic grains is present in a rock, some may be of such a size that their relaxation times are of the

order of days to thousands of years. Such grains will relax to follow the present field, more or less. This is known as VRM. Gentle heating during burial can change the size range so affected, imparting magnetizations over a long period of time which have a higher blocking temperature on the laboratory time scale. This is known as viscous partial thermoremanence or VPTRM. It can often be removed by thermal treatment.

(iv). Isothermal remanent magnetization (IRM).

This is merely the magnetization of a substance by subjecting it to a strong magnetic field. Lightning strikes can give rise to natural IRM. Graham (1961) was able to trace the course of one such lightning current by mapping the direction of magnetization in the surrounding rock.

Since the direction of an IRM is not related to that of the main geomagnetic field, and is generally scattered, it constitutes a source of noise. It can be removed by an alternating field equal to that which produced it. This is often possible (McElhinny & Gough, 1963), but is better avoided by careful choice of sampling sites.

(v). Detrital remanent magnetization (DRM). During deposition of a sediment, magnetic particles can become aligned in the direction of the ambient field and preserve it more or less well during subsequent compaction. DRM is subject

to a number of disturbing influences (King & Rees, 1966). Bottom currents, particle rolling and sloping beds can all cause inclination bias. Non-spherical particles have a tendency to lie flat. If the magnetization is controlled by shape anisotropy as can happen in magnetite, this can also bias the inclination. Experiments by Irving & Major (1964) suggest, however, that a deposited but unconsolidated sediment can acquire a post depositional DRM by rotation of magnetic particles in the interstitial water jacket. This mechanism is not subject to biasing. Although inclination error is well established in varves (Rees, 1961), it does not appear to exist in red beds (Creer, 1967; Strangway et al., 1971). The difference may be due to the magnetic particles being smaller than the quartz matrix, so that interstices of appropriate size exist (Strangway, 1970). In a well sorted sediment, the density difference between quartz and the iron oxides would tend to favour this. Application of Stokes' law suggests that the ratio of quartz diameter to haematite diameter should be 1.6 for spherical grains.

A further disturbing influence is the randomizing effect of Brownian motion, which sets a lower limit on the size of particle which can contribute significantly to DRM. Collinson (1965) suggested that Langevin's derivation of the

susceptibility of a paramagnetic gas was a close analogy. The bulk magnetization as a fraction of the maximum possible DRM (all particles aligned parallel to the field) would be expected to vary as the Langevin function $L(a)$, where

$$a = \frac{\mu_o v J_s H}{k T}$$

and
$$L(a) = \coth(a) - \frac{1}{a} \dots \dots \dots (1.4)$$

Collinson's value of 0.5 A.m^{-1} ($.05 \text{ emu/cc}$) for J_s is no longer appropriate, because haematite in the size range of interest is almost certainly single domained and therefore saturated. His estimate of 10^{-4} cm as the diameter where this effect will become important is therefore not tenable. Insertion of values of 10^3 A.m^{-1} for J_s , 40 A.m^{-1} for the earth's field and 300°K for T gives the values for magnetization efficiency found in Table 1.1b. It will be seen that grains with diameters of $.2\mu\text{m}$ or less (about the limit of optical observation) are not likely to carry a significant part of the bulk DRM.

(vi). Anhysteretic remanent magnetization (ARM).

A rock sample being subjected to alternating field demagnetization in the presence of a small steady field will become magnetized in the direction of the field (Nagata, 1961). The

Table 1.1b The Effect of Thermal Agitation on DRM in
Haematite as a Function of Grain Size

Spherical Grain diameter (μm)	Magnetization (% of saturated DRM)
1.0	84.0
.8	70.0
.6	41.0
.4	13.0
.2	1.7
.1	.2
.05	.03

remanence resides in grains with coercivity equal to the peak alternating field, not the small steady field. This is normally considered to be a laboratory effect, but Nagata (1961) suggests that it might arise in nature if the magnetic field due to a lightning strike was essentially periodic in character. The effect is avoided when not desired in the laboratory by careful cancellation of steady fields and tumbling the sample during demagnetization. Care must be taken to drive the a.f. apparatus with a high purity sine wave. As little as 1% even harmonic distortion is equivalent to a steady field considerably stronger than the earth's at maximum a.f. drive. This problem is minimized in apparatus where the drive coil is part of a sharply tuned series resonant circuit.

1.2 Laboratory Techniques

Laboratory techniques are well described in "Methods in Palaeomagnetism" (eds. Collinson, Creer & Runcorn, 1967). They are therefore only treated briefly here. The natural remanence of a rock sample is generally a composite of the original, or primary magnetization, and various secondary components. These secondary components may be due to weathering or groundwater circulation (CRM), heating (VPTRM), or lightning (IRM). In addition, if the

rock sample has grains with relaxation time less than the age of the rock it will have a VRM. The object of laboratory treatment is to discriminate between these various possible components and identify the primary remanence. The most commonly used discriminants are coercivity and blocking temperature.

The NRM may be divided into coercivity fractions by subjecting the sample to an alternating magnetic field whose peak value is smoothly reduced to zero. This has the effect of randomizing that portion of the remanence with coercivity less than the peak alternating field. This treatment is particularly effective in the removal of IRM and VRM. The primary remanence (TRM, DRM or CRM) is generally harder than the secondary, although this is not necessarily so.

The NRM may be divided into blocking temperature fractions by heating to successively higher temperatures and cooling in zero field, thereby randomizing components with lower blocking temperatures. This treatment is particularly effective in the removal of VPTRM and in discriminating between components residing in different minerals, with different Curie points.

Neither treatment will remove a CRM residing in haematite grains of sufficient size, because these will have

blocking temperatures close to the Curie point of haematite and coercivities beyond the range of the a.f. demagnetization apparatus.

The remanence of the rock sample after treatment may be measured by use of an instrument directly sensitive to the magnetic field of the sample such as an astatic or parastatic magnet system or a fluxgate. Alternatively it may be measured by causing induction in a pickup coil during angular or linear movement of the sample.

Interpretation of the results obtained by partial demagnetization is considerably assisted by a knowledge of the magnetic content of the rock, as provided by microscopic examination of polished thin sections, chemical analysis using an electron microprobe or X-ray diffraction instrument, and separation of the magnetic fraction.

Further insight into the inherent magnetic properties of the rock is provided by giving the rock a stepwise IRM in magnetic fields increasing until saturation is reached. A crude analysis into magnetite, specularite and pigment fractions is possible using the IRM data alone (Dunlop, 1972).

1.3 Analysis of Data

A widely applied method of analysis of palaeomagnetic results has been proposed by Fisher (1953) and elaborated on

by Watson (1956a,b, 1966, 1970), Watson & Irving (1957), Epp, Tukey & Watson (1971), Cox (1969) and McElhinny (1964).

The method is based on treatment of palaeomagnetically determined directions as unit vectors, which may conveniently be represented by points on a sphere. The points are assumed to be distributed about some population mean direction with probability density

$$P_A dA = \frac{\kappa}{4\pi \sinh \kappa} e^{\kappa \cos \theta} \sin \theta d\phi d\theta$$

The parameter κ is a measure of precision. θ is the angle between the mean direction and any given observation. ϕ , the azimuthal angle, is uniformly distributed. The best estimate of the true mean direction of the distribution is given by the vector sum of a random sample. The best estimate k of κ is given by

$$k = \frac{N-1}{N-R}$$

where N is the sample size and R is the length of the vector resultant.

The probability of observing a θ greater than some θ_0 is given by

$$P(\theta > \theta_0) = e^{-\kappa(1-\cos \theta_0)}$$

for k greater than 3. In particular, 63% of the observations will be found within θ_{63} where

$$\theta_{63} = 81 k^{-1/2} \text{ degrees.}$$

This is the analogue of the standard deviation for the Normal distribution.

A cone may be described about the sample mean direction such that the population mean direction may be said to lie within the cone with 95% confidence. The semi-angle of this cone is given by

$$\alpha_{95} = \cos^{-1} \left[1 - \frac{N-R}{R} \left\{ \left(\frac{1}{P} \right)^{\frac{1}{N-1}} - 1 \right\} \right]$$

where P is 0.05 for 95% confidence.

Wilson (1959) has proposed another measure of sample scatter given by

$$\delta = \cos^{-1}(R/N)$$

It makes no assumptions about the form of the distribution and has no precise statistical meaning. For a Fisher dis-

tribution and sufficiently large N it may be shown to be equivalent to the definition of θ_{63} .

Since scatter may arise from a number of causes, it is useful to analyse the results at a number of hierarchical levels. Sampling is arranged at a number of sites spread through a geological formation. Multiple independently oriented samples are obtained at each site, and a number of specimens may be cut from each sample. The specimen directions may be meaned together to provide a sample mean. The between-specimen scatter represents small scale inhomogeneity of remanence and measurement errors. A number of sample means may be combined to form a site mean. The between-sample scatter includes orientation errors and large scale inhomogeneities. A number of site means may be combined to obtain a formation mean. The between-site scatter will include the effect of geomagnetic variations on the between-site time scale. Ideally the formation mean will average out the secular variation and dipole wobble, but not cover sufficient time to include appreciable polar wander. The sampling should therefore span about 10^5 years.

A formation mean direction is most simply compared with results from other formations in different localities by mapping the inferred palaeomagnetic field direction to a

"palaeomagnetic pole" (Irving, 1964) by assuming a geocentric dipole field configuration.

The bearing of the pole from the site location is given by the declination. The palaeomagnetic colatitude p of the sampling site is related to the magnetic inclination I by

$$\cot p = \frac{1}{2} \tan I$$

If the present-day latitude and longitude of the sampling locality are λ and ϕ , then the location of the palaeomagnetic pole λ_p , ϕ_p is given by

$$\lambda_p = \sin^{-1}(\sin \lambda \cos p + \cos \lambda \sin p \cos D)$$

$$\dots \dots \dots (-90^\circ \leq \lambda_p \leq 90^\circ)$$

$$\phi_p = \phi + \beta \dots \dots \dots (\cos p \geq \sin \lambda \sin \lambda_p)$$

$$\phi_p = \phi + 180 - \beta \dots \dots \dots (\cos p < \sin \lambda \sin \lambda_p)$$

where

$$\beta = \sin^{-1}(\sin p \sin D / \cos \lambda_p)$$

$$\dots \dots \dots (-90^\circ \leq \beta \leq 90^\circ)$$

Declination D is taken to be positive clockwise from true north, inclination I is taken positive down (Irving, 1964).

Alternatively, the pole may be found graphically on a spherical projection using D and p (Graham, 1955).

The circular surface trace on the unit sphere of the cone of confidence about the mean direction maps to an oval of confidence about the pole whose major and minor axes, δm and δp are given by

$$\delta p = \frac{1}{2} \alpha_{95} (1 + 3 \cos^2 p) \dots \dots \dots \text{varies from } 0.5-2.0 \alpha_{95} \\ \text{as } I \text{ varies } 0-90^\circ$$

$$\delta m = \alpha_{95} (\sin p / \cos I) \dots \dots \dots \text{varies from } 1-2 \alpha_{95} \\ \text{as } I \text{ varies } 0-90^\circ$$

An alternative method of analysis is to calculate a palaeomagnetic pole corresponding to each site and then obtain a cone of confidence about the mean pole with semi-angle A_{95} . If the sampling sites are widely scattered the second method is preferable, because it takes into account the between-site scatter due to the spatial variations in the dipole field. For sites closely spaced, the two methods give similar results. Which is used depends on whether the distribution of site mean directions or site poles corresponds most closely to Fisher's distribution. Strictly

speaking they cannot both do so.

In this study single sample directions have been combined to give site means, and these combined to give a formation mean. Both individual site poles and the pole of the formation mean direction have been found. Calculations were performed by means of programmes employing an IBM 360/67 computer in remote terminal and batch mode and a Wang 600 programmable calculator. Programming was largely performed by Dr. McMurry with various modifications and programme maintenance by the author.

1.4 The Importance of Precambrian Palaeomagnetic Results

All earth history from the formation of the earth at about 4500 m.y. to the emergence of considerable quantities of animal life at about 600 m.y. is classed as the Precambrian aeon. It thus encompasses the first 7/8 of the history of the earth. Despite this, relatively little work has been done on Precambrian rocks because of their generally poor state of preservation. Precambrian palaeomagnetic results constitute 14% of the entries in the Irving-McElhinny pole lists.

Palaeomagnetic results from Phanerozoic rocks (the last 600 m.y.) have been forthcoming in some quantity from all the continents except Antarctica. With the aid of these

results it has been possible to make palaeogeographic reconstructions (Roy, 1972; Creer, 1968; McElhinny, 1967; Van der Voo, 1970; Irving, 1964) which supplement those made on geometric or geologic grounds (Bullard, Everitt & Smith, 1965; Smith & Hallam, 1970; King, 1965). Information has been gleaned about the intensity, reversal rate and palaeosecular variation of the geomagnetic field (section 1.1). It is clearly of interest to obtain similar information about the other 7/8 of earth history.

Precambrian rocks are more or less well preserved in a number of shield areas, notably those of the Baltic, Canada, southern Africa and western Australia. Palaeomagnetic results obtained from such shield areas may be used to demonstrate that:

(i). A geomagnetic field has existed at least since 2700 m.y. with field strengths similar to the presently observed values (McElhinny & Evans, 1968; Schwarz & Symons, 1968). This implies the existence of a liquid core of considerable size since those times if the dynamo origin of the main field is accepted. This is in turn an important boundary condition in the whole question of the earth's origin.

(ii). The field had a dipole-like configuration over a considerable area of the surface at least at 1200 and

1400 m.y. (Fahrig & Jones, 1969 and chapter 7 of this thesis).

(iii). Relative drift has occurred between the Canadian and southern African shields during the Precambrian (Spall, 1972). This suggests that the mechanism causing more recent drift may have been operative in the Precambrian as well.

(iv). The Canadian shield has remained stable (with the possible exception of the Grenville Province - Irving, Park & Roy, 1972) since at least 1400 m.y. (Chapter 7). Results from the Canadian shield are thus likely to present a consistent picture, and the shield should be a good site for extension of such studies further into the past.

It has been possible in the present study to estimate the time interval between sampling sites. The resulting reversal rate estimate enables a further boundary condition to be placed on any dynamo models.

2. LABORATORY INSTRUMENTATION

2.1 Spinner Magnetometers

The vector remanence of the rock specimens studied was measured on one of two commercial spinner magnetometers. The first, and most used, was the Princeton Applied Research Magnetometer (PAR) Model SM-1 with digital readout. It spins the specimen (a 2.5×2.5 cm cylinder) at 105 Hz inside a pickup coil and employs phase sensitive detection, giving the magnetic moment of the specimen resolved along two orthogonal axes in the plane of spinning. Spinning in several orientations provides the third component and some redundancy of measurement to enable removal of various possible errors. The orientations are arranged to enable each component to be read with each polarity in each channel. This takes six spin positions. An examination of 1103 such six-spin measurements for rocks of various intensities revealed that for specimens with total moment greater than $1 \times 10^{-8} \text{ A.m}^2$ ($1 \times 10^{-5} \text{ emu}$), the difference between the full reading and a subset employing three spins (all components in all channels) was less than 2° in 93% of the cases and less than 5° in 97% of the cases (Appendix 2). On the basis of this only rock specimens with moments less than $1 \times 10^{-8} \text{ A.m}^2$ were measured using the full spin sequence.

The manufacturers claim a minimum detectable moment of $7 \times 10^{-11} \text{ A.m}^2$, but this is not easily reached in practice. The instrument is provided with internal calibration circuitry, but an absolute calibration was made using a 100 turn coil wound on a $2.54 \times 2.54 \text{ cm}$ cylindrical former. The coil current was supplied by a sine wave oscillator, which removed the need to spin the coil. A synchronous, but appropriately phase shifted, square wave from the same oscillator was used to trigger the reference circuits. The magnetic moment of the coil was taken to be

$$P = \sqrt{2} \ n \ I \ A$$

where n is the number of turns, I the root-mean-square current and A the cross sectional area of the coil. The relationship between magnetometer reading and calibration current was found to be linear within experimental errors. Given the daily calibration procedure used in the laboratory of employing the internal calibrate on one channel and transferring it to the other using a standard specimen, the channels are equal to within $\frac{1}{2}\%$. However the readings require to be reduced by 12.6% to be correct in an absolute sense. This correction has not been applied to results reported here.

The second magnetometer was supplied by the Schonstedt Instrument Co. (Model SSM-1). It employs a fluxgate as the sensing element. Although the fluxgate is capable of measuring steady fields, the specimen is spun at 5 Hz so that phase sensitive detection may be employed to discriminate against noise. The arrangement of the sensor on the spin axis makes it particularly easy to extend the dynamic range of the instrument by moving the spinning specimen further away, but it makes the magnetometer very sensitive to specimen inhomogeneity and inaccurate centring for weak specimens. A different spin system was developed for the Schonstedt instrument to minimize this problem. It meets the constraints applied above, and also presents all faces of the specimen holding cube to the sensor. Six spins per measurement are required. A three spin subset appears inadvisable.

A comprehensive set of comparison measurements using the PAR and Schonstedt instruments revealed that direction measurements agreed within 3° in 38%, 5° in 64% and 7° in 80% of cases in the most sensitive position (Appendix 2). In the next most sensitive position the corresponding proportions were 62%, 74% and 90%. At the remaining positions differences were acceptably small. Amplitude comparison using the same readings revealed that

the Schonstedt instrument reads $94 \pm 8\%$ and $91 \pm 6\%$ of the PAR reading in the most sensitive and next most sensitive positions. Since the correct reading in absolute terms is 87.4% of the PAR reading, the Schonstedt readings may be taken as being absolute within the error limits for weak samples. The Schonstedt magnetometer was only used for 2% of the 4000 remanence measurements made in this study.

Hollerith cards were punched from the measurement booking sheets for batch processing on an IBM 360/67 computer. Latterly (the last third of the study) measurements were entered directly into a Wang programmable calculator and all corrections made immediately, so that a close check on the effects of demagnetization could be kept.

2.2 Alternating Field Demagnetizer

The apparatus used is similar to that described by McElhinny (1966), and has been described in detail by Murthy (1969). It employs a two-axis tumbler with 11:16 tumbling ratio so that all directions in the sample may be presented to the maximum demagnetizing field. The peak demagnetizing field available is about 1.4×10^5 A/m (1800 Oe). The peak flux density in air (in milliTesla) rather than the peak field strength is quoted in the remainder of this thesis because it bears a simpler relation

to the electromagnetic unit ($1 \text{ mT} = 10 \text{ gauss}$). This is not strictly correct because the flux density in the sample is dependent on the sample magnetization.

The author has improved the apparatus by rewiring the controls for tumbler, alternating field strength and steady field cancellation. All controls are now in one panel, considerably improving the ease of operation. The reliability has been improved by the elimination of a stepping relay, and the sensitivity of the steady field cancellation increased by the insertion of a workable fine control. The demagnetizing cycle is completely automatic once initiated by a start control on the panel. The control circuit is shown in Appendix 2.

2.3 Magnetically Shielded Room. Testing

A magnetically shielded room has been constructed in the Palaeomagnetism Laboratory. Specifications may be found in Appendix 2.

Immediately after completion, the ambient field inside the room was about 600 nT (600 gamma) reversed with respect to the earth's field. Over the course of some months it aged to about $1/3$ of this, but was finally reduced to the region of the theoretical value of 40 nT (40 gamma) by application of the alternating magnetic field of a

television degaussing coil to all the inner surfaces. This final inside field represents a shielding factor of a little better than 1000.

The production of zero field inside the room can be achieved by giving the walls a controlled remanence (Patton, 1967) but this is inclined to drift and it was thought better to employ a triaxial set of single turn square Helmholtz coil pairs driven by constant current supplies. The gradient in the absence of the coils is about 10-20 nT/m (0.1-0.2 gamma/cm) over the central cubic metre of the room, and is only marginally worse than this outside the central region. There are anomalies associated with individual flaws of up to 40 nT but these are all at the walls and die off rapidly with distance. Anomalies of 150 nT are associated with the door sliding mechanism, which unavoidably includes some steel. This also falls off rapidly with distance. It is undetectable near the room centre. The room is normally operated with the doors shut during sensitive experiments. The door makes an undetectable difference to the field in the further half of the room, but affects cancellation in the near half by as much as 200 nT.

Cancellation in the central region of the coil system may be set to within 2 nT and is stable to within 5 nT over the course of a week. The total field variation

over the space occupied by samples during thermal demagnetization (section 2.4) is about 1 nT.

The shielded room is in routine daily use for thermal demagnetization of rock samples.

2.4 Furnace for Palaeomagnetic Samples

A non-magnetic furnace has been installed in the shielded room by the author. The furnace itself was supplied by the University of Rhodesia, and the triac control unit by Research Incorporated of Minnesota. The furnace coil is non-inductively wound and driven by up to 5 A at 200 V. Since the heated space is small, the thermal inertia of the system is small and up to four heating runs per day may be arranged. A maximum of ten specimens may be heated together in either air or nitrogen at temperatures of up to 800°C. The specimens are placed on stainless steel shelves inside a 5 cm diameter copper tube (Plate 2.4a). The temperature difference between the hottest and coldest sample positions is 4°C at 650°C. The copper cylinder is hard chromium plated to inhibit corrosion. Furnace temperature is measured using a Pt/Pt-13% Rh thermocouple connected to the furnace power supply in a control loop. The power supply is a proportional triac type controller triggered by the difference between the furnace temperature and a pre-set

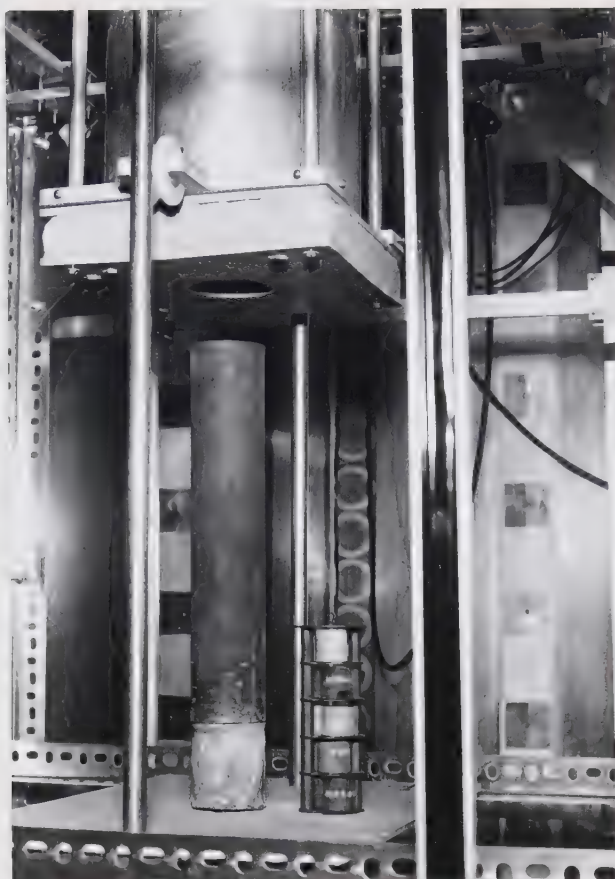


Plate 2.4a The rock magnetism furnace in raised position, showing the copper heating jacket and stainless steel sample shelves.

temperature. The time rate of change and the time integral of the difference signal are also used to achieve a stable control loop. Any given desired temperature in the range 100°C to 800°C may be achieved within 2°C at the thermocouple, but care is required at the lower temperatures to avoid overshoot.

The magnetic field due to the sample containing apparatus is 1 nT or less at the sample positions. Since a magnetic field of about 200 nT is associated with a component in the top of the furnace, samples are cooled with the furnace in a raised position. A cord and pulley system through one of the cable hoods makes it possible to raise the furnace from outside the room with the doors shut. The samples thus normally cool in a field of less than 5 nT (5 gamma).

3. PALAEOMAGNETISM OF THE CAMBRIAN MOUNT CLARK AND ARCTOMYS FORMATIONS

3.1 Objectives of the Studies

The lower Palaeozoic Era presents a number of interesting problems to the palaeomagnetist.

There is a hint that secular variation and dipole wobble were both small in the Cambrian (Briden, 1968), although this has not been found by other workers (Fahrig, Irving & Jackson, 1971; Robertson & Baragar, 1972; Al-Khafaji & Vincenz, 1971). It seems likely that the dipole moment of the geomagnetic field was at a minimum in the lower Palaeozoic (Smith, 1967; Schwarz & Symons, 1968). This contradicts the small secular variation unless non-dipole components were also small.

The paucity of Cambrian, Ordovician and Silurian palaeomagnetic results throughout the world, and particularly for North America, points to the need for work in this area. There do not seem to be many rock formations in this age range suitable for palaeomagnetic study.

The sampling of two Cambrian formations in western Canada was carried out in an attempt to improve the situation by providing palaeomagnetic poles and estimates of secular variation for the Cambrian. Unfortunately, no results

applicable to this end were obtained.

3.2 Mount Clark Formation

3.2.1 Geological setting and sampling

The McConnell Range of the Franklin Mountains along the eastern bank of the MacKenzie River (Figs. 3.2.1a,b) is composed of a thick (10 km) succession of Proterozoic and Palaeozoic sedimentary rocks. The most prominent peaks in the range, Cap Mountain (1560 m, 123.2°W, 63.3°N) and Mount Clark (1462 m, 124.2°W, 64.4°N) are capped by a pink resistant quartzite horizon, the Mount Clark Formation. Williams (1923) produced a tentative stratigraphic succession for the area which has been modified only slightly by more recent work by Douglas and Norris (1963) and the Geological Survey of Canada in Operation Norman (Aitken et al., 1970). Table 3.2.1a, compiled in advance of publication of the Operation Norman reports, shows the succession as it is currently understood. Williams (1923) reported the finding of a number of fossils which caused him to assign the Mount Clark Formation to the lower Cambrian. Douglas and Norris (1963) report the existence of lower Cambrian fossils in the overlying Mount Cap Formation.

Aitken et al. (1970) interpret the regional geology as indicating orogenic uplift immediately post Saline River

Figure 3.2.1a The geographic location of sampling areas.

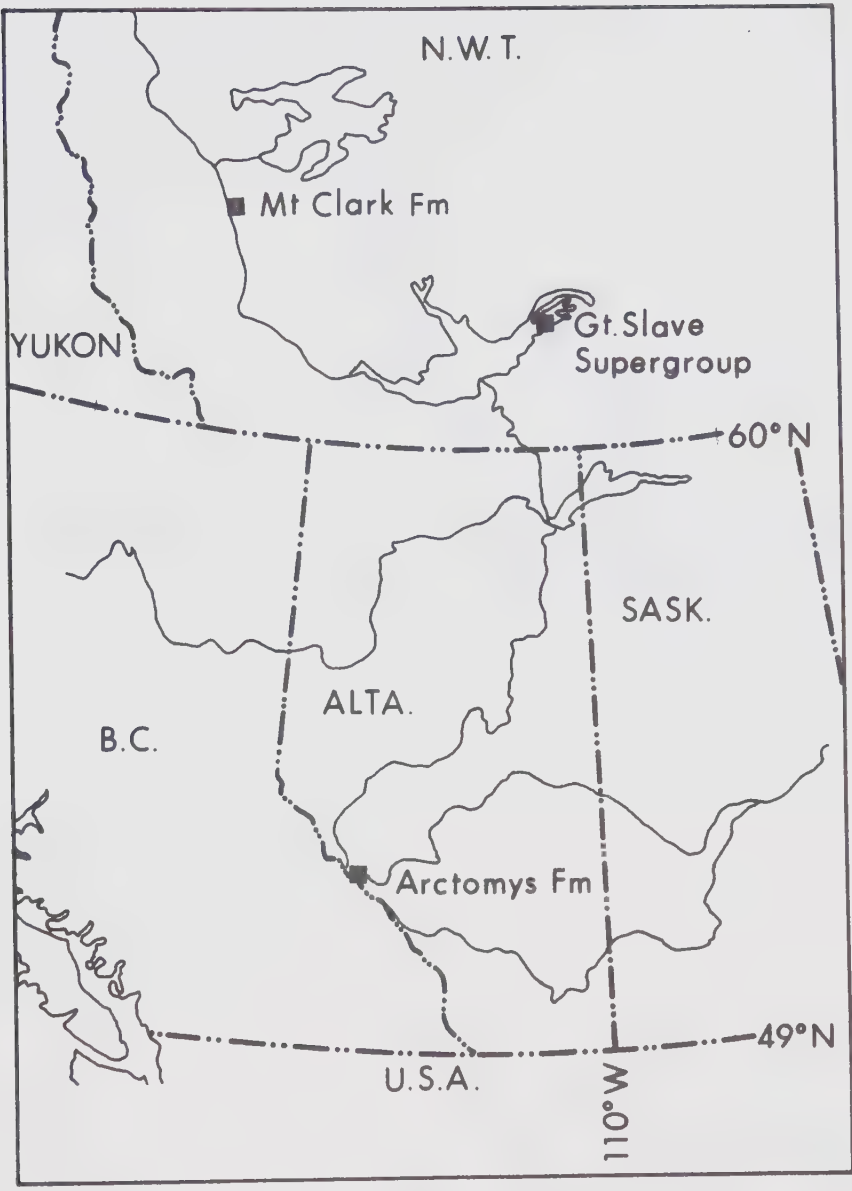
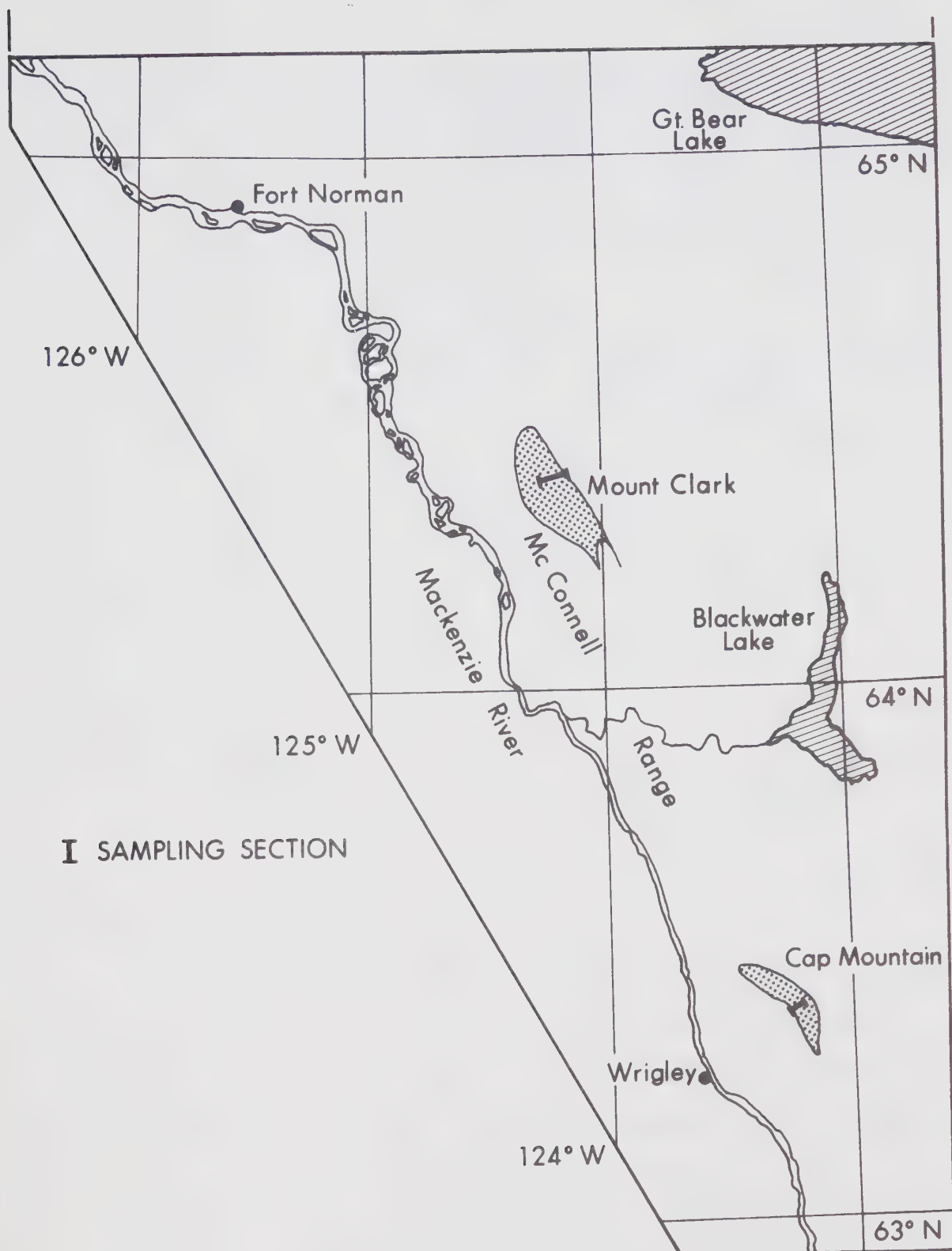


Figure 3.2.1b Location of sampling sections,
Mount Clark Formation.



Formation, i.e. "pre-middle Cambrian" and epeirogenic or gentle, swell-like uplift in pre-upper Ordovician, pre-Devonian, pre-Cretaceous and pre-Tertiary times. Recent glaciation has left erratics at the top of Cap Mountain, and close to the top of Mount Clark.

Samples of the Mount Clark Formation were obtained at Cap Mountain (6 sites) and Mount Clark (9 sites) at 15 - 20 m stratigraphic intervals (Fig. 3.2.1b). The two sampling sections were up gullies cutting into a dip slope. Although they are stratigraphically ordered, they almost certainly overlap. The samples from Cap Mountain covered the top 100 m of the reported total thickness of 150 m. The Mount Clark section covered about 120 m, but its location within the formation is not known. The Mount Cap and Saline River Formations, whose lithology also seemed promising (Table 3.2.1a) could unfortunately not be sampled, because they form a recessive interval and are not exposed.

Sampling was by field drilling using a drill similar to that described by Doell and Cox (1965) and orientation was by direct sun compass observation using an instrument similar to that described by Gough and Opdyke (1963). Five samples were obtained at each site of sufficient size to yield at least two 2.5 cm long specimens. Bedding orientation at each sampling site was measured using a Brunton type

Table 3.2.1a The Cambrian Stratigraphic Succession
in the McConnell Range

Period	Formation	Thickness	Lithology
Lower Cambrian	Saline River Formation	upper 100 m	Banded, calcareous shales with interbeds of red and green shale.
		lower 70 m	Red and grey shale containing salt, gypsum and selenite.
 Covered Interval		
	Mt. Cap Formation	70 m	Grey and green fissile shales. Red sandstone and shale.
	Mt. Clark Formation	150 m	Pink & red quartzite.
Pre- Cambrian	Lone Land Formation	15 m	Red shale & ferruginous sandstone.
		20 m	Haematite, red conglomerate, sandstone.

compass-clinometer, assuming the magnetic declination to be 35.5°E at Cap mountain and 36.7°E at Mount Clark as extrapolated from magnetic charts for 1965.0. Strikes were fairly uniform, except for sites at the base of the Mount Clark section. Dips were in the region of 30° . The dips and strikes at each site, together with the stratigraphic arrangement of sites are listed in Appendix 4.

A typical specimen name is MB5A. M denotes the study (McConnell Range), B the site, 5 the sample and A the specimen.

3.2.2 Natural remanence and A.F. demagnetization

The site level statistics for the NRM's before dip correction are given in Table 3.2.2a. The NRM site mean directions are plotted on an equal area projection in Fig. 3.2.2a. Two sites (MD and MM) have been rejected as random (Watson, 1956) and are not plotted. It will be noted that the site mean directions group about the present field at the site, including it within the circle of 95% confidence about their mean. Thus we cannot reject the hypothesis that the NRM's represent the present field. This could have come about either as a result of recent weathering, which would give a CRM in the present field direction or as a result of the predominance of magnetic material with short relaxation

Table 3.2.2a Mount Clark Formation. Within-site statistics on NRMs. No dip correction applied.

<u>Site</u>	<u>N</u>	<u>D</u>	<u>I</u>	<u>k</u>	<u>α_{95}</u>	<u>R</u>	<u>Notes</u>
MA	5	57.0	76.2	18.9	18.2	4.7844	
MB	5	107.1	69.1	200	5.4	4.9799	
MC	5	45.5	79.4	54	10	4.9255	
MD	5	29.5	55.8	2	73	3.0670	1
ME	5	337.7	59.2	3	51	3.7500	2
MF	5	45.3	71.8	1000	2.4	4.9960	
MG	5	343.6	65.3	37	13	4.8915	
MH	5	306.9	74.4	27	15	4.8513	
MJ	5	297.3	70.1	32	16	3.9074	
MK	5	93.2	72.1	60	10	4.9337	
ML	5	85.3	37.1	5	40	4.1399	
MM	5	103.5	47.2	2	62	3.3889	1
MN	5	350.3	57.6	17	19	4.7607	
MO	6	56.9	60.8	4	41	4.6138	
MP	5	23.0	82.9	151	6	4.9735	

Table 3.2.2a Mount Clark Formation. Within-site statistics
on NRMs. No dip correction applied.

Continued

Mean of 13 non-random sites. $D = 31.5$, $I = 75.9$

$k = 14.0$, $R = 12.1415$, $\alpha_{95} = 11.5$, $\theta_{63} = 20.9$

Present field in sampling area $D = 36$, $I = 81$.

Notes

1. Directions random on Watson's (1956) criterion.
2. Direction not random, but precision reduced by presence of one nearly reversed direction.

N is the number of samples per site included in the mean direction for the site.

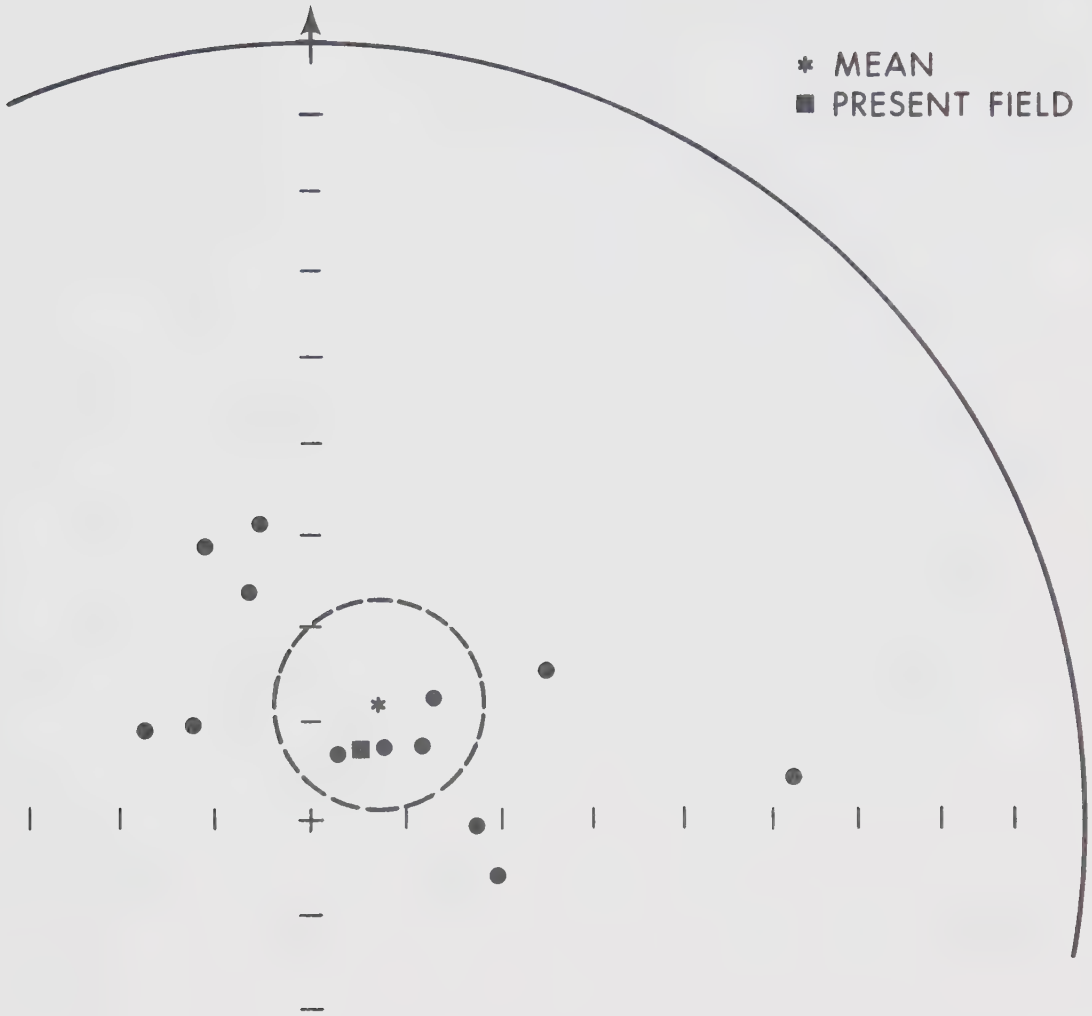
D is the azimuth of the magnetization, in degrees east of true north.

I is the inclination of the magnetization, in degrees below the horizontal.

k and α_{95} are statistical parameters described in Chapter 1.

R is the length of the vector resultant of the five sample directions.

Figure 3.2.2a NRM site mean directions, Mount Clark Formation. No dip correction has been applied. The circle of 95% confidence about the mean is shown.



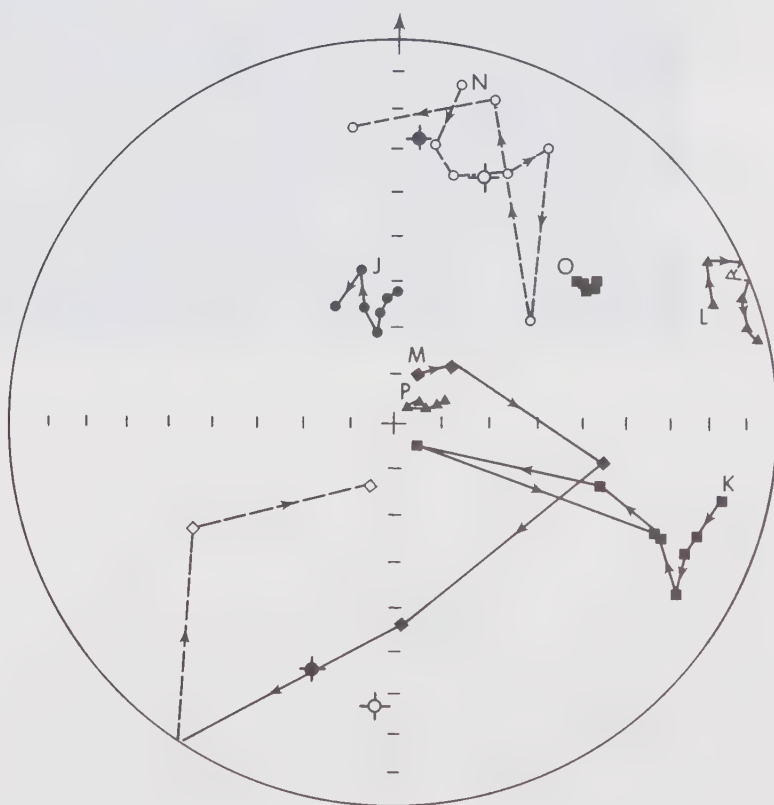
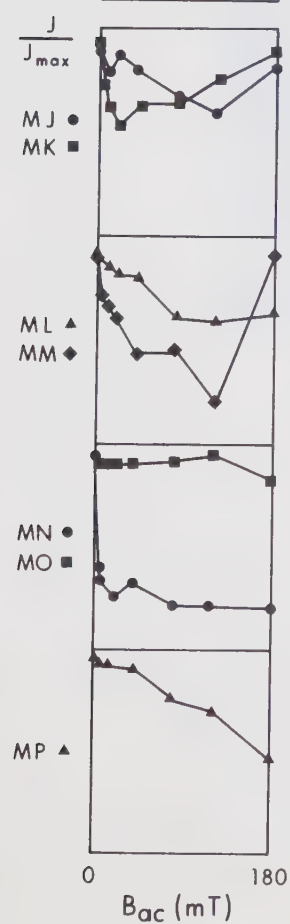
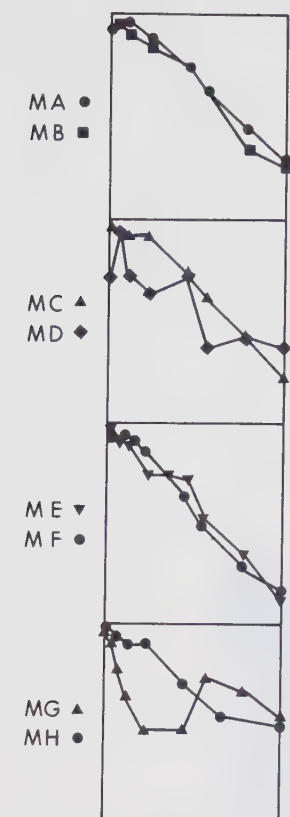
times, giving rise to a VRM. This is further discussed below.

Pilot specimens from each site have been subjected to alternating field demagnetization. The variation in direction and intensity caused by this is depicted in Fig. 3.2.2b. A correction for the dip of the strata has been applied. Detailed results are listed in Appendix 1. Demagnetization produces no coherent trends. The pilot specimens from some sites (MA, B, C, O, P) change direction very little. Others move, but in no consistent manner. Exceptions are the pilots from sites MG, MD and MM which show considerable change in direction, but do not agree with each other at all. The pilot from MM moves to a position almost exactly reversed from its NRM direction. This is not understood. The intensity curves show a considerable drop in most cases. The lack of movement accompanying this drop suggests that there is only one component of magnetization present in many of the samples studied.

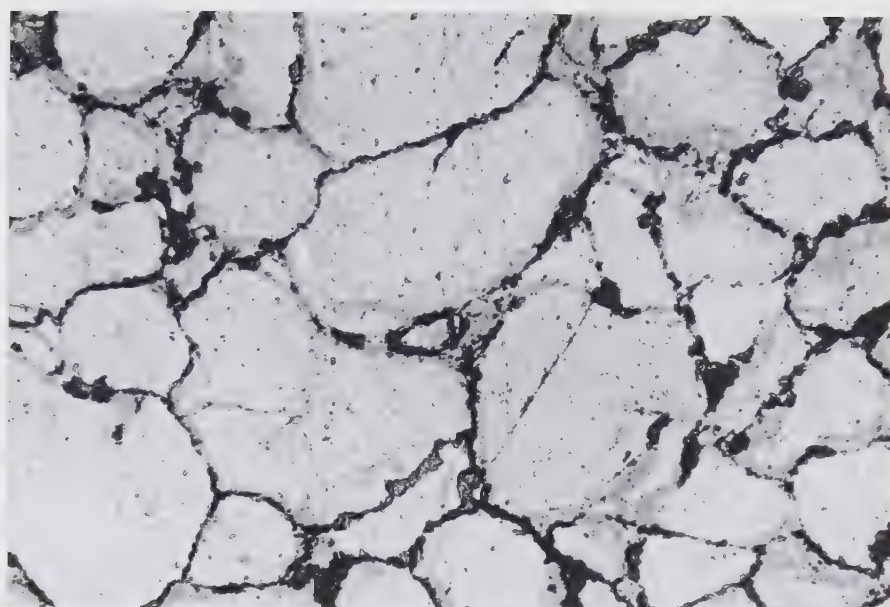
3.2.3 Discussion

Plate 3.2.3a is a photomicrograph of material from site MC. It reveals that the rock is a mature, moderately well sorted quartzite with very little of the inter-

Figure 3.2.2b Alternating Field demagnetization of the Mount Clark Formation. Pilot specimens from each site are shown.



✱ CAMBRIAN DIRECTIONS



—|—|—
200 μm

Plate 3.2.3a Transmitted light photomicrograph of
material from site MC in the Mount
Clark Formation

stitial cement considered important in the magnetism of red sediments (Creer, 1962). No detrital ore grains were observed in the thin section. Any that are present must be very much smaller than the quartz grains making up the rock.

The alternative hypotheses of VRM and CRM may now be examined. Magnetic grains with short relaxation times will normally be expected to have low coercivity (Everitt, 1961). Thus A.F. demagnetization may be expected to remove a VRM component. The response by some specimens described above may well be due to such a removal. On the other hand, remagnetization as a result of gentle heating during burial may be expected to give rise to VPTRM (Section 1.1) which may be quite hard. Such burial has occurred several times (Section 3.2.1 above), so that secondary components could have been acquired with the earth's field in various directions. A CRM resulting from recent weathering could be either hard or soft, depending on the grain size of the particles involved. Since at least some of the specimens demagnetized have a remanence directed along the present field and are not moved by demagnetization, it seems most likely that they have acquired a recent CRM.

Fig. 3.2.2b includes two Cambrian directions deduced from the results of Al-Khafaji and Vincenz (1971).

None of the specimens shows an obvious end point near either of these directions or their antipoles.

It is concluded that a primary NRM direction is not recoverable from the Mount Clark Formation.

3.3 The Arctomys Formation, Southern Rocky Mountains

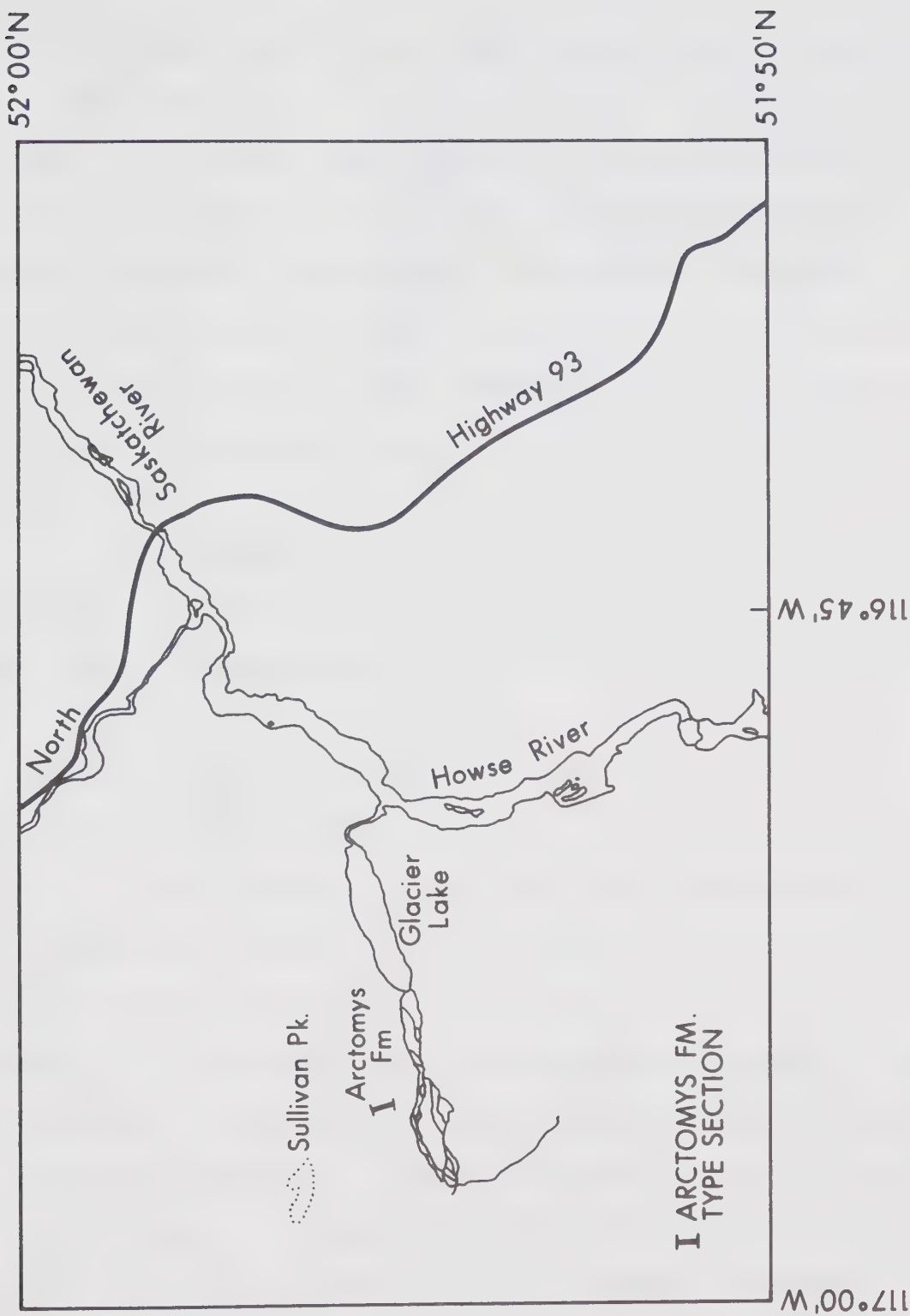
3.3.1 Geological setting and sampling

The Cordilleran Geosyncline of the Southern Rocky Mountains contains some 4-5 km of lower Palaeozoic sediments (Aitken, 1966). These consist primarily of limestone and dolomite, but include some shale, mudstone and siltstone which might give useful palaeomagnetic results.

In particular, the Arctomys Formation (red shale and siltstone) is present over a wide area and is much used as a stratigraphic marker horizon (Aitken & Greggs, 1966). The type section is on the southern slopes of Sullivan Peak (116.9°W , 51.9°N , Figs. 3.2.1a, 3.3.1a). The formation is essentially unfossiliferous, only a few unidentifiable fossil fragments having been found, but it is placed in the middle Cambrian by Aitken and Greggs (1966) on the basis of trilobites in the overlying Waterfowl Formation and the underlying Pika Formation.

A reconnaissance collection was made from the Arctomys Formation. Five hand blocks of red shale were ob-

Figure 3.3.1a Location of the Arctomys Formation type section, where samples were obtained.



tained, one from each of five shale bands spread through the 250 m thick formation at the type section. Orientation was by means of a Brunton type magnetic compass clinometer. The rock in the vicinity was too weakly magnetized to affect magnetic readings. The magnetic declination was extrapolated from charts for 1965.0, and taken to be 23°E . The bedding plane orientation was similarly found. It was uniform throughout the section, having a strike of 127°E and a dip of 16° to the SW.

The samples are labelled AA to AE in order of increasing age. The two specimens cut from each sample are named A and B respectively.

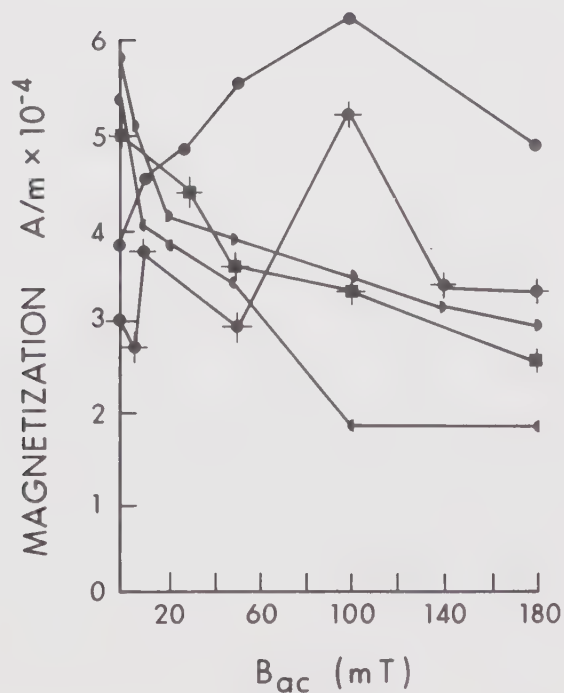
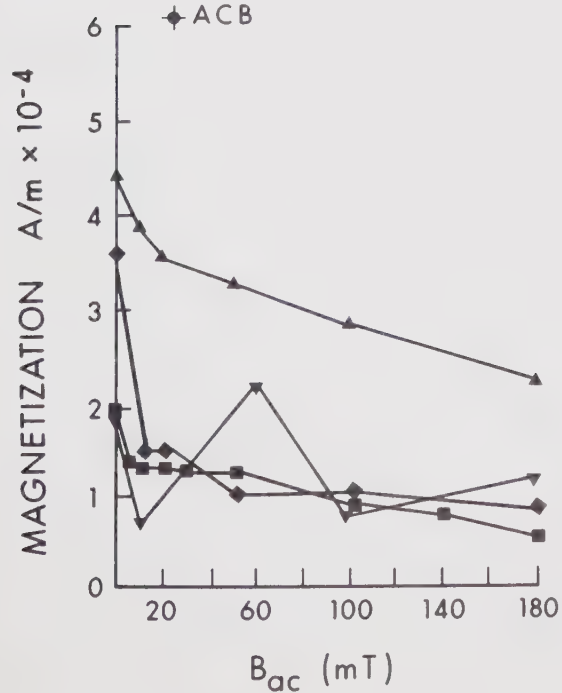
3.3.2 Natural remanence and A.F. demagnetization

The direction and intensity of magnetization of each of the five samples as they vary with demagnetizing field are shown in Fig. 3.3.2a. A correction for the dip of the strata has been applied. It will be noted that although A.F. demagnetization has considerable effect on the direction and intensity of magnetization, no satisfactory end points are reached. The two specimens AAA and AAB show typical intensity decrease for their stable directions. Specimens ABB, ACA and ACB all show intensity increases together with large changes in direction, suggesting that

Figure 3.3.2a A.F. demagnetization of samples from the Cambrian Arctomys Formation. Solid symbols are used for points on the lower hemisphere and open symbols for points on the upper hemisphere.



- | | |
|-------|-----------------------|
| ■ AAA | ▮ ADA |
| ◆ AAB | ◑ ADB |
| ▲ ABA | ⊠ AEA |
| ▼ ABB | * PRESENT FIELD |
| ● ACA | ◆ CAMBRIAN DIRECTIONS |
| ◆ ACB | |



an opposed low coercivity component is being progressively removed. The specimens from samples AD and AE show small movement and smooth demagnetization.

3.3.3 Discussion

Alternating field demagnetization of the Arctomys Formation appears to cause a general movement towards a direction near $D = 140^{\circ}$, $I = -50^{\circ}$, which is not particularly close to the Cambrian directions at this location deduced from the results of Al-Khafaji and Vincenz (1971). Since no end points are reached, no Cambrian pole is calculated here. Further sampling and thermal demagnetization may produce more useful results.

4. NATURAL REMANENCE OF THE PRECAMBRIAN KAHOCHELLA GROUP, GREAT SLAVE SUPERGROUP

4.1 Introduction

4.1.1 Summary

In this chapter the geological setting and sampling of the Kahochella Group is described, and the results of A.F. and thermal demagnetization are presented. It is shown that a well defined mean direction for much of the Group exists, although there are a number of anomalous sites. The removal of a number of secondary components by demagnetization is demonstrated.

4.1.2 Objectives of the study

Very little palaeomagnetic work has been done on North American rocks in the age range 2100 m.y. to 1400 m.y. (see Chapter 7). This seems to have been a time of considerable apparent polar wander, judging from the disparity of about 50° between palaeomagnetic poles at either end of the interval. The Kahochella Group, consisting as it does of a great thickness of well exposed red shales (Section 4.2), offers the opportunity not only to obtain a good palaeomagnetic pole at ca. 1800 m.y., but also to study the time variation of the geomagnetic field around that date.

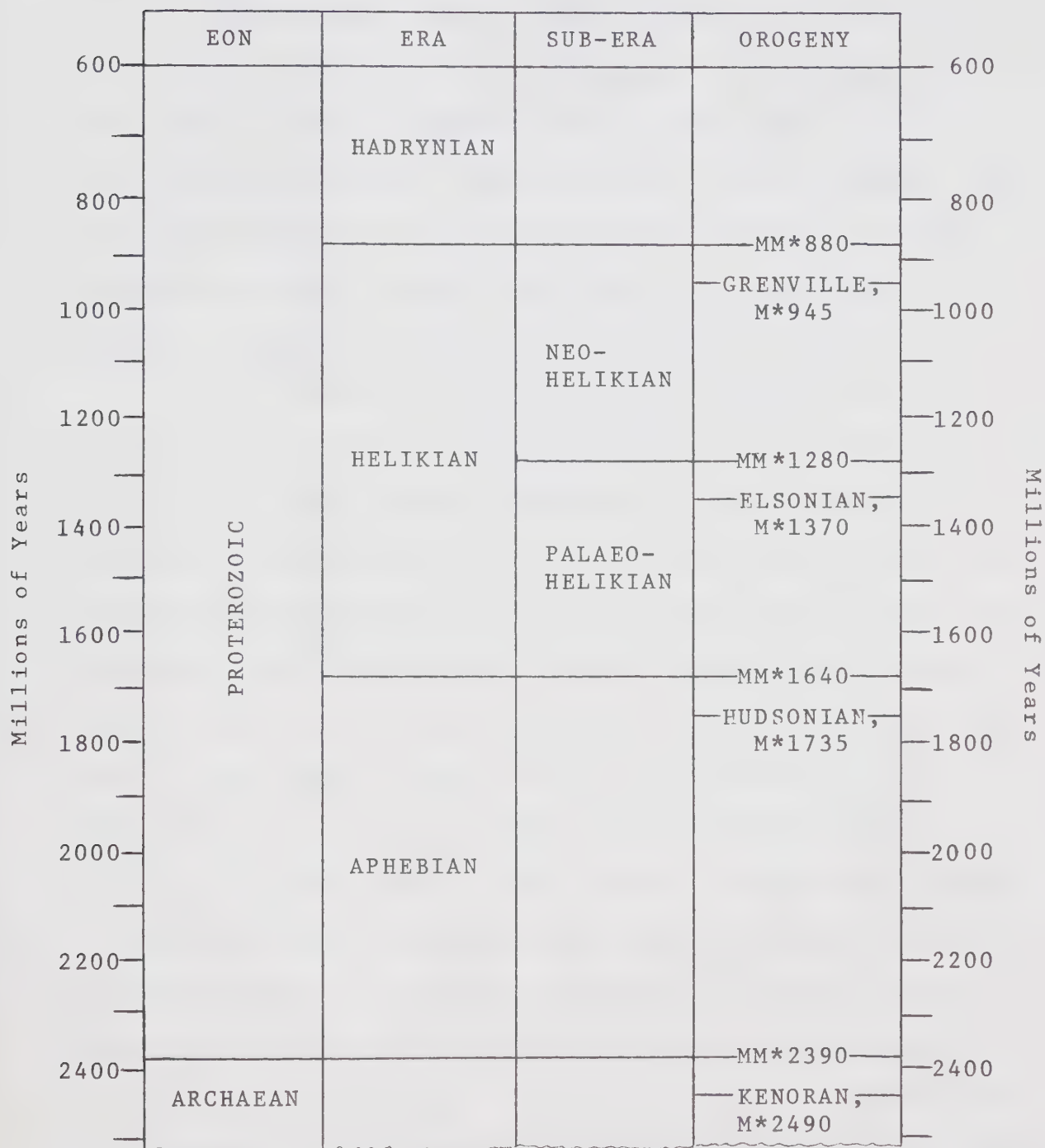
The probable time involved in the deposition of the group (about 50 m.y. - see Section 6.1) is such as to span a time interval comparable to that in which field reversals are known to have occurred in recent times. A reversal rate such as has been observed for the Permian (Irving & Parry, 1963) might well yield no reversals in 50 m.y. Such a time scale may also include a small amount of polar wander. Jones & McElhinny (1967) claim to have resolved a considerable amount of polar wander using results from a thick sequence of red sediments of similar age in Africa.

Thus a carefully designed sampling scheme which makes use of the available stratigraphic control should yield a crude, but nevertheless unique "tape recording" of the geomagnetic field at about 1800 m.y., provided an original remanence has been preserved.

4.2 Geologic Setting and Sampling

A time scale for the Canadian Shield has been proposed by Stockwell (1964, Table 4.2a). It uses orogenies as dated by K/Ar methods to divide the Precambrian into Eras, notably the Aphebian Era between the ends of the Kenoran (2390 m.y.) and Hudsonian (1640 m.y.) orogenies. The shield may also be divided into structural provinces (Stockwell, 1970)

Table 4.2a Precambrian time-scale for the Canadian Shield
from Geol. Surv. Can., Paper 67-2 Part A, 1968.



M* mean age of orogeny in millions of years

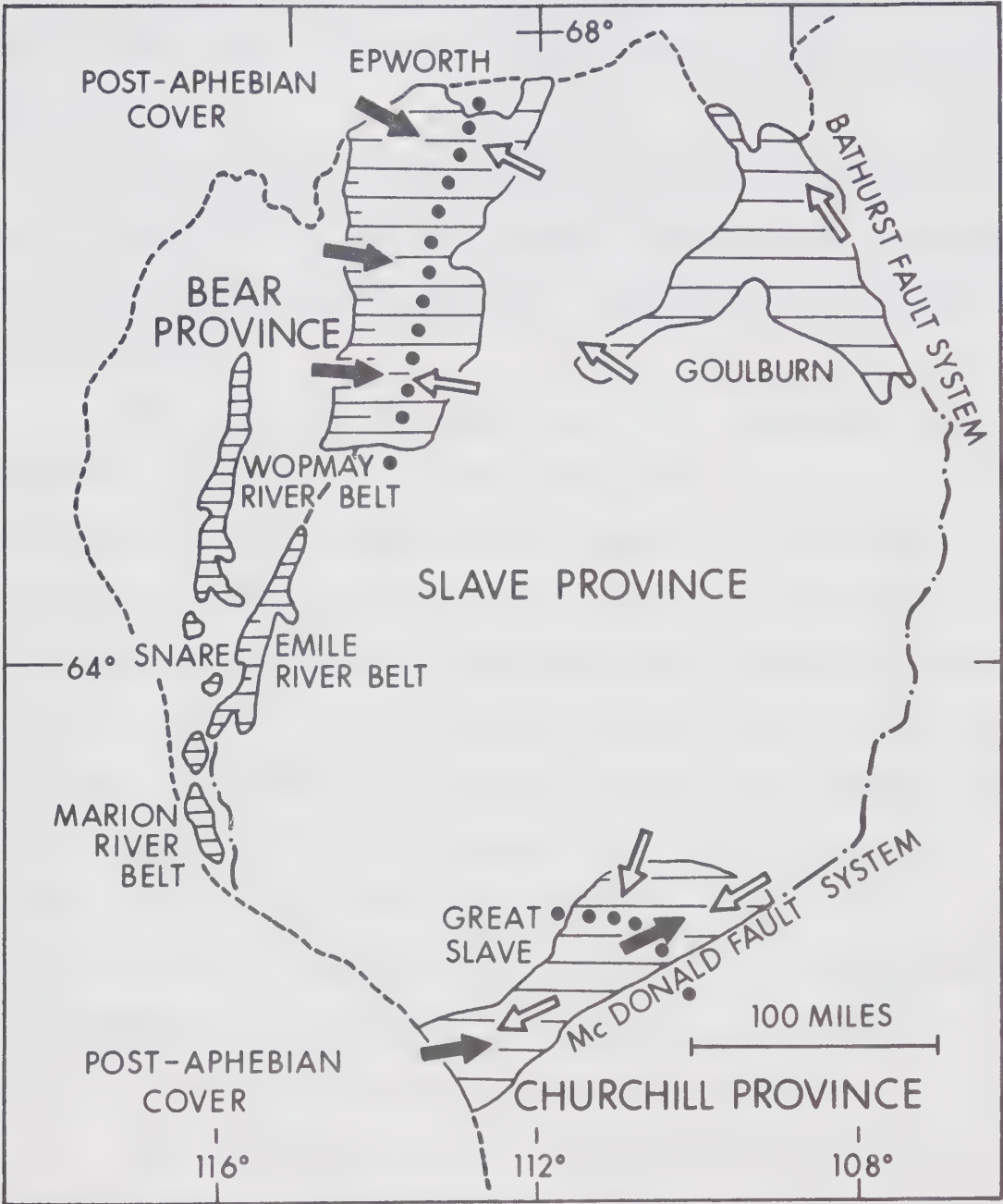
MM* mean age minus one standard deviation (K/Ar determination on orogenic micas)

on the basis of overall differences in internal structural trends and style of folding.

The margins of the Slave Province include four large tracts of Proterozoic sedimentary rocks (Fig. 4.2a). These are the Snare, Epworth and Goulburn Groups and the Great Slave Supergroup. Hoffman et al. (1970) propose that these are remnants of the "Coronation Geosyncline" which developed between a stable platform to the east and a late Archean orogenic belt (the Bear Province) to the west.

In the area of the East Arm of Great Slave Lake, District of Mackenzie, (Geological Survey of Canada Map 1122A, Fig. 3.2.1a) late Archean granites are overlain by the intensely folded Wilson Island and Union Island Groups with total thickness at least 7 km, which are in turn overlain by the Great Slave Supergroup. This is itself gently folded and intruded by quartz diorite laccoliths and diabase dykes and sills. K/Ar ages of biotites from the diorite are 1845, 1795, 1785 and 1630 m.y. (G.S.C. 61-78 and unpublished - quoted by Hoffman, 1969). The diorites intrude all members of the Great Slave Supergroup up to and including the Stark Formation, which they appear to disturb. Hoffman (1969) therefore considers the intrusions to be contemporaneous with the Stark Formation. The diabase dykes and sills have been sampled for palaeomagnetic purposes by Fahrig and Jones

Figure 4.2a The remnants of the Coronation Geosyncline spread around the borders of the Slave Province (After Hoffman et al. (1970)).



(1969, 5 sites) and Irving et al. (1972, 8 sites). They are shown to be a part of the Mackenzie igneous event at about 1200 m.y.

Great Slave Supergroup strata are truncated to the south by the McDonald Fault, and are unconformably overlain by the very late Aphebian or Early Helikian rocks of the Et-then Group.

The Great Slave Supergroup has a maximum total thickness of more than 8 km of lavas, red and green shales and stromatolitic limestone and dolomite but the actual thickness of individual formations varies considerably, depending on the location. Hoffman (1968) proposed that it be elevated to the rank of Supergroup and subdivided it into the Sosan, Kahochella, Pethei and Christie Bay Groups. The stratigraphic nomenclature suggested by Hoffman is shown in Table 4.2b. Olade and Morton (1972) have proposed that the Seton Formation, assigned by Hoffman to the Kahochella Group, might more properly be regarded as part of the Sosan Group, but the distinction is unimportant here.

The Kahochella Group, which consists mainly of unmetamorphosed mudstones and siltstones, forms the basis of this study. It immediately overlies the Seton Formation (red shales and spilitized basalts), dated by Rb/Sr whole rock isochron at 1873 ± 13 m.y. using a 5×10^{10} year half life for Rb^{87} (Baadsgaard, pers. comm.).

Table 4.2b Table of Formations within the
Great Slave Supergroup

Group	Formation	Thickness	Lithology
Christie Bay	Pearson	>170 m	Basalt, Argillite
	Portage Inlet	210 m	Red-brown shale
	Tochatwi	790 m	Red to buff sandstone
	Stark	600 m ?	Red mudstone, dolomite
Pethei	Hearne	90 m	Limestone
	Wildbread	180 m	Stromatolitic limestone
	Pekanatui Pt	100 m	Limestone, argillite, greywacke
	Blanchet	300 m	Greywacke, argillite, limestone
	McLean	120 m	Argillite, limestone
	Utsingi	270 m	Limestone
	Taltheilei	120 m	Dolomite, limestone
	Douglas Pen.	30 m	Marlstone, argillite, limestone

Table 4.2b Table of Formations within the
Great Slave Supergroup

Continued

Group	Formation	Thickness	Lithology
Kahochella	Charlton Bay	150 m	Green argillite
	McLeod Bay	320 m	Red shale, calcareous concretions
	Gibraltar	1050 m	Red shale
	Seton	1300 m	Spilite, tuff, red siltstone
Sosan	Akaitcho R.	300 m	Red siltstone, white sandstone
	Kluziai	440 m	Pink sandstone
	Duhamel	280 m	Dolomite, orthoquartzite, siltstone
	Hornby Channel	1500 m	Sandstone, dolomite

Hoffman (1967) has made numerous palaeocurrent measurements, the results of which are shown in Fig. 4.2b. The predominant flow direction during the deposition of the Kahochella Formation was towards the present SSE. This is important to the palaeomagnetic study mainly because current flow can affect DRM directions (Rees, 1961). It is further discussed in Section 5.7.

The Seton, Kahochella and Pethei Groups were sampled on Keith Island (111.9°W , 62.1°N) in the East Arm of Great Slave Lake (Figs. 3.2.1a, 4.2c). They are very well exposed along the northwest shoreline, polished clean by glaciation and dipping gently along the coast. It was therefore possible to place sampling sites at known stratigraphic distances apart, subject to restrictions of exposure. Fig. 4.2d shows the stratigraphic relationship between the sites, while Fig. 4.2e shows their location and the strike of the strata at each site. Dips (typically 10° - 20°) were measured at each site for later use in a tectonic correction. The attitudes of the strata at each site are listed in Appendix 4. It will be noted that the sampling was distributed more or less uniformly through the Gibraltar and McLeod Bay Formations with one gap of some 400 stratigraphic metres.

Sampling was by field drilling using a hand held drill similar to that described by Doell and Cox (1965),

Figure 4.2b Palaeocurrent directions in the Great Slave Supergroup (Hoffman, 1967).

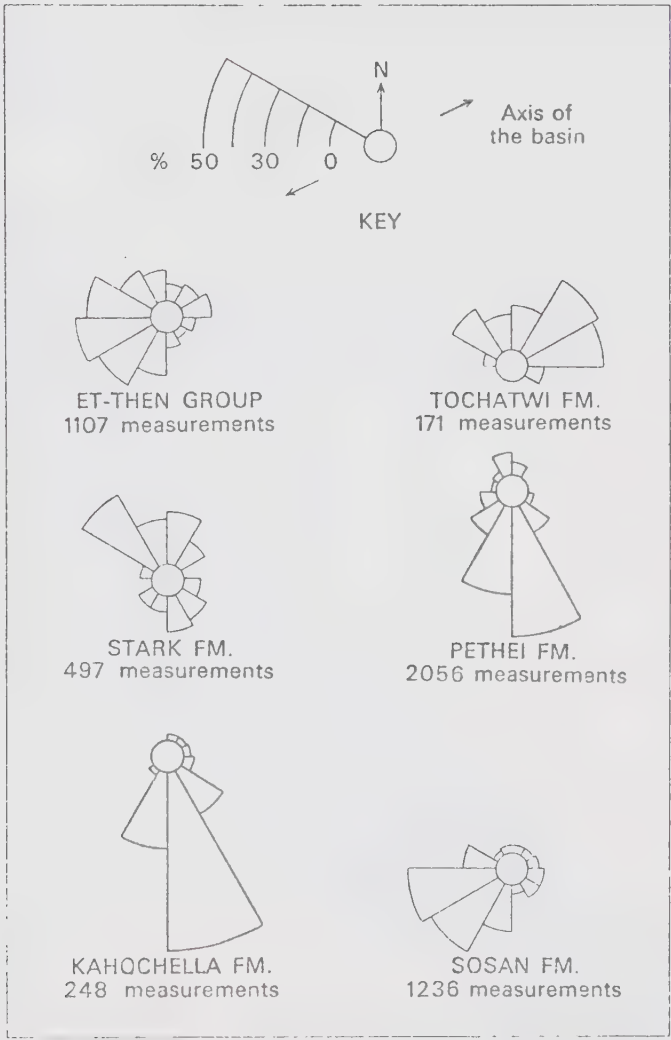


Figure 4.2c Location of sampling area. Keith Island in the East Arm of Great Slave Lake.

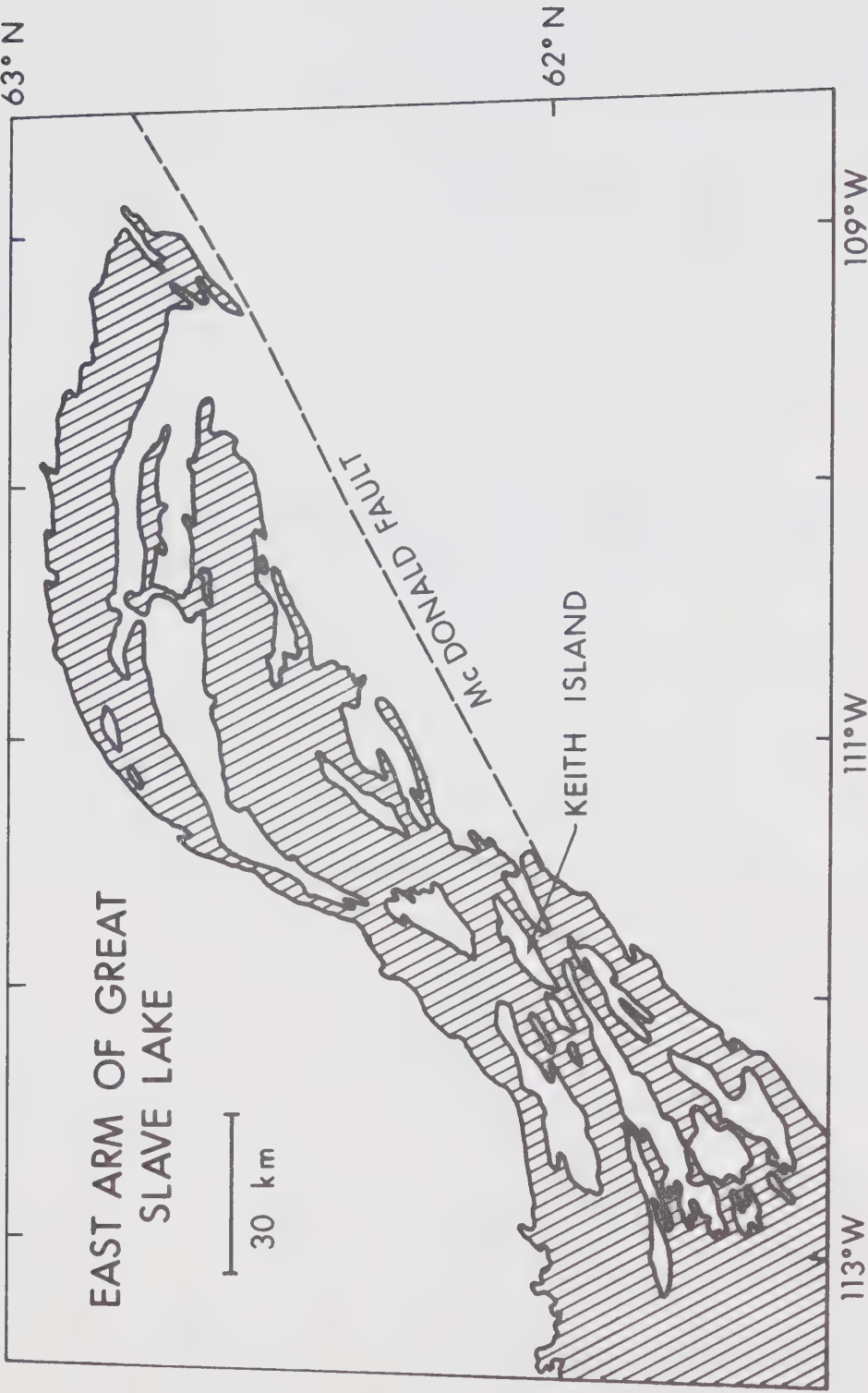


Figure 4.2d The stratigraphic arrangement of sampling sites in the Great Slave Supergroup

GROUP FORMATION SAMPLING

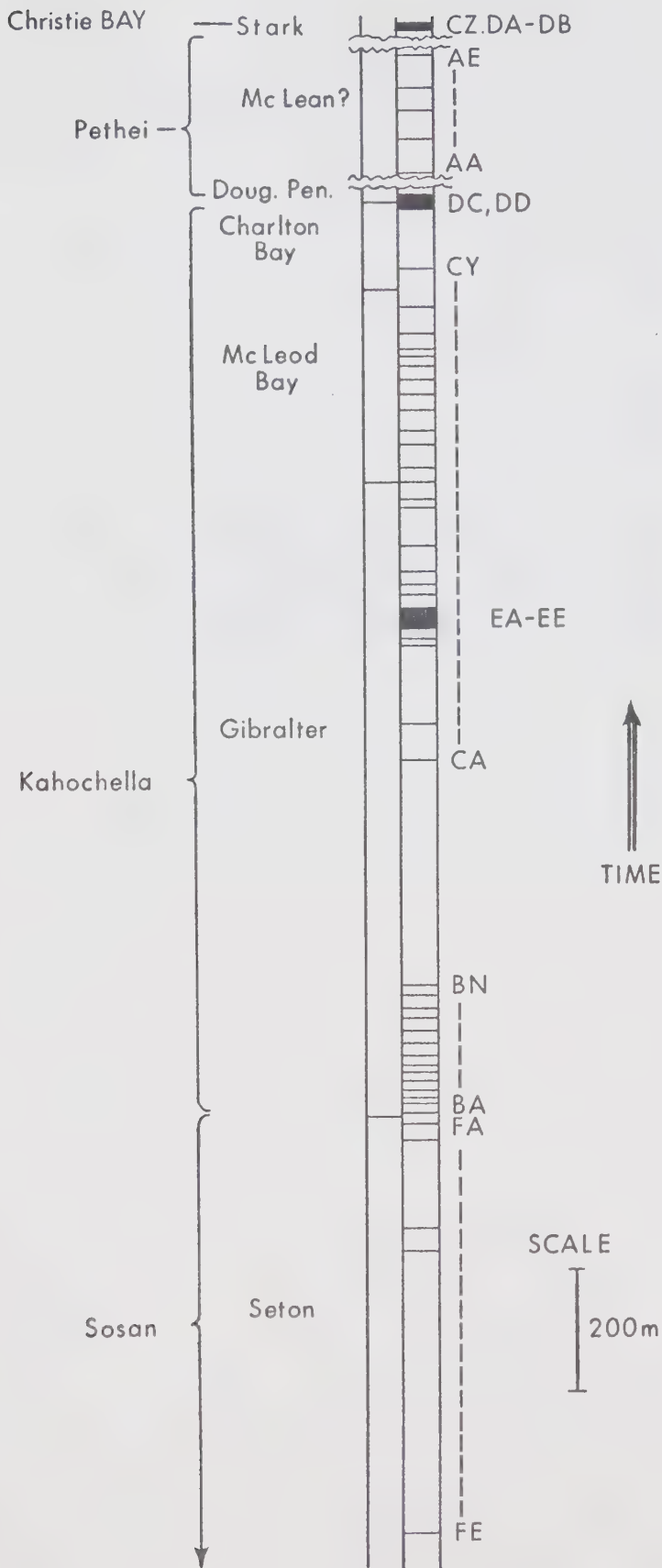


Figure 4.2e The location of sampling sites on the shores of Keith Island, Great Slave Lake. The strike of the strata at each site is shown.

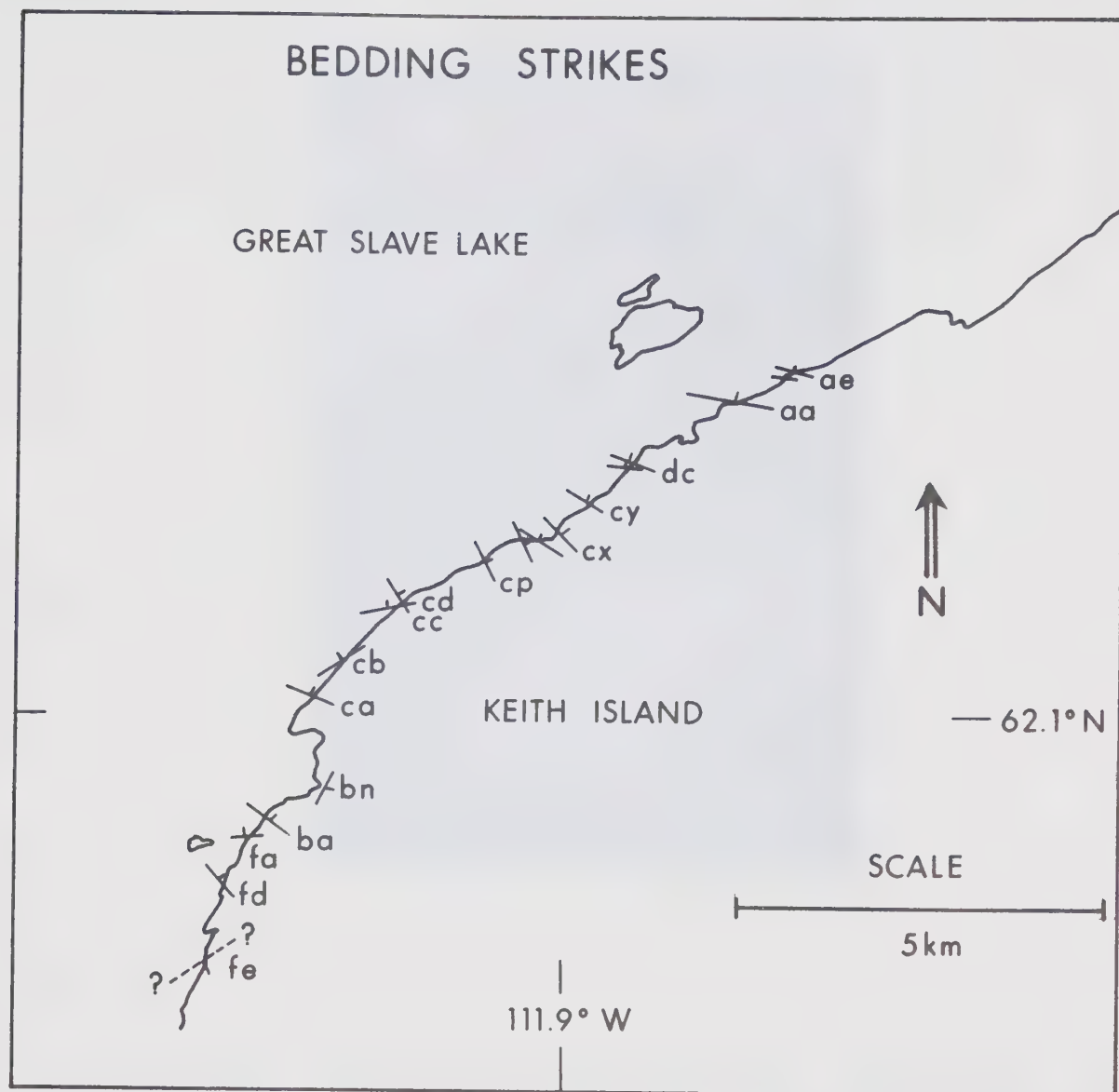




Plate 4.2a The red shales of the Gibraltar Formation on the shores of Keith Island. The planar surface is the result of recent glaciation. Virtually continuous exposure is often available.

although a few hand samples were taken where drilling proved impossible because of the fissile nature of the rock.

Azimuthal orientation of the samples (core and block) was with reference to distant "sight points" whose bearings east of true north were determined by calculation from multiple sun sightings. Since the sun compass included a Brunton type magnetic compass, the magnetic declination could be determined by sightings on the sun or the sight points. It was found to be 30.2°E with a standard deviation of 2.2° (33 observations). Extrapolation from the Dominion Observatory Isogonic Chart for 1965.0 gives 29.7°E . A magnetic compass was used in the determination of bedding strikes. The red sediments were insufficiently magnetic to affect the compass appreciably.

At each site four independently oriented samples of sufficient size to yield at least two specimens each were obtained. As far as possible the samples were obtained from the same horizon. In 32 of 59 cases they were within 2 cm of the same horizon. In only two cases does the stratigraphic spread exceed 1 metre (Appendix 4). The horizontal spacing of the site was made as large as possible within limitations of exposure. It was typically several metres. Sites were grouped in sections within which the between-site spacing could be estimated and approximated 25 m. The larger gaps

between sections were forced by lack of exposure or unsuitable lithology. The figure of 25 m was chosen to enable coverage of the formations of interest in the time available. In all, samples were obtained at 59 sites in 5 sections (Fig. 4.2d). Section E is a detailed section between two sites (CE and CF) in the C section at a spacing of about 4 m stratigraphically. The section was sampled in order to examine geomagnetic field changes that might be missed in the longer intervals. CZ is a sampling site in one of the dioritic intrusions correlative with the Stark Formation mentioned above. Section D is the baked contact of the intrusion. Site DA is at the contact, and DB, DC and DD are 3-6 m, 50 m and 100 m away from the contact.

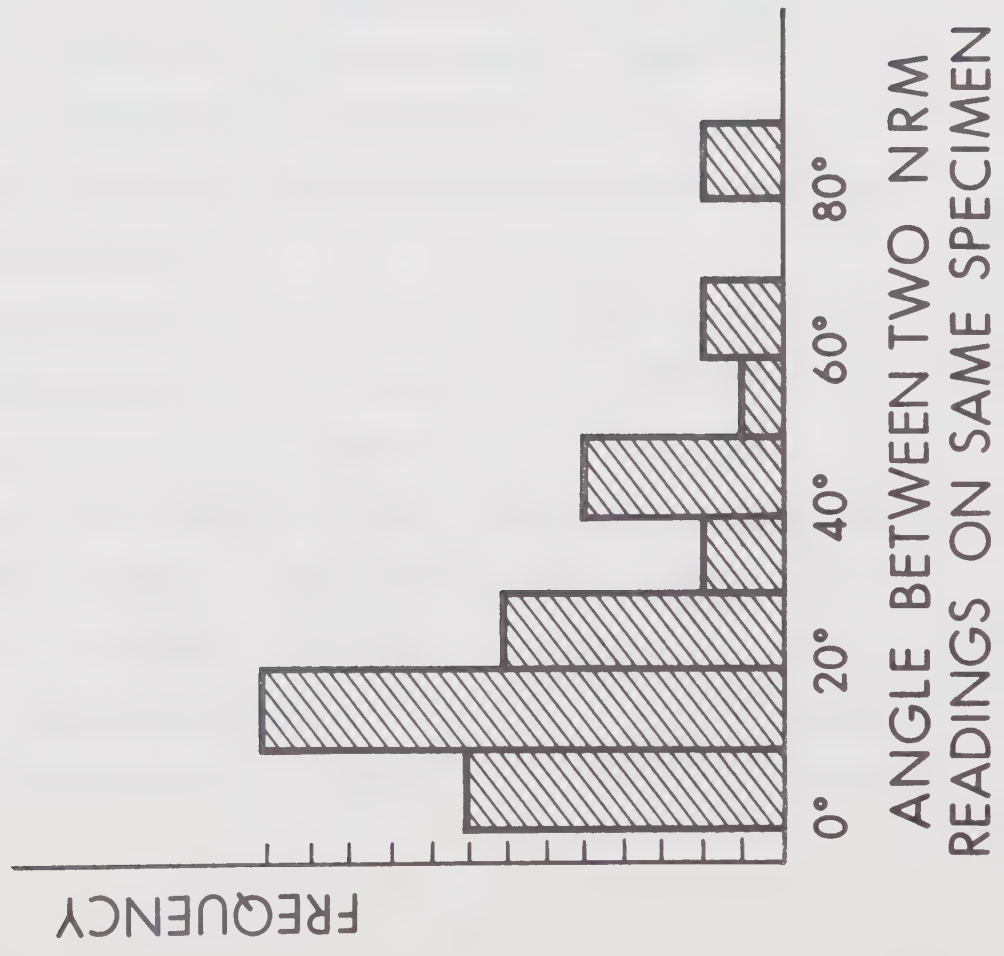
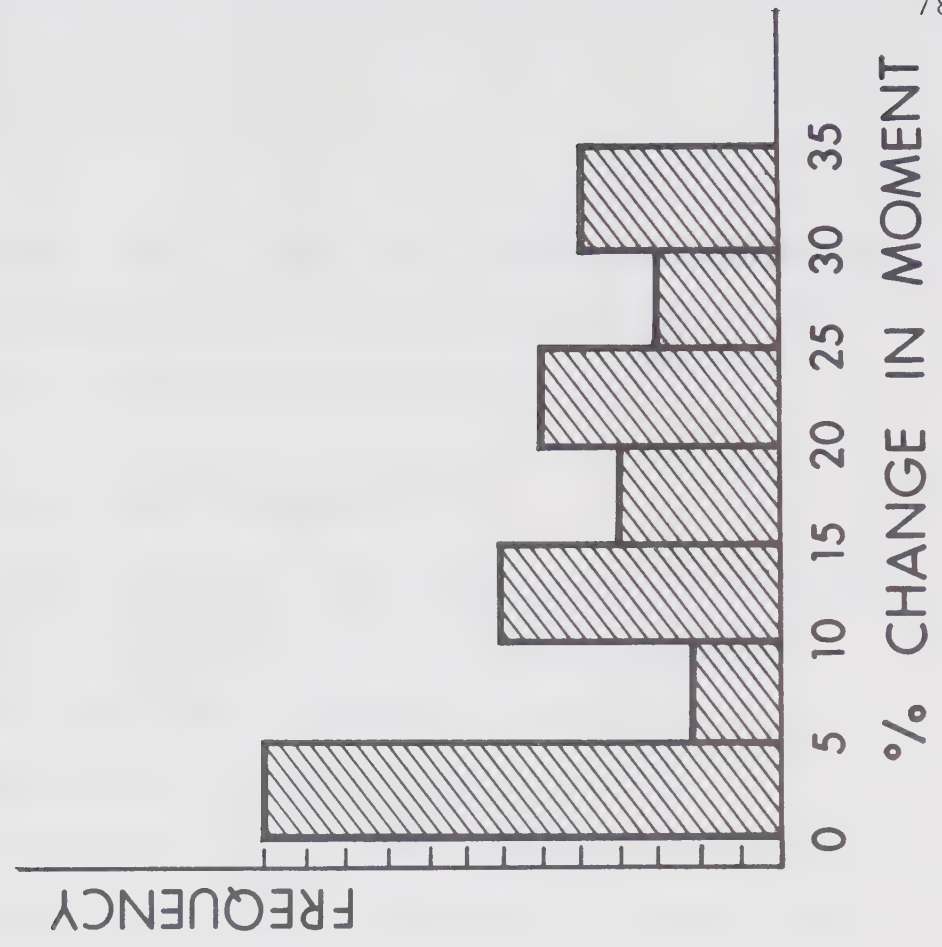
A typical specimen name is CE4B where C denotes the section, E the site, 4 the sample and B the specimen.

4.3 Natural Remanence and Demagnetization

4.3.1 Natural remanent magnetization

The NRM of the Kahochella Group samples was found to include a substantial unstable component. Fig. 4.3.1a shows the differences in angle and moment between pairs of measurements made on each of 40 specimens at times 3 to 6 months apart. Changes of up to 30° in direction and 25% in

Figure 4.3.1a The difference in angle and moment between pairs of measurements made on each of 40 specimens from the Kahochella Group at times 3 to 6 months apart.



moment are common. This suggests the presence of a viscous component with relaxation time in the range of minutes to years, and makes partial demagnetization imperative.

4.3.2 Alternating field demagnetization

One pilot specimen from each site was subjected to alternating field demagnetization. Curves of intensity against demagnetizing field revealed the existence of a large soft magnetization (Figs. 4.3.2b, c, d) which was usually removed by treatment in peak fields of 40 mT (400 Oe).

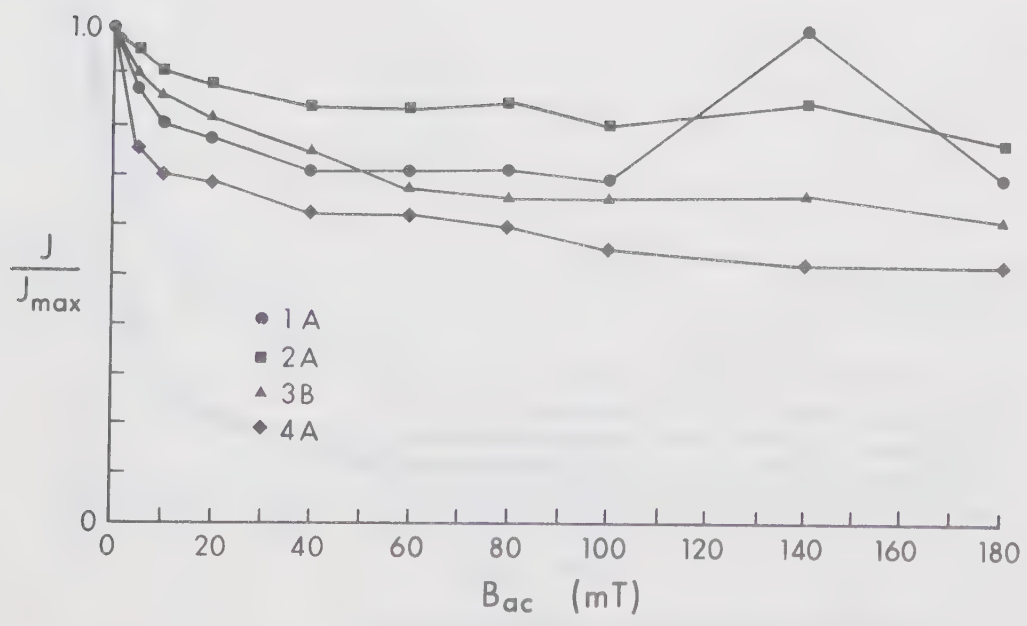
Demagnetization of one specimen per sample was therefore undertaken at three steps to provide evidence of demagnetization end points for each sample. Steps of 40, 60 and 80 mT peak field were employed and these were followed up by treatment in higher fields where no end point had been reached at or before 80 mT.

Typical results for changes in intensity and direction during demagnetization are shown in Figs. 4.3.2a - f. Full details may be found in Appendix 1.

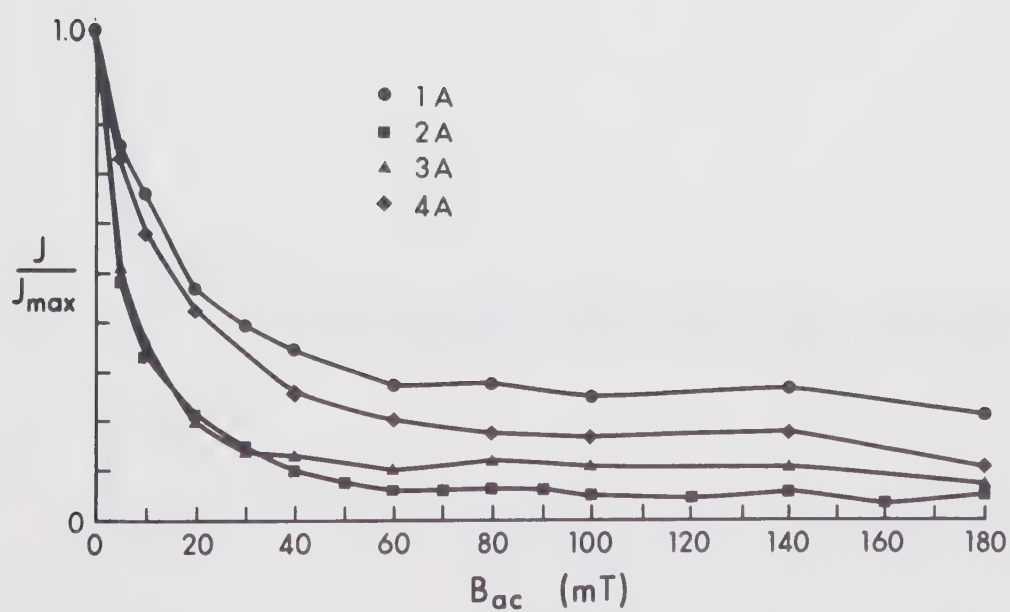
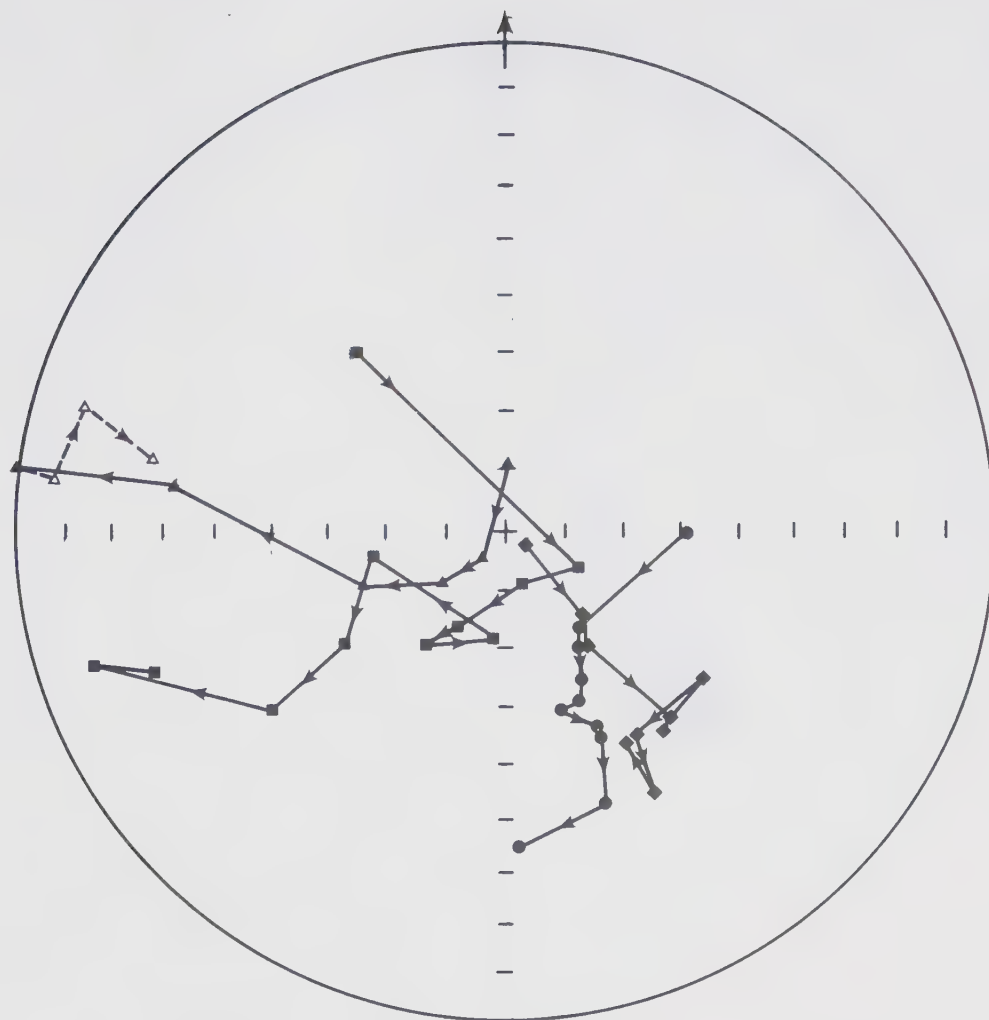
Sites from section A were little affected by demagnetization (Fig. 4.3.2a). They showed almost no direction change while the intensity dropped to a value of 70 - 90% of the NRM after demagnetization in fields of 40 mT and remained roughly constant thereafter. Site AC was magnetized in the

Figure 4.3.2a-f Alternating field demagnetization of specimens from the Kahochella Group. The results from one site per section are shown.

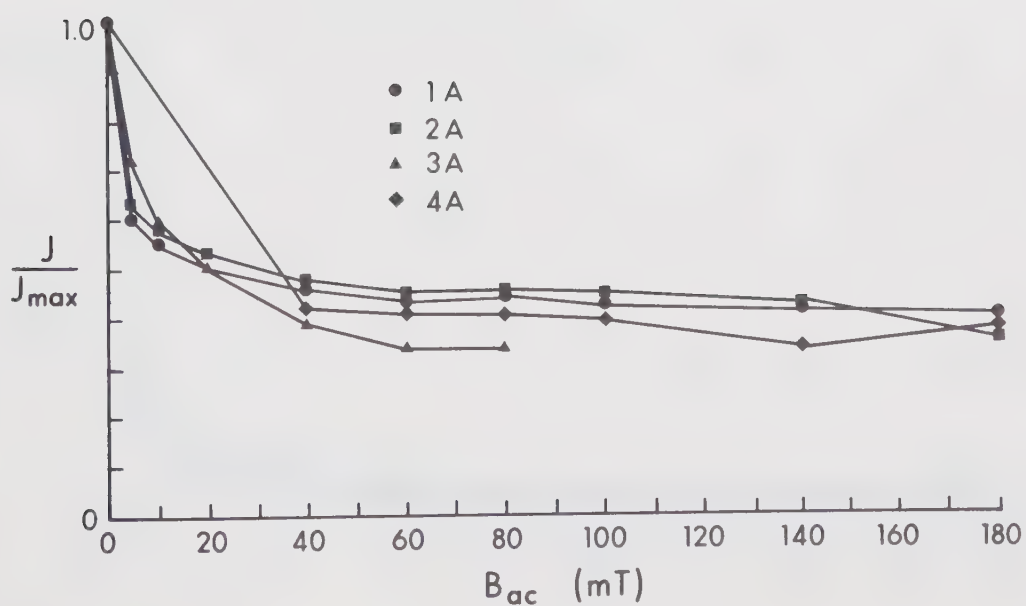
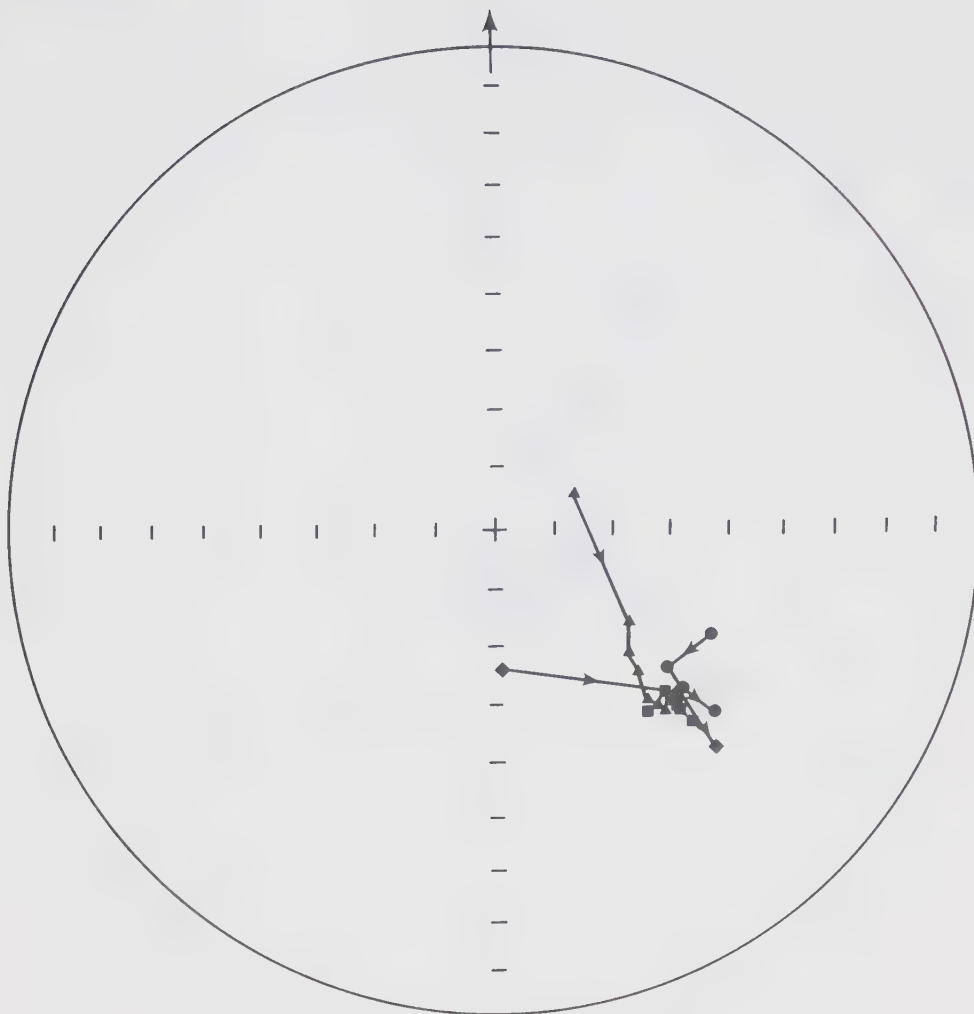
The direction plot employs a polar equal area projection with the north-seeking end of the magnetic vector plotted as an open symbol on the upper hemisphere or a closed symbol on the lower hemisphere. The directions are shown corrected for geologic dip.



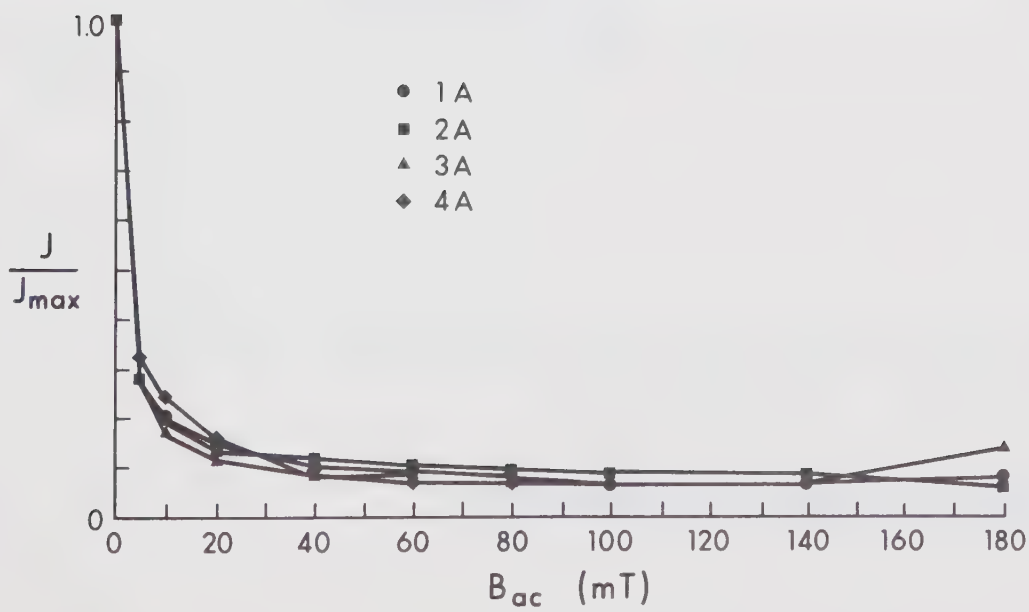
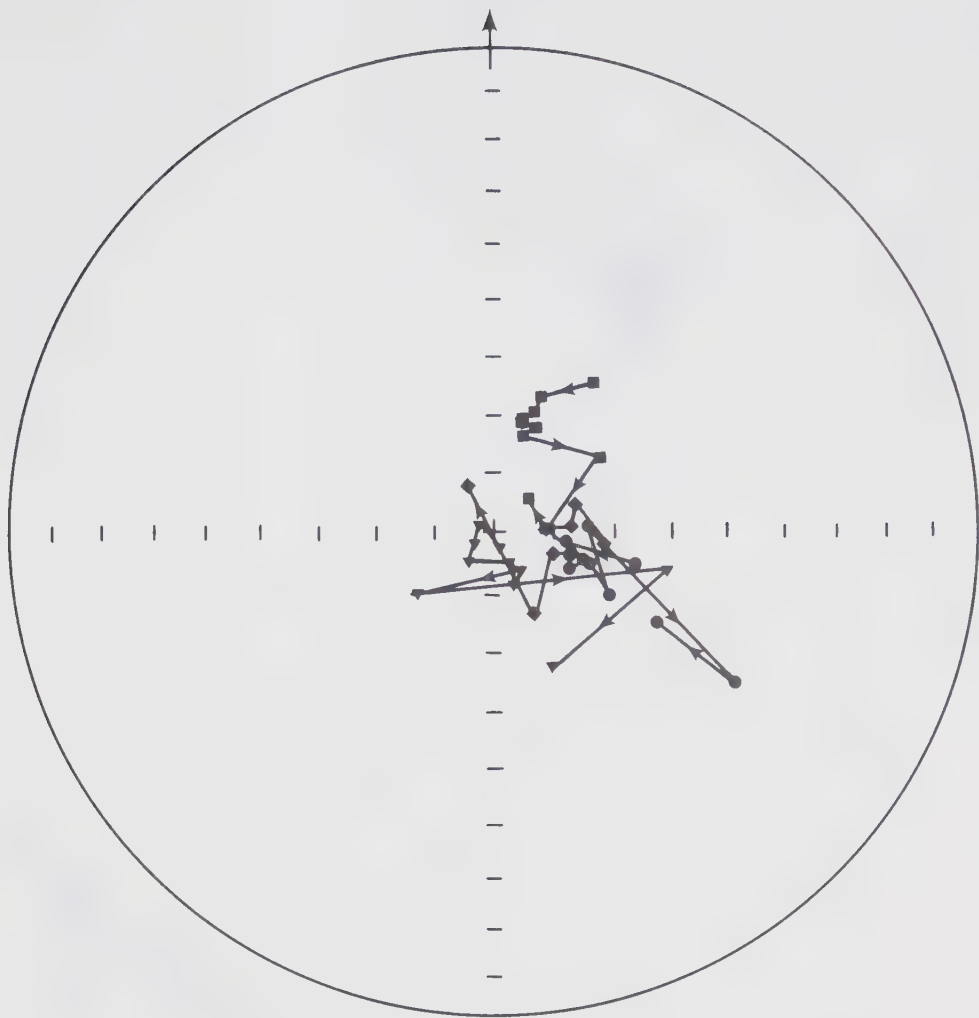
A.F. DEMAGNETIZATION OF SITE AA



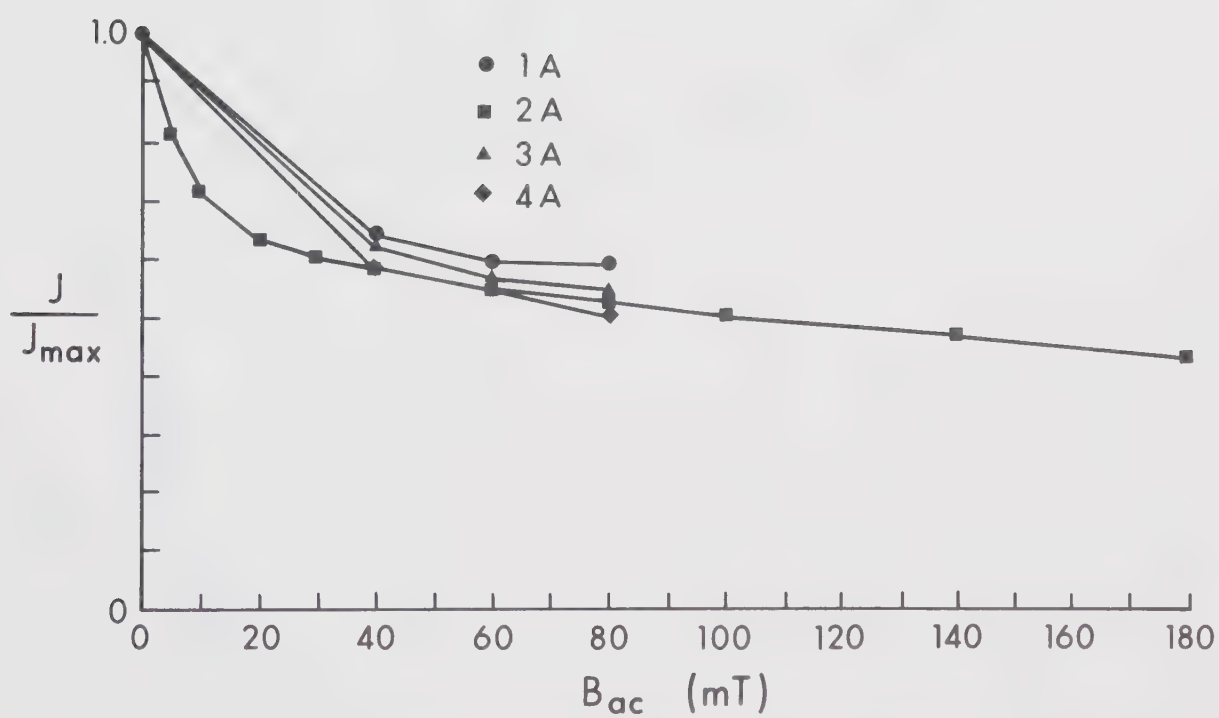
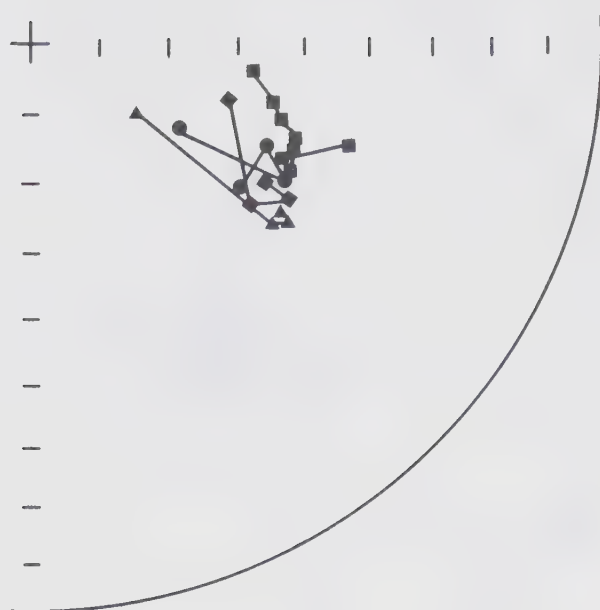
A.F. DEMAGNETIZATION OF SITE BL



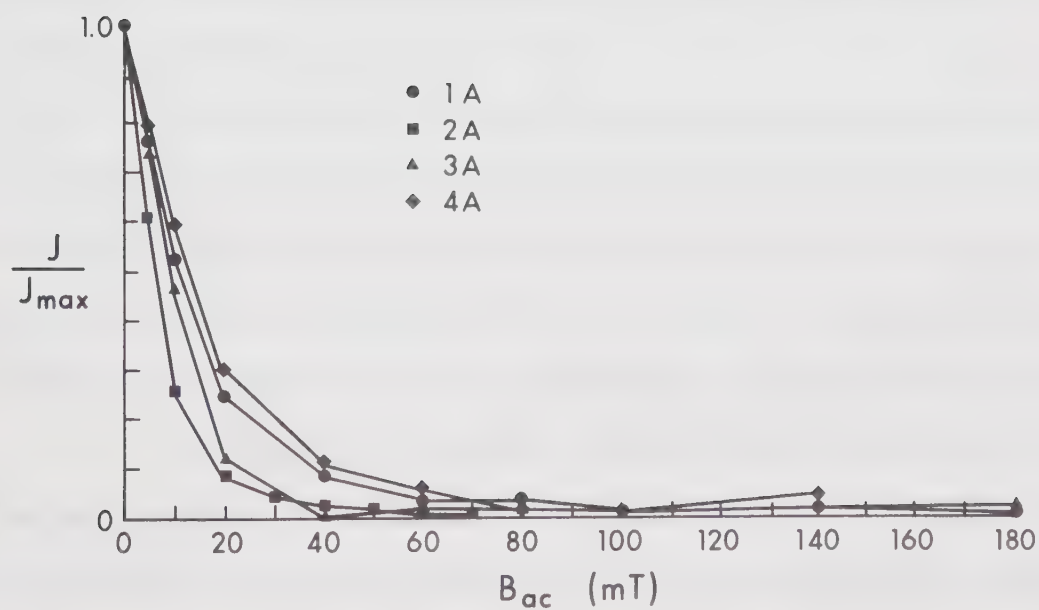
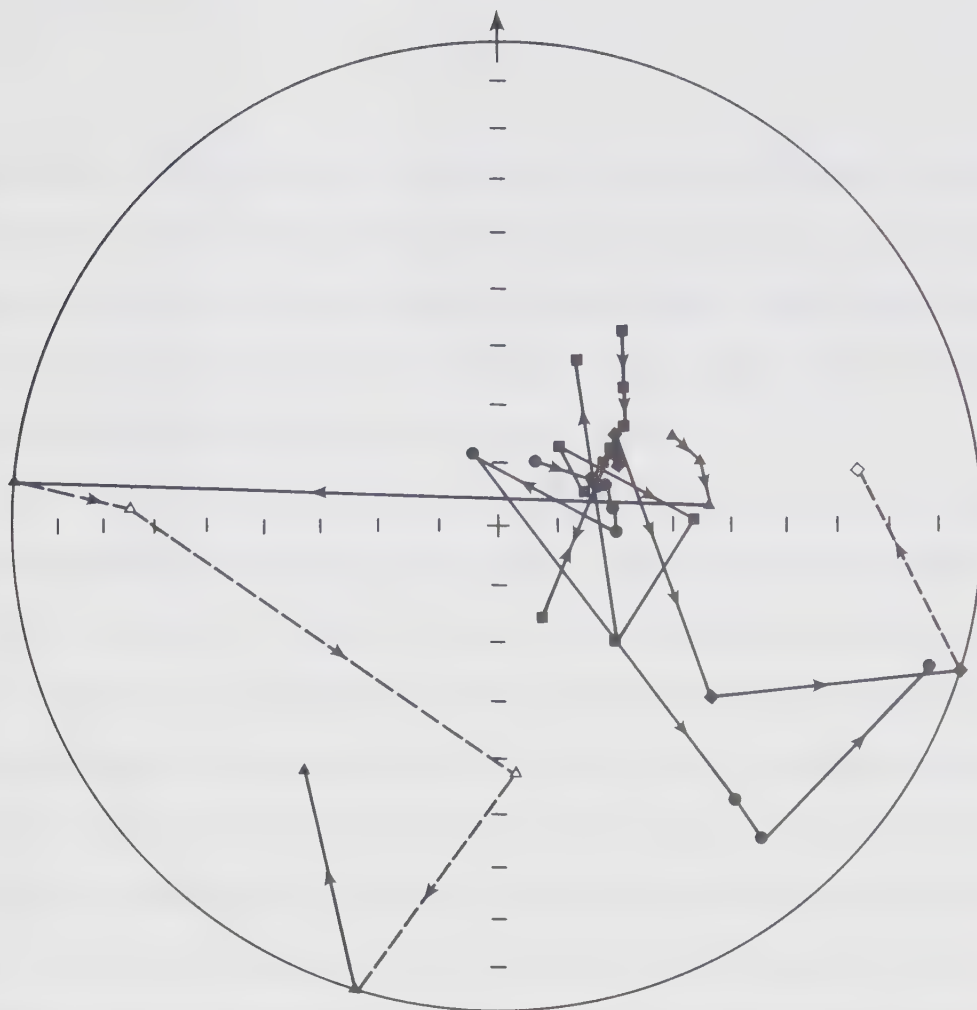
A.F. DEMAGNETIZATION OF SITE CG



A.F. DEMAGNETIZATION OF SITE DA



A.F. DEMAGNETIZATION OF SITE EA



A.F. DEMAGNETIZATION OF SITE FC

direction of the earth's field at the site within its 95% confidence limit (typically 5°), and remained so during demagnetization. Since samples from this site were more heavily weathered than any others collected, it is thought that the magnetization is a recent CRM.

Sites from section B showed considerable response to demagnetization (Fig. 4.3.2b). Intensities dropped to 5-40% of their NRM value in 40 mT and large direction changes were observed. Specimens from the example site BL (Fig. 4.3.2b) show an improved grouping after the first demagnetizing step and then move off in different directions in apparently systematic fashion. The 130° movement shown by specimen BL3A suggests the existence of a reversed component. Such movement is shown by specimens from a number of sites (e.g. BK). In general, demagnetization results in an improvement of within-site precision.

Sites from section C also showed considerable response to demagnetization. Intensities dropped to 40-50% of their NRM value after treatment in 40 mT, and directions generally showed improved grouping (Fig. 4.3.2c). Demagnetization often removed a component in the direction of the present field.

Site DA (the baked contact) has an anomalously soft magnetization (Fig. 4.3.2d). This may be the result of alteration by baking, although such baking often imparts a

very hard TRM (Everitt and Clegg, 1962). Although the intensities drop to only 10% of the NRM values, the direction appears to be fairly stable. The alteration is apparent in sites DA and DB, but DC and DD are sufficiently far away (50 and 100 m) to be unaffected by reheating by an intrusion with observed width of less than 50 m (Carslaw & Jaeger, 1959).

Section E (Fig. 4.2d) is a particularly uniform subsection within the C section. The uniformity is apparent in the tight grouping and close similarity of the demagnetization curves (Fig. 4.3.2e).

Section F within the Seton Formation (Fig. 4.2d) contains both spilitized basalt (FB, FC, FE) and red sediment (FA, FD). The basalt magnetization is very soft. Specimens from site FC (Fig. 4.3.2f) drop to less than 5% of the NRM intensity in fields of 80 mT. No stable end points are reached, and the direction shows large changes at the higher demagnetizing fields, presumably due to the acquisition of an ARM from the demagnetization equipment.

All the above results were subjected to statistical analysis to obtain site mean directions and precision estimates at each demagnetization step. The results giving maximum precision at each site were taken to represent the best cleaned direction unless all the specimen directions moved coherently after attainment of maximum precision. In these

cases and end point was chosen where successive demagnetizations produced no further coherent change. In all cases the precision at the end point was not significantly different at 95% confidence from the maximum value (McElhinny, 1964). Such chosen end points are identified in Table 4.3.2a by a 1. in the remarks column. The table summarizes the results of the A.F. demagnetization experiment, giving the cleaned site mean directions with their associated circle of 95% confidence and precision parameter k . The column headed k/k_0 gives the ratio of the precision parameter after cleaning to its value before demagnetization. Although an improvement in precision is not always shown, the change in site mean direction during demagnetization as a result of removal of a present field component supports the view that the cleaned direction is a better approximation to the original magnetization direction. Statistically significant values of k/k_0 at the 95% confidence level are underlined. The directions have been rotated to correct for the dip of the strata. This means that it has been assumed that the rocks were magnetized before they were tilted. The correction takes no account of possible plunging folds, but for dips of $15^\circ - 20^\circ$ no significant error is introduced by ignoring plunge.

The site mean directions after A.F. demagnetization and geological dip correction are shown in Fig. 4.3.2g grouped

Table 4.3.2a A.F. Demagnetization of Kahochella and Pethei Groups. Site level statistics.

<u>Site</u>	<u>N</u>	<u>mT</u>	<u>D</u>	<u>I</u>	<u>α_{95}</u>	<u>k</u>	<u>k/k_o</u>	<u>Remarks</u>
AA	4	100	175.4	61.3	19	24	.55	1
AB	4	140	139.7	62.9	5.5	284	2.0	
AC	4	20	19.5	72.6	5.1	320	1.95	11
AD	4	10	149.4	49.0	6.7	191	1.55	
AE	4	80	119.3	61.5	11	72	.62	
BA	3	140	276.4	15.0	21	34	3.9	3,6
BA	2	100	157.1	77.9	5.8	1808	<u>400</u>	3
BB	4	100	276.3	79.2	31	9.7	1.62	
BC	4	40	352.5	80.5	9.1	102	<u>12.3</u>	
BD	4	100	98.6	75.3	5.1	326	<u>10.3</u>	
BE	4	140	276.3	67.2	40	6.2	<u>4.4</u>	
BF	4	40	299.1	87.3	33	8.8	<u>5.9</u>	
BG	4	60	152.4	57.6	3.0	919	<u>17.5</u>	
BH	4	60	253.0	12.2	29	11	<u>6.1</u>	6
BI	3	40	138.2	59.2	12	114	.58	3
BJ	Samples move in different directions. (Watson, 1956)						Site random.	
BK	4	100	330.7	1.0	26	13	1.4	6
BL	3	5	140.8	72.1	7.6	265	<u>9.2</u>	9
BM	4	10	217.0	89.1	12	61	<u>6.1</u>	
BN	4	5	142.3	87.1	16	32	<u>4.6</u>	
CA	3	40	160.4	39.3	16	58	.28	7
CB	4	80	145.6	56.1	19	23	.81	1
CC	4	40	164.3	71.7	14	42	2.4	
CD	4	40	118.8	55.9	7.9	135	.48	
CE	4	5	129.2	52.9	8.9	109	1.7	
CF	4	80	148.9	48.8	3.7	634	<u>34</u>	

Table 4.3.2a A.F. Demagnetization of Kahochella and Pethei Groups. Site level statistics.

Continued

<u>Site</u>	<u>N</u>	<u>mT</u>	<u>D</u>	<u>I</u>	<u>α_{95}</u>	<u>k</u>	<u>k/k_o</u>	<u>Remarks</u>
CG	4	60	139.3	43.8	3.4	721	<u>53</u>	
CH	4	180	138.4	46.6	6.9	176	1.6	1
CI	4	40	143.2	58.9	9.9	87	<u>17</u>	
CJ	4	100	80.4	25.8	7.0	176	<u>104</u>	1,4
CK	3	80	125.9	39.1	8.7	202	3.8	2
CL	4	80	125.3	34.4	5.2	319	3.9	1
CM	4	60	135.4	41.7	9.1	103	<u>7.7</u>	
CN	4	40	149.6	69.6	11	65	.86	
CO	4	80	275.9	27.8	13	48	<u>6.1</u>	1,6
CP	4	80	145.5	54.2	5.6	272	<u>7.8</u>	1
CQ	4	80	124.2	49.3	27	13	2.1	1,3
CR	4	60	128.2	53.7	5.0	345	<u>34</u>	1
CS	4	80	136.2	58.5	17	31	2.9	1
CT	4	80	136.7	51.4	12	62	2.6	1
CU	4	60	317.0	-17.3	20	21	3.6	5
CV	4	40	128.0	55.9	4.4	438	<u>34</u>	
CW	4	180	119.4	40.1	10	85	2.2	1
CX	4	60	147.7	73.6	10	78	3.0	
CY	4	40	154.9	69.3	8	132	1.6	
CZ	4	5	8.7	69.8	13	48	1.6	11,12
DA	5	40	82.4	80.9	11	49	3.0	8
DB	3	10	21.1	79.2	10	167	<u>13.5</u>	8,2
DC	4	60	123.0	76.0	9.0	106	<u>6.2</u>	1,10
DD	4	60	163.0	68.7	6.2	221	<u>13.3</u>	10
EA	4	80	121.0	49.7	5.0	336	3.4	
EB	4	80	136.2	52.6	3.4	743	<u>6.1</u>	1

Table 4.3.2a A.F. Demagnetization of Kahochella and Pethei Groups. Site level statistics.

Continued

<u>Site</u>	<u>N</u>	<u>mT</u>	<u>D</u>	<u>I</u>	<u>α_{95}</u>	<u>k</u>	<u>k/k_o</u>	<u>Remarks</u>
EC	4	100	129.2	50.6	5.4	295	2.1	1
ED	4	80	142.9	60.0	15	38	1.6	
EE	4	40	137.0	51.9	4.2	473	<u>316</u>	
FA	4	60	24.0	50.2	13	53	3.6	1
FB	4	5	348.2	50.2	4.3	454	<u>22.4</u>	
FC	4	10	70.3	64.5	11	70	2.0	
FD	4	40	122.0	67.1	6.7	190	<u>4.8</u>	1
FE	4	20	169.0	44.2	3.8	582	<u>16.8</u>	1

N is the number of specimen directions included in the statistical analysis.

mT is the peak demagnetizing field used, quoted in milliTesla.

D is the azimuth of the site mean direction, measured in degrees east of true north.

I is the inclination of the site mean direction, measured in degrees below the palaeohorizontal.

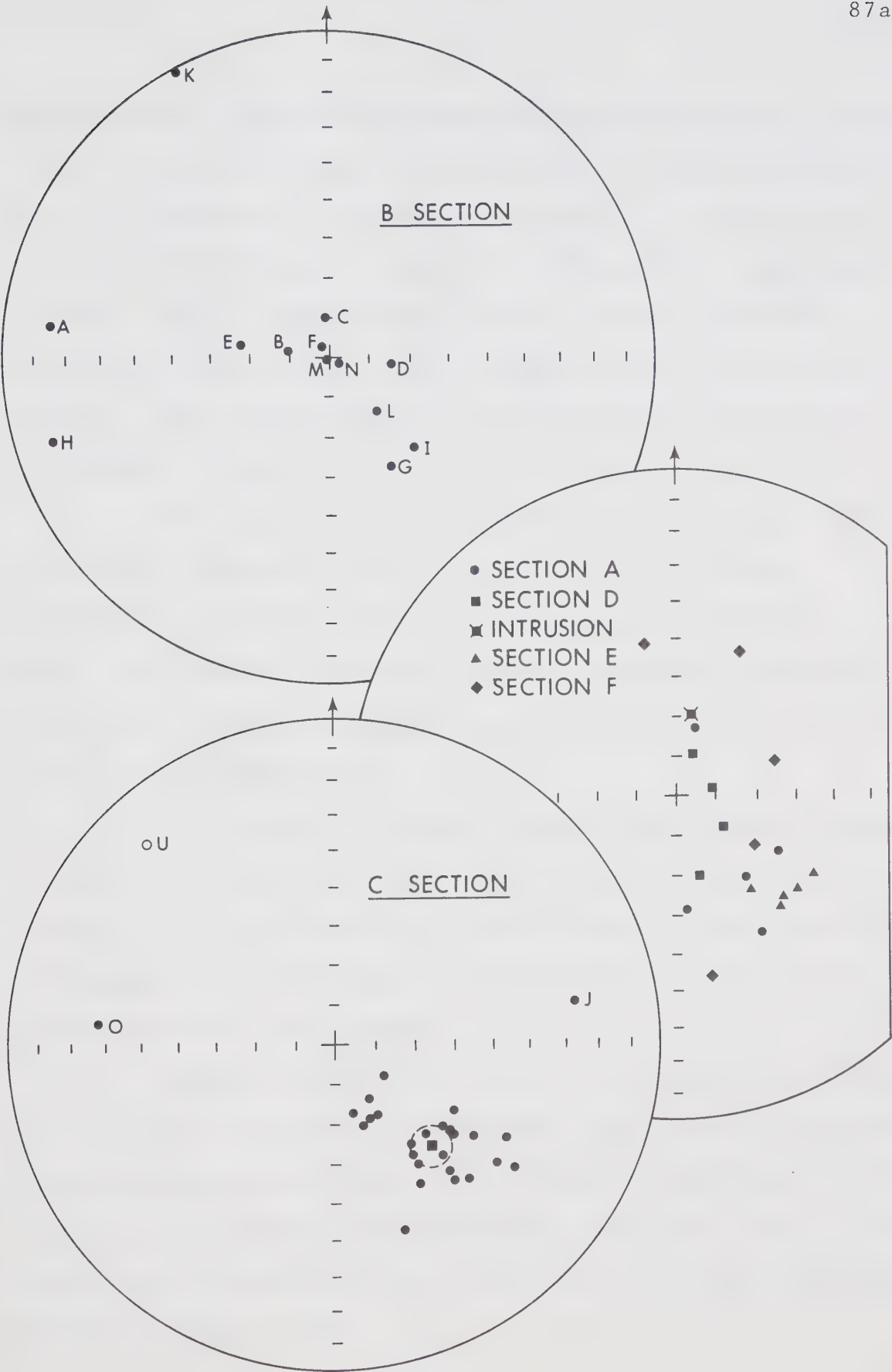
α_{95} and k are statistical parameters described in Chapter 1.

k/k_o is the ratio between the values of k before and after demagnetization. Statistically significant changes in k at 95% confidence are underlined.

Remarks

1. End points chosen beyond maximum k treatment.
2. Only N specimens available.
3. Site stratigraphically split.
4. Probable systematic deviation.
5. Probable reversal.
6. Possible reversal.
7. 4th sample a breccia.
8. Baked contact.
9. One specimen reverses.
10. Grouped with C section.
11. Present field before dip correction.
12. Intrusion

Figure 4.3.2g Site mean directions from the Kahochella
Group after A.F. demagnetization.



by sections. It will be observed that the site mean directions for the A, C and E sections group in the SE quadrant, with the exception of sites CJ, CO and CU. It is thought that CJ may represent a systematic deviation of the field (Lawley, 1970), while CO and CU may represent reversed directions from which a normal component has not been entirely removed. The interpretation of these results is further discussed in Chapter 5.

The results for the B section are somewhat more scattered, although they do group about a very steep southeasterly direction with three site means some way away. Once again, these may represent reversed directions from which a normal component has not been entirely removed by A.F. demagnetization.

The results for the D section seem to show a smear towards the present field direction, which is close to the direction of magnetization of the intrusion. The F section site means are scattered, and include the present field direction within their group.

Section mean directions have been calculated from the site mean directions. They have been combined by section because each section has a characteristic lithology, and the sections are somewhat separated from each other both in space and time of formation (Figs. 4.2d, e). The results are presented in Table 4.3.2b.

Table 4.3.2b A.F. Demagnetization of Kahochella and Pethei Groups. Section level statistics (dip corrected).

<u>Section</u>	<u>N</u>	<u>D</u>	<u>I</u>	<u>α_{95}</u>	<u>k</u>	<u>Remarks</u>
A	4	146.3	60.1	15.1	38	1
B	13	263.0	78.8	22.8	4.2	2
B	10	155.7	83.8	10.8	21	3
C	27	136.4	58.4	11.5	6.8	4
C	24	137.2	55.2	5.2	33	5
E	7	134.7	52.7	5.1	140	6
F	5	167.6	81.4	14.8	28	7
F	5	66.0	74.9	37.9	5.0	8

1. AC excluded, present field CRM.
2. All non-random sites (Watson, 1956).
3. Excluding BA, BH, BK.
4. All non-random sites including DC, DD excluding CZ (Intrusion).
5. Excluding CJ, CO, CU.
6. CE, CF at either end of E section included.
7. Before dip correction.
8. After dip correction.

The calculation of statistics for section F before and after dip correction constitutes a fold test (Graham, 1949). The change in k is significant at the 95% confidence level (McElhinny, 1964). We may conclude that section F was magnetized after folding, because the application of a dip correction significantly reduces the precision.

4.3.3 Thermal demagnetization

Although the results obtained by A.F. demagnetization gave apparently useful results, it was thought advisable to conduct some thermal demagnetization experiments because haematite, a common constituent of red sediments, generally has very high coercivity, and may not be adequately cleaned by A.F. treatment. Pilot studies revealed small but systematic differences between A.F. and thermally cleaned directions.

Pilot specimens were subjected to stepwise thermal demagnetization by heating to successively higher temperatures and cooling in zero field. The pilot studies were performed by the author using the apparatus described in Chapter 2 and by Dr. M. E. Evans using apparatus in the laboratories of the Earth Physics Branch, Department of Energy, Mines and Resources, Ottawa. The Ottawa apparatus was used by kind permission of Drs. E. Irving and J. L. Roy.

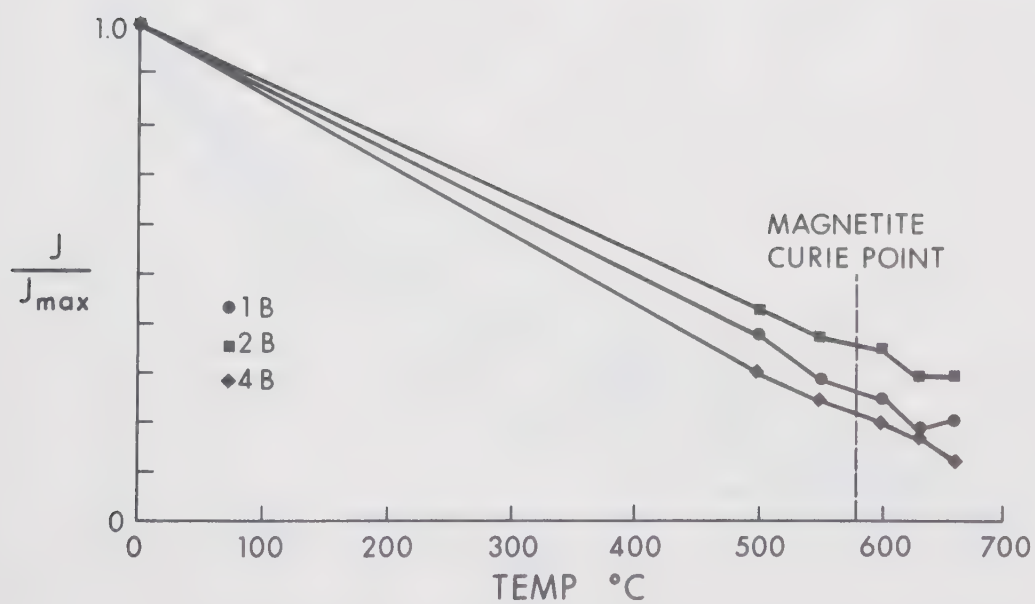
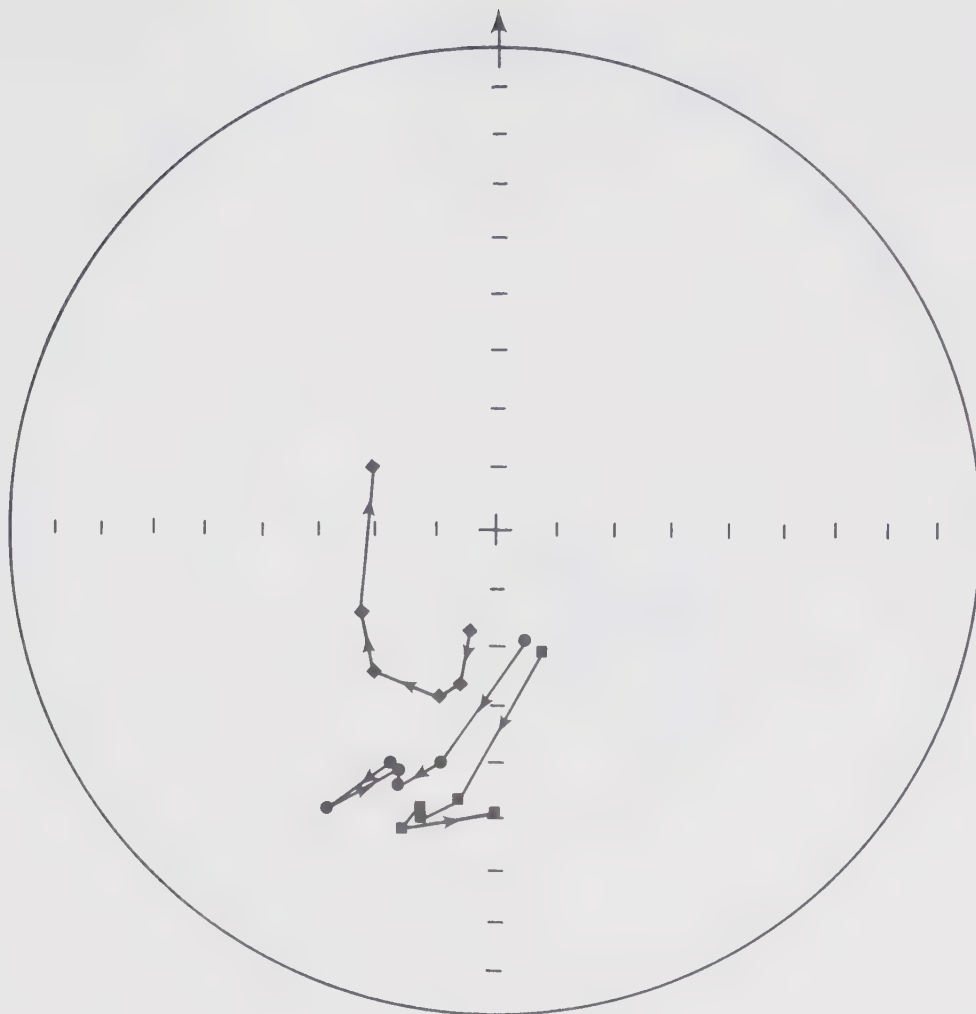
The pilot studies revealed that the specimens were subject to severe alteration if heating was prolonged. All further experiments were therefore performed using the apparatus at the University of Alberta because its temperature could be raised and lowered in about two hours, or more than four times as fast as possible with the apparatus in Ottawa.

The experiments showed blocking temperatures distributed from ambient up to the Curie point of haematite (Figs. 4.3.3b, c) and suggested that the directions of normally and reversely magnetized specimens might be more nearly opposed than had been demonstrated using A.F. demagnetization.

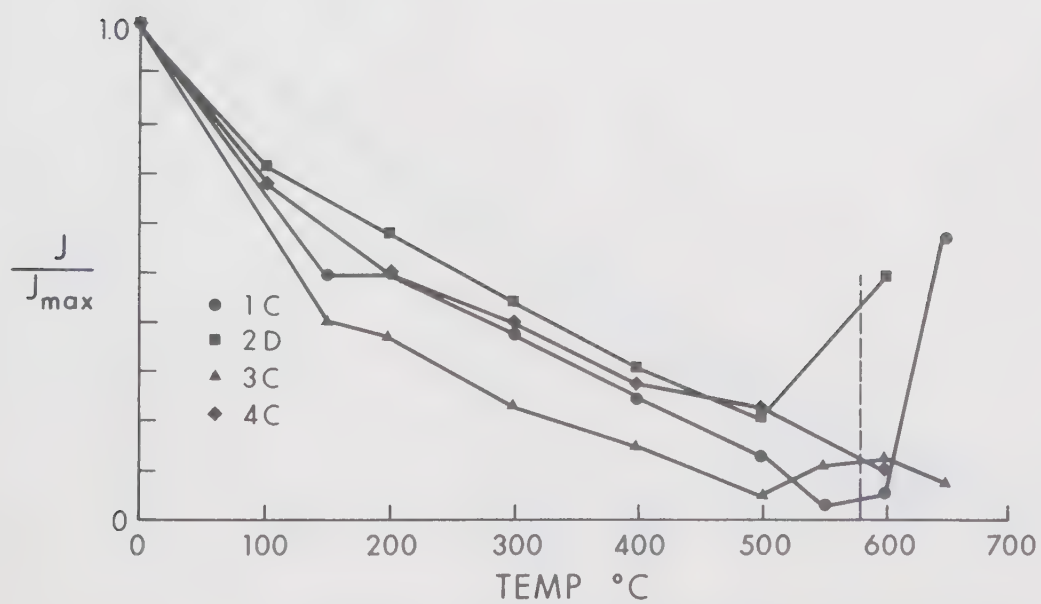
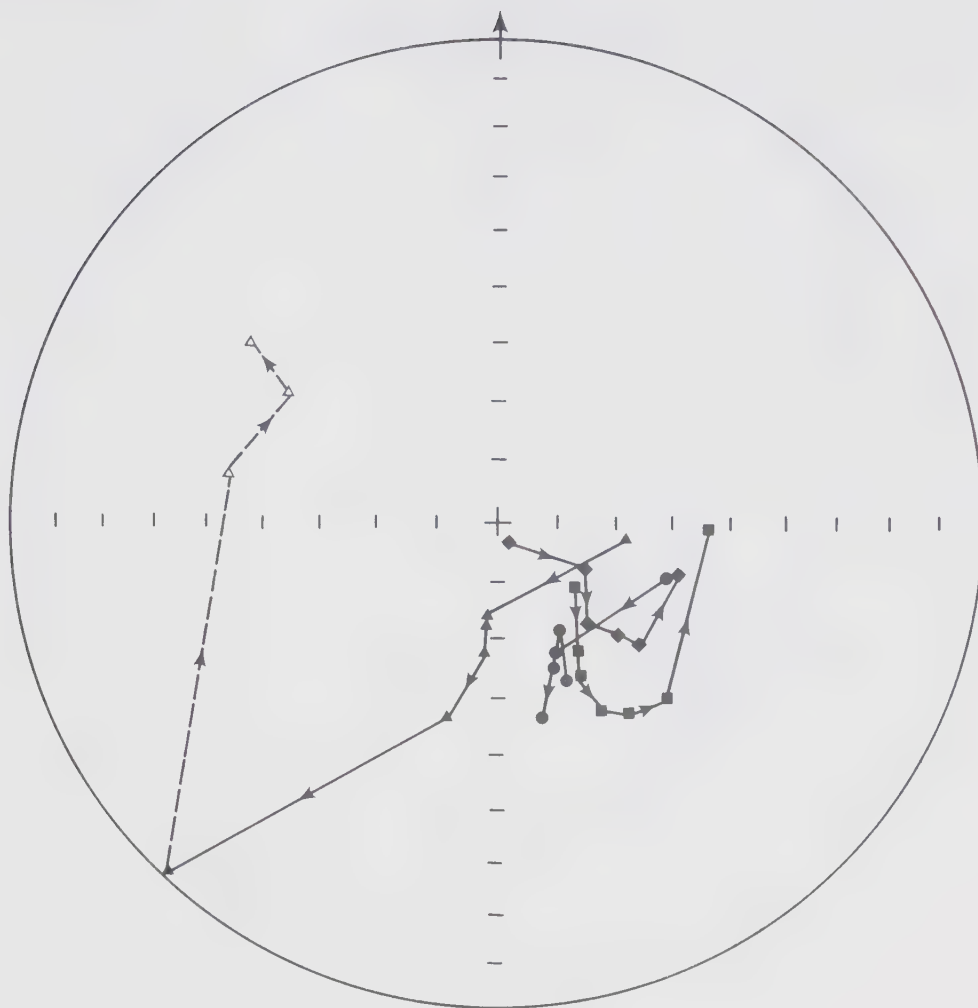
Thermal demagnetization of one specimen per sample from the whole collection (subject to availability of material) was therefore undertaken, using temperature steps of 500, 550, 600, 630 and 660°C to obtain two steps below the Curie point of pure magnetite and some detail above this temperature where haematite is the only mineral still likely to be ferromagnetic. Sample plots of direction and intensity changes are presented in Figs. 4.3.3a-f for the same sites as were displayed after thermal treatment. Full details may be found in Appendix 1.

Specimens from section A were more strongly affected by thermal demagnetization than they were by A.F. treatment (Fig. 4.3.3a). The intensities drop to 10-30% of their NRM

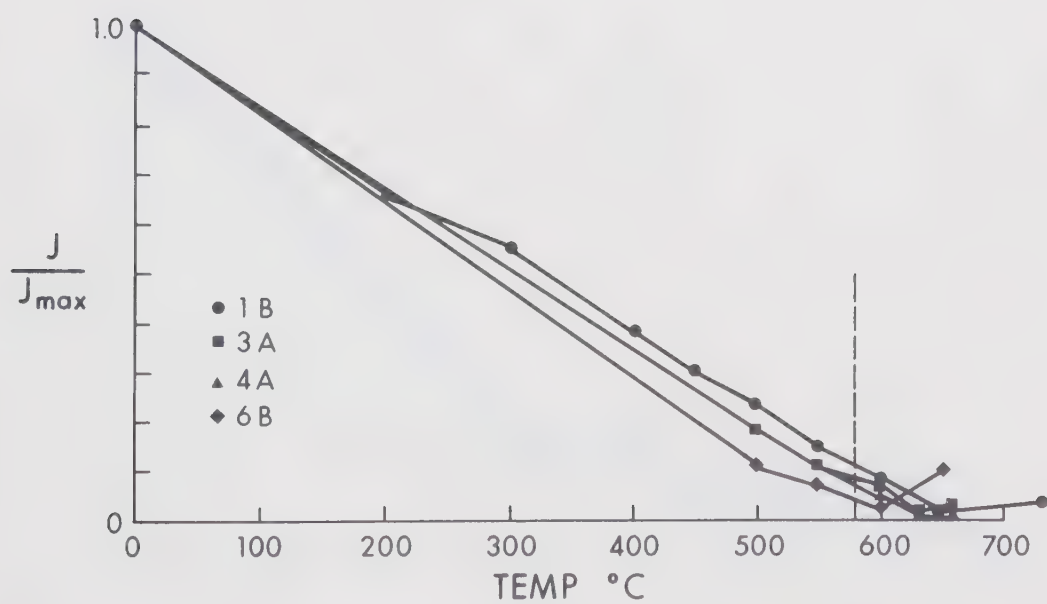
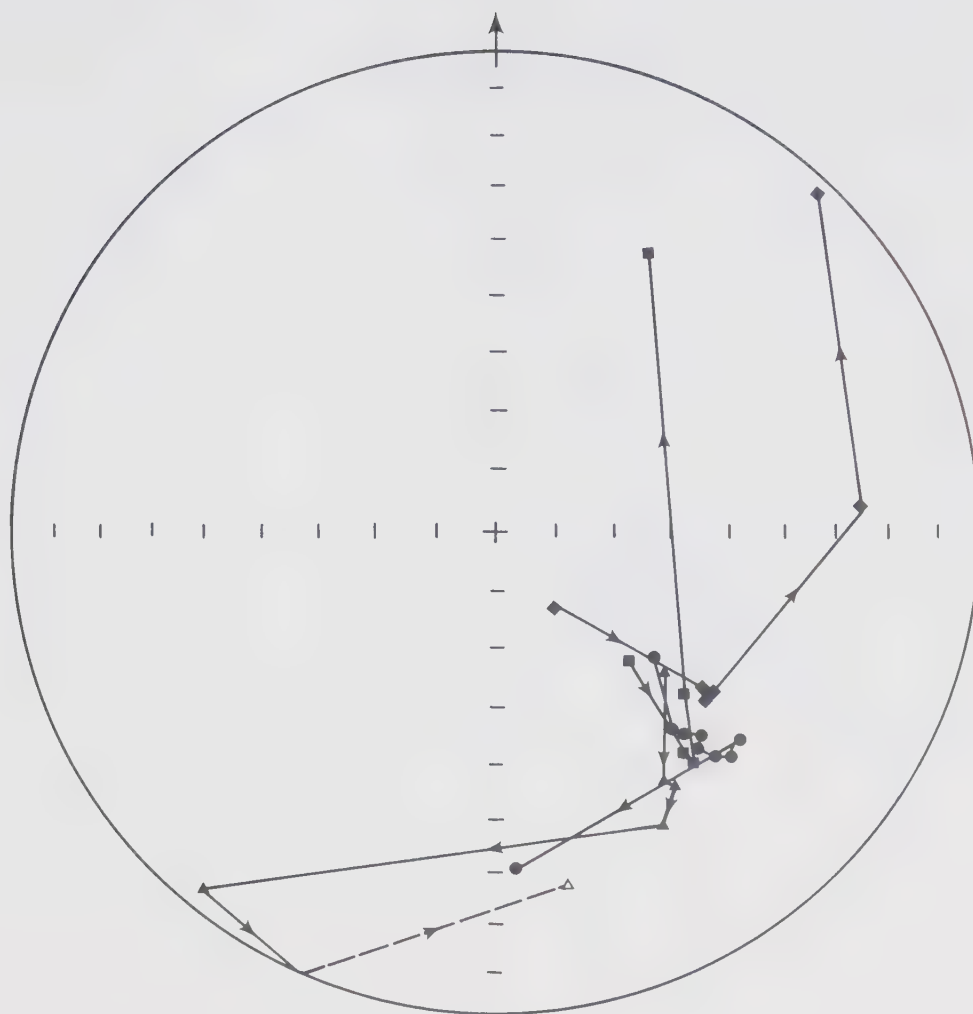
Figure 4.3.3a-f Thermal demagnetization of specimens from the Kahochella Group. The results from one site per section are shown. The direction plot employs a polar equal area projection with the north-seeking end of the magnetic vector plotted as an open symbol on the upper hemisphere or a closed symbol on the lower hemisphere. The directions are shown corrected for geologic dip.



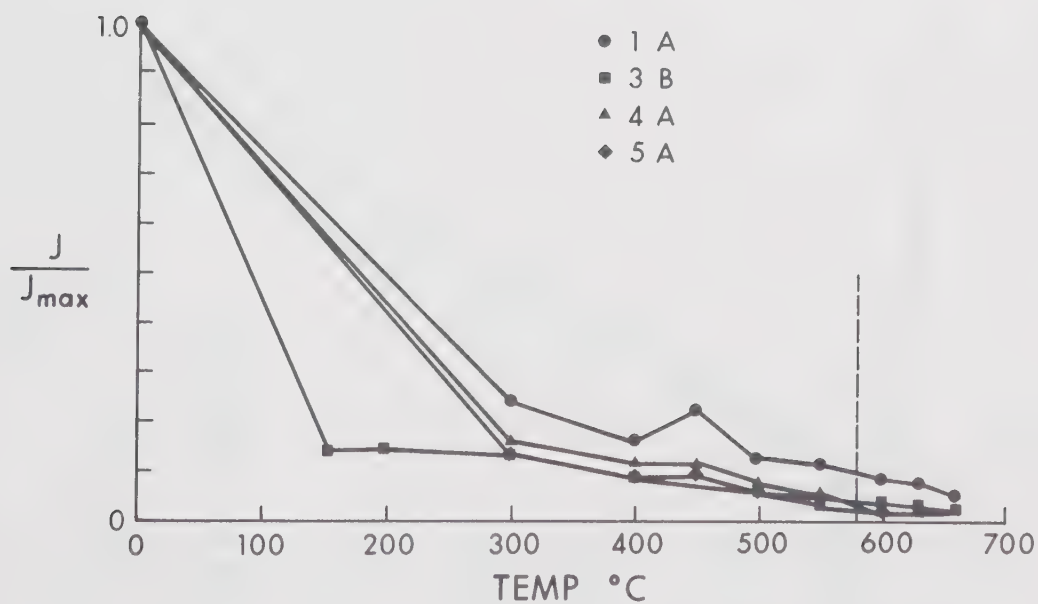
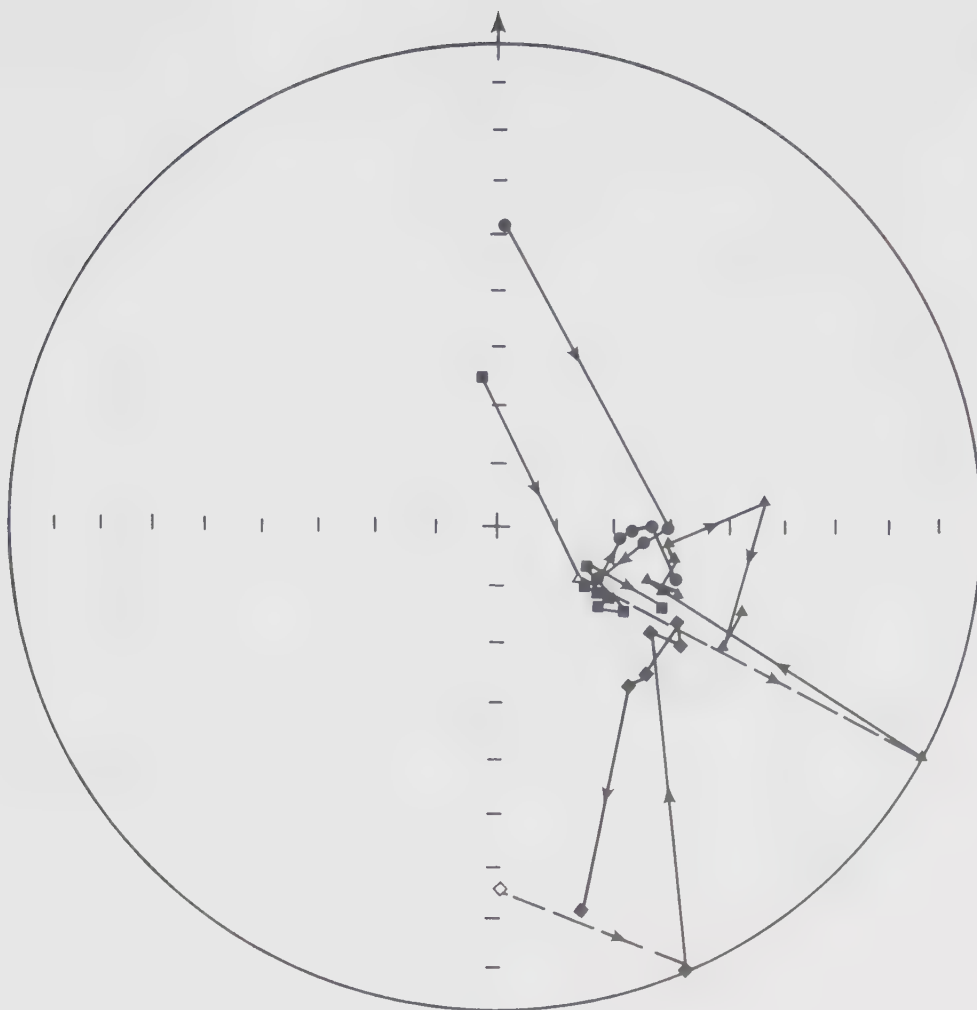
THERMAL DEMAGNETIZATION OF SITE AA



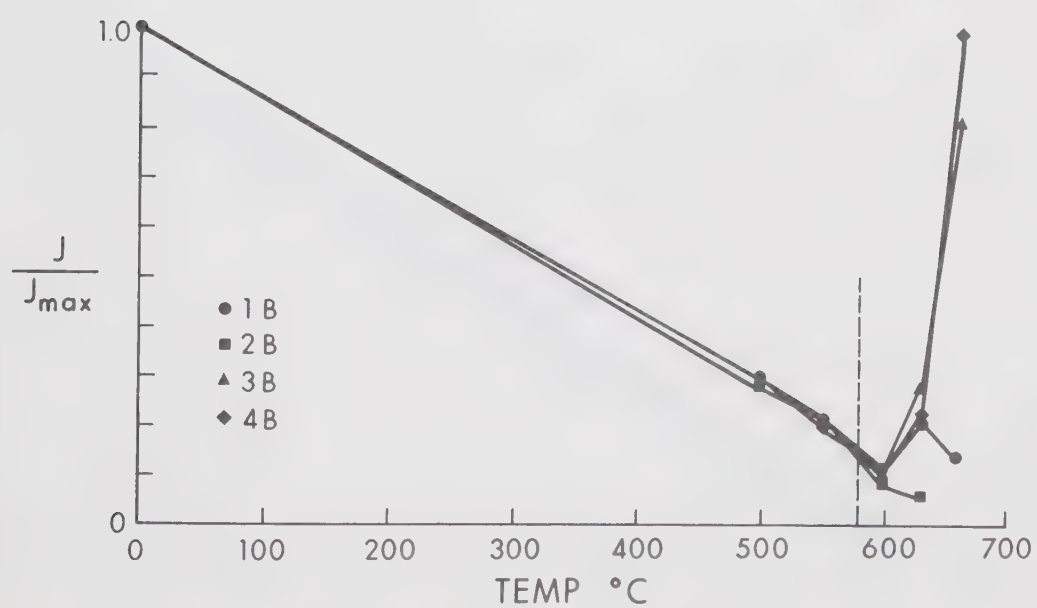
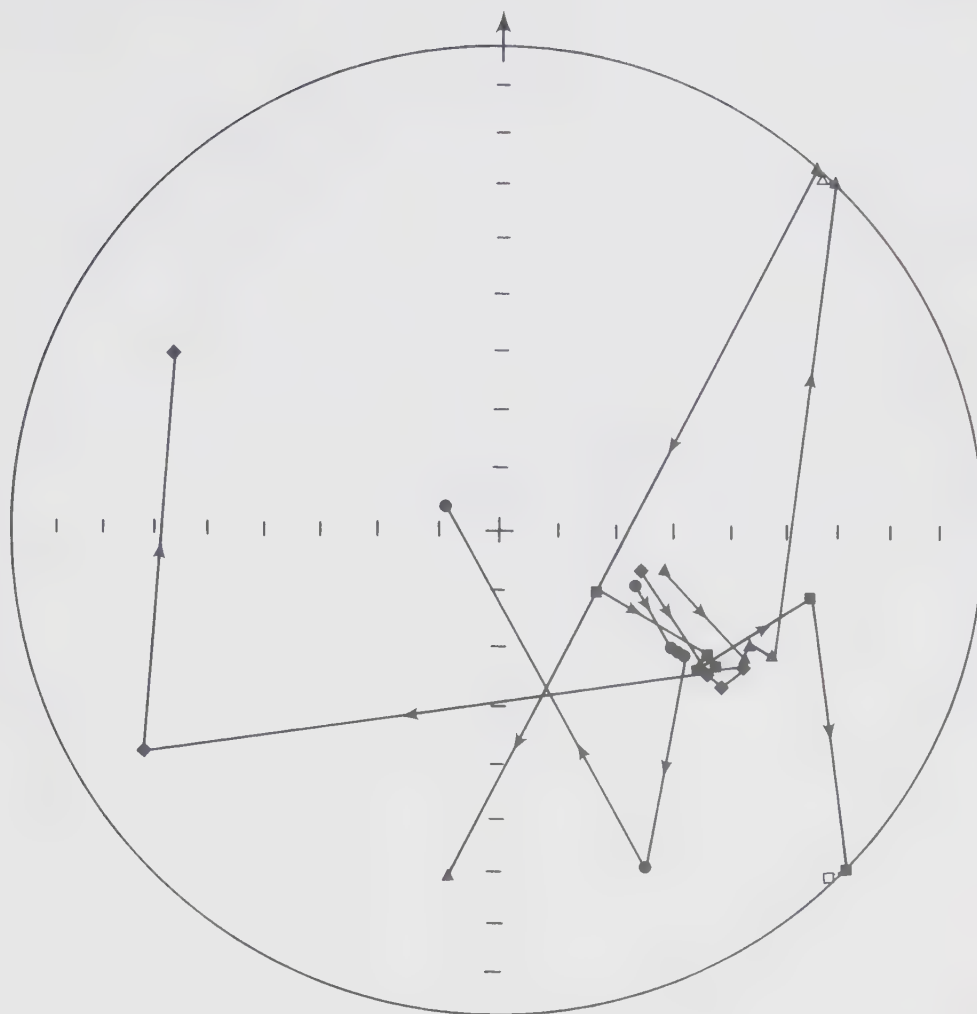
THERMAL DEMAGNETIZATION OF SITE BL



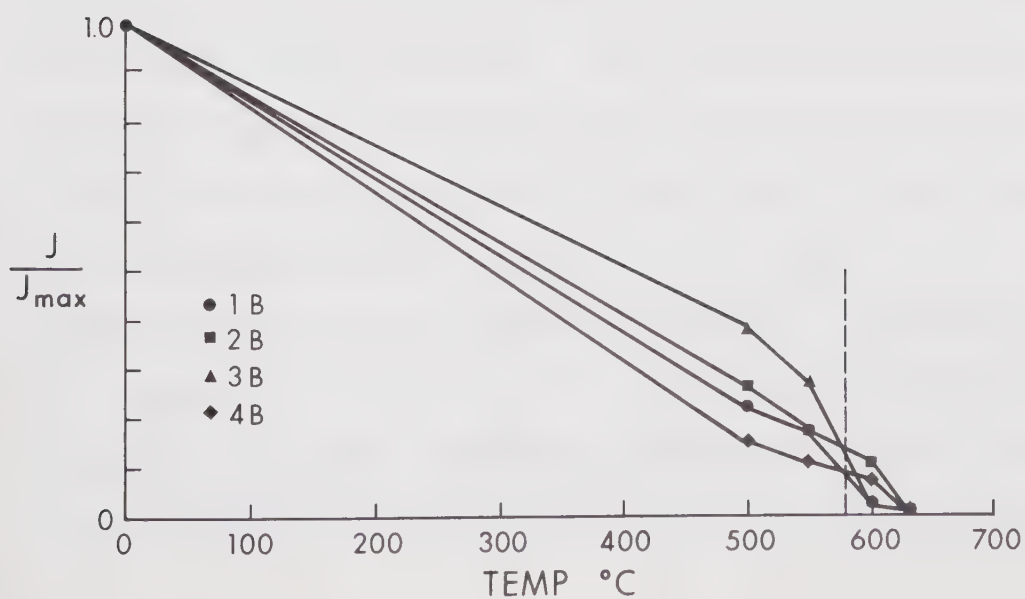
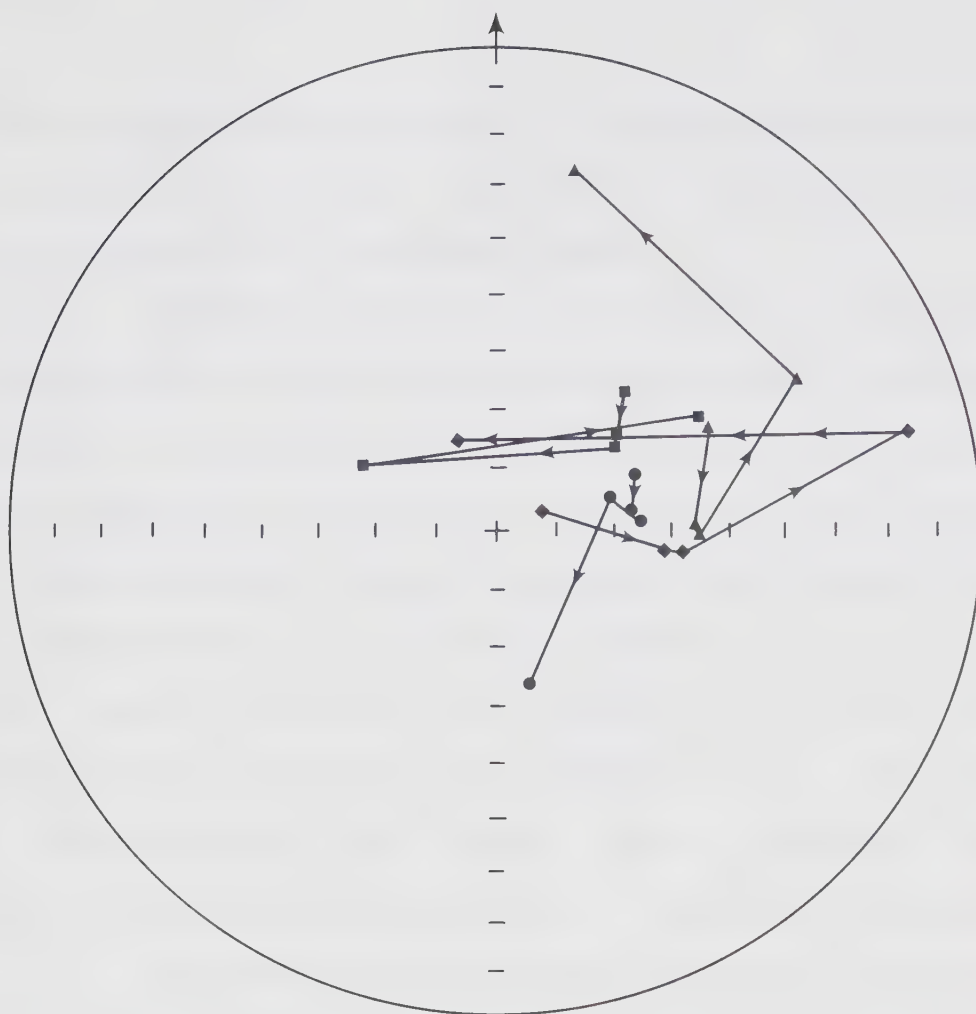
THERMAL DEMAGNETIZATION OF SITE CG



THERMAL DEMAGNETIZATION OF SITE DA



THERMAL DEMAGNETIZATION OF SITE EA



THERMAL DEMAGNETIZATION OF SITE FC

values after heating to 600°C . The directions also show some systematic change. There is no evidence of a magnetite Curie point in the intensity curve.

Specimens from section B (Fig. 4.3.3b) were also strongly affected by thermal demagnetization, dropping to 10-20% of their NRM intensities after heating to 500°C . Three specimens from site BL (the example site) group well in the SE quadrant, while the sample which showed a tendency to reverse during A.F. treatment (BL3) moves to a direction almost exactly reversed with respect to the other three specimens from the site. Examination of the intensity curve for this specimen (Fig. 4.3.3b) shows a maximum at $550 - 600^{\circ}\text{C}$ characteristic of the removal of a reversed component.

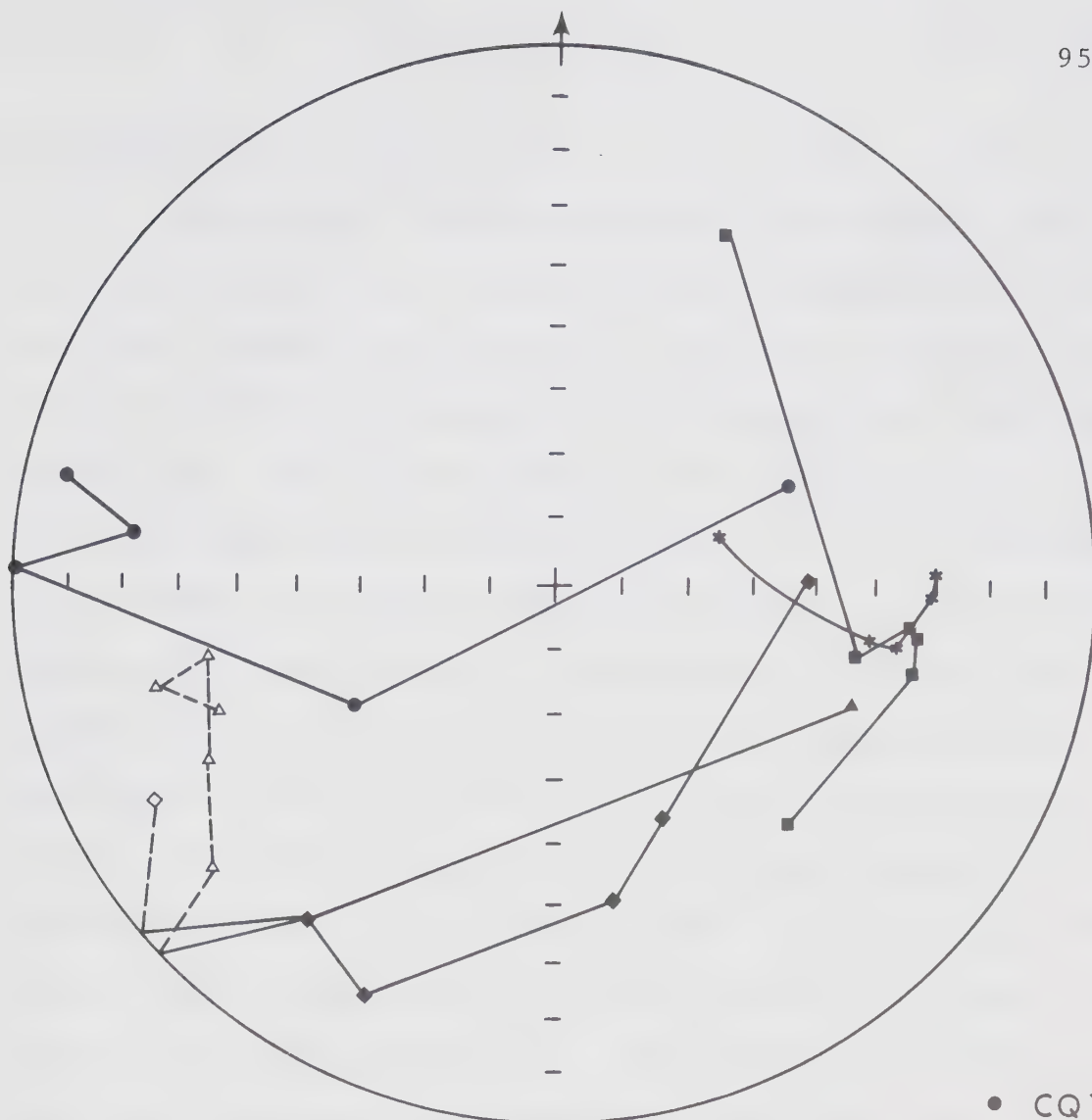
Under thermal treatment specimens from section C (Fig. 4.3.3c) showed a tendency to move to slightly shallower inclinations (i.e. away from the present field) than achieved with A.F. demagnetization. The three anomalous sites (CJ, CO, CU, Fig. 4.3.3h) also moved further away from the present field and reached apparently stable end points. One site (CU) became almost exactly reversed with respect to the main group. Sites CI and CN also showed evidence of a reversed component but did not reach satisfactory end points. Some specimens from site CQ moved towards a reversed direction, but this merely caused the site as a whole to appear random. It is

thought that the stratigraphically distributed nature of the sampling at this site may be responsible for this behaviour. Fig. 4.3.3g shows the stratigraphic relationship of the samples, and their changes in direction during thermal demagnetization. It may be seen that samples CQ1, 2, 5 and 6 all have approximately reversed magnetizations, while sample CQ3 has a normal magnetization. The stratigraphic sequence of the samples thus suggests a reversed period containing a short event of normal polarity.

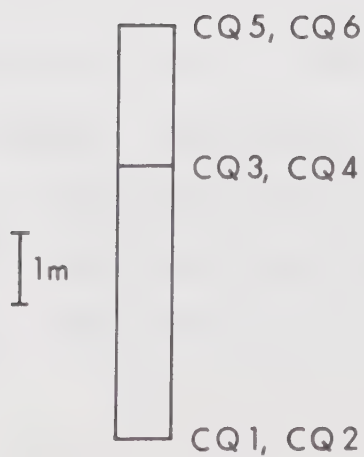
Site DA (Fig. 4.3.3d) appears to be very stable in direction after the initial heating to 150°C . This site is the baked contact of the intrusion CZ, but no stable direction was recovered from the single sample of intrusive material available for thermal treatment. The direction of magnetization in the baked contact is therefore the only evidence of the field direction at the time of intrusion. Sites DC and DD are included in the analysis of the C section data because they are a direct extension of the C section sampling (Fig. 4.2d).

Under thermal demagnetization section E shows extreme uniformity of magnetic properties (Fig. 4.3.3e) as was observed after A.F. demagnetization. The material appears to undergo severe alteration at temperatures above 600°C . This is shown by the steep rise in the intensity

Figure 4.3.3g Stratigraphic interpretation of the mixed polarities observed at site CQ. The stratigraphic relationship of the samples to each other is shown in the lower half of the diagram.



- CQ1B
- ▲ CQ2B
- ★ CQ3A
- CQ3B
- ◆ CQ5A



curve above this temperature.

Thermally cleaned directions were chosen in the same way as in the A.F. studies. The site mean directions with their statistical parameters are listed in Table 4.3.3a. Cleaned directions corresponding to treatment not yielding maximum k are again identified in the "notes" column. The site mean directions are plotted in Fig. 4.3.3h. Sections A, C, D and E once again show a grouping in the SE quadrant, although the grouping is not as good as it was after A.F. demagnetization. Section C now has five anomalous sites, rather than three. Sites CJ, CN, CO and CU are thought to represent reversed directions, while CJ again appears to be a systematic deviation. Section B shows some grouping about a very steep SE direction, but there are as many anomalous sites as there are in the group. Once again, it is thought that these anomalous directions represent field reversals. The problem is discussed further in Chapter 5.

Site mean directions have been grouped in sections for statistical analysis as was done for the results of A.F. treatment. The results are shown in Table 4.3.3b. A fold test has again been performed on section F, and again the reduction of precision resulting from a dip correction is significant at the 95% confidence level, indicating remagnetization after folding. The remagnetization direction

Figure 4.3.3h Site mean directions from the Kahochella Group after thermal demagnetization.

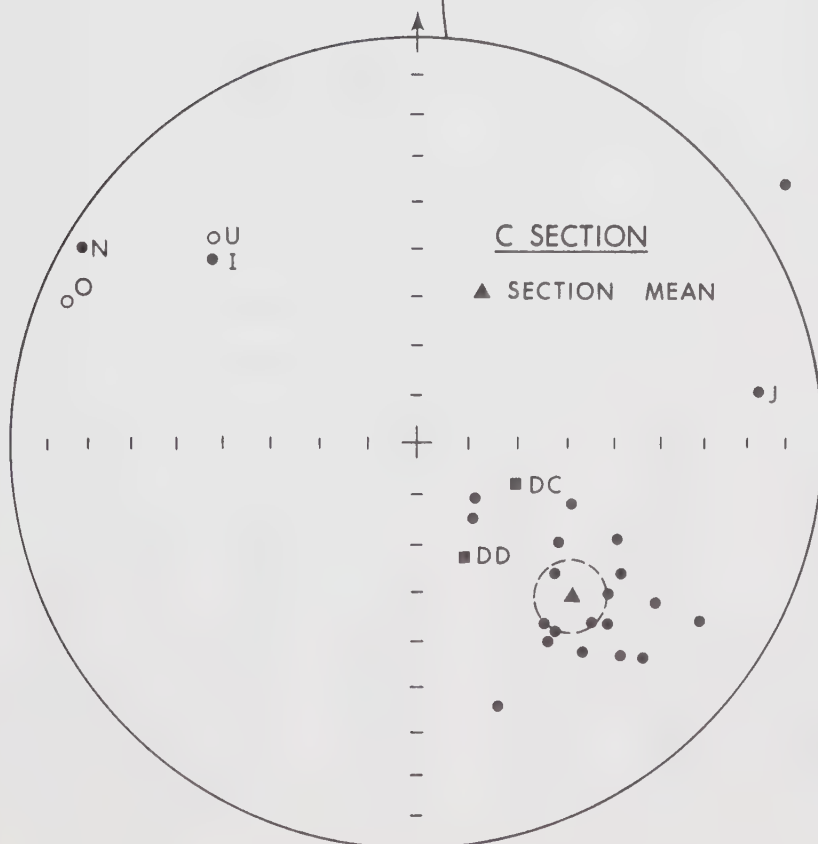
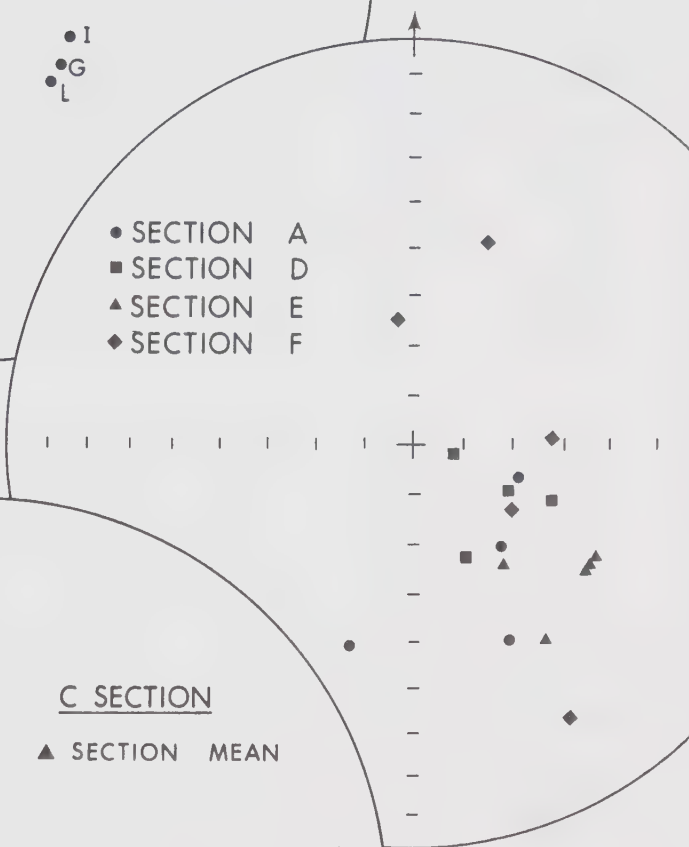
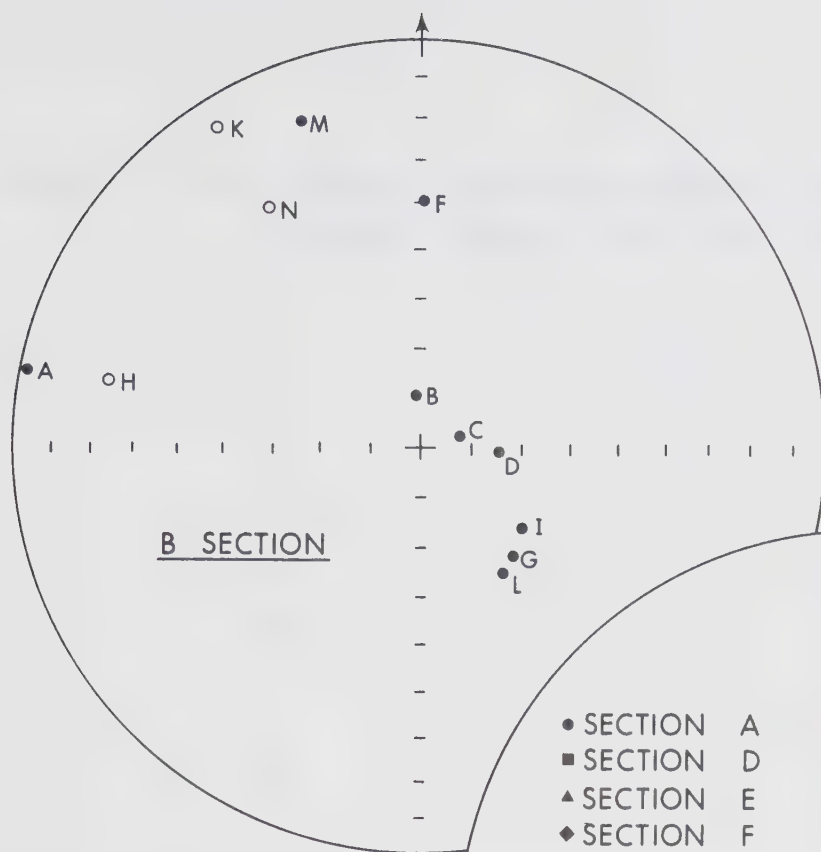


Table 4.3.3a Thermal demagnetization of Kahochella and
Pethei Groups. Site level statistics.

<u>Site</u>	<u>N</u>	<u>T^oC</u>	<u>D</u>	<u>I</u>	<u>α_{95}</u>	<u>k</u>	<u>k/k_o</u>	<u>Notes</u>
AA	3	550	198.6	47.3	18.2	47	.29	1,2
AB	4	500	139.3	63.3	17.3	29	.58	
AC	Random (Watson, 1956)							
AD	4	500	154.3	45.4	7.2	165	.82	
AE	4	500	108.8	67.9	39.1	6.5	<u>.07</u>	
BA	3	630	282.2	2.5	16.0	60	<u>9.5</u>	1,3
BB	4	500	352.9	80.3	41.0	6.0	<u>.12</u>	
BC	4	500	72.7	82.1	16.7	31	.92	
BD	4	500	92.5	74.4	9.7	91	1.4	
BE	Random							
BF	3	550	0.6	39.6	32.0	16	.23	2
BG	4	550	141.0	61.7	2.8	1097	<u>52</u>	
BH	4	630	283.4	-21.6	18.3	26	3.5	
BI	3	500	129.0	64.5	12.5	98	3.0	3
BJ	Random							
BK	4	600	327.7	- 7.6	15.3	37	<u>28</u>	
BL	3	300	146.9	59.9	11.5	117	5.2	1,9
BM	4	600	340.4	16.4	21.9	19	<u>5.0</u>	1
BN	4	660	327.8	-31.1	15.8	35	<u>22</u>	1
CA	3	550	163.5	33.5	8.3	223	3.8	7
CB	4	600	145.7	45.1	27.8	12	.5	1
CC	4	500	126.0	55.3	16.4	32	.81	
CD	4	550	112.4	56.1	16.6	32	<u>.13</u>	1
CE	3	500	142.0	35.4	8.2	222	3.2	2
CF	5	600	147.9	41.5	5.7	181	1.6	1
CG	4	550	135.9	39.0	8.3	122	1.9	1
CH	4	547	134.2	35.6	7.4	153	1.5	

Table 4.3.3a Thermal demagnetization of Kahochella and
Pethei Groups. Site level statistics.

Continued

<u>Site</u>	<u>N</u>	<u>T^oC</u>	<u>D</u>	<u>I</u>	<u>α_{95}</u>	<u>k</u>	<u>k/k_o</u>	<u>Notes</u>
CI	3	630	311.3	32.1	21.7	33	.46	2,6
CJ	4	660	82.5	17.4	5.3	305	3.0	1,4
CK	3	650	123.8	29.9	10.3	144	2.7	2
CL	4	625	123.0	19.2	3.8	579	<u>12.3</u>	1
CM	4	600	134.2	25.0	9.6	93	3.9	1
CN	4	660	300.5	4.2	12.5	55	2.3	6
CO	4	600	291.7	- 7.1	9.8	89	4.1	6
CP	4	630	145.4	41.8	12.7	53	5.2	1
CQ	Random							3
CR	4	550	115.7	45.0	14.9	39	4.1	1
CS	4	500	134.0	51.6	20.8	20	.89	
CT	4	550	137.1	29.0	9.7	92	<u>9.2</u>	1
CU	4	600	314.7	-29.1	11.9	60	<u>5.0</u>	5
CV	3	660	129.3	39.8	9.4	172	1.8	2
CW	5	500	123.0	40.5	7.1	117	<u>9.2</u>	1
CX	4	550	147.4	70.7	6.7	186	<u>9.7</u>	
CY	4	500	132.5	73.6	4.9	357	1.1	
CZ	No material available							
DA	4	400	110.9	60.2	8.8	110	<u>6.3</u>	8
DB	5	300	104.7	81.9	7.6	103	<u>41</u>	8
DC	5	500	113.2	69.5	4.9	243	<u>36</u>	1,10
DD	4	500	156.6	65.4	7.0	174	<u>16.3</u>	10
EA	4	550	121.9	46.9	5.6	273	2.2	
EB	4	550	123.8	47.3	3.9	546	<u>15.5</u>	1
EC	4	550	126.5	46.8	3.3	789	3.0	
ED	4	550	143.6	60.5	13.4	48	<u>7.0</u>	

Table 4.3.3a Thermal demagnetization of Kahochella and
Pethei Groups. Site level statistics.

Continued

<u>Site</u>	<u>N</u>	<u>T°C</u>	<u>D</u>	<u>I</u>	<u>α_{95}</u>	<u>k</u>	<u>k/k_o</u>	<u>Notes</u>
EE	4	600	145.6	41.7	9.1	103	4.1	
FA	4	500	20.5	46.4	19.2	24	<u>10.8</u>	
FB	2	550	351.3	64.0	25.1	101	3.0	2
FC	4	550	84.8	62.5	10.8	74	1.05	
FD	4	550	123.2	66.7	7.7	142	<u>6.7</u>	1
FE	4	550	149.9	23.0	7.2	162	2.4	

Notes

1. End point chosen beyond maximum k treatment.
2. Only N specimens available.
3. Site stratigraphically split.
4. Probable systematic deviation. Good end point.
5. Probable reversal.
6. Possible reversal. End point not reached?
7. 4th sample a breccia.
8. Baked contact.
9. One sample reverses.
10. Grouped with C section.

Statistically significant values of k/k_o underlined
(McElhinny, 1964).

N is the number of specimen directions included in the
site analysis.

D and I are the azimuth (and dip) of the magnetization,
measured in degrees east of true north (below the
horizontal).

k and α_{95} are statistical parameters discussed in Chapter 1.

Table 4.3.3b Thermal demagnetization of Kahochella and
Pethei Groups. Section level statistics
(dip corrected).

<u>Section</u>	<u>N</u>	<u>D</u>	<u>I</u>	<u>α_{95}</u>	<u>k</u>	<u>Remarks</u>
A	4	157.0	60.0	26.3	13.2	1
B	6	123.9	74.5	13.7	25	2
C	21	134.5	45.5	7.2	21	3
E	7	136.1	46.2	8.2	54	4
F	5	85.7	69.4	41.5	4.3	5
F	5	150.8	73.8	14.2	30.2	6

Remarks

1. Site AC random, therefore not included.
2. Sites BB, BC, BD, BG, BI, BL.
3. Excluding CI, CJ, CN, CO, CQ, CU. Including DC, DD.
4. CE, CF included.
5. After dip correction.
6. Before dip correction.

($D = 150.8$, $I = 73.8$) is consistent with a post-folding component of magnetization observed in all sections except A (see Chapter 5).

A number of statistical tests have been performed on the results from section C, excluding the five anomalous sites. The directions have been tested for conformity to a Fisher Distribution (Watson & Irving, 1957). The azimuthal uniformity about the mean was tested by division of the data into four sectors, the expectation population of each sector being 5.25 (21 vectors total). The difference between expectation and the actual counts of 5, 7, 3 and 6 in the four classes enabled the calculation of a χ^2 value of 1.66. The significance point for χ^2 with 1 degree of freedom at $P = 0.05$ is 3.8, so that there is no reason to believe that the azimuthal distribution is not uniform. The density reduction with distance from the mean was tested by dividing the sphere into five zones with equal expectation populations of 4.2. The actual populations (moving away from the mean) were 4, 6, 2, 3 and 6 giving a χ^2 value of 3.0. This is also below the significance point at $P = 0.05$ for one degree of freedom, so that there is no reason to believe that the data for the C section do not conform to a Fisher distribution in this respect also.

A fold test has also been performed on section C data, but the change in k (from 25 to 21) caused by dip correction is not significant at 95% confidence (McElhinny, 1964). The test cannot therefore be applied to determine the age of magnetization.

4.4 Discussion

The results of alternating field and thermal demagnetization are in qualitative agreement (Figs. 4.3.2g, 4.3.3h). In both cases a main group of directions southeast and down has emerged. There are, however, eleven "anomalous" sites in the B and C sections, which require consideration.

The effect of thermal treatment has been to improve the separation of antiparallel components. This must involve the removal of secondary magnetizations. The removal of a post-folding remanence is demonstrated in the next chapter. It is therefore concluded that the thermally cleaned site mean directions more nearly represent a stable magnetization. Possible origins for these magnetizations are discussed in the next chapter.

5. ORIGIN OF THE MAGNETIZATION OF THE KAHOCHELLA GROUP

5.1 Introduction

In any palaeomagnetic study it is clearly important to be able to show that the remanence finally isolated by partial demagnetization is primary and aligned parallel to the ambient field at the time of rock formation. Evidence from a number of sources may be considered. Graham (1949) suggested the classic fold and conglomerate tests, but these rely on fortunate geological circumstances. Where opposed polarities are present, the reversal test (described by Cox & Doell, 1960) may be applied to demonstrate that no appreciable secondary component exists. Baked contacts may be examined to demonstrate that no remagnetizations have occurred (Everitt & Clegg, 1962). The direction and intensity of the remanence removed by demagnetization can yield useful information about the causes of secondary magnetizations. Examination of the coercivity and blocking temperature spectra of the rock makes it possible to identify the mineral phases responsible for the remanence. Finally, petrologic investigations yield indispensable information about the type and mode of occurrence of magnetic minerals present.

The above methods are applied in this chapter to demonstrate that the rocks of the Kahochella group have been

partially remagnetized after folding, and that the remagnetization may be at least partially removed by thermal treatment. It is also demonstrated that the remanence isolated was acquired during lithification and is resident in the mineral haematite.

5.2 Remanence Removed by Partial Demagnetization

It is possible by simple vector subtraction to determine the direction and intensity of the remanence removed at each step by partial demagnetization. Tight grouping of such removed vectors in a direction different from the total remanence direction of the specimens indicates the presence of a component of magnetization which can only be roughly inferred from the standard demagnetization diagrams (Figs. 4.3.2a-f, 4.3.3a-f). Such calculations have been performed on the demagnetization results for the Kahochella Group. A variety of directions was observed, but a remarkably coherent magnetization in the SE direction with steep inclination was removed from specimens with both normal and reversed remanences over the temperature range 550°C - 600°C . The results are shown in Table 5.2a for those sites where the within-site precision parameter exceeded 20 and the removed direction did not coincide with the site mean direction. The latter exclusion was made because a removed vector in the same direction as the

Table 5.2a Vector removed by demagnetization between
550°C and 600°C

<u>Site</u>	<u>N</u>	<u>D_p</u>	<u>I_p</u>	<u>D_a</u>	<u>I_a</u>	<u>k</u>
BA	4	215.1	58.8	212.8	76.6	22
BB	4	157.5	63.1	126.9	71.9	35
BC	4	152.9	62.8	141.0	79.3	88
BD	4	150.9	62.9	107.4	67.4	236
BG	4	144.8	59.2	124.8	58.5	131
BH	4	185.9	57.4	159.7	54.0	37
BM	4	175.7	82.1	130.2	72.8	129
BN	4	153.5	64.2	143.8	54.5	67
CI	4	164.4	53.1	146.9	48.2	51
CN	4	155.1	51.7	136.3	50.6	33
CP	4	148.6	54.6	131.7	51.4	322
CQ	5	139.0	61.3	116.8	48.4	35
DC	4	134.1	53.1	105.0	60.6	146
DD	3	136.7	58.4	114.3	61.7	137
FA	4	140.7	75.9	19.6	62.5	47
Mean	15	155.9	62.8	128.5	65.0	

N is the number of specimen results included in the site mean.

D_p, I_p are the declination and inclination of the mean removed vector with respect to the present horizontal.

D_a, I_a are the declination and inclination of the mean removed vector w.r.t. the palaeohorizontal.

k is the precision estimate of the site mean.

The k values of the mean of site means are 39 and 20 before and after dip correction respectively. The reduction in k is significant at 95% confidence.

base vector implies that a demagnetization end point has been reached.

The mean direction before the application of a correction for geologic dip has significantly higher precision than the mean after dip correction (McElhinny, 1964). Thus the secondary magnetization was acquired after folding, which occurred in late Aphebian time before the deposition of the Et-then Group (Section 4.2).

The removal of this post-folding secondary component is illustrated in Fig. 5.2a which shows the site mean directions of the C section after A.F. and after thermal demagnetization with arrows pointing toward the post-thermal direction. A consistent movement away from a direction close to that of the secondary magnetization is apparent. In some cases (CI, CN) the movement is through more than 90° . It is apparent that thermal demagnetization is fairly successful in removing the secondary component, but the still scattered nature of the reversed directions is an indication that the removal may not be complete. If this were the case, it would be expected that the observed mean cleaned direction would have a higher inclination than the true primary direction. This possibility was investigated by calculating a combined thermally cleaned direction for those sites rejected above (CC, CH, CR, CX, E section) on the grounds that the removed direction was parallel

Figure 5.2a Removal of a secondary magnetization from the rocks of the C section. The site mean directions for the C section are plotted after thermal treatment and after A.F. treatment. The arrows point in the direction of the site mean after thermal treatment. The vector removed from 15 sites by the demagnetization step 550°C to 600°C is also shown, as is the mean direction for the F section after thermal treatment. All directions are plotted with reference to the present horizontal, i.e. without dip correction.

to the total sample cleaned direction. It might reasonably be expected that any secondary magnetization had already been removed from such sites. The mean after dip correction was found to be $D = 129.3$, $I = 51.5$, $k = 31$, $n = 5$, which is not shallower than the mean direction for the C section. The mean direction for the vector removed between 550° and 600°C for these sites was $D = 132.0$, $I = 50.8$, $k = 50$, which is very close to the mean thermally cleaned direction, and supports the contention that no significant secondary magnetization remains in these specimens. Since this direction is no shallower than the mean direction for the C section, it may be concluded that very little secondary remanence remains in these rocks after thermal demagnetization.

It was shown in Chapter 4 that the F section had been remagnetized after folding. The direction of this remagnetization is also shown on Fig. 5.2a. It is not significantly different from the direction deduced by calculation of removed vectors for sections B, C and D. One post-folding remagnetization event is then consistent with the complete remagnetization of the F section and the partial remagnetizations of the B, C and D sections.

5.3 Coercivity and Blocking Temperature Spectra

In this section the intensity data yielded by demagnetization are examined for evidence of the minerals

responsible for remanence. It will be demonstrated that the stable remanence isolated by thermal demagnetization lies in the haematite, while that removed lies either in magnetite or in haematite of fine grain size.

5.3.1 Alternating field demagnetization curves

Representative curves have already been presented in Section 4.3.2. They showed the presence of a soft part of the magnetization whose relative magnitude varied from section to section. Table 5.7a (see Section 5.7) shows the absolute amount of magnetization residing in grains with coercivities below and above 80 mT (800 Oe). These are referred to as the soft and hard parts of the magnetization respectively. The coercivity of the natural remanence at each site is also shown. It may be seen that the A section sites contain small amounts of magnetic material (J_{soft} and J_{hard} columns) while the magnetic content of the B and C sections is rather higher. The difference between the B and C sections (displayed best in the J_{hard} column) appears to lie in greater absolute quantities of hard material in the C section samples.

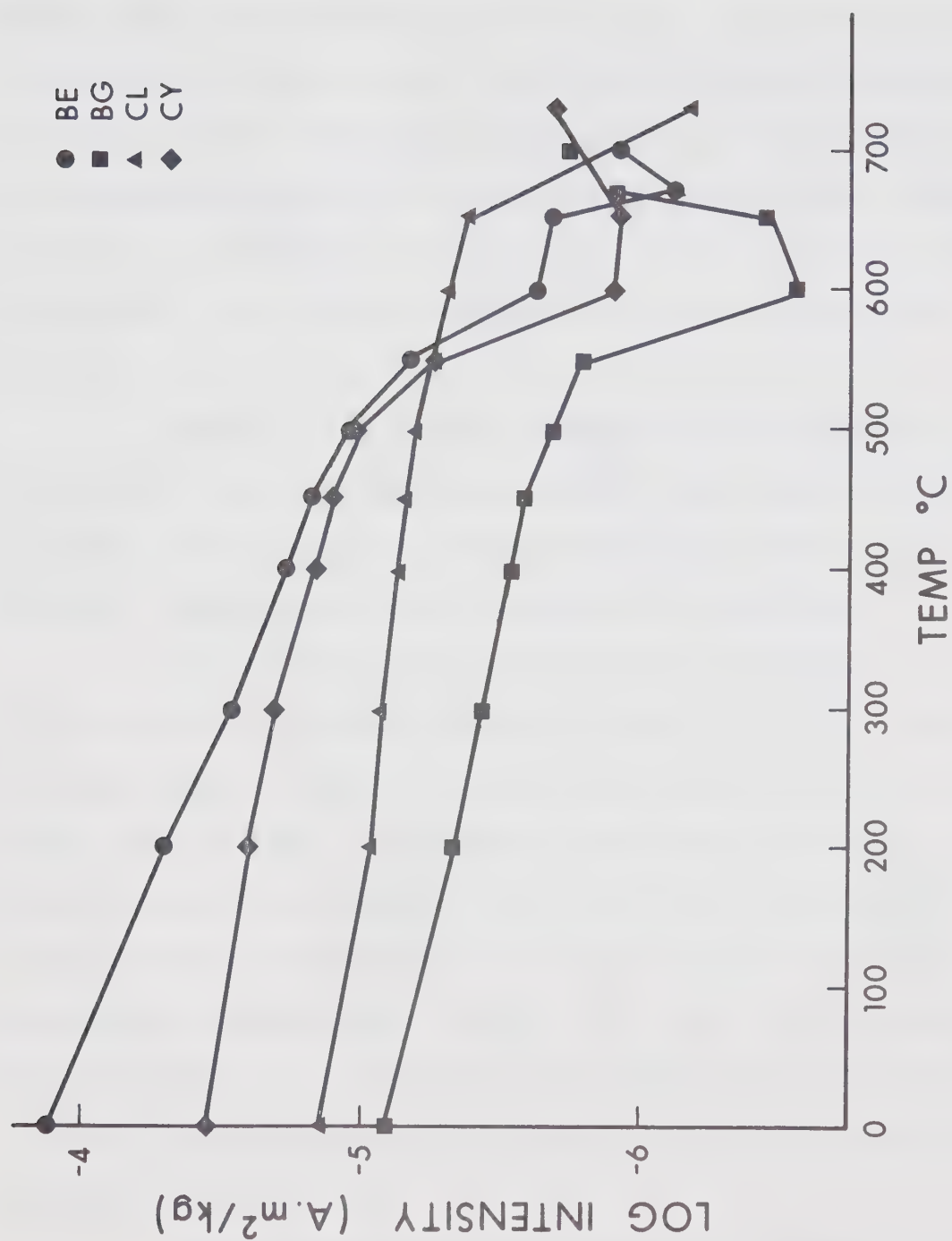
The soft part of the magnetization may be due to the presence of small quantities of a mineral such as magnetite or maghemite, whose coercivity is below 80 mT, or to

ultrafine haematite near the superparamagnetic size limit (Creer, 1959, 1961). Its origin is considered further in following sections.

5.3.2 Blocking temperature spectra

The partially unstable nature of the NRM (Fig. 4.3.1a) and the distribution of blocking temperatures from ambient up to the Curie point of haematite (Figs. 4.3.3a-f, 5.3.2a) suggest a grain size distribution in haematite from the superparamagnetic size limit to greater than $0.4\text{ }\mu\text{m}$ (Table 1.1a). The alternative possibility that this range of blocking temperatures is actually a range in titanomagnetite Curie points may be discarded because a complete range of compositions from magnetite to ulvospinel would be required to give the observed spectrum. This would require improbable conditions during crystallization of the opaque minerals. The intensity curves of Fig. 5.3.2a show some other interesting features. Three of the four curves (for sites, BE, BG, CY) show evidence of alteration by heating in their intensity rise at high temperatures. The rise is suggestive of the production of magnetic material which becomes magnetized on cooling in either the stray fields present in the apparatus of about 5 nT (5 gamma) or in the interaction fields between magnetic grains. The nature of this magnetic material is investigated

Figure 5.3.2a Intensity versus treatment curves for pilot specimens from some sites after thermal demagnetization. Distributed blocking temperatures are clearly displayed.



in Section 5.4. The same three curves in Fig. 5.3.2a show sharp drops after heating to 600°C , i.e. just above the Curie point of magnetite. This may be regarded either as evidence for the existence of magnetite or as evidence that the haematite grain size distribution has a peak a little above $0.4\text{ }\mu\text{m}$ (Table 1.1a) i.e. just at the limit of optical resolution. The optical observations are discussed in Section 5.5.

Some of the thermal demagnetization curves do not show such a drop on heating to 600°C (e.g. site CL in Fig. 5.3.2a). The large drop between 650°C and 730°C is a definite indication of the presence of haematite.

Fig. 5.3.2b shows the results of thermal treatment of the spilitic basalts sampled in the F section. They show a decade drop in intensity on heating above the magnetite Curie point. Fig. 4.3.3f shows the erratic changes in direction which accompany this drop. The nature of the rock rules out the possibility of a large amount of haematite of appropriate grain size, so that this drop may be taken as good evidence of the existence of magnetite in the rocks of site FE. This conclusion is backed up by petrologic observations (Section 5.5).

Fig. 5.3.2c shows the results of thermal treatment of specimens already A.F. demagnetized in 180 mT, along with

Figure 5.3.2b Thermal demagnetization of specimens from the lavas of the F section. All display magnetite Curie points.

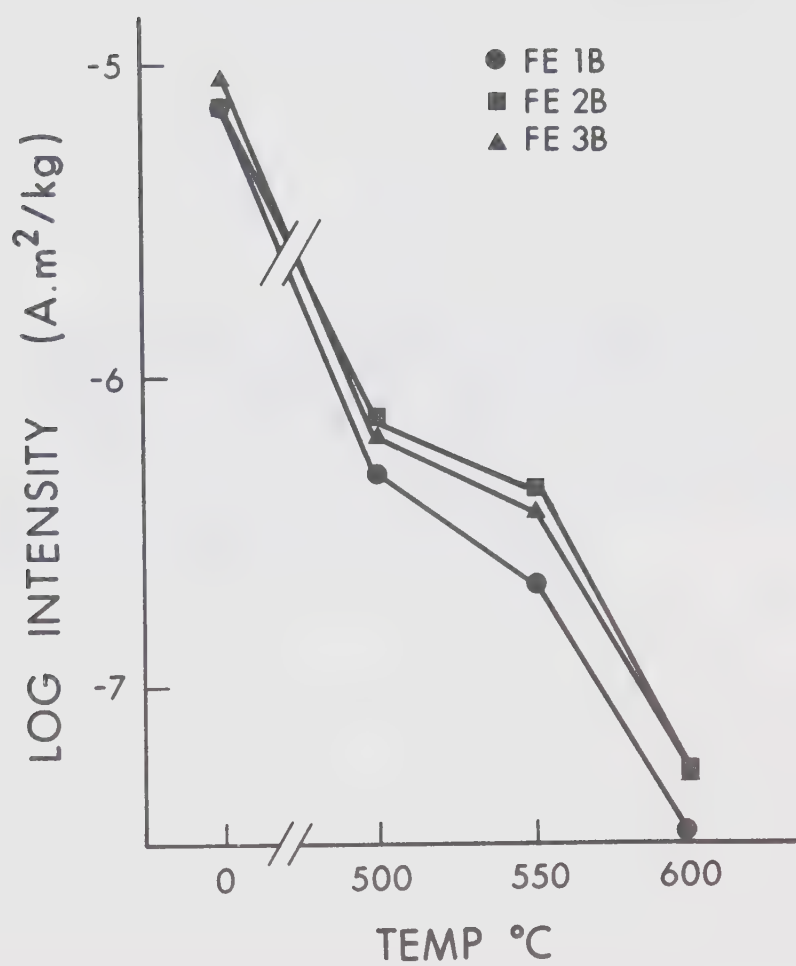
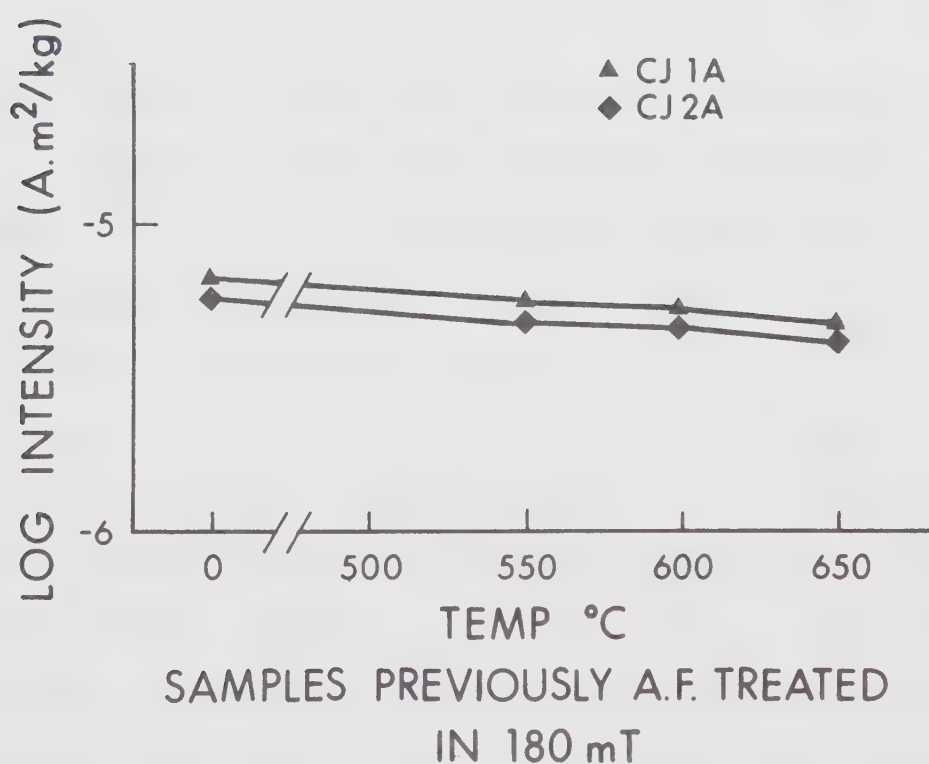
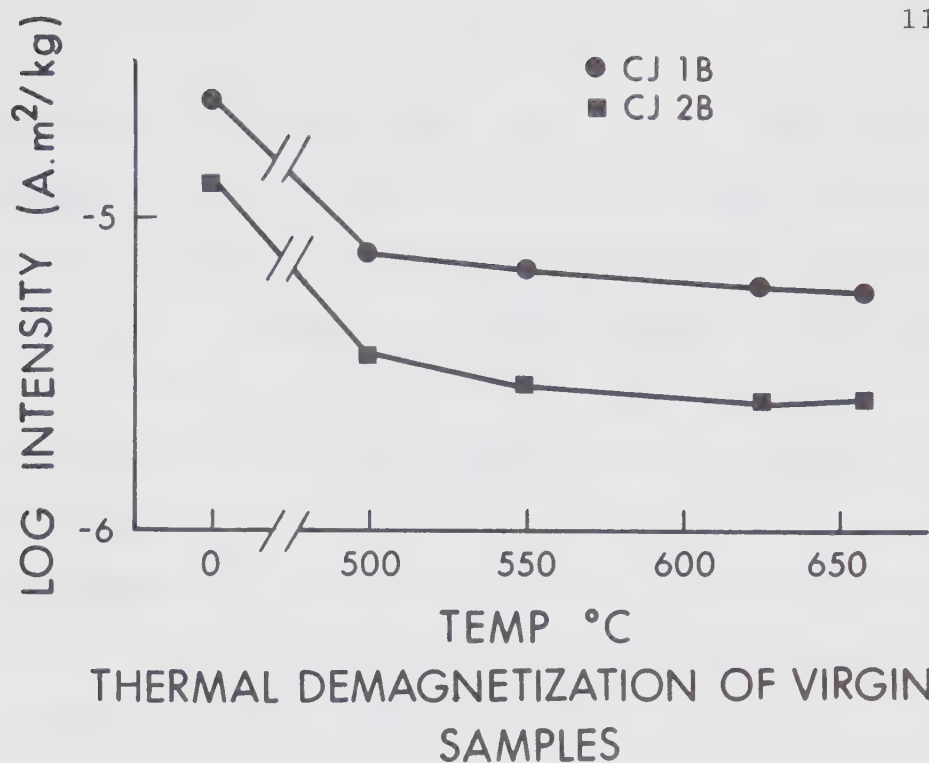


Figure 5.3.2c Thermal demagnetization of specimens previously cleaned of low coercivity components by A.F. treatment. Demagnetization of virgin partner specimens from the same sample is also shown.



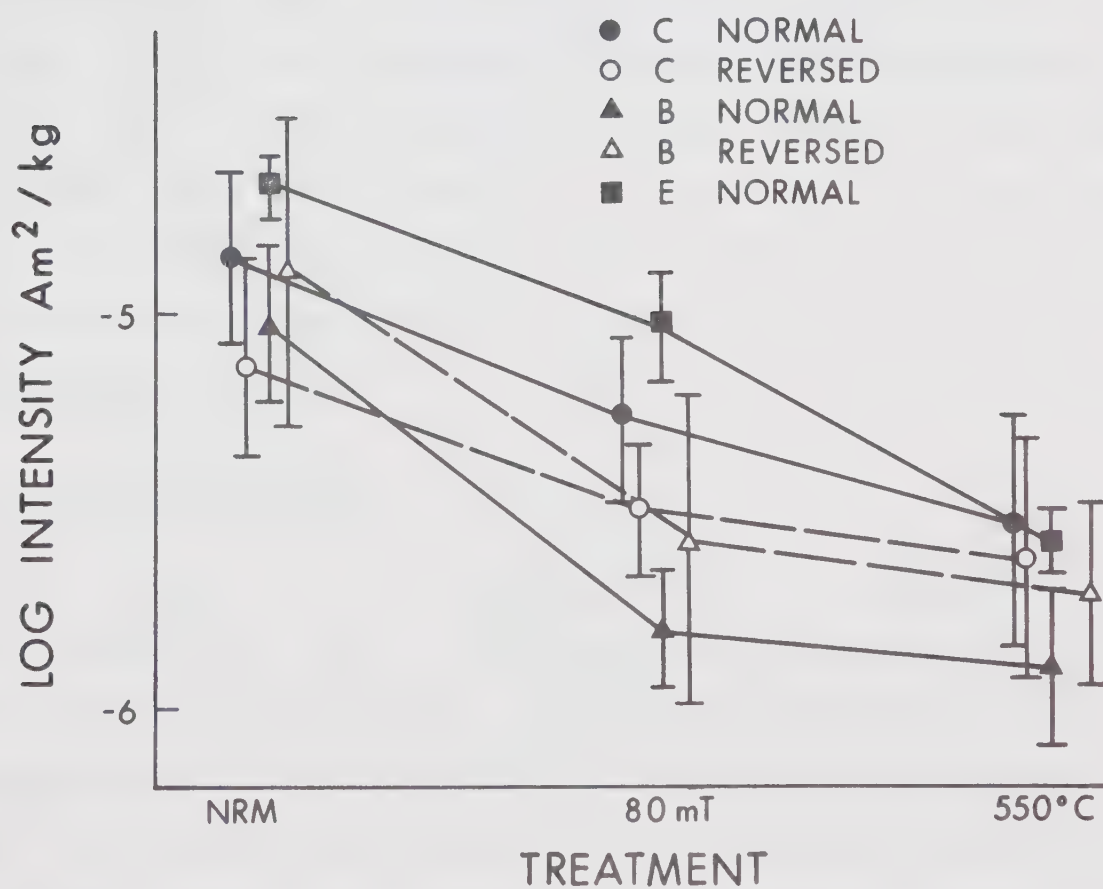
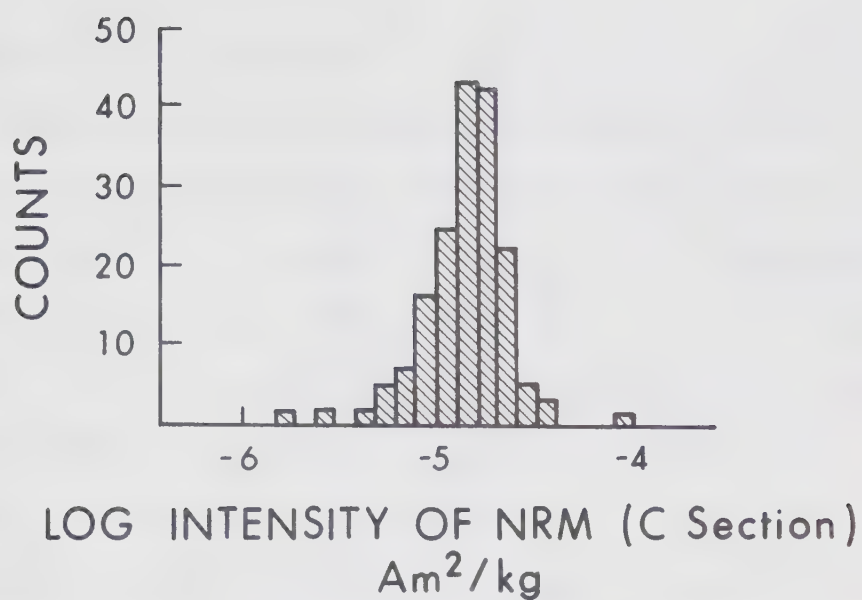
two fresh specimens from the same site. It is clear that A.F. demagnetization has removed that part of the magnetization residing in grains with low blocking temperature. At least for this site, A.F. treatment at 180 mT appears to be about equivalent to thermal demagnetization at 500°C.

The results described above strongly suggest that the mineral responsible for most of the remanence of the sediments is haematite, with a wide range of grain sizes, while magnetite containing relatively little titanium is the major magnetic mineral in the basalts.

5.3.3 Intensities and reversals

The geometric mean NRM intensities and standard deviations for section B, C and E have been calculated. They are shown in Fig. 5.3.3a divided into normal and "reversed" groups, together with the results after A.F. treatment in 80 mT and thermal treatment in 550°C. The histogram of the C section NRM intensities is included to justify the calculation of geometric rather than arithmetic means. The histogram shows that the intensities are distributed in log Gaussian fashion. The figure demonstrates that the intensities of the normal and reversed sites are different, although reversed sites are more intensely magnetized than normal sites in the B section and vice versa in the C section.

Figure 5.3.3a Geometric mean intensities and standard deviations for specimens from the Kahochella Group. Natural intensities and those after treatment in 80 mT and in 550°C are shown. The actual distribution is included for one case (C section normal NRM).



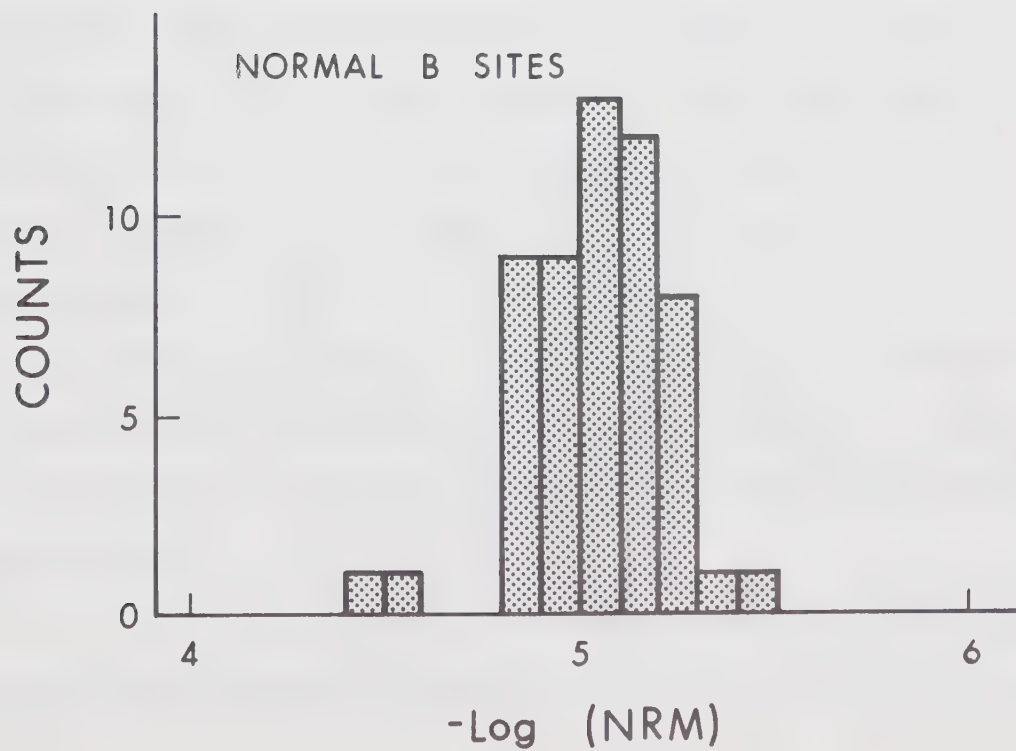
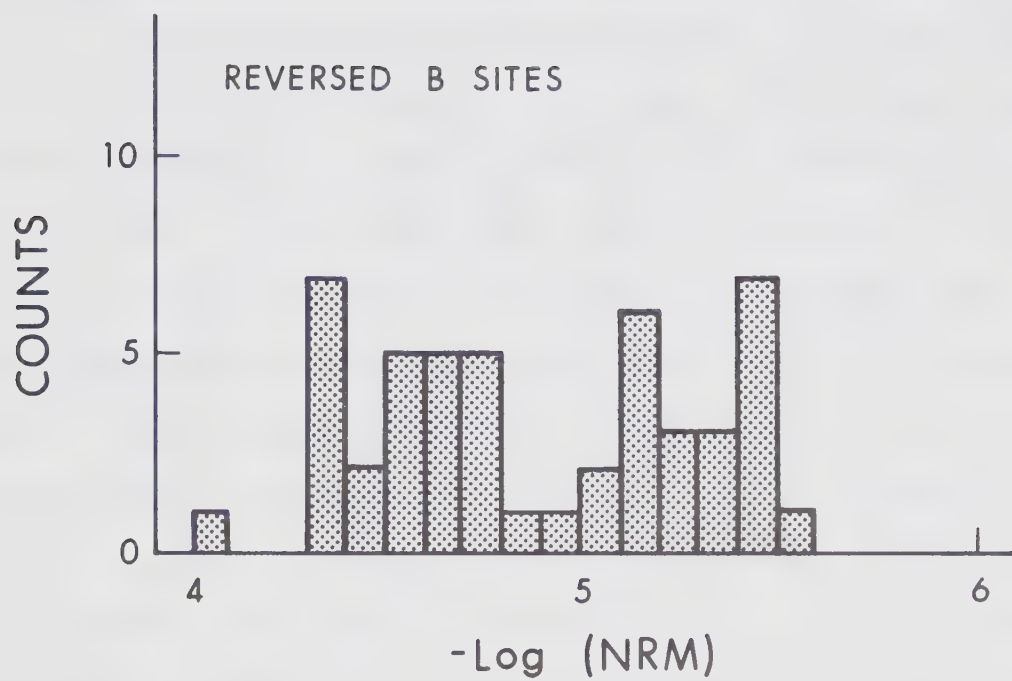
This behaviour is not understood. The presence of a remagnetization component roughly directed along the normal direction should systematically reduce the intensity of reversed specimens. A clue may be found in the histograms of the normal and reversed NRM intensities for the B sections (Fig. 5.3.3b). The reversed group has an apparently bimodal distribution, which increases its apparent standard deviation.

One trend clear from Fig. 5.3.3a is that E section material is most strongly magnetized, and B section material least strongly. The simplest explanation of this is that it reflects the different amounts of magnetic material present, and is a useful clue in establishing which phase of haematite is responsible for the remanence. It is likely to be the phase most concentrated in E section material and least concentrated in B section material. This is shown in Section 5.5 to be fine-grained haematite.

5.4 Isothermal Remanence

Dunlop (1972) has suggested that it is possible to make a rough separation of a red sediment into magnetic fractions by considering the coercivity spectrum as revealed by magnetizing a rock specimen in a progressively increasing field. He assumes that coercivities in the range 0-100 mT (0-1000 Oe), 100-300 mT and 300 mT to saturation are charac-

Figure 5.3.3b Histograms of the intensity distribution
of NRM for the normal and reversed sites
of the B section.



teristic of magnetite, specular haematite (specularite) and fine grained haematite (pigment) respectively.

This technique has been applied to 29 specimens from the Kahochella Group in an attempt to elucidate their magnetic mineralogy. The specimens were magnetized in fields of 5, 10, 20, 30, 50, 100, 200, 300, 500 mT and 1, 2, 3, 5 T (50 Oe to 50 kOe) using an iron cored electromagnet for the lower steps and a superconducting magnet with room temperature access to the magnetic field for steps above 0.5 T. All the specimens were close to saturation at 5 T. The results have been analysed in two ways. The coercivity of remanence of each specimen was found by interpolation. It was defined as the field in which the specimen gained half its saturation remanence. This is tabulated as H_{cr} (IRM) in Table 5.7a. It is noteworthy that H_{cr} is in general very much higher than the coercivity of the NRM as deduced from A.F. demagnetization which is defined as the peak A.F. field required to halve the NRM intensity. This is listed under H_{cr} (A.F.) in Table 5.7a. The difference between the two values of H_{cr} is interpreted as meaning that the highest coercivity minerals do not contribute as much to the NRM as might be expected from their concentration.

The second result obtained from the coercivity spectrum analysis was a crude estimate of the concentrations

of the three mineral fractions in the rock samples as described above. Brooks and O'Reilly (1970) have employed rotational hysteresis results to achieve a similar analysis.

It has been assumed that the saturation remanences of magnetite and haematite are 18.4 and $0.17 \text{ Am}^2/\text{kg}$ (emu). These figures should be taken as rough guides only. They are based on measurements of Roquet (1954) and Dunlop (1971) for magnetite and haematite respectively.

The fraction by mass of each mineral deduced to be present in the rock is shown in Table 5.4a. Two interpretations of the soft part of the coercivity spectrum are given in the table. The 0-100 mT coercivity range has been interpreted in terms of both magnetite and ultrafine haematite (columns labelled Magnetite and Soft Haematite). The haematite interpretation is clearly untenable in the four cases BE1B, BL3B, CH1A and CK4B where the rock has been altered by heating. The amount of ultrafine haematite required to explain the soft remanence ranges from 37% to 101% by mass, which is not likely for red shales. It therefore appears that thermal alteration has resulted in magnetite (or possibly maghemite) production. It does not seem to have been derived from any of the other magnetic minerals present, because they all show an increase after heating. The increases cannot always be regarded as significant, because they involve the measurement

Table 5.4a Concentrations of magnetic minerals in samples
from the Kahochella Group deduced from IRM data

<u>Sample</u>	<u>Magnetite</u>	<u>Specu-</u> <u>larite</u>	<u>Haematite</u>	<u>Soft</u> <u>Haematite</u>	<u>Notes</u>
AC1A	1.3E-6	9.9E-4	2.2E-3	1.4E-4	
AD1A	6.8E-7	8.6E-4	4.4E-3	7.1E-5	
BB1A	6.7E-5	4.8E-3	1.0E-2	7.0E-3	
BD1B	3.8E-5	8.5E-3	2.7E-2	4.0E-3	
BE1A	5.1E-5	7.3E-3	3.2E-2	5.3E-3	
BE1B	9.6E-3	4.0E-2	6.2E-2	1.0E00	1
BE1A	2.5E-5	7.1E-3	1.9E-2	2.6E-3	
BJ4A	4.9E-5	7.8E-3	2.6E-2	5.2E-3	
BK1A	2.5E-5	5.7E-3	2.1E-2	2.7E-3	
BL3A	3.9E-5	6.6E-3	1.3E-2	4.1E-3	
BL3B	3.7E-3	2.6E-1	5.1E-2	3.9E-1	1
CC3A	5.2E-5	1.4E-2	4.8E-2	5.4E-3	
CD1A	1.3E-4	3.4E-2	1.0E-1	1.4E-2	
CE1A	4.9E-5	1.5E-2	1.0E-1	5.1E-3	
CE5A	7.0E-5	1.3E-2	1.2E-1	7.3E-3	
CG1A	5.3E-5	1.1E-2	6.0E-2	5.6E-3	
CG2A	5.7E-5	1.1E-2	8.5E-2	5.9E-3	
CH1A	3.5E-3	3.0E-1	6.2E-2	3.7E-1	1
CH1B	4.9E-5	8.7E-3	4.2E-2	5.2E-3	
CJ3A	3.5E-5	8.2E-3	4.3E-2	3.6E-3	
CK4A	2.4E-5	7.9E-3	4.3E-2	2.5E-3	
CK4B	7.6E-3	2.2E-1	6.8E-2	8.0E-1	1
CL1A	3.3E-5	6.8E-3	4.9E-2	3.5E-3	
C04B	3.8E-5	6.5E-3	3.6E-2	4.0E-3	
CP5A	4.7E-5	6.1E-3	4.5E-2	5.0E-3	

Table 5.4a Concentrations of magnetic minerals in samples
from the Kahochella Group deduced from IRM data

Continued

<u>Sample</u>	<u>Magnetite</u>	<u>Specu- larite</u>	<u>Haematite</u>	<u>Soft Haematite</u>	<u>Notes</u>
CS1B	2.8E-5	3.6E-3	3.1E-2	3.0E-3	
CU1A	3.8E-5	5.6E-3	6.1E-2	4.0E-3	
CV1B	2.0E-5	2.5E-3	2.7E-2	2.1E-3	
CX1A	4.1E-5	1.2E-2	1.7E-1	4.3E-3	

Notes

1. Specimen altered by thermal demagnetization
before IRM produced.

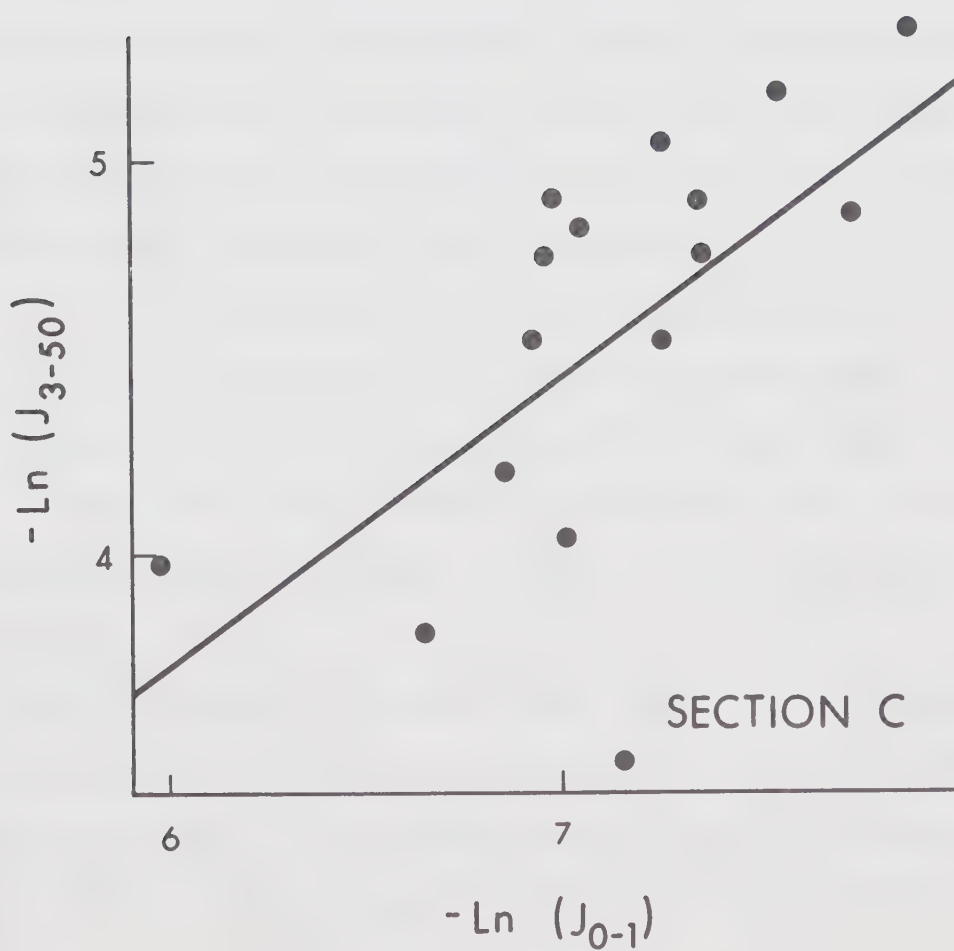
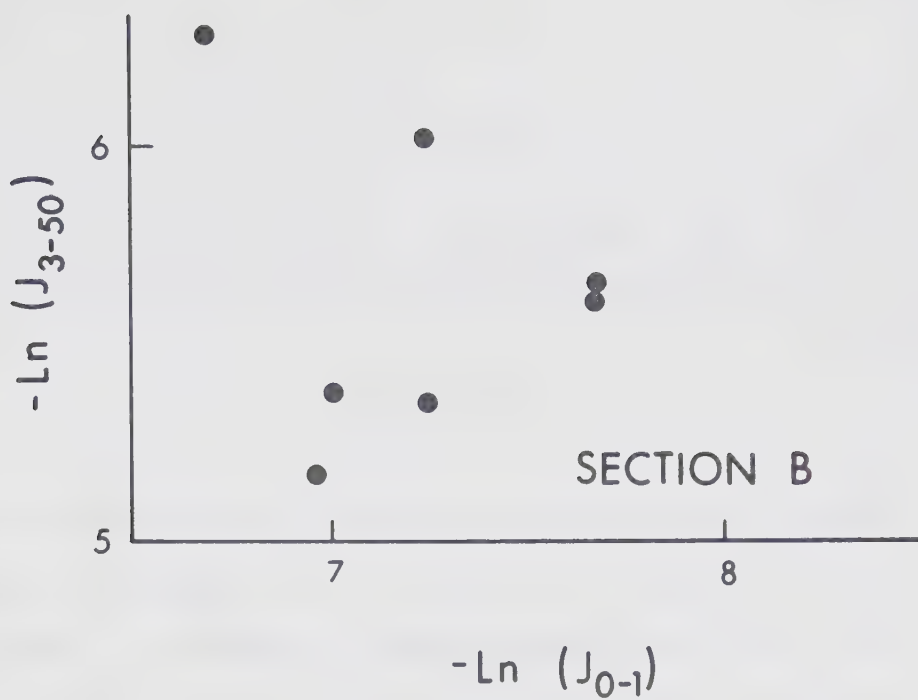
The E in the above table denotes exponentiation.
 Thus 1.3E-6 means 1.3×10^{-6} .

of small changes in the high coercivity range in the presence of a very strong moment due to the saturated magnetite. However, the large increases shown in the Specularite column after heating are probably due to some magnetite which saturates in fields a little above 100 mT rather than to an actual increase in the number of large detrital haematite grains present.

The suggestion that the soft part of the magnetization may be due to ultrafine haematite is more tenable in the unheated samples. Examination of the Haematite and Soft haematite columns shows that the ultrafine haematite content deduced on this model for each sample is consistently one order of magnitude less than the content of harder haematite. This would be expected if the grain size distribution is similar from site to site, but varying in absolute amount. This has been pursued further in Fig. 5.4a, which is a scatter diagram of the amount of saturation remanence residing in the hard part of the spectrum against that residing in the soft part of the spectrum. The diagrams are divided by section and the scales are logarithmic.

For the B section diagram, the coefficient of correlation between the variables plotted is $-.195$. For hypothesis testing this is mapped to the normally distributed w function using Fisher's formula

Figure 5.4a Scatter diagrams of the amount of hard remanence against the amount of soft remanence in specimens from the B and C sections as revealed by IRM studies. J_{0-1} is the remanence gained between zero and 100 mT. J_{3-50} is the remanence gained between 300 mT and 5T.



$$w = \frac{1}{2} \ln \left\{ \frac{(1+r)}{(1-r)} \right\}$$

where r is the coefficient of correlation (Hoel, 1966). The standard error in the mean of the w distribution is

$$\sigma_w = (n-3)^{-\frac{1}{2}}$$

where n is the number of points in the scatter diagram. For the B section diagram, $r = -.195$, $w = -.198$, $n = 7$, $\sigma_w = .5$. For $P = 0.05$, we require a significance point at $1.96 \times \sigma_w$. The significance point is then at .98, and we may not reject the hypothesis that the correlation is zero. In other words, there is no statistical reason to believe that the hard and soft magnetizations are contained in different size ranges of the same mineral phase for the B section.

For the C section diagram, the figures are:

$r = .632$, $w = .745$, $n = 16$, $\sigma_w = .278$, significance point at 95% confidence is .54. We may therefore reject the hypothesis that the variables are uncorrelated. The conclusion remains the same if either or both the extreme values are discarded.

The statistical evidence thus supports the contention that the soft and hard parts of the remanence reside in different size fractions of the same mineral phase. The negative results for the B section suggest that some other mineral

phase may be an important part of the remanence as well. The identification of these mineral phases is ambiguous using IRM data alone. There appear to be two candidates for the phase giving rise to both the soft and hard magnetizations. It could be detrital haematite grains with residual magnetite cores, or it could be the fine-grained haematite. Both are observed to be present (Section 5.5). The former suggestion is somewhat at variance with the coercivity model on which these calculations are based, because the large haematite grains should have their greatest effect on the values in the Specularite column of Table 5.4a, and these values were not used in the correlation calculation. However it cannot be rejected without an examination of the relative proportions of the two possible minerals.

The IRM data may thus be used to demonstrate that thermal alteration produced magnetite, but not by reduction of haematite, and they may be used to support the suggestion that the hardest and softest magnetizations reside in different parts of the same mineral phase, except in the B section.

5.5 Observations Using the Ore Microscope

Polished thin sections of material from some of the sampling sites have been examined by transmitted and reflected light. Quantitative observations were made of ore grain

reflectivity and size distribution. The rock colour in hand sample was classified according to a standard scheme. Dr. S. E. Haggerty kindly examined and commented on a selection of thin sections.

5.5.1 Qualitative observations

Rocks of the B, C, D and E sections are shales and mudstones whose major constituent is quartz in grains of 10 - 50 μm diameter. The grains are sub-rounded and moderately well sorted. The major ore mineral present is haematite. Dr. S. E. Haggerty has identified six modes of occurrence of haematite. These are:

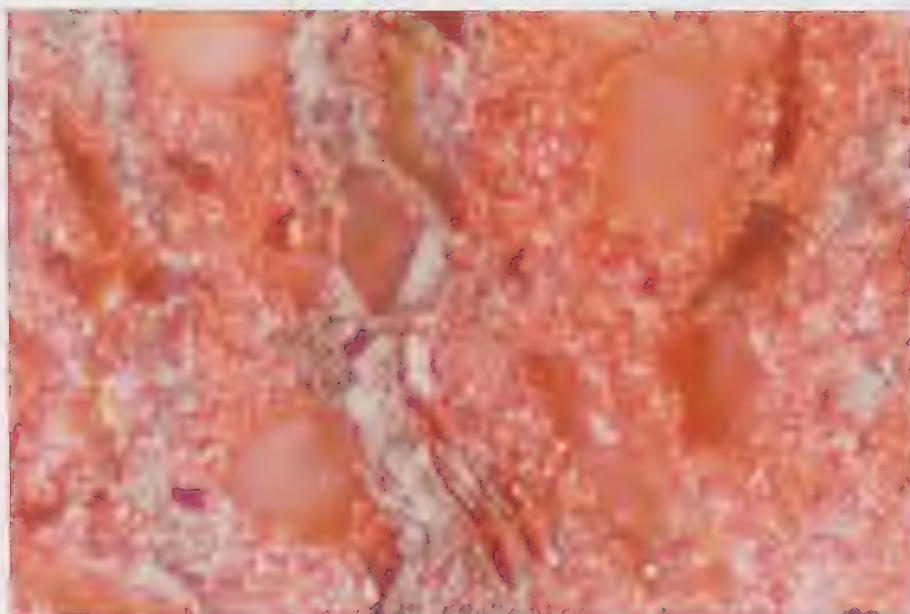
(i) Primary sedimentary banding of haematite grains less than 1 μm in diameter. This is a major constituent of some thin sections, making them opaque to transmitted light. This is a primary phase (Plate 5.5.1a).

(ii) Veinlets of haematite transgressing the sedimentary banding. These are due to remobilization of haematite under conditions of elevated temperature and pressure such as might be expected under a load of 8 km of sediment (Section 4.2). With a typical thermal gradient of $30^{\circ}\text{C}/\text{km}$ (Garland, 1971) a temperature of 260°C would occur at this depth. This mineral phase is secondary (Plate 5.5.1a).

Plate 5.5.1a Photomicrographs of polished sections from sites CC and CH. Magnification 10^3 . i.e. 1 cm = 10 μ m.

Upper Photograph: Site CC, showing sedimentary banding of fine-grained haematite. Bedding is vertical.

Lower Photograph: Site CH, showing ore grain of haematite with residual patches of magnetite, and veinlets of remobilized secondary haematite (upper right).



(iii) Knots of haematite and possible colloform goethite formed by dehydration of primary or secondary goethite. Since the upper stability limit of goethite is 140°C this is evidence of heating above 140°C .

(iv) Wafers of haematite derived from goethite by dehydration.

(v) Discrete grains of haematite in the size range 1 - 30 μm showing subhedral to euhedral crystalline outlines. These must be primary detrital grains, because they show evidence of a previous igneous origin.

(vi) Haematite with residual magnetite cores. These may have been deposited as magnetite, and altered since deposition to haematite (Plate 5.5.1a).

The quantity of fine haematite (Type 1 above) is variable, but the concentration is generally higher in C, D and E section rocks than in A and B section rocks.

Rutile is present as a detrital mineral in many of the thin sections. Magnetite is the main magnetic mineral in the lavas of the F section. Dr. Haggerty (pers. comm.) is of the opinion that the mineral assemblage in the thin section from site CY (pseudobrookite, rutile and haematite) is characteristic of heating to 500°C for a few hours. Alternatively it could be the result of heating to some lower temperature (say 200°C) for several million years.

The rocks of the A section were sampled from a calcareous rock formation of biogenic nature. Not much magnetic mineral is present in the rock, but some grains of detrital haematite do exist.

5.5.2 Size distribution of ore grains

The quantity of ore grains greater than 1 μm in diameter is variable from site to site. Fig. 5.5.2a shows histograms of the size distribution and volume fraction of such ore grains for two thin sections as deduced by grain counting. Here KBL has notably more ore grains in all size ranges, but especially in the larger sizes. The counts may be low for the 1 - 2 μm class. This is near enough to the optical limit to make counting difficult. The total volume fraction of opaques larger than 1 μm for all the thin sections for which counts were made is reported in Table 5.7a.

The possibility that the soft part of the magnetization is associated with the large grains (or the magnetite cores in some of them) may be examined by reference to Fig. 5.5.2b, which compares the observed total amount of such ore grains to the amount of natural remanence lost by demagnetization in 80 mT (800 Oe). The variation of the opaque content by a factor of 8 appears to cause no change in the amount of soft magnetization. The vertical scale bars in the

Figure 5.5.2a The size distributions of opaque grains larger than 1 μm in thin sections from sites BL and CC. The equivalent volume fractions are shown dotted.

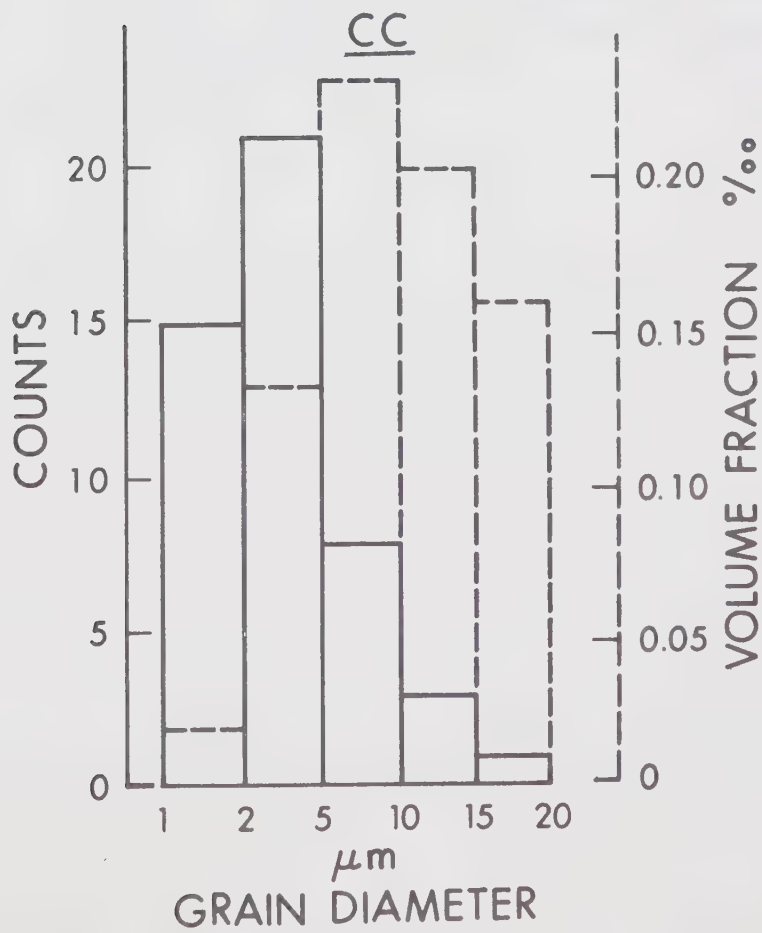
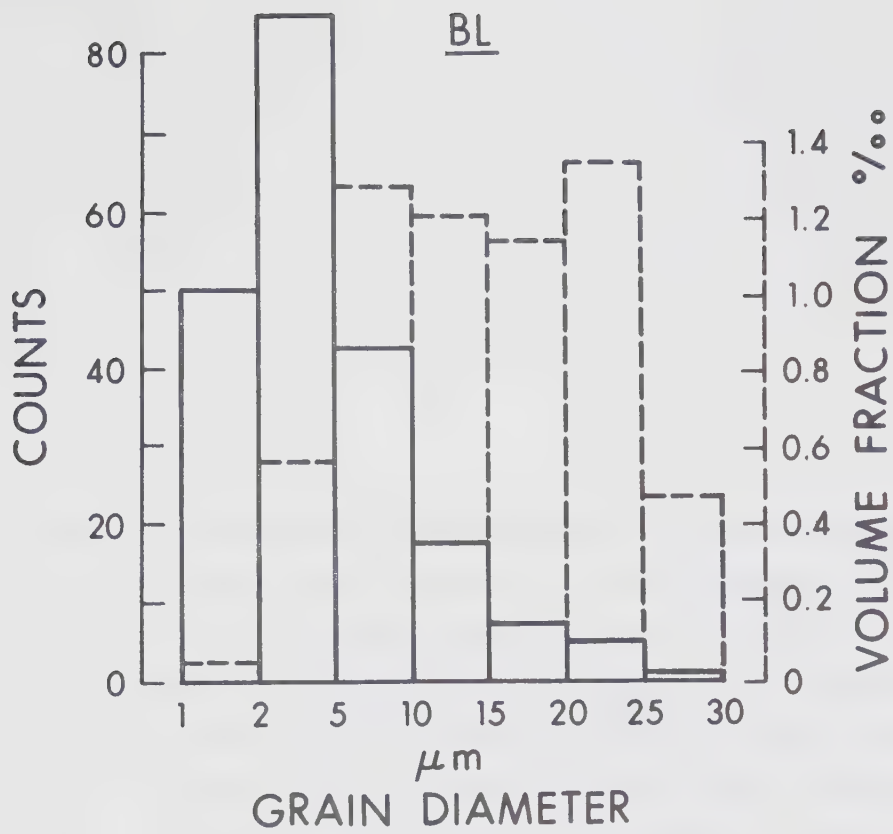


Figure 5.5.2b Comparison of the amount of opaques in the rock to the amount of soft remanence in the rocks of sites BB, BK, BL, CC, CH, CJ, CP, CU and CX. J_{soft} is the amount of remanence removed by treatment in 80 mT peak alternating field. % opaques is the volume fraction of the rock made up of ore grains larger than 1 μm . The range in J_{soft} shown is the range within each site.

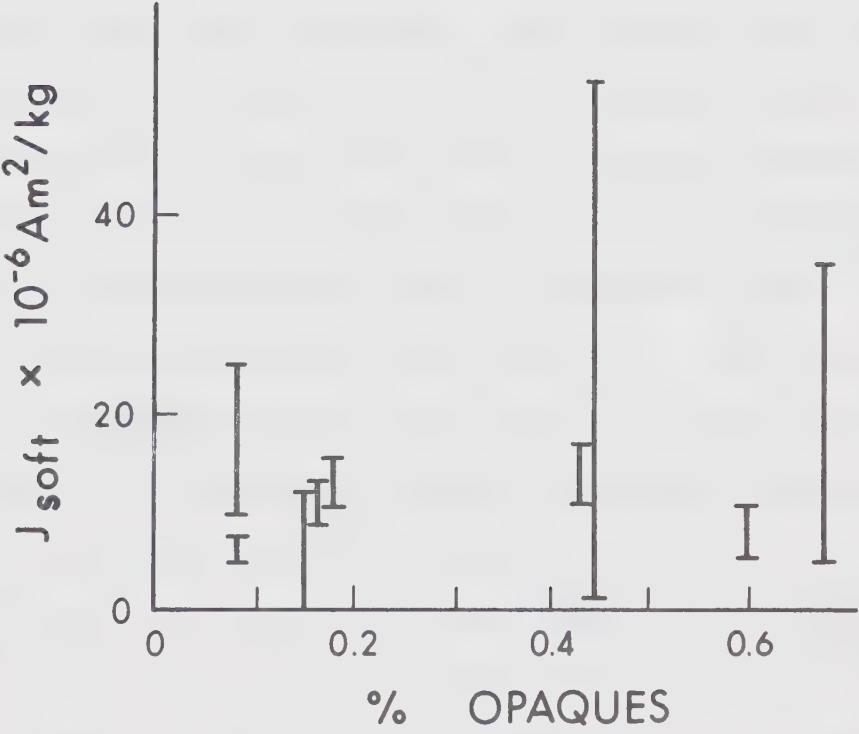


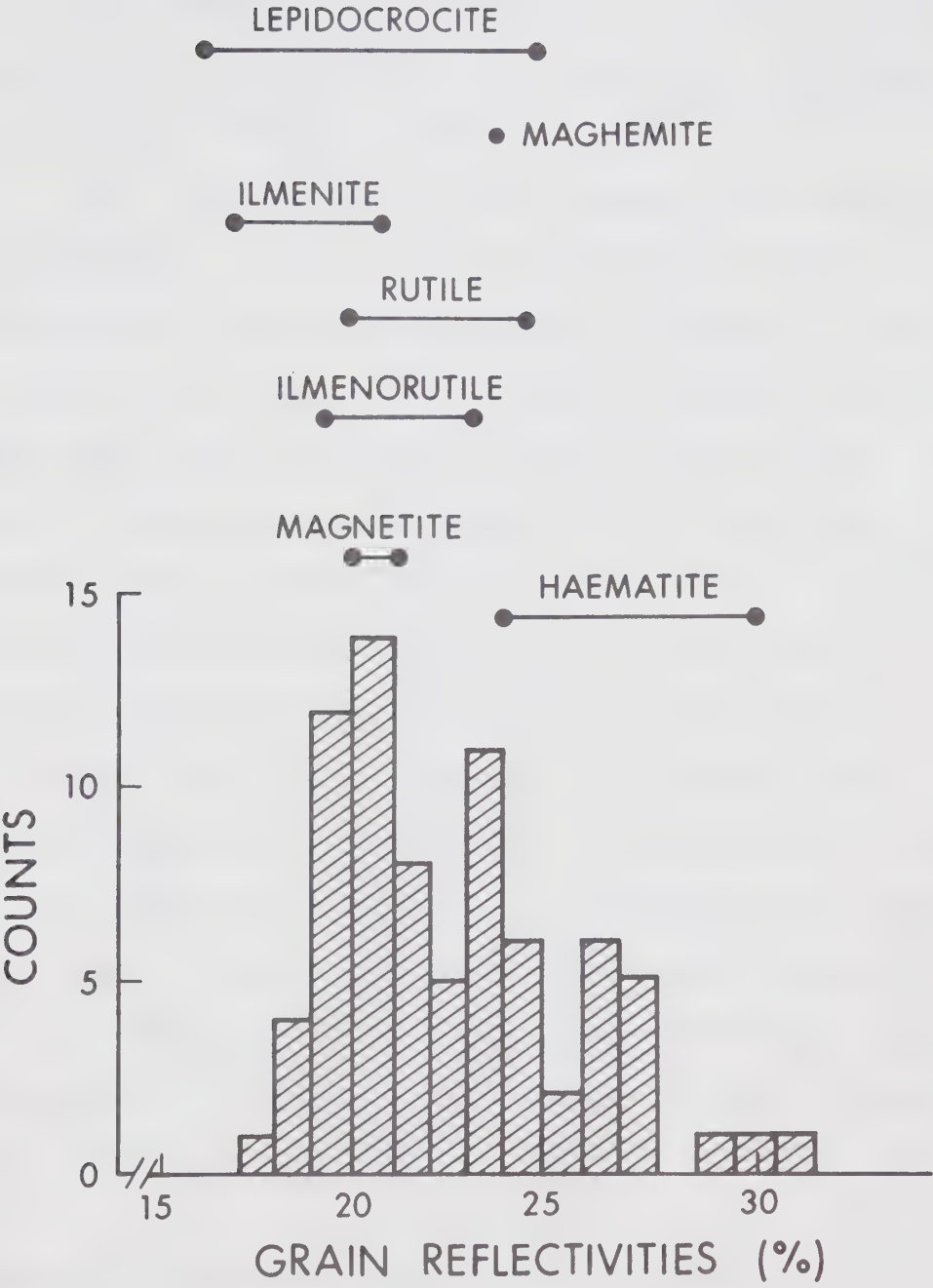
figure show the within-site range in the intensity of the soft magnetization. It therefore seems unlikely that the soft magnetization can be attributed entirely to the magnetite cores in some of the large haematite grains.

5.5.3 Ore grain reflectivities

The reflectivities of ore grains greater than 5 μm in diameter have been measured. The standard wavelength of 546 nm (green) was used, and a calibration point at 20.6% reflectivity was established using a standard sample. A 10 μm illumination spot with a 5 μm diameter reading circle was used. The results are shown in histogram form in Fig.

5.5.3a. The reflectivities of common iron and titanium oxides and hydroxides are also shown in the figure. They are taken from the reflectivity tables of McLeod and Chamberlain (1969). In interpretation of these data it should be remembered that a large grain, well polished, showing no alteration will give the value quoted. Many grains in actual rocks will give values slightly less, so that a skewing towards lower reflectivities is to be expected. The histogram gives definite confirmation of the presence of haematite, but suggests the existence of another mineral as well. It is likely to be ilmenorutile or rutile. This is suggested both by direct observation and by electron microprobe analysis (Section 5.6).

Figure 5.5.3a The distribution of reflectivities for ore grains larger than 5 μm in diameter. Results from all sampling sections except section F are included.



5.5.4 Colour of rock samples

The "redness" of a sediment has long been recognised as a qualitative indicator of its suitability for palaeomagnetic studies (Runcorn, 1957).

The rock samples in hand specimen have been classified according to colour by use of the Rock-Color Chart distributed by the Geological Society of America (1970). Colours are classified by hue, value (lightness) and chroma (saturation). The results are shown in Table 5.5.4a. Where no colour is assigned to the rocks from a site, their colour was intermediate between those on either side. The most notable feature is that the majority of sites from the B section are classed as 5RP (red-purple) while most of the rock from the C section is classed as 5R (red) in hue. This difference represents a difference in the haematite content in the size range which produces a red colouration (around 1 μm and less). This supports the microscope observation of the same phenomenon. The sedimentary banding of the fine haematite is evident in the colour banding in hand specimen at three sites (CC, CD, CX).

5.6 Electron Microprobe Analysis of Ore Grains

Ore grains in three petrographic sections were analysed for Titanium and Iron content using an ARL-EMX

Table 5.5.4a Colour classification of rock samples from
the Kahochella Group

Based on the Rock-Color Chart distributed by the Geological
Society of America

<u>Site</u>	<u>Colour</u>
KAA	5R 4/2 in 5R 8/2
KAB	5RP 6/2 in white (N 10)
KAC	5RP 6/2 in 5RP 8/2
KAD	5RP 7/2
KAE	5RP 5/2
KBA	5RP 4/1
KBB	5RP 4/1
KBF	5P 4/1
KBH	5RP 5/1
KBM	5RP 4/2
KCA	5RP 6/1
KCB	5RP 6/1
KCC	5RP 6/2 & 5R 5/6 banded
KCD	5R 5/4 & N 5 banded
KCE	5R 2/4
KCF	5R 4/4
KCG	5R 4/4
KCH	5R 4/2
KCI	5R 4/2
KCJ	5R 4/2 & 10Y 6/2
KCK	10Y 5/2, 5R 8/2, 5R 5/2
KCL	5R 6/2, 5R 4/2
KCM	5R 5/2

Table 5.5.4a Colour classifications of rock samples from
the Kahochella Group

Based on the Rock-Color Chart distributed by the Geological
Society of America

Continued

<u>Site</u>	<u>Colour</u>
KCQ	5R 5/2, 5RP 6/2, 10G 6/2
KCR	5R 4/2
KCS	5R 5/2
KCT	5R 5/4, 5R 7/2
KCU	5R 5/2, 5R 8/2
KCV	5R 4/2, 5R 7/2
KCW	5R 5/2, 5R 8/4
KCX	5R 6/4, N 6 banded
KCY	5R 5/2, N 7
KCZ	5YR 6/2
KDA	5R 5/6
KDB	N 5
KDC	5R 5/2
KDD	5R 4/2, 5R 8/2
KEA	5R 4/4, 5R 6/2
KEE	5R 5/2
KFA	5RP 4/2, N 6
KFB	10G 7/2
KFC	10G 6/1
KFD	5RP 4/1
KFE	10G 5/2

Electron Microprobe Analyser. The Analyser was operated at 15 kV with a beam current of 0.1 μ A and a beam diameter of about 1 μ m. The secondary X-rays emitted were analysed using LiF crystals.

The background count for iron and for titanium was found by counting on either side of the element peak with a standard sample in the instrument. The mean of the upper and lower backgrounds for each element was taken as the background count for that element. Count rates at the titanium and iron peaks for ilmenite and haematite standards were also found in order to calibrate the instrument. Calibration and background determination were carried out before and after analysing the unknowns. Count rates were sufficiently low (2 kHz) to make a correction for dead time unnecessary. No corrections were made for absorption and fluorescence effects. These would not greatly affect the results because a standard giving a similar count rate to that given by the unknowns was used. Total counts were in the range 16 - 20 k, giving an expected standard deviation of about 1%.

The analysis results of point counts for 2 - 6 locations on 10 grains are reported in Table 5.6a. The grain names refer to numbered negatives of optical photographs of the grain which are kept in the laboratory negative file. The letter pair at the beginning of the grain name denotes the

Table 5.6a Electron Microprobe Ore Grain Analyses

<u>Grain</u>	<u>% Ti</u>	<u>% Fe</u>	<u>Grain</u>	<u>% Ti</u>	<u>% Fe</u>	<u>From</u>
FB 5-18	3.7	66.5	FB 5A	2.6	64.4	F Section
	3.6	66.2		2.7	63.8	
	2.9	66.3		51.5	5.6	
	56.4	2.8	FB 5-17	2.7	63.9	
	55.4	3.2		3.0	60.7	
	55.6	2.7		4.9	60.3	
				56.5	2.5	
BL 5-13	3.7	63.9	BL 5-1	1.0	67.2	B Section
	3.2	63.6		1.1	66.6	
	3.9	63.0		1.1	66.4	
	52.0	4.4	BL	.65	66.4	
	52.5	3.4		.86	66.5	
BL 5-15	2.2	66.6		56.5	2.6	
	2.5	65.8		55.6	2.4	
CH 4-3	2.0	62.1	CH 4-2	50.7	5.8	C Section
	2.3	62.3		49.6	4.3	
	4.9	61.6		50.0	5.8	
	4.1	61.2		6.5	57.7	
CH 4-18	1.4	65.4		4.1	57.9	
	1.4	63.8				
	1.5	63.7				

Table 5.6a Electron Microprobe Ore Grain Analyses

Continued

Stoichiometric Concentrations in Common Ore Minerals.

<u>Mineral</u>	<u>% Ti</u>	<u>% Fe</u>	<u>% O</u>	<u>% H</u>
Haematite Fe_2O_3	0.0	69.94	30.06	0.0
Magnetite Fe_3O_4	0.0	72.36	27.64	0.0
Ilmenite FeTiO_3	31.57	36.80	31.63	0.0
Ulvospinel Fe_2TiO_4	21.42	49.95	28.62	0.0
Rutile TiO_2	59.95	0.0	40.05	0.0
Wustite FeO	0.0	77.73	22.27	0.0
Goethite FeOOH	0.0	62.85	36.01	1.13

site from which it was derived.

Most of the grains analysed were known from optical observation to have two mineralogic phases. This is shown by FB 5-18, for example, where counts on different parts of the grain yield either high titanium or high iron content. Comparison with the stoichiometric concentrations of iron and titanium in some common minerals shows that all the results may be explained in terms of titan-haematite or titanomagnetite and ilmenorutile, where the concentrations are close to haematite and rutile respectively. All the iron concentrations for counts giving high iron are a little less than for haematite or magnetite (which cannot be distinguished with 1% resolution) while all the titanium concentrations for counts giving high titanium are a little less than for rutile. The difference in each case is made up by the other element. Given the Microprobe resolution of 1 μm or a little larger it is hard to confine an analysis exclusively to one mineral phase at a time, so that the percentage of Ti in the Fe rich phase and vice versa may be high.

The analyser was also operated in a scanning mode, enabling photographs to be made of the variation of iron and titanium content over the scanning area. Photographs of iron, titanium, aluminium (in one case) and the equivalent optical picture of the grain are shown in Plates 5.6a,b,c. In Plate

Plate 5.6a Electron microprobe and optical photographs of
 an ore grain from site BL.

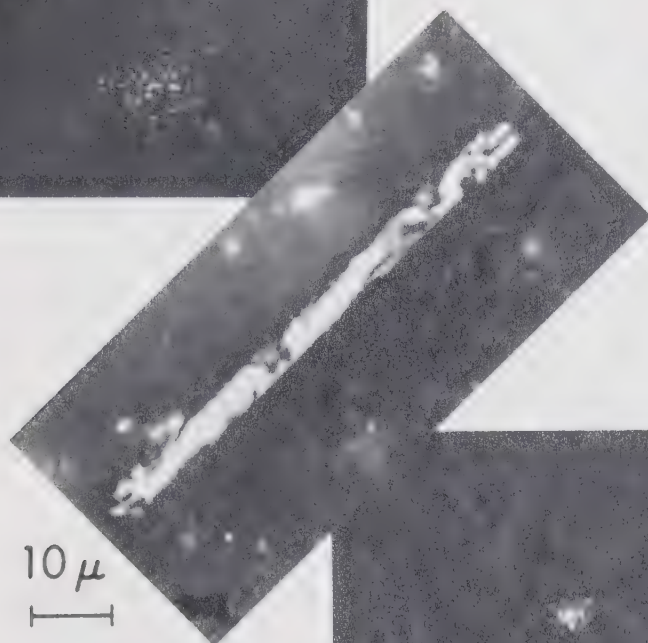
Upper Left: Microprobe picture of iron.

Middle: Optical picture of complete grain,
showing two-phased nature.

Lower Right: Microprobe picture of titanium.
Some titanium is found in the regions high in
iron.

The microprobe pictures are enlarged by a factor
of about 1.8 with respect to the optical
photograph.

143a



10 μ

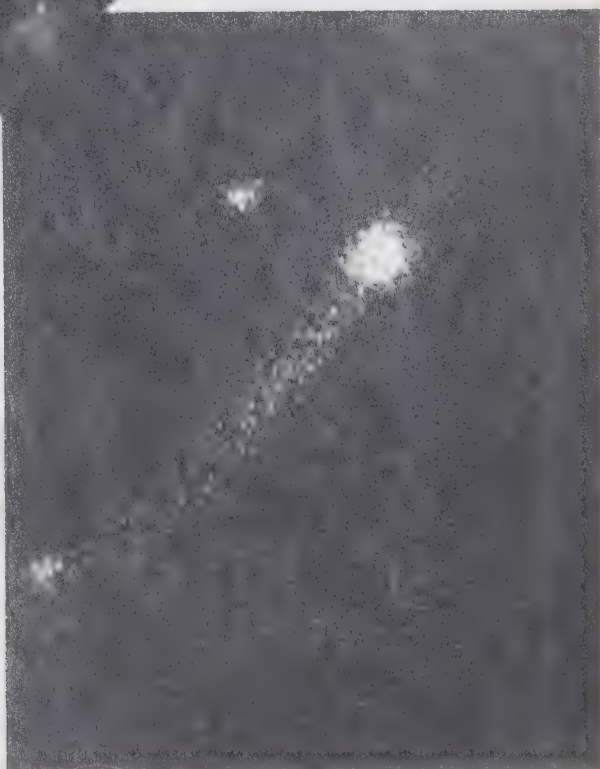


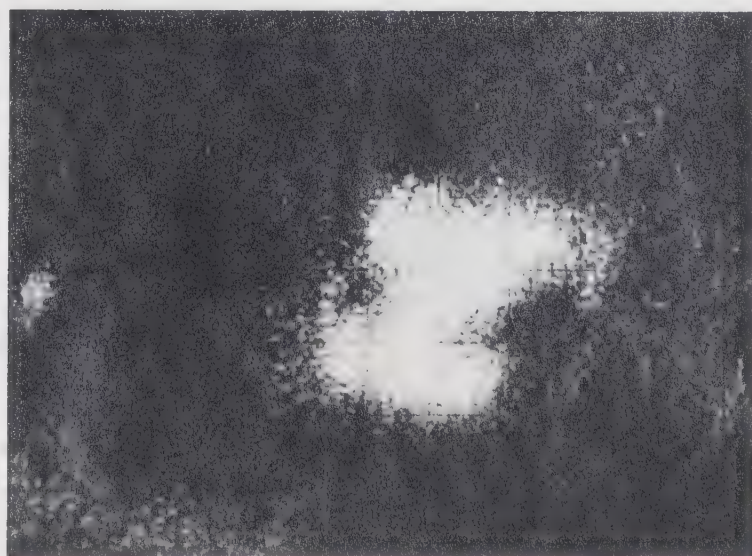
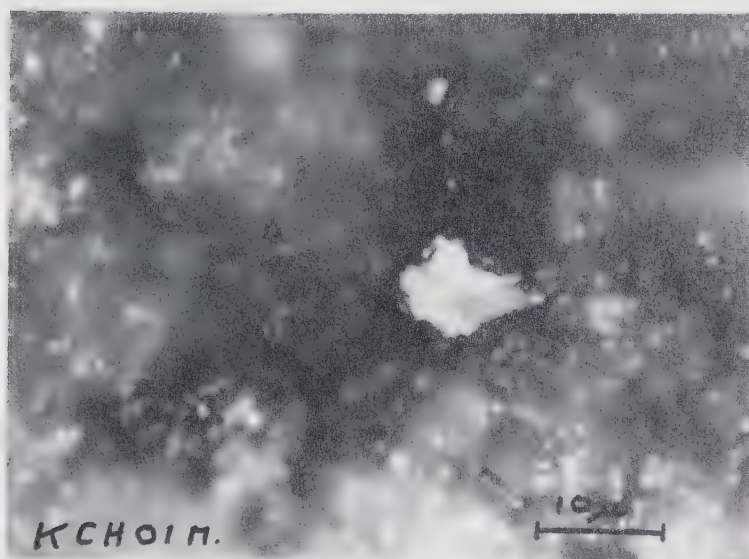
Plate 5.6b Electron microprobe and optical photographs
 of an ore grain from site CH.

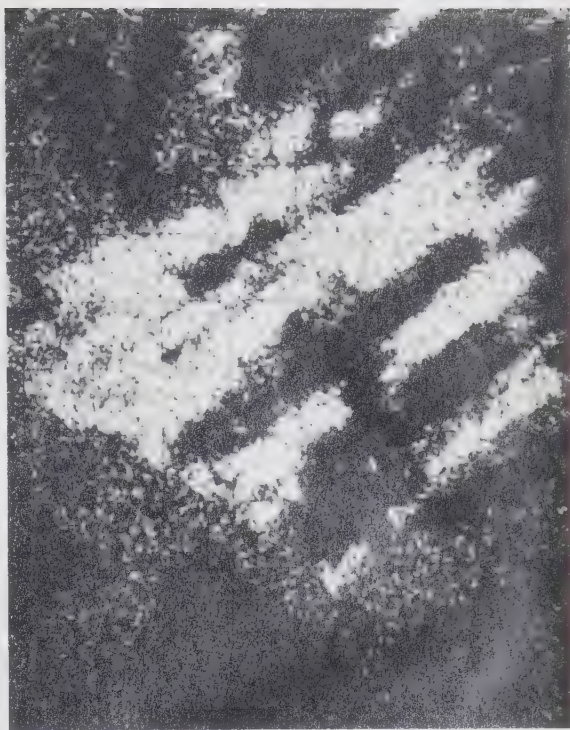
Upper: Microprobe picture of titanium.

Middle: Optical picture of the grain, showing
two-phased nature.

Lower: Microprobe picture of iron. The
titanium and iron are mutually exclusive
within the limits of resolution of the
microprobe.

The microprobe pictures are enlarged with
respect to the optical picture by a factor
of about 1.8.





10 μ
I

5.6a (Sample BL3) it can be seen that the Ti rich phase contains effectively no iron, while the Fe rich phase contains small quantities of titanium. This is also true of Plates 5.6b (Sample CH1) and 5.6c (Sample FB1). Thus in all three cases it is likely that the Ti rich phase is rutile, while the Fe rich phase is titan-haematite with a fairly small titanium content (2-3%) in the first two cases and titanomagnetite in the third case. It is suggested that magnetite is the iron rich phase in the third case because the rock is a spilitized basalt, shows a magnetite Curie point, and shows evidence of magnetite rather than haematite on optical examination (Haggerty, pers. comm.).

The Microprobe results show no difference between the B and C sections in their iron/titanium ratio, so that a similar source region for the detrital material in both sections is likely. The results also reinforce the identification of haematite and rutile by direct observation and reflectivity measurement.

5.7 Discussion. Primary and Secondary Remanence

The conclusions reached in the previous six sections may be summarized as follows:

The existence of a post-folding secondary magnetization in the direction $D = 155.9$, $I = 62.8$ has been demonstrated.

It is removed at least partially by thermal demagnetization but not by A.F. treatment.

The NRM contains both soft and hard magnetizations. The hard magnetization has greater intensity in the C, D and E sections than in the B section. The hard magnetization resides in grains with high blocking temperature. Blocking temperatures are distributed, suggesting either a grain size or a composition distribution. Magnetite Curie points are displayed by the lavas from section F.

The results from studies of IRM suggest that the soft and hard magnetizations may both arise from the same mineral phase.

Microscope observations reveal the presence of primary grains of detrital haematite, primary fine-grained haematite, secondary haematite grains (with magnetite cores) and secondary fine-grained haematite (remobilized veinlets). They also suggest a period of reheating. They demonstrate that higher concentrations of fine-grained haematite exist in the C, D and E section rocks than do in the B section rocks. Examination of the colour of the rock samples supports this contention.

Microprobe measurements indicate that the large ore grains are haematite (or magnetite) and rutile, but that little titanium is to be found in the iron rich minerals.

The apparent correlation between the amount of fine, bedded haematite present and the intensity of the cleaned magnetization suggests that the magnetization of the rocks studied is largely resident in this mineral phase. However the presence of sufficient specular haematite grains to make a significant contribution to the remanence may be easily demonstrated by multiplying the concentration of such grains as determined by grain counting by the magnetization appropriate to single domained, saturated haematite grains. A magnetization comparable to the NRM intensity is obtained. Such large haematite grains would be expected to have high coercivities and blocking temperatures. They could have a DRM (the primary detrital grains) or a CRM (the grains with residual magnetite cores).

There appear to be three possible alternatives:

(i) The remanence isolated by thermal demagnetization resides in the fine-grained bedded haematite and is a CRM acquired during lithification.

(ii) The cleaned remanence resides in the large specular haematite grains.

(iii) Both the above make important contributions to the remanence.

The apparent correlation between intensity and amount of fine-grained haematite present in the C, D and E sections

favours the first alternative for these rocks. The suggestion is further supported by the correlation between soft and hard remanence demonstrated for the C section. The soft remanence with distributed blocking temperature is much more likely to reside in ultrafine haematite with a range in grain size than it is to be in titanomagnetite with a range in compositions. No such compositional range has been found in the microprobe studies, but the haematite size range extends through the optical limit.

These arguments have less force when considering the rocks of section B, because no correlation between soft and hard magnetizations can be demonstrated for these rocks. It therefore appears likely that the large haematite grains contribute significantly to the NRM of the B section.

Finally, the rocks of section A contain very little magnetic mineral other than detrital grains, so that the remanence of the A section rocks is likely to be dominated by a DRM.

Since the existence of a secondary component of magnetization has been demonstrated, it is of interest to enquire where it might reside. The characteristics of this secondary magnetization are that it is not removed by A.F. demagnetization, but is removed by thermal treatment. This almost certainly rules out magnetite, because only magnetite

Table 5.7a Various magnetic parameters discussed
in this chapter

Site	$J_{\text{soft}} \times 10^{-6}$	$J_{\text{hard}} \times 10^{-6}$	$H_{\text{cr}} \text{ (A.F.)}$	$H_{\text{cr}} \text{ (IRM)}$	% Opaques
AA	.05-.2	.2-.3	180	-	
AB	.03-.1	.1-.2	180	-	
AC	.03-.7	.2-.7	40-180	420	
AD	0-0.08	.6-1	180	568	
AE	.6-2	.6-2	134	703	
BA	15-35	2-5	4	-	
BB	5-35	1-2	3.4	274	.67(.47)
BC	5-15	1-2	4.1	-	
BD	15-20	2-3	4	444	
BE	4-300	1-3	6.6	467	
BF	2-4	1-2	25	427	
BG	4-5	2-3	23	-	
BH	1-3	1-2	35	-	
BI	4-6	1-2	22	-	
BJ	4-10	1-5	4-150	449	
BK	1-52	2-40	11-180	460	.44(.12)
BL	5-10	.6-2	4-15	350	.6(.29)
BM	30-50	.3-2	3-4	-	
BN	15-45	1-4	3-4	-	
CA	8-11	3-7	47	-	
CB	2-12	3-4	172	-	
CC	5-7	5-9	38-180	452	.074(.016)
CD	6-8	6-9	180	439	
CE	6	6-9	30-180	617	
CF	3-14	12-15	180	-	

Table 5.7a Various magnetic parameters discussed
in this chapter

Continued

Site	$J_{\text{soft}} \times 10^{-6}$	$J_{\text{hard}} \times 10^{-6}$	$H_{\text{cr}} \text{ (A.F.)}$	$H_{\text{cr}} \text{ (IRM)}$	% Opaques
CG	8-15	6-13	20-33	572	
CH	11-17	5-6	9-18	521	.43 (.2)
CI	4-15	3-7	180	-	
CJ	8-12	6-7	9-35	547	.17 (0)
CK	2-5	6-7	180	-	
CL	5-11	6-8	180	637	
CM	2-7	3-7	180	-	
CN	4-8	2-3	9	-	
CO	1-10	2-3	6-180	545	
CP	10-15	4-5	7	-	.17 (.016)
CQ	5-18	1-5	4-10	-	
CR	2-20	4-5	7	-	
CS	8-20	2-4	6	713	
CT	5-12	2-4	7	-	
CU	0-12	1-6	180	770	.14 (.013)
CV	1-15	3-5	180	796	
CW	7-16	2-5	5	-	
CX	9-25	5-7	9	817	.07 (0)
CY	20-30	5-8	12	99	
CZ	1-5	.1-16	3-5	-	
DA	30-65	3-6	3-4	406	
DB	20-30	1-2	3-5	-	
DC	.12-20	3-4	8-12	-	
DD	1-2	1-2	23	-	

Table 5.7a Various magnetic parameters discussed
in this chapter

Continued

Site	J_{soft} $\times 10^{-6}$	J_{hard} $\times 10^{-6}$	$H_{\text{cr}}(\text{A.F.})$	$H_{\text{cr}}(\text{IRM})$	% Opaques
EA	7-9	9-14	116	-	
EB	4-15	11-13	180	-	
EC	9-15	10-15	180	-	
ED	7-17	6-11	180	-	
EE	12-15	8-10	32	-	
FA	10-20	3-11	4-9	-	
FB	75-170	1-3	3-6	-	
FC	200-400	2-12	6-13	-	
FD	9-12	1-4	4	-	
FE	5-9	.2-.4	4	-	

The ranges shown are the ranges within each site.

J_{soft} is the intensity of magnetization (Am^2/kg or emu/gm) removed by A.F. treatment in 80 mT (800 Oe) peak field.

J_{hard} is the intensity remaining after treatment in 80 mT.

$H_{\text{cr}}(\text{A.F.})$ is the "A.F. coercivity" i.e. the interpolated A.F. treatment at which the sample lost half its NRM. Quoted in mT.

$H_{\text{cr}}(\text{IRM})$ is the "I.R.M. coercivity" or steady field in which the sample gained a remanence equal to half its saturation remanence. Quoted in mT.

% Opaques is the volume percentage of ore grains greater than $1\ \mu\text{m}$ diameter as determined by microscope observation of polished sections. The volume percentage of grains greater than $15\ \mu\text{m}$ is given in parentheses.

in the single domain range stabilized by considerable shape anisotropy has sufficiently high coercivity. Haematite with size appropriate to blocking temperatures between 550 and 600°C could, however, be responsible. The calculations shown in Table 1.1a suggest that this size is a little greater than 0.4 μm diameter, i.e. the optical limit of resolution. In this size range there are two distinct modes of occurrence of haematite. One is the remobilized phase displayed in veinlets transgressing the bedding. The other is the bedded haematite itself. The former phase by its very nature should contain a secondary CRM. The latter will acquire a secondary VPTRM under appropriate conditions. It is not possible to distinguish between the alternatives here.

5.8 Discussion. Interpretation of the Palaeomagnetism

The discussion of the previous section has suggested that the magnetization isolated for the C, D and E sections is primarily a CRM acquired during lithification, while that of the B section includes the possibility of a DRM and that of the A section is primarily DRM. In addition, small secondary components may still exist in the "cleaned" magnetization. Such secondary components, probably directed approximately parallel to the normal magnetization isolated, will have much less effect on normally magnetized sites than on reversely

magnetized sites. The reversed sites are therefore probably less reliable indicators of direction than they are of polarity. They may still be used in the construction of a polarity time scale.

It was mentioned in Section 4.2 that the palaeocurrent direction observed for the Kahochella group is in the SE quadrant (Fig. 4.2b) and might be expected to influence DRM directions. Insofar as it is accepted that the magnetization of the C section is a CRM, this may be ignored, but some effect may be expected for the B section. The somewhat scattered nature of the B section results does not allow close examination of this possibility, but the mean direction of the B section normal sites was found to have a declination of 123.9° , which is about 40° removed from the flow direction. No decisive effect is therefore apparent. The possibility of palaeocurrent influence on the A section data may also be discounted, because there is an angle of about 20° between the section declination and the palaeocurrent direction for the Pethei Group.

It is concluded that the cleaned directions of magnetization for the A, C, D and E sections probably represent the direction of the magnetic field at the time of deposition (section A) and lithification (C,D,E). The results from the B section are less well understood, and should perhaps only be

used for polarity determination. It is possible that the sites with normal polarity are usable for direction determination.

6. VARIATION WITH TIME OF THE PALAEOMAGNETIC FIELD AT ca 1800 M.Y.

6.1 Introduction

In this chapter, the time interval covered by the deposition of the Kahochella Group is estimated, and this estimate is used to establish a polarity scale. The serial correlation in the data is employed to establish a tentative picture of polar wander on a time scale of 20-30 m.y. The scatter in the data is used to estimate the magnitude of secular variation and dipole wobble on time scales of about 0.6 m.y. and 20-30 m.y. Finally, palaeomagnetic poles for the A, B, C and E sections are presented together with a pole for the remagnetization event discussed in Chapter 5.

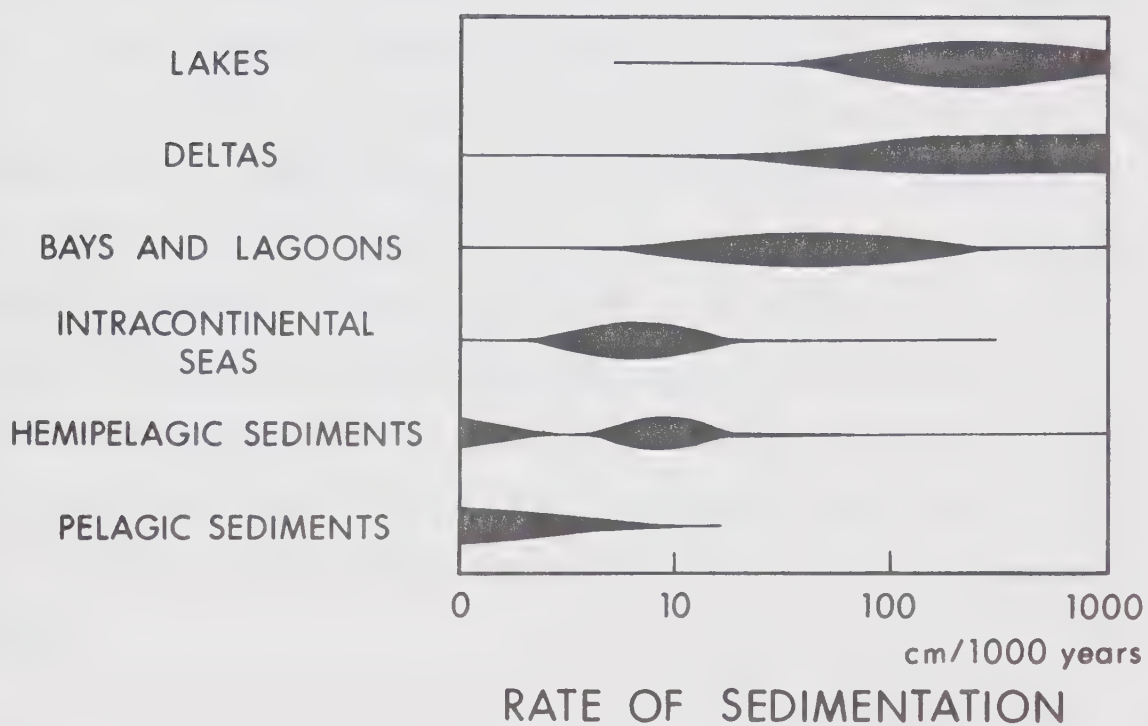
6.2 Time Resolution of Sampling

With rocks of the age of the Kahochella Group, radiometric dating methods do not have sufficient resolution to enable an estimate of the time duration involved in the deposition to be made. It therefore becomes necessary to use less direct methods. A possible candidate when studying sediments of fairly uniform lithology is the sedimentation rate. The method has been widely employed in the past (Hudson, 1964) as a means of interpolation between radiometric dates.

The maximum thickness of sediment, regardless of lithology, is usually used for the interpolation. The maximum known thickness of sediment deposited since the upper Cambrian is 375,000 ft (Hudson, 1964). This implies a maximum sedimentation rate of 20 cm per thousand years, and must certainly be higher than the sedimentation rate for shales. It does, however, form a useful upper limit to sedimentation rates estimated by other methods.

Kukal (1971) has made an extensive compilation of contemporary sedimentation rates in a variety of situations. Fig. 6.2a summarizes this compilation. The class most appropriate to a geosyncline would appear to be the intra-continental seas. The Coronation Geosyncline was roughly circular with a diameter of about 500 km, i.e. a medium sized inland sea. Since the sedimentation rate in inland seas appears to be an inverse function of the size of the basin (Kukal, 1971), this would suggest that the Coronation Geosyncline should have a sedimentation rate in the range 5 to 20 cm per thousand years (Fig. 6.2a). 10 cm/1000 years may be taken as typical. This sediment would then suffer compaction during lithification. Hoffman (1968) has estimated the amount of compaction present in the McLeod Bay Formation of the Kahochella Group (Section 4.2) by consideration of the bowing of shale laminations around calcareous concretions

Figure 6.2a Contemporary sedimentation rates observed in a variety of depositional environments. After Kukal (1971).



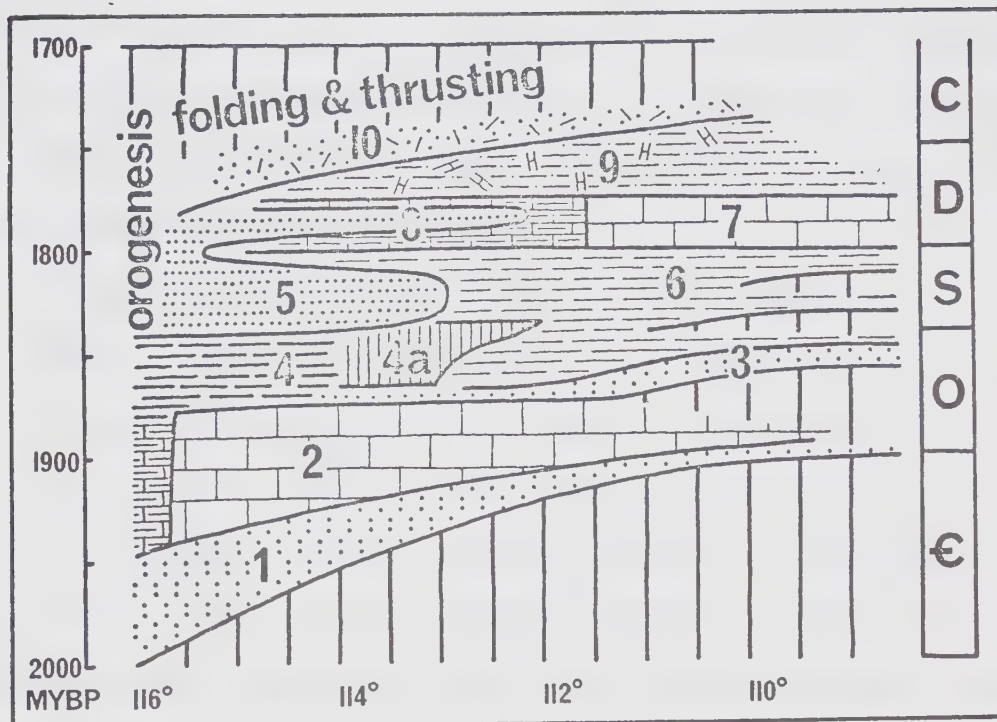
which are assumed to have undergone no compaction. He concludes that the shales have been reduced to 40% of their originally deposited thickness. This suggests that the appropriate time scale for the Kahochella Group is about 4 cm/1000 years.

Nascimbene (1963) has estimated the time scale of deposition of marine shales in the upper Cretaceous Bearpaw Sea of the southern Alberta plains by K/Ar dating of sanidine and biotite from bentonite (volcanic ash) layers in the sediments. He obtains 100 - 150 ft per million years or 3-5 cm/1000 years. Folinsbee et al. (1961), using the same method, estimate a deposition rate as measured in compacted rocks of 150 ft/m.y. or 5 cm/1000 years for the whole Cretaceous Period in the Alberta and Peace River Basins. This includes marine shales and continental sandstones, and is therefore likely to be higher than estimates for shales alone.

Hoffman et al. (1970) have proposed a detailed time-stratigraphic model for the Coronation Geosyncline based on analogies with Palaeozoic geosynclines. Their model (Fig. 6.2b) implies an age for the volcanics of the Seton Formation of 1870 to 1840 m.y. and a deposition rate for the Kahochella shales of 3.8 cm/1000 years. The first prediction has been verified by Rb/Sr dating (Section 4.2).

Figure 6.2b Time-stratigraphic model of the depositional history of the Coronation Geosyncline. After Hoffman et al. (1970).

10. Tochatwi Fm.
9. Stark Fm.
8. Pethei Gp. Off-shelf carbonate.
7. Pethei Gp. Carbonate shelf.
6. Kahochella shale.
5. Recluse Flysch.
- 4a. Seton formation volcanics.
3. Kluziai Fm.
2. Duhamel carbonate shelf.
1. Hornby Channel terrigenous shelf.



The second is taken as another estimate of the deposition rate particularly appropriate to the problem in hand.

Thus analogies with deposition rates from the present day, the Cretaceous Period and the Palaeozoic Era all yield thickness-time ratios for shales of about 4 cm/1000 years. Fig. 6.2a suggests that this is subject to variation by a factor of about two, and we have an upper bound of 20 cm/1000 years (see above).

The best estimate of the time represented by the span between sampling sites in the Kahochella Group is then 6×10^5 years (25 m at 4 cm/1000 years), while the total times represented by the B and C sections of sites are 6 and 25 m.y. respectively. The gap between the sections is about 10 m.y. All these estimates should be considered to be uncertain by a factor of two. The total time that includes all sites in the study may be estimated from Fig. 6.2b to be about 60 m.y. (from the Seton Formation to the middle of the Pethei Group at 112°W).

6.3 Reversal Rate Estimates

The polarity time scale for the Cenozoic Era has been reasonably well defined by studies of ocean magnetic anomalies. The reversal rate appears to vary from 1 to 4 reversals per million years (Section 1.1). McElhinny and

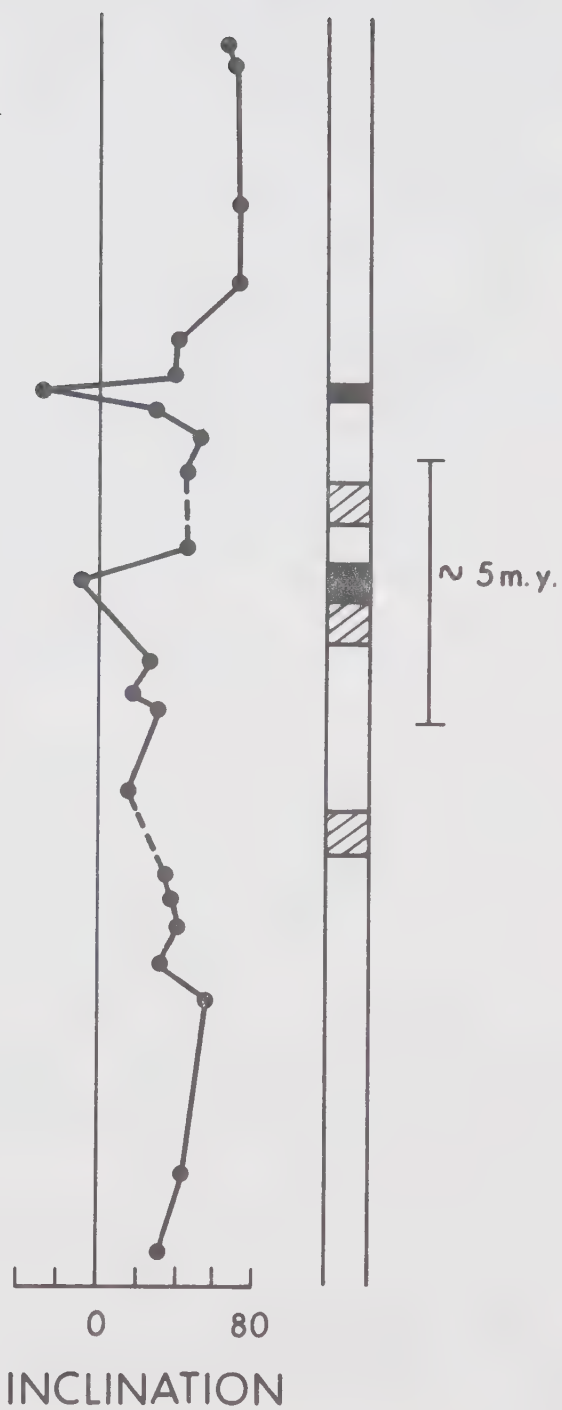
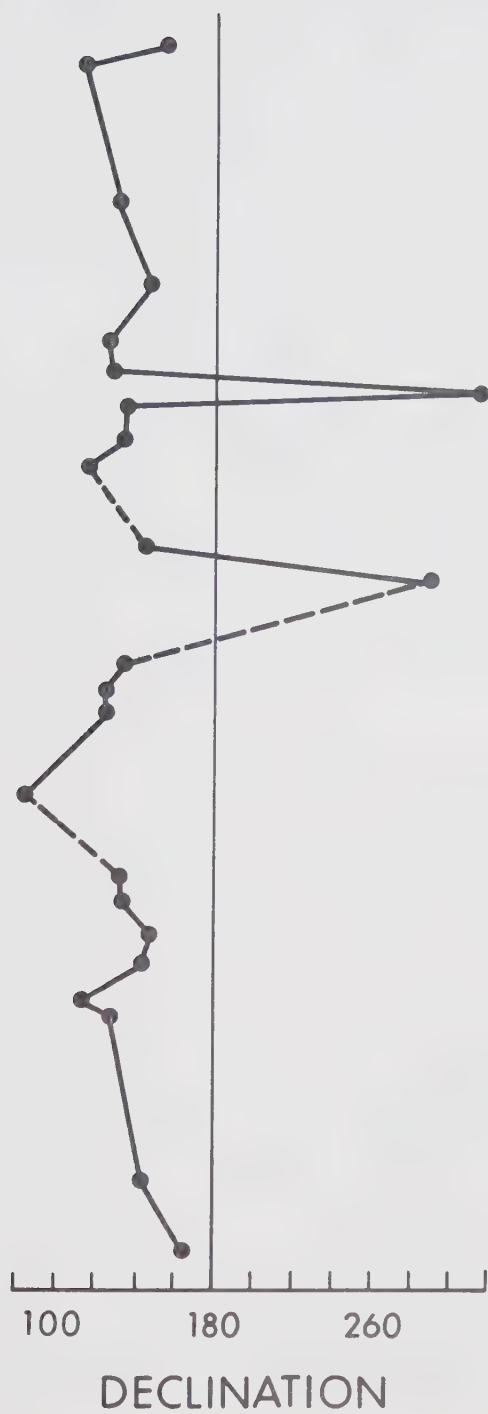
Burek (1971) have proposed a polarity time scale for the Mesozoic Era from all available information, including the results of Helsley and Steiner (1969) which indicate the existence of a predominantly normal interval during the Cretaceous. This time scale suggests that reversal rates can be as low as 0.1 per million years. A predominantly reversed interval during the Permian is now well established (Irving & Parry, 1963 ; McMahon & Strangway, 1967) although normal events within it have been reported (McElhinny & Burek, 1971).

McElhinny & Burek (1971) have proposed a nomenclature for such polarity time scales whereby geologic time is divided into "intervals" of length 10^7 or 10^8 years during which the reversal behaviour was constant, i.e. predominantly normal, predominantly reversed or of mixed polarity with a perhaps high reversal rate. Within the intervals they propose that shorter periods of polarity of about 10^6 years or less be known as zones. The term then embraces the previous terms epoch and event proposed by Cox et al. (1963, 1964).

Fig. 6.3a shows the equivalent polarity time scale for the period covered by the C section of the Kahochella Group. It comprises a predominantly normal interval containing four reversed zones. The sections labelled uncertain

Figure 6.3a Proposed variation of direction and polarity of the palaeomagnetic field with time for the C section of the Kahochella Group.

 NORMAL
UNCERTAIN
REVERSED



(shaded in Fig. 6.3a) are assigned reversed polarity because they all show some evidence of a reversed component, albeit not completely separable from a normal magnetization. The polarities "normal" and "reversed" are assigned on the convention that a normal polarity exists when the magnetization vector gives a palaeomagnetic pole on the polar wander path which ends at the present day north pole (see Chapter 7).

The upper "uncertain" zone (the stratigraphically distributed site CQ) is probably a reversed zone containing a very short normal zone. The total number of reversals (i.e. changes of polarity) detected in the C section is then 10, spread over a time span of about 25 m.y. or a reversal rate of about 0.4 per million years at about 1800 m.y.

Five sites out of a total of 27 in the C section show evidence of reversed field. The best estimate of the probability of observing reversed field at 1800 m.y. is thus $5/27$ or 0.2, which is much lower than recent measurements which give 0.5, and somewhat higher than estimates for the Cretaceous and Permian Periods which are below 0.1 (McElhinny & Burek, 1971).

A reversal time scale similar to Fig. 6.3a may be constructed for the B section, although the assignment of polarity must of necessity be a little more arbitrary. Such

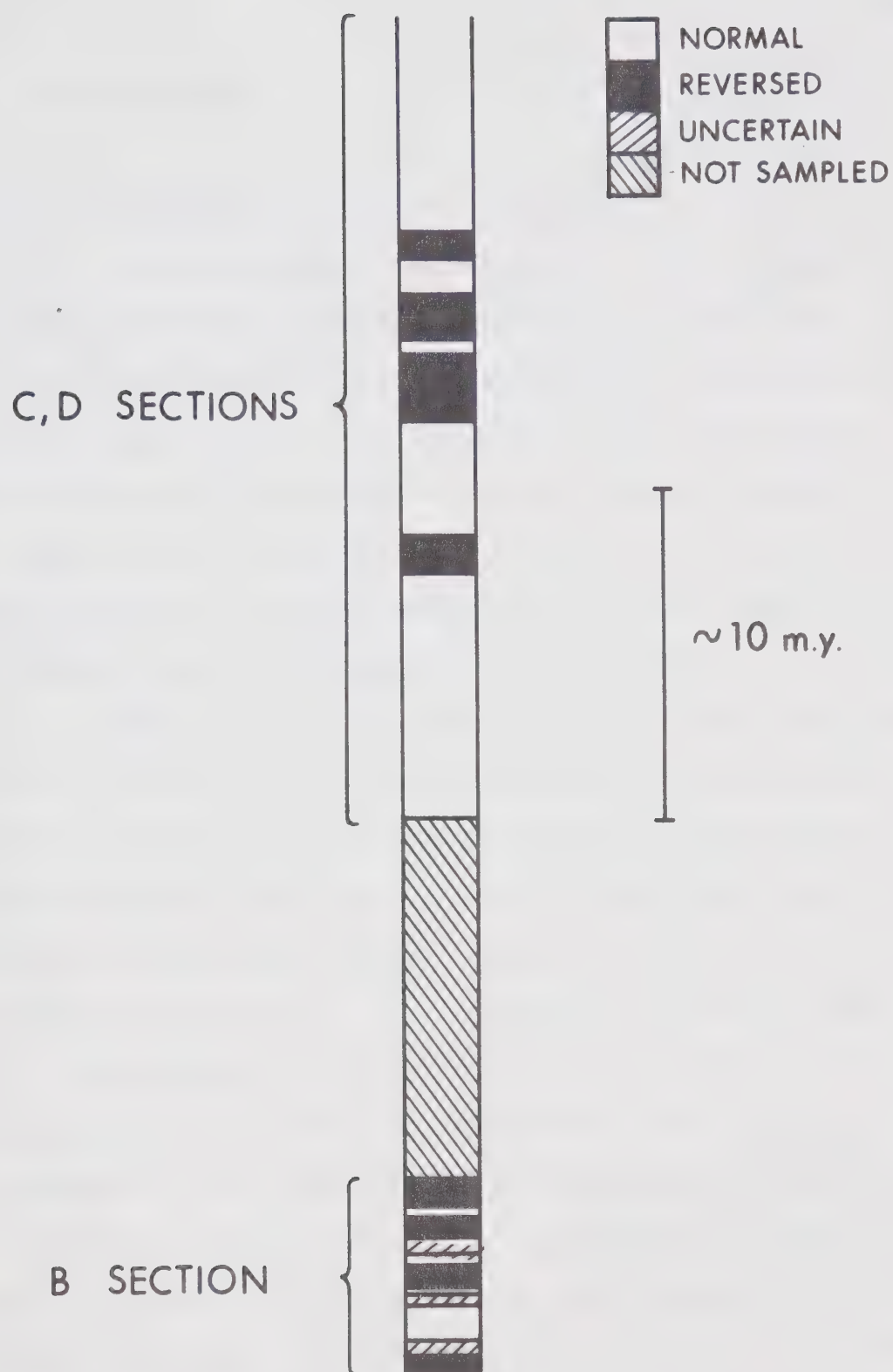
a time scale is shown in Fig. 6.3b for the whole Kahochella Group. Polarity has been assigned to all sites showing tendencies to either normal or reversed directions. It has not been assigned only where the site was random or showed no clear tendency to either polarity. A large interval for which no data are available exists between the B and C sections. It may be seen that the B section has a higher proportion of reversed sites than was found in the C section. Of the eleven sites to which a polarity may be assigned, five are reversed. Furthermore, at least seven reversals may be identified, giving a minimum reversal rate of a little more than 1/m.y.

Thus reversal rates for the B and C sections may be assigned minimum values of 1.1 and 0.4 reversals per million years respectively. Section A has normal polarity at all sites from which a direction is recoverable, but there is a considerable time gap between it and the top of the C section.

6.4 Secular Variation, Dipole Wobble and Apparent Polar Wander

The approximately known time relationship between sites in this study may further be exploited to examine the variations in direction shown by the geomagnetic field. In this section, the secular variation is examined on two time scales (0.6 and 25 m.y.) and the motions of the palaeomagnetic

Figure 6.3b Proposed variation of polarity of the palaeomagnetic field with time for the B and C sections of the Kahochella Group.



pole are examined.

6.4.1 Calculation of between-site scatter

The statistical parameter θ_{63} (the circular standard deviation given approximately by $81/\sqrt{k^0}$) may be employed as a measure of the dispersion in the data caused by variations in the field direction with a time scale shorter than the time spanned by the sampling (Creer, 1962). The value of θ_{63} calculated for the distribution of site mean directions is influenced by the uncertainties in the site mean directions themselves. This effect may be removed in favourable cases by the application of a two-tier analysis (Watson & Irving, 1957) which enables an estimate to be made of the value of θ_{63} freed of the effects of within-site scatter. Such an analysis has been applied to the C and E section site mean directions after thermal cleaning (Table 4.3.3b). The E section data include sites CE and CF, giving 7 sites in all. The analysis is strictly only applicable when the within-site precision is similar at all sites. This is only approximately true here, but the results may be considered to constitute a good indication. Tables 6.4.1a and 6.4.1b show the results of this analysis. The parameters calculated are the within-site and between-site precisions and their corresponding standard deviation angles. They are called

Table 6.4.1a Two-tier analysis of variance, C section

Number of sites, $B = 21$.

Number of specimens, $N = 83$

Resultant of specimens, $R = 78.248546$

Resultant of site means, $R_s = 20.03397$

Sum of the site resultants, $\sum_i R_i = 82.00698$

Weighted mean number of specimens per site

$$\bar{N}_i = (N - \sum_i N_i^2 / N) / (B - 1) = 3.94819$$

N_i is the number of observations at the i th site.

Source of Dispersion	Degrees of Freedom	Sum of Squares	Mean Square	Expectation of MSQ
Between Sites	$2(B-1)$ 40	$\sum_i R_i - R$ 3.7584	$\frac{\sum_i R_i - R}{2(B-1)}$.09396	$\frac{1}{2} \left(\frac{1}{\kappa_w} + \frac{\bar{N}_i}{\kappa_b} \right)$
Within Sites	$2\{\sum_i (N_i - 1)\}$ 124	$\sum_i (N_i - R_i)$.99302	$\frac{\sum_i (N_i - R_i)}{2 \sum_i (N_i - 1)}$ 8.00822E-3	$\frac{1}{2\kappa_w}$
Total	$2(N-1)$ 164	$N - R$ 4.751454		

The variance ratio $F = 11.73$. The significance point for $P = 0.01$ is 1.75, so the between-site variance must be considered significant.

Hence κ_w , the within-site precision, = 62.4 and $\theta_{63w} = 10.2^\circ$.

κ_b , the between-site precision, = 22.9.

$\theta_{63b} = 16.9^\circ$.

Table 6.4.1b Two-tier analysis of variance, E section

Number of sites, $B = 7$

Number of specimens, $N = 28$

Resultant of specimens, $R = 27.422123$

Resultant of site means, $R_s = 6.888738$

Sum of the site resultants, $\sum R_i = 27.85711$

Weighted mean number of specimens per site = 3.98809

Source of Variance	Degrees of Freedom	Sum of Squares	Mean Square
Between Sites	12	.434987	3.62489E-2
Within Sites	42	.14289	3.402E-3
Total	54	.577877	

$$F = \frac{3.62489E-2}{3.402E-3} = 10.7: \text{Significance point at } P = 0.01 \text{ is } 2.64.$$

Between site variance is therefore significant.

$$\text{Hence } \kappa_w = 147, \theta_{63w} = 6.7^\circ \quad \text{and} \quad \kappa_b = 61, \theta_{63b} = 10.4^\circ.$$

k_w , k_b , θ_{63w} and θ_{63b} respectively here. In both cases, the values of between-site precision with the effects of within-site variation removed (i.e. k_b) are very little different from the values calculated from

$$k = \frac{N-1}{N-R}$$

This indicates that the within-site scatter has little effect because it is small.

The palaeolatitude for the Kahochella Group deduced from the inclination of the C and E section directions is 27° . θ_{63} for this latitude has been calculated for the 1945 field by Irving (1964), taking an average around a line of geographic latitude and using both hemispheres. He obtains a value of 14° . Brock (1971) calculates a best fitting value of 14.5° for this palaeolatitude from an analysis of palaeomagnetic results for all ages. The results obtained for the C and E sections are 16.9° and 10.4° .

We may test the hypothesis that the calculated values of θ_{63b} are different from the 1945 values by referring the ratio of their equivalent k values to the tables given by Cox (1969). The assumption inherent in the use of this test is that the standard value (for the 1945 field here) is precisely known. In neither case is there reason to believe (at 95% confidence) that the scatters observed for the C and

E sections are different from the 1945 values or the best fitting palaeomagnetic values.

Since one value of k_b is higher than the present day value while the other is lower, the possibility exists that they are different from each other. We may test this hypothesis by referring the ratio $k_b(E)/k_b(C)$ to the F-ratio tables for 40 and 12 degrees of freedom (Watson, 1956a; McElhinny, 1964). The ratio has the value 2.66. The 95% critical point is 2.0. The hypothesis that the two values are indistinguishable from each other may thus be rejected.

Thus although the calculated values of scatter for the C and E sections cannot be distinguished from the scatter of the 1945 field, they can be distinguished from each other. This being the case, it is of interest to consider how this difference might arise.

The time span of the E section, calculated by the same deposition rate analogy as used in Section 6.2 is about 0.6 m.y. (23 metres from CE to CF at 4 cm/1000 years) compared to the time span of 20 - 30 m.y. estimated for the whole C section. It is thus likely that the difference between the two estimates of scatter is due to the inclusion in the C section data of a field variation with characteristic time longer than 0.6 m.y. The discussion of Section 1.1 suggests that the E section time span should adequately average out

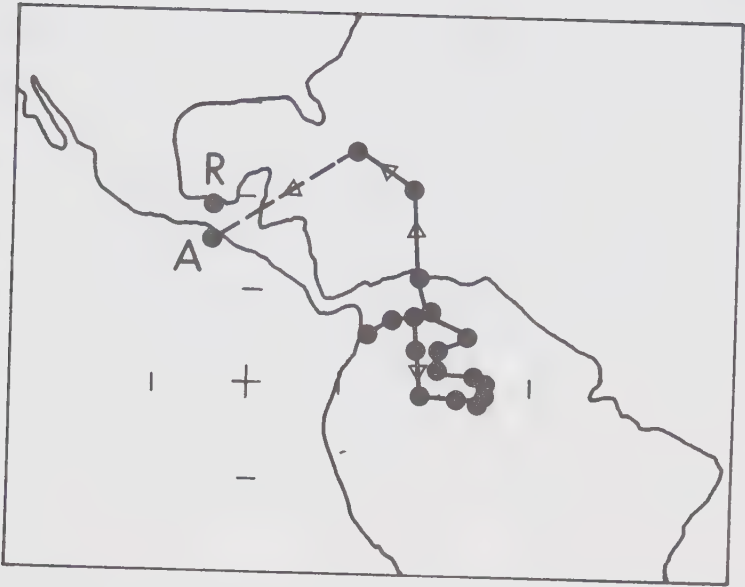
secular variation and dipole wobble, while the C section time span may well include some apparent polar wander or random walking of the rotation axis.

These suggestions are somewhat dependent on the assumption that the characteristic times of the above phenomena have not changed substantially since 1800 m.y. and that the estimated time spans are correct to within an order of magnitude. Irrespective of these assumptions, the time span of the E section cannot be far from 1/40 of the time span of the C section and their standard deviation angles are 10.4° and 16.9° . It seems most likely that the C section mean includes some apparent polar wander.

6.4.2 Apparent polar wander and dipole wobble

Examination of Fig. 6.3a suggests that the plots of declination and inclination against time for the C section show some serial correlation. This was investigated by calculating a 5 site running mean direction, and mapping the mean directions so found to palaeomagnetic poles. The results are shown in Fig. 6.4.2a. There appears to be one cycle of variation followed by a northward trend. Included in the plot are the poles for the A section (somewhat later in time than the top of the C section) and the remagnetization direction discussed in Chapter 5. The trend does not lie along

Figure 6.4.2a Variation with time of the palaeomagnetic pole for the C section of the Kahochella Group. Calculated from a five site running mean of the directions at each site. The remagnetization and A section poles are also shown.



the polar wander path deduced from other palaeomagnetic results for this age range (Chapter 7). Two possibilities exist. Either further detail in the apparent polar wander path for this age range (with perhaps an extra loop) is necessary, or the results display a short time scale random walk which is averaged out over longer time scales to give the deduced polar wander path. If the latter suggestion is correct, we may expect that other results where the serial correlation over similar time scales may be examined, will yield similar fine structure. Helsley and Steiner (1971) have found a similar serial correlation in the lower Triassic Moenkopi Formation, but they estimate the time span of their data to be about 3 m.y. They suggest that the three cycles they observe over this period represent secular variation.

6.5 A Palaeomagnetic Pole for the Kahochella Group

The mean directions for the A, B, C, E and F sections have been mapped to palaeomagnetic poles using the usual geocentric dipole assumption. The results are shown in Table 6.5a and on Fig. 6.5a.

Fig. 6.5a has several noteworthy features. The poles for the C and E sections coincide, which is to be expected, since the E section was sampled between two sites in the C section. The poles for sections A and F and the

Table 6.5a Palaeomagnetic poles for the Great Slave
Supergroup

<u>Section</u>	<u>N</u>	<u>Longitude</u>	<u>Latitude</u>	<u>dp</u>	<u>dm</u>	<u>Notes</u>
A	4	94.1°W	14.6°N	30°	40°	
B	6	80.0°W	40.3°N	23°	25°	
B	3	81.6°W	20.5°N	9°	11°	1
C	21	72.2°W	6.2°N	6°	9°	2
E	5	73.6°W	6.3°N	7°	10°	
F	5	94.7°W	34.0°N	23°	26°	3
Remag.	15	94.0°W	18.0°N	8°	10°	4

Notes

1. Sites BG, BI, BL.

2. Includes DC, DD.

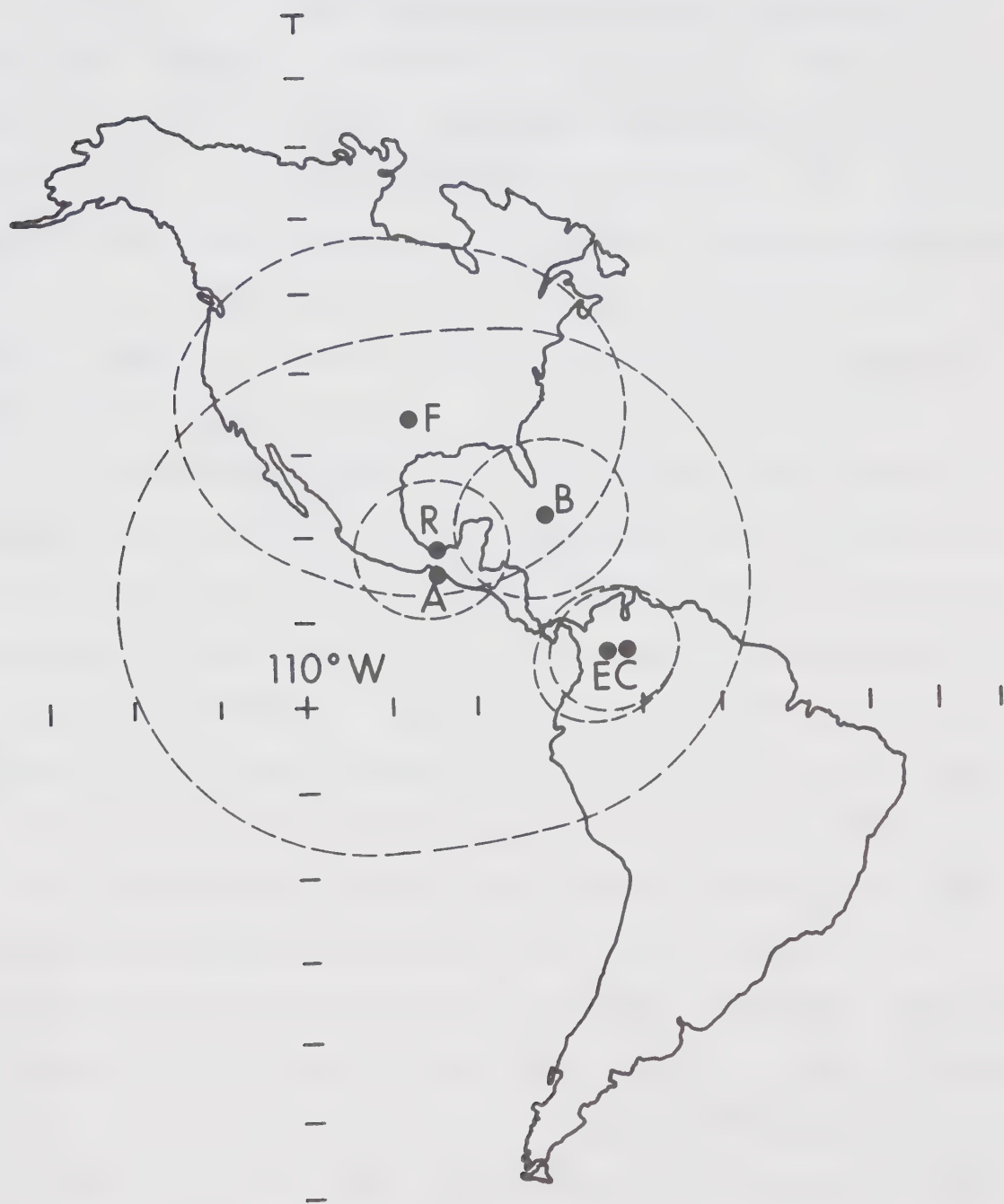
3. Before dip correction.

4. Calculated from removed vectors (Section 5.2).

N is the number of sites included in the analysis.

dp, dm are the major axes of the oval of 95% confidence
about the pole.

Figure 6.5a Section mean palaeomagnetic poles for the rocks of the Kahochella Group. The B section pole is calculated from three "normal" site directions.



remagnetization all have considerable overlaps of their ovals of confidence. It has been suggested earlier (Section 5.2) that the F section is completely remagnetized. This is consistent with the almost complete overlap between the R and F ovals. The close agreement between the R and A poles suggests that the remagnetization may have taken place during deposition of the Pethei Group, but the conclusion is far from unique, especially considering the large oval of confidence about the A section pole.

The results for the B section have been further examined by calculating the palaeomagnetic pole corresponding to each site direction for the six normal sites. The results are shown in Fig. 6.5b. It is clear that the distribution is far from Fisherian. Since the sites are ordered in time, we may propose a polar wander path for the time represented by the sites near the bottom of the B section. Examination of Fig. 6.5b suggests either that a field excursion has been recorded by these sites or that they show the path of a reversal between the reversed site BA and the normal group of BI, BG and BL. If this is the case, the best normal direction for the B section is the mean of the site directions at sites BG, BI and BL. This direction maps to a palaeomagnetic pole at 81.6°W , 20.5°N (Table 5.6a).

This interpretation of the results from the B section provides a possible solution to a problem raised in Chapter 5,

Figure 6.5b Palaeomagnetic poles for each "normal" site in the B section. The time ordering of the poles suggests that a field excursion may have been observed.



that the mean intensity of the reversed B section sites is greater than the mean intensity of the normal sites. If the normal group includes three transitional directions, it is not surprising that the mean intensity is lower, because the intensity of the field is observed to decrease by a factor of about five during transitions (Lawley, 1970). Splitting the intensity results into normal B section and transitional B section yields small populations (twelve) for this type of analysis. In fact, no significant difference is detected.

It is thought that the poles for the C and E sections best represent the position of the palaeomagnetic pole at 1800 m.y., freed of the effects of remagnetization. However the relatively large scatter of the "reversed" site directions (compared with normal sites) for the B and C sections suggests that a substantial remagnetized component remains after cleaning. This may also be true for the normal sites, although the direction of the remagnetization is such as to affect normal sites rather less. If this is the case the mean direction for the normal sites quoted may be too steep. A shallower inclination would result in a palaeomagnetic pole southeast of the pole quoted here.

The palaeolatitude implied by the C and E section poles is 27° if an axial dipole is assumed. This is in agreement with the palaeolatitude spectrum of redbeds compiled by

Briden and Irving (1964) which shows 88% of the occurrences to be within 30° of the palaeoequator.

7. ANALYSIS OF PRECAMBRIAN RESULTS FOR NORTH AMERICA

All publications known to the author which give palaeomagnetic results for the Precambrian of North America are listed in the bibliography of palaeomagnetic results at the end of this chapter. Selection criteria have been applied to these results to eliminate those whose meaning is uncertain. The remainder are listed in Table 7.3a and depicted in Fig. 7.3a, together with the Precambrian polar wander path which most simply fits the results.

7.1 Acceptance Criteria

No results for the rocks of the Grenville Province have been accepted because Irving, Park and Roy (1972) have suggested that the Grenville Province has moved as a whole relative to the rest of North America. No results for the Sudbury Irruption are given because, despite considerable work, (Laroche, 1969) it is not yet possible to say what tectonic corrections should be applied to the north and south ranges of the body.

Results were not accepted unless the stability of magnetization was demonstrated by A.F. or thermal treatment.

Results were not accepted if only single samples at each site were taken, unless such studies on rocks of the same age could be combined.

Finally, results were not accepted unless some indication (radiometric or stratigraphic) of the age of the rock was available. When a large number of results for a particular age was available (e.g. for the Keweenawan) only the more recent were used.

Where possible, results for rocks of the same age were combined (see Table 7.3a) to yield an average pole for the time in question.

The results remaining after these selection criteria were applied are listed in Table 7.3a. The criteria were relaxed in the cases where the rock units studied were particularly old (i.e. the Matachewan, Molson and Marathon dykes) so that no better result of similar age was available.

Those selected results for which the number of sites exceeded 10 (9 in the case of the Stillwater Complex - the oldest result) or which were the result of combining multiple studies have their circles or ovals of 95% confidence marked on Fig. 7.3a. These points were used to outline the polar wander path.

7.2 Dating Problems

Recent efforts by the GSC to obtain K/Ar dates on all formations studied geologically have made it possible to define a K/Ar age for nearly all palaeomagnetic results from

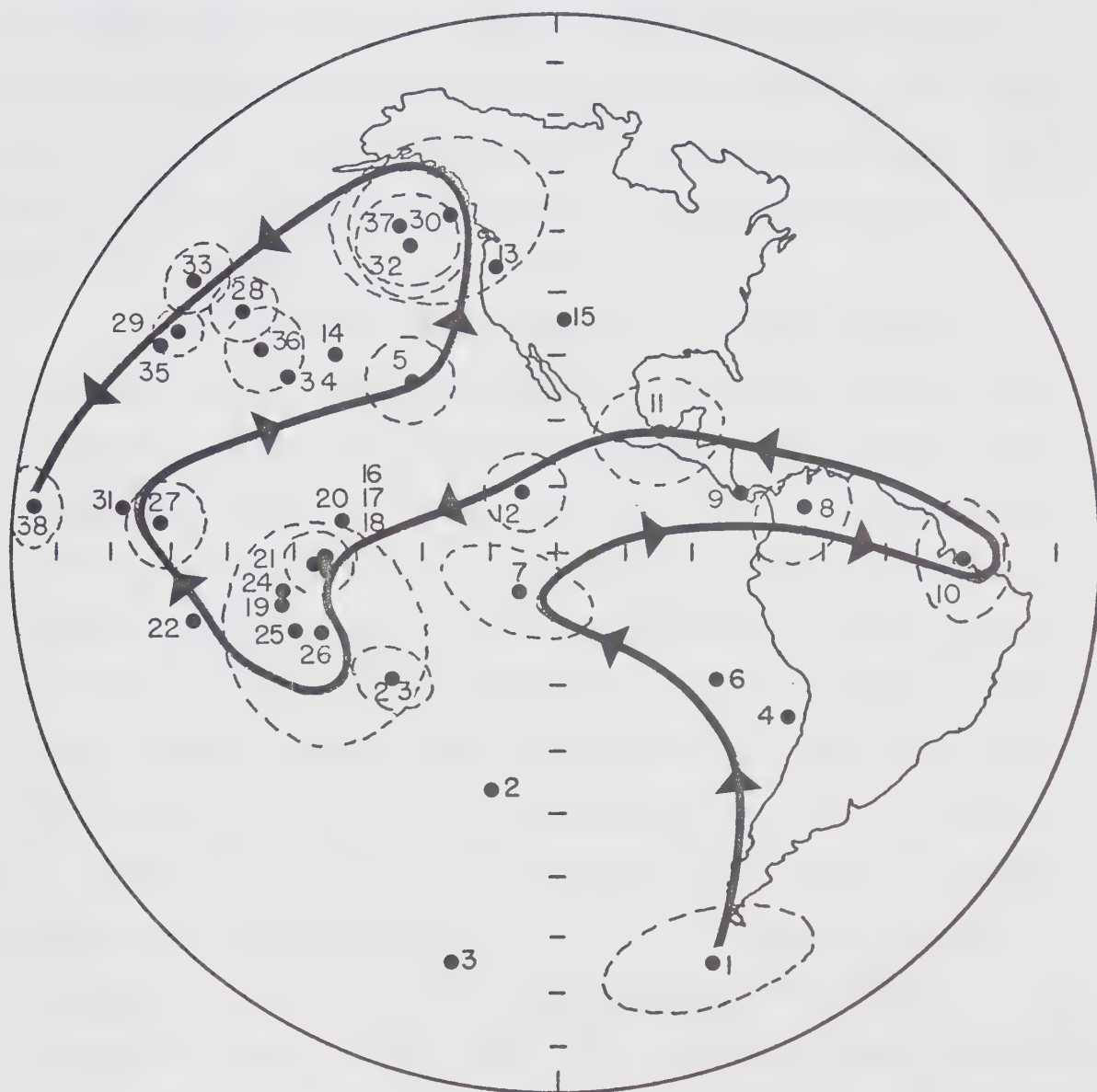
the Canadian Shield. The susceptibility of such dates to resetting by orogenic events has been exploited to date the orogenies themselves (Table 4.2.1). It is therefore uncertain in many cases whether the K/Ar date represents the time of magnetization of the rock. Where available, Rb/Sr whole rock isochron ages have been quoted. Even these are, however, open to question on occasion. Note 24 for Table 7.3a illustrates a case where isochron ages obtained on the same rock formations can disagree significantly. The age of the Mackenzie event has been taken to be 1200 m.y. as the result of comprehensive K/Ar and isochron dating, but Gates (1971) has obtained isochron ages of 1600 m.y. from two formations considered to belong to the Mackenzie event. Since Gates' results have only appeared in thesis form, while the others are open to criticism in the literature, the 1200 m.y. age has been taken in this case.

7.3 The Precambrian Polar Wander Path for North America

The polar wander path deduced from selected Precambrian results from North America is shown in Fig. 7.3a.

Some features of particular interest are apparent. The clustering of results at 145°W , 1°S for rocks whose ages are close to 1400 m.y. is an indication of the dipolar nature of the palaeomagnetic field at 1400 m.y. The rock units

Figure 7.3a A Precambrian apparent polar wander curve for North America. The numbers refer to Table 7.3a. Circles or ovals of confidence are plotted for the poles which include measurements from rocks sampled at ten or more sites.



EQUAL AREA PROJECTION CENTRED ON
110°W 0°N

contributing to this group have been sampled from widely scattered locations in North America, and have magnetic inclinations varying from 10° to 44° of both polarities. The result may also be taken as an indication of the integrity of the continent since 1400 m.y. Similar conclusions may be drawn from the clustering of results from the Mackenzie igneous event at 1200 m.y.

It is to be expected that the polar wander path postulated will change somewhat in the near future. Preliminary results for the Stark Formation of the Great Slave Supergroup (Dr. D. K. Bingham, pers. comm.) indicate that further detail is likely to be added to the curve in the Aphebian age bracket. Irving, Park and Roy (1972) display a polar wander path for the later Precambrian which includes a much deeper "Logan Loop" (Robertson & Fahrig, 1971) than is displayed in Fig. 7.3a. The tip of the loop is defined by poles 30, 32, 37 at a latitude of about 50°N . The loop displayed by Irving, Park and Roy (1972) extends almost to the pole. This is not justified by results available in the literature, but they say that they are using unpublished data which, when published, will lead to alterations to the curve in this region.

The pole from the Kahochella Group has joined with that from the Et-then Group in revealing a loop in the polar

wander curve across South America whose existence has not previously been suspected (see Spall, 1972). The close agreement between poles for the Kahochella and Dubawnt Groups suggests that their ages may be very close. The position of the remagnetization pole for the Kahochella Group suggests that the remagnetization event is pre-Western Channel Diabase.

7.4 Comparison With Other Palaeoblocks

The only other continent for which comprehensive Precambrian results are available is Africa (McElhinny et al., 1968). The North American and African polar wander paths have recently been compared by Spall (1972). He points out that it is not possible to superimpose the two curves, indicating relative drift between North America and Africa during at least parts of the Precambrian. The modifications to the path for North America brought about by poles 8, 9 and 10 do not alter this conclusion. This is in qualitative agreement with the relative movements between Africa and North America proposed by Schenk (1971) on geological grounds.

Table 7.3a Precambrian Pole Positions Relative to North America

<u>Formation</u>	<u>Date</u>	<u>Method</u>	<u>Long.</u>	<u>Lat.</u>	<u>dp</u>	<u>dm</u>	<u>N</u>	<u>Author</u>
1. Stillwater	2450±210	WR-Iso	68W	62S	8	13	9	Bergh, 1970
2. Matachewan SW	2485	WR-K/Ar	120.8W	37.2S	6	12	39*	Fahrig et al., 1965
3. Matachewan NE	2690±93	WR-Iso	139.7W	62.9S	13	22	15*	Fahrig et al., 1965
4. Abitibi ENEN	2147±68	WR-Iso	73W	24S	12	20	2	Larocheville, 1966
5. Abitibi ENEW	1230	Min-K/Ar	134W	27N	6	7	10	Larocheville, 1966
6. Nipissing	2162±27	WR-Iso	86.4W	19S	23		2	Symons, 1970, 1971
7. Indian Harbour	2080±42	WR-K/Ar	117W	6S	6	12	12	Murthy & Deutsch, 1972
8. Kahochella C.	1800	WR-Iso	72.2W	6.2N	6	9	21	This thesis
9. Dubawnt	1732±9	WR-Iso	82W	8N	?	?	?	See notes
10. Et-then	-	-	48.0W	1S		8	14	Irving, Park & McGlynn, 1972
11. Kahochella Remag.	See notes	-	94W	18N	8	10	15	This thesis
12. Western Channel	See notes	-	115W	9N		6	35	Irving, Donaldson & Park, 1972
13. Wind R.	1880 2060	Min-K/Ar	121W	43N	23	23	4	Spall, 1971a
14. Marathon	1810	WR-K/Ar	146.8W	29N	12	16	9*	Fahrig et al., 1965
15. Molson	1445	WR-K/Ar	108.9W	36.2N	27	28	5*	Fahrig et al., 1965
16. Michikamau	1400	Min-K/Ar	144.7W	0.5S	5.6		6	Murthy et al.

Table 7.3a Precambrian Pole Positions Relative to North America

Continued

<u>Formation</u>	<u>Date</u>	<u>Method</u>	<u>Long.</u>	<u>Lat.</u>	<u>dp</u>	<u>dm</u>	<u>N</u>	<u>Author</u>
17. Missouri Tuffs	1300-	Min-Rb/Sr Min-K/Ar	142.6W	1.2S	5	7	11	Hsu et al., 1966
18. Missouri Ign.	1400	WR-Iso	144.3W	1.3S	8	12	5**	Hays & Scharon, 1966
19. Front Range Granites	1410±30	WR-Iso	151W	8S	6	9	5	Eggler & Larson, 1968
20. Croker Isl.	1475±50	WR-Iso	142.8W	5.4N	7	10	23*	Palmer, 1969
21. 13-17 Above	1400		145.1W	1.1S	5.5		5**	
22. Colorado diabase	1400?		167.4W	8.6S	?	?	32	Kellogg, 1971
23. Grinnell (prov.)	1325±15	WR-Iso	136W	18S	4	6	27	McMurry, pers. comm.
24. Kintla	1325±15	WR-Iso	152W	6.7S	11		3	Norris & Black, 1961
25. Purcell	1325±15	WR-Iso	149.8W	11.2S	12		5**	Black, 1963
26. 20-22Above	1325±15		146.1W	12S	16		3**	
27. Mackenzie	1205±50	WR-Iso						
	1660±145	WR-Iso	171W	3N	6		7**	See notes
	1200 Multiple K/Ar		167W	33N	5		7**	Beck, 1970
28. Normal Rocks Kew.			177.1W	29.2N	4		4**	Palmer, 1970
29. Normal Rocks Kew.			133.5W	50.7N	13		6**	Palmer, 1970
30. Rev. Rocks Kew.			179W	6N	4	8	4	Spall, 1970a
31. Pikes Peak	1040	WR-Iso						

Table 7.3a Precambrian Pole Positions Relative to North America

<u>Formation</u>	<u>Date</u>	<u>Method</u>	<u>Continued</u>				<u>Author</u>
			<u>Long.</u>	<u>Lat.</u>	<u>dp</u>	<u>dm</u>	
32. Logan Sills	1050	WR-K/Ar	140W	47N	8		Robertson & Fahrig, 1971
33. Logan Dikes	1020	WR-K/Ar	179W	35N	5		Fahrig, 1971
34. Oklahoma Gran. Baked cont.	1107±22	WR-K/Ar	154W	25N	14	19	Spall, 1970b
35. Arizona Sills	1140	Min-K/Ar	179W	27N	6	9	Helsley & Spall, 1972
	1150±30	Concord.					
36. Texan Granites	953±13	WR-Iso	160W	28N	5	6	Spall, 1971b
37. Mugford Basalt	948±90	WR-K/Ar	143W	49N	9	11	Murthy & Deutsch, 1972
38. Franklin Int.	675±25	WR-K/Ar	165.3E	4.8N	4.7		Robertson, & Baragar, 1972
							Fahrig et al., 1971

Date is quoted in millions of years.

Method. WR-Iso. Rb/Sr whole rock isochron.

WR-K/Ar. K/Ar whole rock analysis.

Min-K/Ar. K/Ar mineral analysis.

Concord. U/Pb concordia plot.

Table 7.3a Precambrian Pole Positions Relative to North America

Continued

Long., Lat. Longitude and latitude of palaeomagnetic pole.
 dp,dm. Angular semi-axes of the oval of 95% confidence about the pole.
 Where one figure is given, it is A_{95} , the radius of 95% confidence about a mean pole.

N. The number of sites sampled from independent rock units. * denotes samples. ** denotes formations or studies. Author refers to the bibliography of palaeomagnetic results.

Notes on Table 7.3a

1. Corrected for tilt of layering. Date by Fenton and Faure (1969). Dating picture confused by previous publications in abstract form by Fenton & Faure. Date quoted by Bergh is an early abstract preprint.
- 2,3. Fahrig et al. quote K/Ar whole rock date of 2485 m.y. and a K/Ar hornblende date of 1740 ± 200 . Gates (1971) obtains 2690 ± 93 by Rb/Sr whole-rock isochron.
- 4,5. Fahrig and Wanless (1963) quote a K/Ar age of 1230. Gates (1971) obtains 2147 ± 68 by Rb/Sr whole-rock isochron on samples from the ENEW trend. Polarity reversed for ENEN pole. ENEN errors calculated from quoted value of k.
6. Fairbairn et al. (1969) obtain a date of 2162 ± 27 by Rb/Sr whole-rock isochron on samples from the Nipissing Diabase. Van Schmus (1965) obtains 2155 ± 80 by the same method. A mineral isochron gives 1700 ± 50 , indicating metamorphism at this date. Palaeomagnetic results recalculated giving unit weight to sills and ignoring some scattered site directions.
7. Murthy and Deutsch quote a K/Ar whole-rock date of 2080 ± 42 .
8. Calculated by deposition rate model from Rb/Sr whole-rock isochron age of 1873 ± 13 on underlying Seton Formation (H. A. Baadsgaard, pers. comm.).
9. Park et al. (1972) (Can. J. Earth Sci., in press), quoted by Irving, Donaldson and Park (1972). Pole position esti-

mated from diagram. Date by Fraser, Donaldson, Fahrig and Tremblay (1970).

10. Irving et al. give the age as late Aphebian or early Palaeohelikian.
11. Remagnetization is post-folding. This occurred before the deposition of the Et-then Group which is late Aphebian or early Palaeohelikian. The pole is calculated using the vectors removed by thermal treatment over the step $550^{\circ}\text{C} - 600^{\circ}\text{C}$.
12. Irving et al. bracket the age between a K/Ar (biotite-hornblende) date of 1400 ± 75 and the K/Ar age of the country rock (1785 m.y.). Sites are probably not all in separate sills.
13. Spall quotes a range of K/Ar whole rock and mineral ages from 1680 to 2060.
14. Fahrig et al. quote a K/Ar whole rock age of 1810.
15. Fahrig et al. quote a K/Ar whole rock age of 1445.
16. Murthy et al. quote a K/Ar biotite date of 1400.
17. Result recalculated giving unit weight to site mean directions. See 15 for dates.
18. Result recalculated giving unit weight to formations. Rb/Sr whole-rock isochrons of 1315 ± 35 and 1420 ± 30 by Bickford and Odom, 1968.

19. Eggler and Larson quote a Rb/Sr isochron at 1410 ± 30 . Error estimates recalculated giving unit weight to sites.
20. Van Schmus (1965) obtains a Rb/Sr whole rock and mineral isochron age of 1475 ± 50 . Site mean directions show some smear to the present field direction.
21. Calculated giving unit weight to studies, to obtain a mean pole for 1400 m.y. from rocks spread all over the shield, and inclinations varying from 10° to 44° .
22. Abstract. Errors and dating method not quoted.
23. Provisional result from study at the University of Alberta. Dates on the Belt and Purcell Groups obtained by Obradovich and Peterman (1968). Mineral and whole rock Rb/Sr isochrons give 1325 ± 15 . Correlations by Harrison (1972).
24. For age see 23. Calculated giving unit weight to sites.
- 25,26. See 23 for age.
27. Mean of 7 studies spread over most of Canadian Shield. Summarized by Fahrig and Jones, 1969. Van Schmus (1965) gives a Rb/Sr whole rock isochron age of 1205 ± 50 for Sudbury diabase. Leech (1966) gives K/Ar whole rock ages on chilled margins of Mackenzie dykes in Yellowknife area of 1000-1250. Gates (1971) obtains a Rb/Sr whole rock isochron age of 1660 ± 145 for the Sudbury diabase and claims to recalculate a date of 1685 from the results of Van Schmus (above). He also obtains a date of 1660 (no error given) by Rb/Sr isochron on the Mackenzie dykes near

Yellowknife. Fahrig and Jones summarize comprehensive K/Ar dating by the GSC giving ages around 1200 m.y. Age of Mackenzie event taken as 1200 here.

- 28,30. Keweenawan rocks variously dated as follows: Middle Keweenawan 1115 ± 15 U/Pb concordia plot, 3-20% discordant. Silver and Green, 1963. Duluth Gabbro 1115 ± 15 Rb/Sr whole rock isochron, Faure et al., 1969. Endion Sill 1092 ± 15 Rb/Sr whole rock isochron, Faure et al., 1969. Results grouped in formations because most sites are single sample sites.
31. Age quoted by Spall as 1040 from Rb/Sr whole rock isochron.
32. Robertson and Fahrig quote an inferred age from K/Ar whole rock dates of 1050.
33. Robertson and Fahrig quote a K/Ar whole rock age of 1020.
34. Result from the baked contact of a granite intrusion. The baking is dated at 1107 ± 22 by K/Ar whole rock analysis.
35. Helsley and Spall quote a K/Ar biotite age of 1140 ± 40 and a U/Pb zircon concordia age of 1150 ± 30 .
36. Spall quotes a Rb/Sr whole rock and feldspar isochron age of 953 ± 13 . The k value for 4 formations is 557, which suggests that the formations (which may have cooled simultaneously) have not averaged out short-term field variations.
37. Murthy and Deutsch quote a K/Ar whole rock age of 948 ± 90 .
38. Fahrig, Irving and Jackson (1971) summarize numerous K/Ar whole rock and mineral ages. They obtain an age of 675 ± 25 .

BIBLIOGRAPHY OF PALAEOMAGNETIC RESULTS FROM
PRECAMBRIAN ROCKS OF NORTH AMERICA

- Balsley, J. R. and A. F. Buddington, Remanent magnetism of the Russell Belt of Gneisses, northwest Adirondack Mountains, New York, *Adv. Phys.* 6, 317-322, 1957.
- Beck, M. E., Paleomagnetism of Keweenawan intrusive rocks, Minnesota, *J. Geophys. Res.* 75, 4985-4996, 1970.
- Beck, M. E. and N. C. Lindsley, Paleomagnetism of the Beaver Bay Complex, Minnesota, *J. Geophys. Res.* 74, 2002-2013, 1969.
- Bergh, H. W., Paleomagnetism of the Stillwater Complex, Montana, in: *Palaeogeophysics*, p. 143-158, Proceedings NATO Conference, Newcastle, ed. S. K. Runcorn, Academic Press,
- Bickford, M. E. and A. L. Odom, Rb-Sr geochronology of Igneous events in the Precambrian of the St. Francis mountains, southeastern Missouri, *Geol. Soc. Amer. special papers* #121, Abstracts for 1968, Annual meeting in Mexico City.
- Black, R. F., Palaeomagnetism of part of the Purcell System in southwestern Alberta and southeastern British Columbia, *Geol. Surv. Can.*
- Books, K. G., W. S. White and M. E. Beck, Magnetization of Keweenawan Gabbro in northern Wisconsin and its relation to time of intrusion, *U.S. Geol. Surv. Prof. Paper* 550-D, p. D117-D124, 1966.
- Collinson, D. W. and S. K. Runcorn, Polar wandering and continental drift: evidence from paleomagnetic observations in the United States, *Geol. Soc. Amer. Bull.* 71, 915-958, 1960.
- Cox, A. V. and R. R. Doell, Review of Paleomagnetism, *Geol. Soc. Amer. Bull.* 71, 645-768, 1960.
- Doell, R. R., Palaeomagnetic study of rocks from the Grand Canyon of the Colorado River, *Nature* 176, 1167, 1955.

- DuBois, P. M., Comparison of paleomagnetic results for selected rocks of Great Britain and North America, *Adv. Phys.* 6, 177-186, 1957.
- DuBois, P. M., Correlation of Keweenawan rocks of Lake Superior district by palaeomagnetic methods *Proc. Geol. Assoc. Can.* 11, 115-128, 1959. (*Geol. Surv. Can. reprint* 12, 1960).
- DuBois, P. M., Palaeomagnetism and correlation of Keweenawan rocks, *Geol. Surv. Can. Bull.* 71, 75, 1962.
- Eggler, D. H. and E. E. Larson, Palaeomagnetic study of dated Precambrian rocks of the Front Range, Colorado-Wyoming, *Geophys. J. Roy. Astr. Soc.* 14, 497-504, 1968.
- Elston, D. P. and G. R. Scott, Paleomagnetism of some Precambrian basalts and red beds, eastern Grand Canyon, Arizona, *Trans. Amer. Geophys. Union* 52, 822 (Abstract), 1971.
- Fahrig, W. F., E. H. Gaucher and A. Larochelle, Palaeomagnetism of diabase dykes of the Canadian Shield, *Can. J. Earth Sci.* 2, 278-298, 1965.
- Fahrig, W. F., E. Irving and G. D. Jackson, Paleomagnetism of the Franklin diabases, *Can. J. Earth Sci.* 8, 455-467, 1971.
- Fahrig, W. F. and D. L. Jones, Paleomagnetic evidence for the extent of the Mackenzie igneous events, *Can. J. Earth Sci.* 6, 679-688, 1969.
- Fahrig, W. F. and R. K. Wanless, Age and significance of diabase dyke swarms of the Canadian Shield, *Nature* 200, 934-937, 1963.
- Fairbairn, H. W., P. M. Hurley, K. D. Card and C. J. Knight, Correlation of radiometric ages of Nipissing diabase and Huronian metasediments with Proterozoic orogenic events in Ontario, *Can. J. Earth Sci.* 6, 489-497, 1969.
- Faure, G., S. Chaudhuri and M. D. Fenton, Ages of the Duluth Gabbro Complex and of the Endion Sill, Duluth, Minnesota, *J. Geophys. Res.* 74, 720-725, 1969.

- Fenton, M. D. and G. Faure, The age of the igneous rocks of the Stillwater Complex of Montana, *Geol. Soc. Amer. Bull.* 80, 1599-1604, 1969.
- Fraser, J. A., J. A. Donaldson, W. F. Fahrig and L. P. Tremblay, Helikian basins and geosynclines of the Northwestern Canadian Shield, in: *Basins and Geosynclines of the Canadian Shield*, ed. A. J. Baer, *Geol. Surv. Can. Paper* 70-40, 213-238, 1970.
- Gates, T. M., Improved dating of Canadian Precambrian dikes and a revised polar wandering curve, *Ph.D. Thesis, M.I.T.*, 1971.
- Graham, J. W., Changes of ferromagnetic minerals and their bearing on magnetic properties of rocks, *J. Geophys. Res.* 58, 243-260, 1953.
- Hargraves, R. B. and D. M. Burt, Paleomagnetism of the Allard Lake anorthosite suite, *Can. J. Earth Sci.* 4, 357-369, 1967.
- Harrison, J. E., Precambrian Belt Basin of northwestern United States: its geometry, sedimentation, and copper occurrences, *Geol. Soc. Amer. Bull.* 83, 1215-1240, 1972.
- Hays, W. W. and L. Scharon, A paleomagnetic investigation of some of the Precambrian igneous rocks of southeast Missouri, *J. Geophys. Res.* 71, 553-560, 1966.
- Helsley, C. E., Palaeomagnetic results from Precambrian rocks of central Arizona and Duluth, Minnesota, *Trans. Amer. Geophys. Union* 46, 67, (Abstract), 1965.
- Helsley, C. E. and H. Spall, Paleomagnetism of 1140 to 1150 million-year diabase sills from Gila County, Arizona, *J. Geophys. Res.* 77, 2115-2128, 1972.
- Hood, P. J., Palaeomagnetic studies of some Precambrian rocks in Ontario, *Ph.D. Thesis, Univ. of Toronto*, 1958.
- Hood, P. J., Paleomagnetic study of the Sudbury Basin, *J. Geophys. Res.* 66, 1235-1241, 1961.
- Howell, L. G., J. D. Martinez and E. H. Statham, Some observations on Rock Magnetism, *Geophys.* 23, 285-298, 1958.

- Hsu, I-Chi, R. E. Anderson and L. Scharon, Paleomagnetic properties of some of the Precambrian rocks in Missouri, *J. Geophys. Res.* 71, 2645-2650, 1966.
- Irving, E., J. A. Donaldson and J. K. Park, Paleomagnetism of the western channel Diabase and associated rocks, Northwest Territories, *Can. J. Earth Sci.* 9, 960-971, 1972.
- Irving, E., J. K. Park and J. C. McGlynn, Paleomagnetism of the Et-then Group and the Mackenzie diabase in the Great Slave Lake area, *Can. J. Earth Sci.* 9, 744-755, 1972.
- Irving, E., J. K. Park and J. L. Roy, Palaeomagnetism and the origin of the Grenville Front, *Nature* 236, 344-346, 1972.
- Jahren, C. E., Magnetization of Keweenawan rocks near Duluth, Minnesota, *Geophys.* 30, 858-874, 1965.
- Kellogg, K. S., Reversal of magnetic direction induced by thermal demagnetization of a Precambrian diabase from north-central Colorado, *Trans. Amer. Geophys. Union* 52, 822 (Abstract), 1971.
- Larochelle, A., Palaeomagnetism of the Abitibi Dyke Swarm, *Can. J. Earth Sci.* 3, 671-683, 1966.
- Larochelle, A., The palaeomagnetism of the Sudbury Diabase dyke swarm, *Can. J. Earth Sci.* 4, 323-332, 1967.
- Larochelle, A., Preliminary results of a study of the paleomagnetism of the Sudbury Irruptive, *Geol. Surv. Can. Paper* 69-19, 1969.
- Leech, A. P., Potassium-Argon dates of basic intrusive rocks of the District of Mackenzie, N.W.T., *Can. J. Earth Sci.* 3, 389-412, 1966.
- McElhinny, M. W., J. C. Briden, D. L. Jones and A. Brock, Geological and geophysical implications of Paleomagnetic results from Africa, *Rev. Geophys.* 6, 201-238, 1968.
- Murthy, G. S., The paleomagnetism of diabase dikes from the Grenville Province, *Can. J. Earth Sci.* 8, 802-812, 1971.

- Murthy, G. S. and E. R. Deutsch, Paleomagnetism of igneous rock units from the Coast of Labrador, *Can. J. Earth Sci.* 9, 207-212, 1972.
- Murthy, G. S., W. F. Fahrig and D. L. Jones, The paleomagnetism of the Michikamau anorthositic intrusion, Labrador, *Can. J. Earth Sci.* 5, 1139-1144, 1968.
- Nairn, A. E. M., D. V. Frost and B. G. Light, Palaeomagnetism of certain rocks from Newfoundland, *Nature* 183, 596-597, 1959.
- Norris, D. K. and R. F. Black, Application of palaeomagnetism to thrust mechanics, *Nature* 192, 933-935, 1961.
- Obradovich, J. D. and Z. E. Peterman, Geochronology of the Belt Series, Montana, *Can. J. Earth Sci.* 5, 737-747, 1968.
- Palmer, H. C., The paleomagnetism of the Croker Island Complex, Ontario, Canada, *Can. J. Earth Sci.* 6, 213-218, 1969.
- Palmer, H. C., Paleomagnetism and correlation of some middle Keweenawan rocks, Lake Superior, *Can. J. Earth Sci.* 7, 1410-1436, 1970.
- Park, J. K. and E. Irving, Magnetism of dikes of the Frontenac Axis, *Can. J. Earth Sci.* 9, 763-765, 1972.
- Robertson, W. A., Palaeomagnetic results from northern Canada suggesting a tropical Proterozoic climate, *Nature* 204, 66-67, 1964.
- Robertson, W. A., Magnetization directions in the Muskox intrusion and associated dykes and lavas, *Geol. Surv. Can. Bull.* 167, 1969.
- Robertson, W. A. and W. R. A. Baragar, The petrology and paleomagnetism of the Coronation sills, *Can. J. Earth Sci.* 9, 123-140, 1972.
- Robertson, W. A. and W. F. Fahrig, The great Logan paleomagnetic loop - The polar wandering path from Canadian Shield rocks during the Neohelikian Era, *Can. J. Earth Sci.* 8, 1355-1372, 1971.

- Runcorn, S. K., Paleomagnetic survey in Arizona and Utah: Preliminary results, *Geol. Soc. Amer. Bull.* 67, 301-316, 1956.
- Runcorn, S. K., Paleomagnetic results from Precambrian sedimentary rocks in the western United States, *Geol. Soc. Amer. Bull.* 75, 687-704, 1964.
- Schenk, P. E., Southeastern Atlantic, Canada, Northwestern Africa and continental drift, *Can. J. Earth Sci.* 8, 1218-1251, 1971.
- Silver, L. T. and J. C. Green, Zircon ages for middle Keweenawan rocks of the Lake Superior region, *Trans. Amer. Geophys. Union* 44, p. 107 (Abstract), 1963.
- Sopher, S., Palaeomagnetic study of the Sudbury Irruptive, *Geol. Surv. Can. Bull.* 90, 1963.
- Spall, H., Paleomagnetism of basement granites of southern Oklahoma and its implications; progress report, *Oklahoma Geol. Surv. Notes* 28, 65-80, 1968.
- Spall, H., Palaeomagnetism of the Pikes Peak Granite, Colorado, *Geophys. J. Roy. Astr. Soc.* 21, 427-440, 1970a.
- Spall, H., Paleomagnetism of basement granites in southern Oklahoma: final report, *Oklahoma Geol. Surv. Notes* 30, 136-150, 1970b.
- Spall, H., Paleomagnetism and K/Ar age of mafic dikes from the Wind River Range, Wyoming, *Geol. Soc. Amer. Bull.* 82, 2457-2472, 1971a.
- Spall, H., Paleomagnetism of Precambrian rocks from El Paso, Texas, *Phys. Earth Planet. Int.* 4, 329-346, 1971b.
- Spall, H., Did southern Africa and North America drift independently during the Precambrian? *Nature* 236, 219-221, 1972.
- Strangway, D. W., Magnetic properties of Diabase dikes, *J. Geophys. Res.* 66, 3021-3031, 1961.
- Strangway, D. W., Rock magnetism and dike classification, *J. Geol.* 72, 648-663, 1964.

- Symons, D. T. A., A paleomagnetic study on the Gunflint, Mesabi and Cuyuna Iron Ranges in the Lake Superior region, *Econ. Geol.* 61, 1336-1361, 1966.
- Symons, D. T. A., Paleomagnetism of Precambrian rocks near Cobalt, Ontario, *Can. J. Earth Sci.* 4, 1161-1169, 1967.
- Symons, D. T. A., Paleomagnetic evidence on the genesis of the hard haematite ore deposits of the Vermilion Range, Minnesota, *Can. J. Earth Sci.* 4, 449-460, 1967.
- Symons, D. T. A., A paleomagnetic study of concentrating iron ores from northern Michigan, *Econ. Geol.* 62, 118-137, 1967.
- Symons, D. T. A., Paleomagnetic evidence on the origin of the Marquette and Steep Rock hard hematite and goethite deposits, *Can. J. Earth Sci.* 4, 1-20, 1967.
- Symons, D. T. A., Paleomagnetism of the Nipissing diabase, Cobalt area, Ontario, *Can. J. Earth Sci.* 7, 86-90, 1970.
- Symons, D. T. A., A paleomagnetic study of the Nipissing Diabase, Blind River-Elliott Lake area, Ontario, *Geol. Surv. Can. Paper* 70-63, 1971.
- Van Schmus, R., The geochronology of the Blind River - Bruce mines area, Ontario, Canada, *J. Geol.* 73, 755-780, 1965.
- Vincenz, S. A., Phenomenon of partial self-reversal in Keweenawan rocks. 1. Magnetization of Portage Lake lavas, *J. Geophys. Res.* 73, 2729-2752, 1968.
- Vincenz, S. A. and K. Yaskawa, Phenomenon of partial self-reversal in Keweenawan rocks. 2. Magnetization of Upper Keweenawan lavas and sediments and of Lower Keweenawan dikes, *J. Geophys. Res.* 73, 2753-2767, 1968.

BIBLIOGRAPHY

- Aitken, J. D., Middle Cambrian to Middle Ordovician cyclic sedimentation, southern Rocky Mountains, Alberta, *Bull. Can. Petrol. Geol.* 14, 405-411, 1966.
- Aitken, J. D., G. D. Cook and H. R. Balkwill, Operation Norman, District of Mackenzie, *Geol. Surv. Can. Paper 70-1, Pt. A*, Report of activities, April to October, 1969, p. 203-206, 1970.
- Aitken, J. D. and R. G. Greggs, Upper Cambrian Formations, Southern Rocky Mountains of Alberta, an interim report, *Geol. Surv. Can. Paper 66-49*, 1966.
- Al-Khafaji, S. A. and S. A. Vincenz, Magnetization of the Cambrian Lamotte Formation in Missouri, *Geophys. J. Roy. Astr. Soc.* 24, 175-205, 1971.
- Banerjee, S. K., Characteristic difference between TRM and CRM in ultrafine hematite, *Trans. Amer. Geophys. Union* 52, 191 (Abstract), 1971a.
- Banerjee, S. K., New grain size limits for palaeomagnetic stability in haematite, *Nature* 232, 15-16, 1971b.
- Briden, J. C., Paleomagnetism of the Ntonya Ring Structure, Malawi, *J. Geophys. Res.* 73, 725-734, 1968.
- Briden, J. C. and E. Irving, Palaeolatitude spectra of sedimentary palaeoclimatic indicators, in: *Problems in Palaeoclimatology*, ed. A. E. M. Nairn, Publ. Interscience, London, New York, Sydney, 705 p., 1964.
- Brock, A., An experimental study of palaeosecular variation, *Geophys. J. Roy. Astr. Soc.* 24, 303-317, 1971.
- Brooks, P. J. and W. O'Reilly, Magnetic rotational hysteresis characteristics of red sandstones, *Earth & Planet. Sci. Letters* 9, 71-76, 1970.
- Bullard, E. C., The secular change of the earth's magnetic field, *Mon. Not. R.A.S. Geophys. Suppl.* 5, 248, 1948.

- Bullard, E. C., J. E. Everett and A. G. Smith, The fit of the continents around the Atlantic, *Phil. Trans. Roy. Soc.* 258, 41-51, 1965.
- Carslaw, H. S. and J. C. Jaeger, *Conduction of Heat in Solids*, 2nd edition, Publ. Oxford Univ. Press, 510 pages, 1959.
- Chamalaun, F. H., Origin of the secondary magnetization of the Old Red Sandstones of the Anglo-Welsh Cuvette, *J. Geophys. Res.* 69, 4327-4337, 1964.
- Collinson, D. W., Depositional remanent magnetization in sediments, *J. Geophys. Res.* 70, 4663-4668, 1965.
- Collinson, D. W., Investigations into the stable remanent magnetization of sediments, *Geophys. J. Roy. Astr. Soc.* 18, 211-222, 1969.
- Collinson, D. W., K. M. Creer and S. K. Runcorn, *Methods in Palaeomagnetism*, Publ. Elsevier, Amsterdam, London, New York, 609 pages, 1967.
- Cox, A. V., Lengths of geomagnetic polarity intervals, *J. Geophys. Res.* 73, 3247-3260, 1968.
- Cox, A. V., Research note: Confidence limits for the precision parameter κ , *Geophys. J. Roy. Astr. Soc.* 17, 545-549, 1969.
- Cox, A. V., Latitude dependence of the angular dispersion of the geomagnetic field, *Geophys. J. Roy. Astr. Soc.* 20, 253-269, 1970.
- Cox, A. V. and R. R. Doell, Review of paleomagnetism, *Geol. Soc. Amer. Bull.* 71, 645-768, 1960.
- Cox, A. V. and R. R. Doell, Long period variations of the geomagnetic field, *Bull. Seism. Soc. Amer.* 54, Pt. B, 2243-2270, 1964.
- Cox, A. V., R. R. Doell and G. B. Dalrymple, Geomagnetic polarity epochs and Pleistocene geochronology, *Nature* 198, 1049-1051, 1963.
- Cox, A. V., R. R. Doell and G. B. Dalrymple, Reversals of the earth's magnetic field, *Science* 144, 1537-1543, 1964.

- Cox, A. V., R. R. Doell and G. B. Dalrymple, Time scale for geomagnetic reversals, in: *History of the Earth's Crust*, ed. R. Phinney, Princeton Univ. Press, Princeton, New Jersey, 1968.
- Creer, K. M., A.C. demagnetization of unstable Keuper Marls from S.W. England, *Geophys. J. Roy. Astr. Soc.* 2, 261-275, 1959.
- Creer, K. M., Superparamagnetism in red sandstones, *Geophys. J. Roy. Astr. Soc.* 5, 16-28, 1961.
- Creer, K. M., The dispersion of the geomagnetic field due to secular variation and its determination for remote times from palaeomagnetic data, *J. Geophys. Res.* 67, 3461-3476, 1962.
- Creer, K. M., On the origin of the magnetization of Red Beds, *J. Geomag. Geoelec.* 13, 86-100, 1962.
- Creer, K. M., Systematic errors in the Palaeomagnetic inclination of sedimentary rocks? *Nature* 213, 482-483, 1967.
- Creer, K. M., Arrangement of the continents during the Palaeozoic era, *Nature* 219, 41-44, 1968.
- Deer, W. A., R. A. Howie and J. Zussman, *An Introduction to the Rock-forming Minerals*, Publ. Longmans, London, 528 pages, 1966.
- Doell, R. R., Paleomagnetism of the Kau Volcanic Series, Hawaii, *J. Geophys. Res.* 74, 4857-4868, 1969.
- Doell, R. R. and A. Cox, Measurement of the remanent magnetization of igneous rocks, *U.S. Geol. Surv. Bull.* 1203-A, A1-A32, 1965.
- Doell, R. R. and A. Cox, The Pacific geomagnetic secular variation anomaly and the question of lateral uniformity in the lower mantle, in: *The Nature of the Solid Earth*, in honour of Francis Birch, ed. E. C. Robertson, J. F. Hays and L. Knopoff, Publ. McGraw-Hill, 677 pages, 1972.
- Douglas, R. J. W. and D. K. Norris, Dahadinni and Wrigley map-areas, District of Mackenzie, Northwest Territories, 65N and 950, *Geol. Surv. Can. Paper* 62-33, 1963.

- DuBois, P. M., Correlation of Keweenawan rocks of Lake Superior district by palaeomagnetic methods, *Proc. Geol. Assoc. Can.* 11, 115-128, 1959. (Geol. Surv. Can. Reprint 12, 1960).
- Dunlop, D. J., Magnetic properties of fine-particle hematite, *Ann. Geophys.* 27, 269-293, 1971.
- Dunlop, D. J., Magnetic mineralogy of unheated and heated red sediments by coercivity spectrum analysis, *Geophys. J. Roy. Astr. Soc.* 27, 37-55, 1972.
- Epp, R. J., J. W. Tukey and G. S. Watson, Testing unit vectors for serial correlation, *J. Geophys. Res.* 76, 8480-8483, 1971.
- Everitt, C. W. F., Thermoremanent Magnetization. I. Experiments on single domain grains, *Phil. Mag.* 6, 713-726, 1961.
- Everitt, C. W. F. and J. A. Clegg, A field test for palaeomagnetic stability, *Geophys. J. Roy. Astr. Soc.* 6, 312-319, 1962.
- Fahrig, W. F., E. Irving and G. D. Jackson, Paleomagnetism of the Franklin diabases, *Can. J. Earth Sci.* 8, 455-467, 1971.
- Fahrig, W. F. and D. L. Jones, Paleomagnetic evidence for the extent of Mackenzie igneous events, *Can. J. Earth Sci.* 6, 679-688, 1969.
- Fisher, R. A., Dispersion on a sphere, *Proc. Roy. Soc. Ser. A* 217, 295-305, 1953.
- Folinsbee, R. E., H. Baadsgaard and J. Lipson, Potassium-Argon dates of Upper Cretaceous ash falls, Alberta, Canada, *N.Y. Acad. Sci. Annals* 91, Art. 2, 352-363, 1961.
- Garland, G. D., *Introduction to Geophysics. Mantle Core and Crust*, Publ. W. B. Saunders, Philadelphia, London, Toronto, 420 pages, 1971.
- Geological Society of America, Rock-Color Chart, Distributed by the Geological Society of America, Boulder, Colorado, Reprinted, 1970.

- Gough, D. I. and N. D. Opdyke, The palaeomagnetism of the Lupata alkaline volcanics, *Geophys. J. Roy. Astr. Soc.* 7, 457-468, 1963.
- Graham, J. W., The stability and significance of magnetism in sedimentary rocks, *J. Geophys. Res.* 54, 131-167, 1949.
- Graham, J. W., Evidence of Polar Shift since Triassic time, *J. Geophys. Res.* 60, 329-348, 1955.
- Graham, K. W. T., The remagnetization of a surface outcrop by lightning currents, *Geophys. J. Roy. Astr. Soc.* 6, 85-102, 1961.
- Hargraves, R. B., Magnetic anisotropy and remanent magnetism in hemo-ilmenite from ore deposits at Allard Lake, Quebec, *J. Geophys. Res.* 64, 1565-1578, 1959.
- Hedley, I. G., Chemical remanent magnetization of the FeOOH , Fe_2O_3 system, *Phys. Earth Planet. Int.* 1, 103-121, 1968.
- Heirtzler, J. R., G. O. Dickson, E. M. Herron, W. C. Pitman, III, and X. LePichon, Marine magnetic anomalies, geomagnetic field reversals, and motions of the ocean floor and continents, *J. Geophys. Res.* 73, 2119-2136, 1968.
- Helsley, C. E. and M. B. Steiner, Evidence for long intervals of normal polarity during the Cretaceous Period, *Earth & Planet. Sci. Letters* 5, 325-332, 1969.
- Helsley, C. E. and M. B. Steiner, Secular variation in the Lower Triassic Moenkopi Formation, *Trans. Amer. Geophys. Union* 52, 189 (Abstract), 1971.
- Hide, R., Motions of the earth's core and mantle, and variations of the main geomagnetic field, *Science* 157, 55-56, 1967.
- Hide, R. and K. Stewartson, Hydromagnetic oscillations of the earth's core, *Rev. Geophys. & Space Phys.* 10, 579-598, 1972.
- Hoel, P. G., *Elementary Statistics*, 2nd edition, Publ. Wiley, New York, London, Sydney, 351 pages, 1966.

- Hoffman, P. F., Stratigraphy, sedimentology and paleocurrents in the East Arm of Great Slave Lake, *Geol. Surv. Can., Report of Activities, Pt. A*, May-October, 1966, Paper 67-1, Pt. A., 1967.
- Hoffman, P. F., Stratigraphy of the Lower Proterozoic (Aphebian), Great Slave Supergroup, East Arm of Great Slave Lake, District of Mackenzie, *Geol. Surv. Can. Paper 68-42*, 1968.
- Hoffman, P. F., Proterozoic paleocurrents and depositional history of the East Arm fold belt, Great Slave Lake, N.W.T., *Can. J. Earth Sci.* 6, 441-462, 1969.
- Hoffman, P. F., J. A. Fraser and J. C. McGlynn, The Coronation geosyncline of Aphebian age, district of Mackenzie, in: *Basins and Geosynclines of the Canadian Shield*, ed. A. J. Baer, *Geol. Surv. Can. Paper 70-40*, 201-212, 1970.
- Hudson, J. D., Sedimentation rates in relation to the Phanerozoic time scale, in: *The Phanerozoic Time-Scale*, ed. W. B. Harland, A. Gilbert Smith and B. Wilcock, A symposium dedicated to Professor Arthur Holmes, *Geol. Soc. London*, 37-42, 1964.
- Irving, E., Palaeomagnetic directions and pole positions: Pt. 1, *Geophys. J. Roy. Astr. Soc.* 3, 96-111, 1960.
- Irving, E., Paleomagnetic directions and pole positions, Pt. 2, *Geophys. J. Roy. Astr. Soc.* 3, 444-449, 1960.
- Irving, E., Palaeomagnetic directions and pole positions: Pt. 3, *Geophys. J. Roy. Astr. Soc.* 5, 72-79, 1961.
- Irving, E., Palaeomagnetic directions and pole positions: Pt. 4, *Geophys. J. Roy. Astr. Soc.* 6, 263-267, 1962.
- Irving, E., Palaeomagnetic directions and pole positions: Part 5, *Geophys. J. Roy. Astr. Soc.* 7, 263-274, 1962.
- Irving, E., *Paleomagnetism and its Application to Geological and Geophysical Problems*, Publ. Wiley & Sons, New York, London, Sydney, 399 pages, 1964.

- Irving, E., Palaeomagnetic directions and pole positions, Pt. 7, *Geophys. J. Roy. Astr. Soc.* 9, 185-194, 1965.
- Irving, E. and A. Major, Post-depositional detrital remanent magnetization in a synthetic sediment, *Sedimentology* 3, 133-143, 1964.
- Irving, E., J. K. Park and J. C. McGlynn, Paleomagnetism of the Et-then Group and Mackenzie Diabase in the Great Slave Lake Area, *Can. J. Earth Sci.* 9, 744-755, 1972.
- Irving, E., J. K. Park and J. L. Roy, Palaeomagnetism and the origin of the Grenville Front, *Nature* 236, 344-346, 1972.
- Irving, E., L. G. Parry, The magnetism of some Permian rocks from New South Wales, *Geophys. J. Roy. Astr. Soc.* 7, 395-411, 1963.
- Irving, E., P. M. Stott, Palaeomagnetic directions and pole positions: Part 6, *Geophys. J. Roy. Astr. Soc.* 8, 249-257, 1963.
- Jacobs, J. A., *The Earth's Core and Geomagnetism*, Pergamon Press, Oxford, London, Paris, Frankfurt, MacMillan, New York, 137 pages, 1963.
- Jones, D. L. and M. W. McElhinny, Stratigraphic interpretation of paleomagnetic measurements on the Waterberg Red Beds of South Africa, *J. Geophys. Res.* 72, 4171-4179, 1967.
- King, L. C., Geological relationship between South Africa and Antarctica, *Alex L. DuToit memorial lecture no. 9*, *Trans. Geol. Soc. South Africa annexure to vol. 68*, 1965.
- King, R. F. and A. I. Rees, Detrital magnetism in sediments: an examination of some theoretical models, *J. Geophys. Res.* 71, 561-571, 1966.
- Kukal, Z., *Geology of Recent Sediments*, Academia Publ. House of the Czechoslovak Academy of Sciences, Prague, Published in English by Academic Press, London & New York, 1971.

- Lawley, E. A., The intensity of the geomagnetic field in Iceland during Neogene polarity transitions and systematic deviations, *Earth & Planet. Sci. Letters* 10, 145-149, 1970.
- McElhinny, M. W., Research note: Statistical significance of the fold test in palaeomagnetism, *Geophys. J. Roy. Astr. Soc.* 8, 338-340, 1964.
- McElhinny, M. W., An improved method of demagnetizing rocks in alternating magnetic fields, *Geophys. J. Roy. Astr. Soc.* 10, 369-374, 1966.
- McElhinny, M. W., The palaeomagnetism of the southern continents. A survey and analysis, in: *Continental Drift Emphasizing the History of the South Atlantic Area*, Published in microfilm only by the Amer. Geophys. Union, 1967.
- McElhinny, M. W., Palaeomagnetic directions and pole positions: Pt. 8, Pole numbers 8/1 to 8/186, *Geophys. J. Roy. Astr. Soc.* 15, 409-430, 1968.
- McElhinny, M. W., Palaeomagnetic directions and pole positions: Pt. 9, Pole numbers 9/1 to 9/159, *Geophys. J. Roy. Astr. Soc.* 16, 207-224, 1968.
- McElhinny, M. W., Notes on Progress in Geophysics - Palaeomagnetic Directions and Pole Positions - X, *Geophys. J. Roy. Astr. Soc.* 19, 305-327, 1969.
- McElhinny, M. W., Notes on progress in Geophysics, Palaeomagnetic directions and pole positions - XI, Pole numbers 11/1 to 11/90, *Geophys. J. Roy. Astr. Soc.* 20, 417-429, 1970.
- McElhinny, M. W., Geomagnetic reversals during the Phanerozoic, *Science* 172, 157-159, 1971.
- McElhinny, M. W. and P. J. Burek, Mesozoic Palaeomagnetic Stratigraphy, *Nature* 232, 98-102, 1971.
- McElhinny, M. W. and M. E. Evans, An investigation of the strength of the geomagnetic field in the early Precambrian, *Phys. Earth Planet. Int.* 1, 485-497, 1968.

- McElhinny, M. W. and D. I. Gough, The palaeomagnetism of the Great Dyke of Southern Rhodesia, *Geophys. J. Roy. Astr. Soc.* 7, 287-303, 1963.
- McLeod, C. R. and J. A. Chamberlain, Reflectivity and Vickers Microhardness of ore minerals, *Geol. Surv. Can. Paper* 68-64, 1969.
- McMahon, B. E. and D. W. Strangway, Kiaman Magnetic Interval in the Western United States, *Science* 155, 1012-1013, 1967.
- Moriya, T., Anisotropic superexchange interaction and weak ferromagnetism, *Phys. Rev. Series* 2, 120, 91-98, 1960.
- Murthy, G. S., Paleomagnetic studies in the Canadian Shield, *Ph.D. Thesis, Univ. of Alberta*, 1969.
- Nagata, T., *Rock Magnetism*, Publ. Maruzen, Tokyo, 350 pages, 1961.
- Nascimbene, G. G., Bentonites and the geochronology of the Bearpaw sea, *M.Sc. Thesis, Geology Dept., Univ. of Alberta*, 1963.
- Neel, L., Some theoretical aspects of rock magnetism, *Adv. Phys.* 4, 191-243, 1955.
- Olade, M. A. D. and R. D. Morton, Observations on the Proterozoic Seton Formation, East Arm of Great Slave Lake, Northwest Territories, *Can. J. Earth Sci.*, in press.
- Patton, B. J., Magnetic shielding, in: *Methods in Palaeomagnetism*, ed. D. W. Collinson, K. M. Creer and S. K. Runcorn, Publ. Elsevier, Amsterdam, London, New York, 609 pages, 1967.
- Porath, H., Magnetic studies on specimens of intergrown maghemite and hematite, *J. Geophys. Res.* 73, 5959-5965, 1968.
- Rees, A. I., The effect of water currents on the magnetic remanence and anisotropy of susceptibility of some sediments, *Geophys. J. Roy. Astr. Soc.* 5, 235-251, 1961.

- Robertson, W. A. and W. R. A. Baragar, The petrology and paleomagnetism of the Coronation Sills, *Can. J. Earth Sci.* 9, 123-140, 1972.
- Roquet, J., Sur les remanences des oxydes de fer et leur interet en geomagnetisme. Premiere Partie, *Ann. Geophys.* 10, 226-247, 1954.
- Roy, J. L., Red Beds: DRM or CRM? *Phys. in Can.* 28, 45 (Abstract), 1972.
- Roy, J. L., A pattern of rupture of the eastern North American - western European paleoblock, *Earth & Planet. Sci. Letters* 14, 103-114, 1972.
- Runcorn, S. K., The sampling of rocks for palaeomagnetic comparisons between the continents, *Adv. Phys.* 6, 169-176, 1957.
- Schenk, P. E., Southeastern Atlantic Canada, Northwestern Africa, and Continental Drift, *Can. J. Earth Sci.* 8, 1218-1251, 1971.
- Schwarz, E. J. and D. T. A. Symons, On the intensity of the paleomagnetic field between 100 million and 2500 million years ago, *Phys. Earth & Planet. Int.* 1, 122-128, 1968.
- Smith, A. G. and A. Hallam, The fit of the southern continents, *Nature* 225, 139-144, 1970.
- Smith, P. J., The intensity of the ancient geomagnetic field, *Geophys. J. Roy. Astr. Soc.* 12, 321-362, 1967.
- Smith, P. J., The intensity of the ancient geomagnetic field: A Summary of conclusions, in: *Palaeogeophysics*, ed. S. K. Runcorn, Academic Press, London and New York, 518 pages, 1970.
- Smith, R. W. and M. Fuller, Alpha-haematite: stable remanence and memory, *Science* 156, 1130-1133, 1967.
- Spall, H., Did Southern Africa and North America Drift independently during the Precambrian? *Nature* 236, 219-221, 1972.

- Stacey, F. D., The physical theory of rock magnetism, *Adv. Phys.* 12, 45-133, 1963.
- Stockwell, C. H., Fourth Report on Structural Provinces, orogenies and time-classification of rocks of the Canadian Precambrian Shield, in: *Age Determinations and Geological Studies, Pt. II, Geol. Surv. Can. Paper 64-17, Pt. II*, 1-21, 1964.
- Stockwell, C. H., Geology of the Canadian Shield, in: *Geology and Economic Minerals of Canada* (5th edition), Information Canada, 1970.
- Strangway, D. W., *History of the Earth's Magnetic Field*, McGraw-Hill, 168 pages, 1970.
- Strangway, D. W., R. M. Hones, B. E. McMahon and E. E. Larson, The magnetic properties of naturally occurring goethite, *Geophys. J. Roy. Astr. Soc.* 25, 345-359, 1968.
- Strangway, D. W., B. E. McMahon, T. R. Walker and E. E. Larson, Anomalous Pliocene paleomagnetic pole positions from Baja California, *Earth & Planet. Sci. Letters* 13, 161-166, 1971.
- Symons, D. T. A., Paleomagnetic evidence on the origin of the Marquette and Steep Rock hure haematite and goethite deposits, *Can. J. Earth Sci.* 4, 1-20, 1967.
- Van der Voo, R., New palaeomagnetic evidence for the rotation of the Iberian Peninsula, in: *Palaeogeophysics*, ed. S. K. Runcorn, Academic Press, London and New York, 518 pages, 1970.
- Watson, G. S., Analysis of dispersion on a sphere, *Mon. Not. Roy. Astr. Soc. Geophys. Suppl.* 7, 153-159, 1956a.
- Watson, G. S., A test for randomness of directions, *Mon. Not. Roy. Astr. Soc. Geophys. Suppl.* 7, 160-161, 1956b.
- Watson, G. S., The statistics of orientation data, *J. Geol.* 74, 786-797, 1966.

- Watson, G. S., Orientation statistics in the earth sciences, *Bull. Geol. Inst., Univ. Uppsala*, New Series 2, 73-89, 1970.
- Watson, G. S. and E. Irving, Statistical methods in rock magnetism, *Mon. Not. Roy. Astr. Soc. Geophys. Suppl.* 7, 289-300, 1957.
- Williams, M. Y., Reconnaissance across Northeastern British Columbia and the geology of the northern extension of Franklin Mountains, Northwest territories, *Geol. Surv. Can. Summary Report* 1922, Pt. B, 65B-87B, 1923.
- Wilson, R. L., Remanent magnetism of late Secondary and early Tertiary British rocks, *Phil. Mag.* 4, 750-755, 1959.

APPENDIX 1 DETAILED RESULTS OF PALAEOMAGNETIC MEASUREMENTS

The magnetization vector for each specimen is given after each stage of treatment. The specimen names used are the abbreviated ones employed in the thesis. An expanded name is written on each specimen. Thus results for EB2B are for a specimen whose full name is KEB02B. K denotes the collection (Kahochella Group). The samples from the Mount Clark Formation with typical specimen name MC3B here have the name CCC03B written on the actual specimen, where CC denotes the study. The remainder of the naming convention is explained in the text.

Treatment of the specimens is keyed by letter.

- N - Natural Remanent Magnetization
- M - A.F. treatment
- T - Thermal demagnetization using Ottawa furnace
- C - Thermal demagnetization using Edmonton furnace
- W - Remeasurement some time after an A.F. demagnetization run

The intensity of the treatment is given in mT (if M) or °C (if C or T).

The intensity of the remanence vector (J) is given in Am²/kg (emu/gm). A number such as 3.07-7 denotes 3.07×10^{-7} .

Declination and inclination of the vector w.r.t.
and the palaeohorizontal are given in degrees east of true
north and below the horizontal.

APPENDIX 2 LABORATORY APPARATUS

A2.1 Spinner Magnetometers

The magnetometers were tested in two ways:

(i) Readings from the PAR spinner taken over a 6 month period were examined to see what error would be introduced by spinning each specimen about 3 axes rather than 6. The angle between the vector deduced from 6 spins and that deduced from a subset of the readings equivalent to 3 spins are displayed in histogram form in Fig. A2a (upper) for specimens with moments greater than 10^{-8} Am^2 (10^{-5} emu). Only in a few cases of very unstable magnetization is the difference appreciable.

(ii) Measurements made on both the PAR and Schonstedt magnetometers were compared using weakly magnetized specimens so that the Schonstedt magnetometer could be operated in its two most sensitive configurations. In these configurations the effects of specimen inhomogeneity are most easily observed. Histograms of the difference in angle between readings on the two instruments are shown for the most sensitive (position 4) and next most sensitive (position 3) configurations in Fig. A2b. It can be seen that specimen inhomogeneity has appreciable effect in the most sensitive configuration.

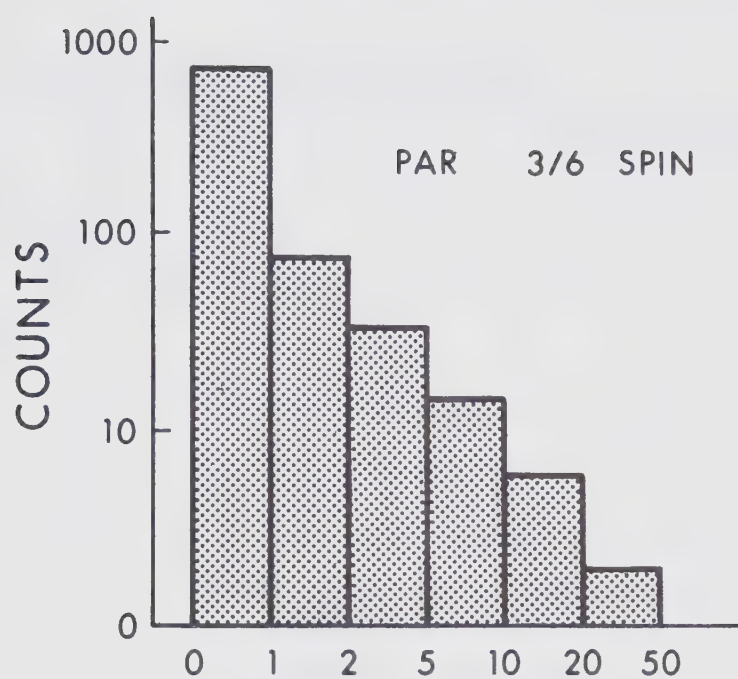


Fig A2a ANGLE BETWEEN 6 AND 3-spin (°)

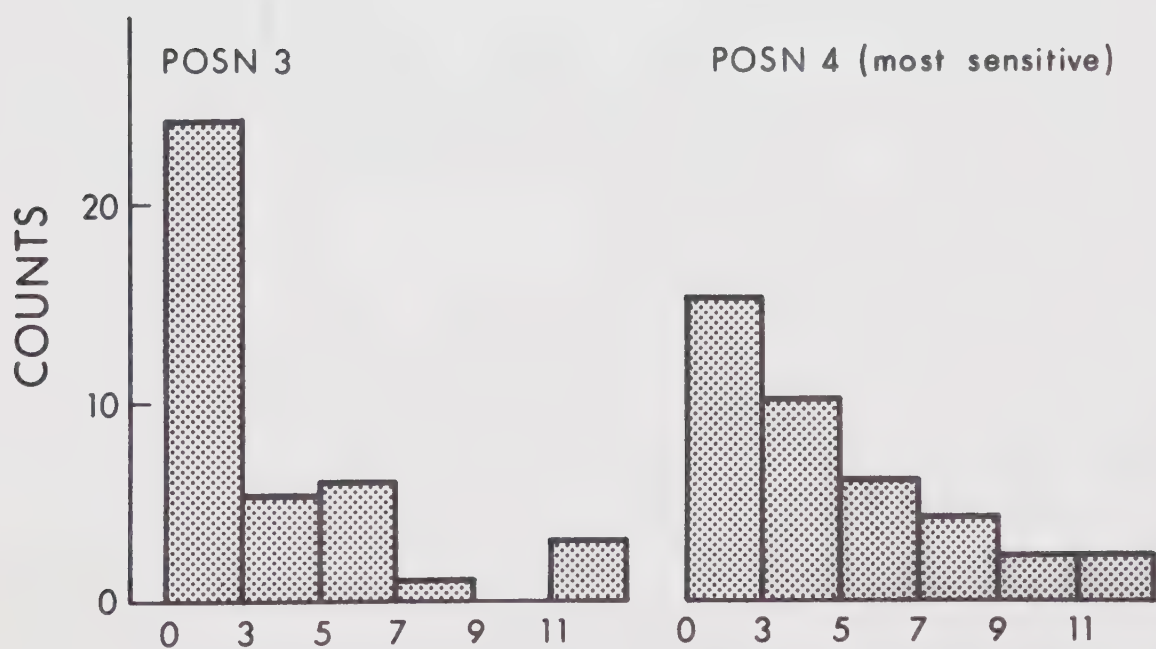


Fig A2b DISCREPANCY BETWEEN PAR & SCHONSTEDT (°)

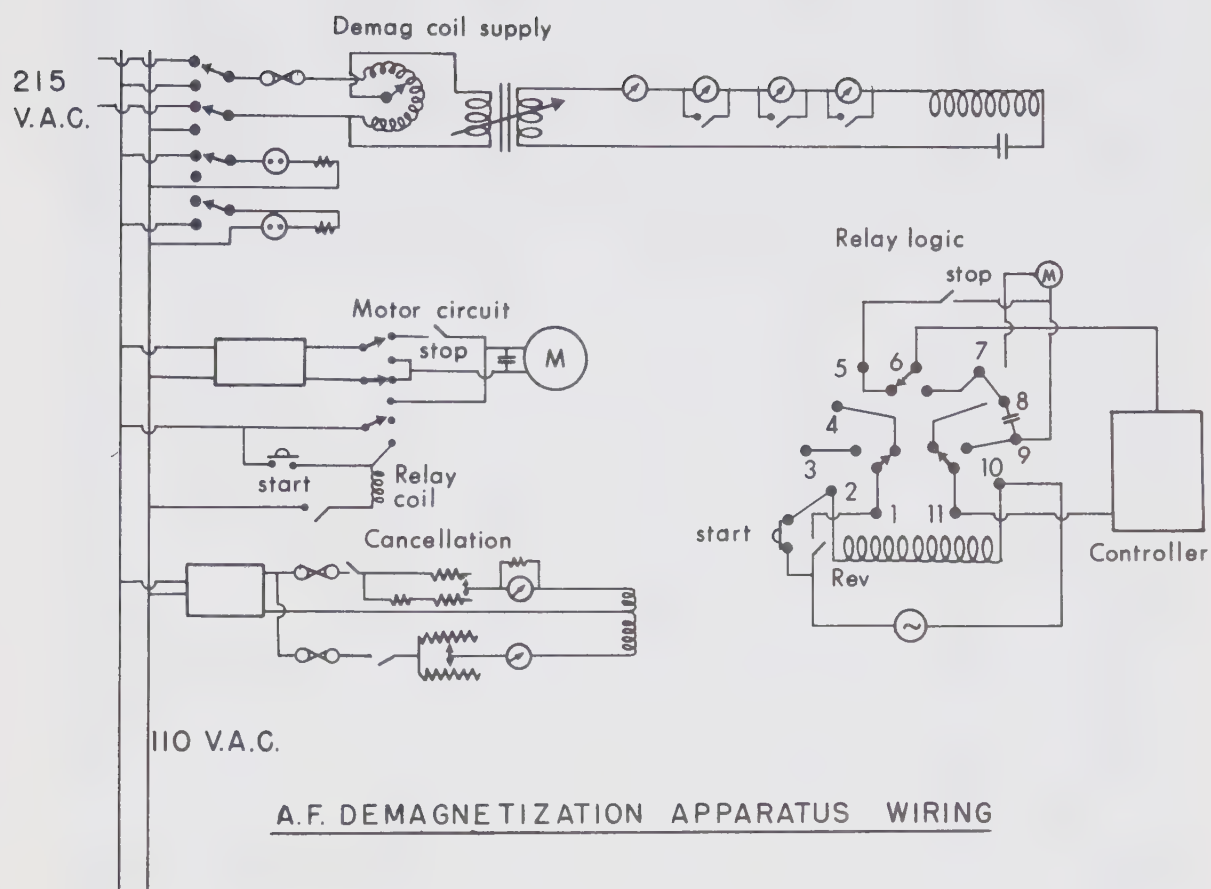
A2.2 Magnetically Shielded Room

(i) Material: Moly-permalloy supplied by the Allegheny Ludlum Steel Corp. Frame built entirely of plywood, laminated where necessary to obtain sufficient thickness.

(ii) Size: Double cubical shield. Inner of side 80" (2.03 m), shielding material 52 thou (1.3 mm). Outer of side 100" (2.54 m), shielding material 60 thou (1.5 mm). Material applied in strips 20" wide (.508 m) with batten strips 3" (7.6 cm) clamped over the joints as described by Patton (1967).

(iii) Doors: Opening is 68" × 35" (1.72 × .88 m). Inner and outer doors also clad with shielding material and slide on Al rails. During operation the doors are held together by a pressure reduction between them of ca. 1/30 atm. provided by a commercial vacuum cleaner.

Fig. A2c Improved control panel wiring for A.F.
demagnetization apparatus.



SPEC	TREAT	J	D	I	SPEC	TREAT	J	D	I	SPEC	TREAT	J	D	I	SPEC	TREAT	J	D	I				
AA1A	N	0	4.24-7	164	64	AA4A	N	0	3.15-7	152	73	AD1B	C	300	1.72-6	147	46	AE3A	M	80	1.71-6	123	56
AA1A	M	5	3.94-7	173	57	AA4A	M	5	2.47-7	152	71	AD1B	C	400	1.50-6	148	46	AE3A	M	100	1.62-6	123	56
AA1A	M	10	3.62-7	170	55	AA4A	M	10	2.61-7	154	69	AD1B	C	450	1.33-6	148	47	AE3A	M	140	1.58-6	120	53
AA1A	M	20	3.48-7	167	56	AA4A	M	20	2.54-7	150	69	AD1B	C	500	1.18-6	147	45	AE3A	M	180	1.38-6	119	56
AA1A	M	40	3.22-7	168	56	AA4A	M	40	2.25-7	144	69	AD1B	C	550	1.03-6	150	45	AE3A	C	550	3.82-7	148	-24
AA1A	M	60	3.21-7	171	53	AA4A	M	60	2.21-7	145	73	AD1B	C	600	8.98-7	149	47	AE3A	C	500	3.13-7	149	16
AA1A	M	80	3.23-7	177	64	AA4A	M	80	2.02-7	146	70	AD1B	C	650	7.70-7	147	50	AE3A	C	450	2.95-7	142	35
AA1A	M	100	3.13-7	182	49	AA4A	M	100	2.04-7	141	69	AD1B	C	670	4.86-7	139	63	AF3B	N	0	1.67-6	116	78
AA1A	M	140	4.50-7	164	83	AA4A	M	140	1.35-7	135	65	AD1B	C	700	7.33-7	302	35	AF3B	C	500	4.40-7	164	60
AA1A	M	180	3.16-7	163	48	AA4A	M	180	1.76-7	134	65	AD2A	N	0	1.30-6	150	46	AE3B	C	550	3.67-7	176	61
AA1F	N	0	4.12-7	166	71	AA4H	N	0	2.73-7	85	76	AD2A	M	5	1.29-6	151	46	AE3B	C	600	2.93-7	182	53
AA1R	C	500	1.56-7	194	40	AA4R	C	500	4.17-8	94	59	AD2A	M	10	1.29-6	151	46	AE3B	C	630	3.75-7	214	32
AA1R	C	550	1.19-7	202	44	AA4R	C	550	3.18-8	99	70	AD2A	M	20	1.28-6	150	46	AE3B	C	660	2.02-7	225	38
AA1R	C	600	1.04-7	204	46	AC1A	N	0	1.01-6	28	73	AD2A	M	40	1.28-6	150	46	AE4A	N	0	1.48-6	105	68
AA1R	C	630	7.96-8	212	37	AC1A	M	5	1.01-6	30	73	AD2A	M	60	1.27-6	151	46	AE4A	M	5	1.06-6	111	63
AA1R	C	650	4.45-8	202	45	AC1A	M	10	9.43-7	30	74	AD2A	M	80	1.27-6	151	46	AE4A	M	20	8.99-7	114	60
AA2A	N	0	3.46-7	191	59	AC1A	M	20	9.66-7	29	73	AD2A	M	100	1.24-6	152	45	AE4A	M	40	8.76-7	114	59
AA2A	M	5	3.32-7	176	52	AC1A	M	40	9.70-7	31	73	AD2A	M	140	1.20-6	148	43	AE4A	M	60	8.38-7	116	57
AA2A	M	10	3.16-7	176	50	AC1A	M	60	7.71-7	32	72	AD2A	M	180	1.13-6	144	40	AE4A	M	80	8.24-7	114	57
AA2A	M	20	3.07-7	178	50	AC1A	M	80	7.10-7	36	74	AD2B	N	0	3.89-5	150	50	AE4A	M	100	8.22-7	113	52
AA2A	M	40	2.93-7	176	48	AC1A	M	100	6.29-7	41	74	AD2B	C	500	2.10-5	152	43	AE4A	M	140	8.12-7	114	53
AA2A	M	60	2.93-7	181	47	AC1A	M	140	4.97-7	45	74	AD2B	C	550	1.82-5	152	43	AE4A	M	180	7.62-7	104	46
AA2A	M	80	2.97-7	181	47	AC1A	M	180	4.48-7	50	74	AD2B	C	600	1.65-5	153	45	AE4A	C	550	1.89-7	50	-52
AA2A	M	100	2.77-7	181	47	AC1B	N	0	1.14-6	20	76	AD2B	C	630	1.73-5	152	75	AF4A	C	400	1.87-7	35	-44
AA2A	M	140	2.93-7	177	44	AC1B	C	500	4.52-7	353	69	AD2B	C	660	2.70-5	153	70	AF4A	C	650	1.53-7	357	-44
AA2A	M	180	2.65-7	180	46	AC1B	C	550	3.94-7	345	69	AD3A	N	0	6.89-7	145	49	AE4B	N	0	1.41-6	102	71
AA2B	N	0	4.23-7	161	69	AC1F	C	600	3.02-7	20	74	AD3A	M	5	6.86-7	145	49	AE4B	C	500	1.47-7	162	56
AA2B	C	500	1.84-7	189	43	AC1F	C	630	2.78-7	25	64	AD3A	M	10	6.86-7	145	48	AE4B	C	550	6.44-6	80	45
AA2B	C	550	1.55-7	195	38	AC1B	C	650	2.25-7	5	77	AD3A	M	20	6.66-7	148	48	AE4B	C	600	6.71-8	19	-33
AA2B	C	600	1.46-7	195	41	AC2A	N	0	3.10-7	30	64	AD3A	M	40	6.65-7	148	47	AE4B	C	630	1.07-7	342	-50
AA2B	C	630	1.24-7	198	35	AC2A	M	5	2.95-7	24	75	AD3A	M	60	6.67-7	150	39	AE4B	C	660	3.43-7	1	-10
AA2B	C	660	1.25-7	191	41	AC2A	M	10	2.92-7	27	73	AD3A	M	80	6.08-7	150	46	BA1A	N	0	1.99-5	359	29
AA3B	N	0	3.95-7	178	76	AC2A	M	20	3.31-7	15	74	AD3B	N	0	7.73-7	150	51	BA1A	N	0	2.06-5	57	55
AA3B	M	5	3.60-7	173	76	AC2A	M	30	2.64-7	21	73	AD3B	C	500	3.93-7	159	42	BA1A	M	5	8.12-6	325	52
AA3B	M	10	3.42-7	170	76	AC2A	M	40	3.46-7	6	69	AD3B	C	550	3.10-7	154	42	BA1A	M	10	6.74-6	295	52
AA3B	M	20	3.23-7	172	75	AC2A	M	50	2.89-7	13	78	AD3B	C	600	2.64-7	156	45	BA1A	M	20	5.73-6	280	45
AA3B	M	40	2.97-7	169	73	AC2A	M	60	2.74-7	46	58	AD3B	C	630	5.90-7	26	26	BA1A	M	40	5.04-6	287	36
AA3B	M	60	2.69-7	172	72	AC2A	M	70	2.97-7	52	58	AD3B	C	660	1.04-6	133	-7	BA1A	M	60	5.00-6	281	32
AA3B	M	80	2.63-7	173	72	AC2A	M	80	2.73-7	341	60	AD4A	N	0	1.02-6	139	59	BA1A	M	80	4.80-6	281	29
AA3B	M	100	2.64-7	174	70	AC2A	M	90	2.08-7	51	73	AD4A	M	5	9.95-7	137	59	BA1A	M	100	4.80-6	280	29
AA3B	M	140	2.65-7	166	75	AC2A	M	120	2.01-7	35	71	AD4A	M	10	9.71-7	148	57	BA1A	M	140	4.95-6	278	26
AA3B	M	180	2.45-7	194	77	AC2A	M	160	1.70-7	56	75	AD4A	M	20	9.64-7	140	57	BA1A	M	180	4.34-6	282	26
AA4A	N	0	4.86-7	144	81	AC2A	M	180	1.56-7	354	88	AD4A	M	40	9.51-7	145	55	BA1B	N	0	1.95-5	357	41
AA4A	M	5	3.68-7	149	80	AC2A	M	160	1.56-7	98	80	AD4A	M	60	9.25-7	148	55	BA1B	C	500	3.56-7	284	16
AA4A	M	10	3.45-7	144	78	AC2A	M	180	1.56-7	354	88	AD4A	M	80	9.40-7	143	54	BA1B	C	550	3.51-6	284	10
AA4A	M	20	3.33-7	147	77	AC2B	N	0	3.73-7	46	73	AD4A	M	100	9.37-7	141	59	BA1B	C	600	3.28-6	287	2
AA4A	M	40	3.02-7	145	75	AC2B	C	500	6.78-8	14	10	AD4A	M	140	8.62-7	148	57	BA1B	C	630	3.36-6	290	0
AA4A	M	60	3.00-7	144	76	AC2B	C	550	6.07-8	12	4	AD4A	M	180	8.93-7	144	50	BA1B	C	660	4.15-6	333	-4
AA4A	M	80	2.94-7	143	75	AC2B	C	600	5.68-8	20	-16	AD4B	N	0	2.64-5	147	61	BA2A	N	0	3.56-5	62	36
AA4A	M	100	2.75-7	139	77	AC2B	C	630	4.77-8	71	-11	AD4B	C	500	1.12-5	159	52	BA2A	M	80	2.20-6	288	39
AA4A	M	140	2.60-7	161	75	AC2B	C	660	2.46-9	6	0	AD4B	C	550	9.64-6	172	46	BA2A	M	100	2.38-6	281	50
AA4A	M	180	2.60-7	150	61	AC3A	N	0	5.21-7	21	72	AD4B	C	600	8.84-6	178	49	BA2A	M	140	2.41-6	272	19
AA4B	N	0	3.23-7	167	72	AC3A	M	5	4.93-7	25	73	AD4B	C	630	8.99-6	154	39	BA2A	M	180	2.29-6	275	34
AA4B	C	500	9.58-8	194	66	AC3A	M	10	4.78-7	25	71	AD4B	C	660	6.02-6	342	66	BA2B	N	0	1.86-5	290	45
AA4B	C	550	7.84-8	199	60	AC3A	M	20	4.49-7	33	71	AE1A	N	0	1.28-6	143	80	BA2B	C	500	1.83-6	256	35
AA4B	C	600	6.55-8	222	58	AC3A	M	40	3.77-7	32	71	AE1A	M	5	9.22-7	67	73	BA2B	C	550	1.72-6	269	17
AA4B	C	630	5.83-8	239	67	AC3A	M	60	3.12-7	49	67	AE1A	M	10	8.18-7	76	73	BA2B	C	600	1.60-6	271	3
AA4B	C	660	4.28-8	297	67	AC3A	M	80	2.90-7	45	76	AE1A	M	20	7.62-7	83	73	BA2B	C	630	1.67-6	274	-1
AB1A	N	0	2.67-7	151	67	AC3A	M	100	2.67-7	28	64	AE1A	M	40	7.05-7	90	71	BA2B	C	660	2.25-6	255	-4
AB1A	M	5	2.52-7	151	62	AC3A	M	140	2.24-7	73	59	AE1A	M	60	6.87-7	98	72	BA3A	N	0	1.70-5	349	53
AB1A	M	10	2.40-7	150	61	AC3A	M	180	2.11-7	70	76	AE1A	M	80	6.67-7	97	69	BA3A	M	5	3.07-6	263	17
AB1A	M	20	2.35-7	153	60	AC3B	N	0	4.12-7	52	73	AE1A	M	100	7.01-7	97	70	BA3A	M	100	3.31-6	267	3
AB1A	M	40	2.34-7	150	60	AC3B	C	200	3.15-7	71	69	AE1A	M	140	6.30-7	90	72	BA3A	M	140	3.41-6	280	0
AB1A	M	60	2.22-7	151	62	AC3B	C	300	2.20-7	71	68	AE1A	M	180	5.19-7	101	64	BA3B	N	0	2.30-5	273	63
AB1A	M	80	2.40-7	149	61	AC3B	C	400	1.16-7	76	58	AE1B	N	0									

SPEC	TREAT	J	D	I	SPEC	TREAT	J	D	I	SPEC	TREAT	J	D	I	SPEC	TREAT	J	D	I
RF1A	C 500	2.27-7	341	49	RD1P	M 80	2.85-6	112	72	BF2A	W 80	5.63-7	176	23	BH2B	N 0	7.43-6	88	70
RD1P	C 560	6.15-7	347	27	RD1P	M 100	2.74-6	117	71	BF2A	C 500	9.95-7	341	6	BH2B	C 500	1.44-6	261	-13
RF1A	C 600	7.73-7	328	-8	RD1P	M 140	2.75-6	122	69	BF2A	C 550	1.39-6	353	1	BH2B	C 550	1.62-6	263	-22
RF1P	C 630	7.64-7	337	-24	RD2A	N 0	1.76-5	4	66	BF2A	C 600	9.77-7	337	30	BH2B	C 600	1.82-6	262	-27
RF1P	C 660	8.14-7	326	-5	RD2A	M 80	2.58-6	110	75	BF2A	C 630	1.17-5	233	9	BH2B	C 630	1.87-6	272	-27
RF2A	N 0	1.66-5	236	69	RD2A	M 100	2.18-6	94	75	RF3A	N 0	5.16-6	5	66	PH2B	C 660	1.79-6	296	-4
RF2A	M 90	1.50-6	227	59	RD2A	M 140	2.33-6	109	69	BF3A	M 60	1.72-6	146	74	BH3A	N 0	4.16-6	240	49
RF2A	M 100	1.13-6	225	54	RD2B	N 0	1.72-5	58	71	BF3A	M 40	1.73-6	153	62	BH3A	M 40	1.52-6	227	20
RF2A	M 140	1.27-6	225	62	RD2B	C 500	2.42-6	94	72	RF3A	M 80	1.63-6	143	70	BH3A	M 60	1.51-6	234	15
RF2A	M 180	0.91-7	242	44	RD2B	C 550	1.77-6	96	68	BF3B	N 0	5.76-6	295	61	BH3A	M 80	1.39-6	233	11
RF2P	N 0	1.61-5	40	62	RD2P	C 600	1.14-6	90	72	BF3B	C 200	2.94-6	317	86	BH3B	N 0	6.46-6	285	56
RF2P	C 500	1.52-6	201	59	RD2P	C 630	7.93-7	76	56	PF3B	C 300	2.43-6	5	87	BH3B	C 500	1.35-6	270	-11
RF2P	C 560	1.28-6	205	54	RD2B	C 660	9.96-7	69	45	PF3B	C 400	2.06-6	34	87	BH3B	C 550	1.55-6	275	-21
RF2P	C 600	9.81-7	216	32	RD3A	N 0	1.92-5	359	81	BF3B	C 450	1.73-6	352	81	BH3B	C 600	1.71-6	279	-26
RF2P	C 630	1.04-6	213	23	RD3A	M 80	3.05-6	94	81	BF3B	C 670	9.15-6	237	8	BH3B	C 630	1.78-6	286	-20
RF2P	C 660	1.43-6	224	17	RD3A	M 100	2.63-6	87	76	BF3B	C 500	1.63-6	13	64	BH3B	C 660	4.79-6	273	-4
RF3A	N 0	0.92-4	312	33	RD3A	M 140	2.43-6	91	80	BF3B	C 550	2.26-6	23	37	BH4B	N 0	6.31-6	182	68
RF3A	M 90	1.26-6	34	78	RD3P	N 0	1.96-5	356	74	BF3B	C 600	1.66-6	65	23	BH4B	C 500	1.49-6	301	-11
RF3A	M 100	1.07-6	4	74	RD3P	C 500	3.04-6	68	84	PF3B	C 650	2.50-6	77	3	BH4B	C 550	1.58-6	302	-17
RF3A	M 140	1.09-6	36	82	RD3P	C 550	2.44-6	68	83	BF3B	C 700	5.48-6	163	44	BH4B	C 600	1.69-6	308	-22
RF3A	M 180	0.22-7	199	95	RD3P	C 600	1.62-6	1	84	BF4A	N 0	5.04-6	70	-75	BH4B	C 630	1.72-6	304	-22
RF3P	N 0	1.57-5	28	74	RD3P	C 630	1.47-6	31	83	BF4A	M 40	1.66-6	240	87	BH4P	C 660	1.66-6	302	-22
RF3P	C 500	1.18-6	28	67	RD3B	C 660	1.95-6	123	52	PF4A	M 60	1.30-6	193	85	BH5A	N 0	3.94-6	11	57
RF3P	C 560	1.01-6	23	49	RD4A	N 0	2.38-5	30	55	BF4A	M 80	1.12-6	260	76	BH5A	M 40	4.58-7	55	63
RF3P	C 600	7.15-7	17	27	RD4A	M 80	1.94-6	91	73	BF4B	N 0	1.18-5	222	84	BH5A	M 60	4.1-7	295	16
RF3P	C 630	6.83-7	21	15	RD4A	M 100	1.73-6	90	77	BF4B	C 500	1.64-6	351	38	BH5A	M 80	1.94-7	40	71
RF3P	C 660	0.09-7	23	14	RD4A	M 140	1.37-6	113	74	BF4B	C 550	1.71-6	7	38	BH5A	M 100	1.46-7	22	15
RF4A	N 0	1.49-5	27	57	RD4B	N 0	2.90-5	38	77	BF4B	C 600	2.20-6	354	19	BH5A	M 140	6.51-7	118	6
RF4A	M 90	1.01-6	181	77	RD4B	C 500	2.26-6	105	66	BF4B	C 630	4.22-6	319	22	BH5A	M 180	7.69-6	347	21
RF4A	M 100	0.92-7	182	90	RD4P	C 550	1.67-6	106	65	BG1A	N 0	6.70-6	281	79	BH5B	N 0	2.84-6	215	-45
RF4A	M 140	0.18-7	179	71	RD4P	C 600	1.11-6	101	63	BG1A	M 5	5.05-6	155	60	BH5B	M 40	9.89-7	284	17
RF4A	M 180	0.21-7	42	43	RD4P	C 630	1.05-6	116	57	BG1A	M 10	4.34-6	169	75	BH5P	M 60	1.09-6	288	23
RF4P	N 0	1.11-5	325	77	RD4P	C 660	2.53-6	156	31	BG1A	M 20	3.50-6	155	69	BH5P	M 80	1.16-6	289	30
RF4P	C 500	0.88-7	119	96	RF1A	N 0	1.46-5	289	-68	BG1A	M 40	2.60-6	154	61	BH5P	M 100	9.60-7	277	-13
RF4P	C 560	4.00-7	141	79	RF1A	M 5	9.49-5	292	-67	BG1A	M 60	2.34-6	154	55	BH5P	M 140	1.00-6	294	-41
RF4P	C 600	4.08-7	59	83	RF1A	M 10	2.66-5	296	-61	BG1A	M 80	2.33-6	153	50	BH5P	M 180	7.07-7	268	-24
RF4P	C 630	2.70-7	38	73	RF1A	M 20	3.77-6	311	46	BG1A	M 100	1.96-6	157	58	BH5P	M 200	9.60-7	277	-13
RF1A	N 0	1.64-5	234	71	RF1A	M 40	3.17-6	310	45	BG1A	M 140	1.71-6	152	45	BH5P	M 240	1.00-6	294	-41
RF1A	M 5	6.44-6	348	81	RF1A	M 60	2.80-6	309	40	BG1A	M 180	2.05-6	162	62	BH5P	M 280	1.00-6	294	-41
RF1A	M 10	5.00-6	342	81	RF1A	M 80	2.30-6	324	33	BG1B	N 0	0.86-6	146	76	BH5P	M 320	1.00-6	294	-41
RF1A	M 20	3.76-6	3	82	RF1A	M 100	2.22-6	318	36	BG1B	C 200	4.01-6	157	73	BH5P	M 360	1.00-6	294	-41
RF1A	M 40	2.90-6	16	76	RF1A	M 140	2.24-6	317	33	BG1B	C 300	3.78-6	153	69	BH5P	M 400	1.00-6	294	-41
RF1A	M 60	2.46-6	7	77	RF1A	M 180	2.55-6	322	25	BG1B	C 400	2.67-6	155	68	BH5P	M 440	1.00-6	294	-41
RF1A	M 80	2.25-6	23	78	RF1P	N 0	1.34-4	292	-33	BG1B	C 450	2.64-6	148	70	BH5P	M 480	1.00-6	294	-41
RF1P	N 0	1.13-5	17	73	RF1P	C 200	5.19-5	301	-50	BG1B	C 500	2.07-6	145	67	BH5P	M 520	1.00-6	294	-41
RF1P	C 500	2.13-6	73	90	RF1P	C 300	2.97-5	302	-54	BG1B	C 550	1.62-6	140	63	BH5P	M 560	1.00-6	294	-41
RF1P	C 560	1.70-6	58	75	RF1P	C 400	1.87-5	302	-53	BG1B	C 600	2.72-7	205	21	BH5P	M 600	1.00-6	294	-41
RF1P	C 600	1.18-6	42	69	RF1P	C 450	1.49-5	304	-54	BG1B	C 650	3.47-7	121	-34	BH5P	M 640	1.00-6	294	-41
RF1P	C 630	2.43-7	50	66	RF1P	C 500	1.06-5	307	-51	BG1B	C 700	1.17-6	121	65	BH5P	M 680	1.00-6	294	-41
RF1P	C 660	7.96-7	57	83	RF1P	C 550	6.70-6	309	-45	BG1B	C 750	1.79-6	348	23	BH5P	M 720	1.00-6	294	-41
RF2A	N 0	7.56-6	50	45	RF1P	C 600	2.32-6	321	4	BG2A	N 0	6.32-6	15	71	BH5P	M 760	1.00-6	294	-41
RF2A	M 90	2.13-6	328	83	RF1P	C 650	2.97-6	327	14	BG2A	M 40	2.83-6	158	66	BH5P	M 800	1.00-6	294	-41
RF2A	M 100	1.77-6	330	86	RF1P	C 700	7.36-7	265	37	BG2A	M 60	2.23-6	153	58	BH5P	M 840	1.00-6	294	-41
RF2A	M 140	1.64-6	246	90	RF1P	C 750	1.15-6	101	2	BG2A	M 80	2.04-6	158	50	BH5P	M 880	1.00-6	294	-41
RF2A	M 180	1.61-6	287	79	RF2A	N 0	5.36-5	289	-38	BG2B	N 0	1.79-5	124	71	BH5P	M 920	1.00-6	294	-41
RF2A	M 100	1.49-6	171	73	RF2A	M 100	1.76-6	309	47	BG2B	C 500	2.01-6	144	61	BH5P	M 960	1.00-6	294	-41
RF2A	M 140	0.94-7	183	63	RF2A	M 140	2.49-6	281	53	BG2B	C 550	1.63-6	136	59	BH5P	M 1000	1.00-6	294	-41
RF2P	N 0	1.05-5	5	60	RF2A	M 180	1.20-6	308	43	BG2B	C 600	6.62-7	172	65	BH5P	M 1040	1.00-6	294	-41
RF2P	C 500	1.61-6	154	76	RF2P	N 0	4.61-5	298	-34	BG2B	C 630	6.65-7	256	62	BH5P	M 1080	1.00-6	294	-41
RF2P	C 560	1.71-6	150	75	RF2P	C 500	2.77-6	301	10	BG2B	C 660	1.72-6	272	1	BH5P	M 1120	1.00-6	294	-41
RF2P	C 600	7.78-7	156	40	RF2P	C 550	1.70-6	303	17	BG3A	N 0	7.61-6	10	70	BH5P	M 1160	1.00-6	294	-41
RF2P	C 630	6.10-7	190	70	RF2P	C 600	1.25-6	323	37	BG3A	M 40	2.88-6	153	68	BH5P	M 1200	1.00-6	294	-41
RF2P	C 660	4.85-7	16	7	RF2P	C 630	1.17-6	323	4	BG3A	M 60	2.20-6	148	61	BH5P	M 1240	1.00-6	294	-41
RF3A	N 0	6.60-6	80	66	RF3A	C 660	1.35-6	242	21	BG3A	M 80	2.05-6	154	62	BH5P	M 1280	1.00-6	294	-41
RF3A	M 90	3.28-6	330	72	RF3A	C 700	2.95-6	125	50	BG3B	N 0	1.26-5	251	76	BH5P	M 1320	1.00-6	294	-41
RF3A	M 100	3.08-6	334	71	RF3A	M 100	2.96-6	162	60	BG3B	C 500	2.14-6	146	63	BH5P	M 1360	1.00-6	294	-41
RF3A	M 140	2.56-6	326	70	RF3A	M 140	2.34-6	191	68	BG3B	C 550	1.67-6	144	63	BH5P	M 1400	1.00-6	294	-41
RF3P	N 0	1.02-5	51	61	RF3P	M 180	2.16-6	147	62	BG3B	C 600	9.73-7	150	67	BH5P	M 1440	1.00-6	294	-41
RF3P	C 200	4.34-6	120	71	RF3P	C 200	4.42-6	114	63	BG3B	C 630	6.72-7	132	70	BH5P	M 1480	1.00-6	294	-41
RF3P	C 300	3.52-6	329	77	RF3P	C 300	9.73-7	112	63	BG3B	C 660	6.79-7	43	15	BH5P	M 1520	1.00-6	294	-41
RF3P	C 400	2																	

SPEC	TREAT	J	D	I	SPEC	TREAT	J	D	I	SPEC	TREAT	J	D	I	SPEC	TREAT	J	D	I				
RJ1A	M	5	6.27-6	343	44	RJ5B	M	5	4.99-6	129	80	BL1A	M	100	1.20-6	156	52	FL3C	C	300	2.47-6	186	69
RJ1A	M	10	5.32-6	341	36	RJ5B	M	10	4.00-6	144	76	BL1A	M	100	1.43-6	161	41	FL3C	C	400	1.65-6	195	67
RJ1A	M	20	4.56-6	340	24	RJ5B	M	20	2.92-6	151	72	BL1A	M	140	1.12-6	179	36	FL3C	C	500	5.44-7	223	6
RJ1A	M	40	4.60-6	342	11	RJ5B	M	40	2.32-6	147	68	BL1A	M	180	4.89-6	195	-7	FL3C	C	551	1.30-6	280	-45
RJ1A	M	60	4.00-6	339	4	RJ5B	M	60	1.60-6	154	63	BL1A	C	500	6.00-7	181	30	FL3C	C	600	1.15-6	302	-46
RJ1A	M	80	4.54-6	339	1	RJ5B	M	80	1.45-6	161	64	BL1A	C	550	5.28-7	194	40	FL3C	C	650	9.44-7	306	-37
RJ1A	M	100	4.50-6	339	3	RJ5B	M	100	1.20-6	148	68	BL1A	C	600	3.52-7	204	39	FL4A	N	0	4.57-6	129	61
RJ1A	M	140	4.67-6	339	2	RJ5B	M	140	1.23-6	182	55	FL1A	C	630	2.34-7	212	28	FL4A	M	5	6.18-6	130	71
RJ1A	M	180	3.79-6	344	0	RJ5B	M	180	1.27-6	129	57	FL1B	N	0	4.75-6	99	78	FL4A	M	10	4.99-6	146	67
RJ1A	M	180	5.11-6	52	32	RK1A	N	0	6.17-6	15	36	BL1B	T	100	6.96-6	57	74	FL4A	M	20	3.67-6	149	66
RJ1A	C	500	3.77-6	343	-3	RK1A	M	5	5.91-6	354	28	FL1B	T	215	5.80-6	49	81	FL4A	M	40	2.27-6	141	49
RJ1A	C	550	3.70-6	343	-5	RK1A	M	10	5.58-6	352	22	FL1B	T	306	3.79-6	117	73	FL4A	M	60	1.75-6	143	47
RJ1A	C	600	3.70-6	343	-5	RK1A	M	20	5.40-6	351	16	FL1B	T	409	3.18-6	135	58	FL4A	M	80	1.50-6	127	49
RJ1A	C	630	4.16-6	46	5	RK1A	M	40	5.31-6	452	9	FL1B	T	505	1.58-6	158	80	FL4A	M	100	1.46-6	147	46
RJ1A	C	650	8.21-6	260	1	RK1A	M	60	5.08-6	351	7	FL1B	T	547	1.53-6	209	84	FL4A	M	140	1.54-6	152	38
RJ1B	N	0	0.60-6	7	46	RK1A	M	80	5.26-6	351	6	FL1B	T	600	4.23-6	282	54	FL4A	M	180	1.01-6	149	48
RJ1B	M	5	6.03-6	348	34	RK1A	M	100	5.23-6	348	7	BL1B	T	650	2.42-6	55	43	FL4B	N	0	1.18-6	80	73
RJ1B	M	10	6.08-6	344	26	RK1A	M	140	5.21-6	347	3	BL1B	T	775	1.28-6	44	50	FL4B	T	100	9.38-6	37	85
RJ1B	M	20	5.50-6	342	14	RK1A	M	180	4.61-6	349	9	BL1C	N	0	4.13-6	108	60	FL4B	T	215	7.28-6	62	83
RJ1B	M	40	5.56-6	339	4	RK1B	N	0	5.79-6	333	55	BL1C	C	152	4.02-6	156	66	FL4B	T	306	5.00-6	101	84
RJ1B	M	60	5.52-6	339	-3	RK1B	M	5	6.21-6	334	41	BL1C	C	200	4.02-6	157	64	FL4B	T	409	4.75-6	352	84
RJ1B	M	80	5.44-6	340	-4	RK1B	M	10	5.23-6	334	34	BL1C	C	700	3.09-6	156	61	FL4B	T	505	2.55-6	60	68
RJ1B	M	100	5.61-6	338	-5	RK1B	M	20	4.87-6	332	23	BL1C	C	400	2.08-6	150	62	FL4B	T	547	1.44-6	5	80
RJ1B	M	140	5.36-6	340	-9	RK1B	M	40	4.46-6	336	13	FL1C	C	500	1.05-6	156	56	FL4B	T	600	4.32-6	54	40
RJ1B	M	180	3.73-6	331	-6	RK1B	M	60	4.48-6	335	10	FL1C	C	551	2.75-7	225	13	FL4B	T	650	5.12-6	300	28
RJ2A	N	0	0.70-6	325	66	RK1B	M	80	4.54-6	336	8	FL1C	C	600	4.48-7	237	59	FL4B	T	775	1.66-6	14	56
RJ2A	C	500	4.41-7	238	37	RK1B	M	100	4.53-6	334	6	FL1C	C	650	4.66-6	279	58	FL4C	N	0	1.09-6	162	87
RJ2A	C	550	4.07-7	261	-22	RK1B	M	140	3.43-6	327	0	FL2A	N	0	0.58-6	123	80	FL4C	C	100	7.41-6	119	73
RJ2A	C	600	7.33-7	278	-42	RK1B	M	180	2.77-6	330	5	FL2A	M	5	4.60-6	119	77	FL4C	C	200	5.48-6	133	63
RJ2A	C	630	7.40-7	332	-19	RK1B	M	180	6.09-6	36	11	FL2A	M	10	3.14-6	166	81	FL4C	C	300	4.37-6	137	83
RJ2A	C	650	1.00-6	155	17	RK1B	C	500	3.58-6	333	-1	FL2A	M	20	2.02-6	207	72	FL4C	C	400	3.07-6	132	61
RJ2A	N	0	6.91-6	295	95	RK1B	C	550	2.60-6	334	-3	FL2A	M	30	1.32-6	217	68	FL4C	C	500	2.43-6	131	68
RJ2A	M	5	4.60-6	140	72	RK1B	C	600	3.71-6	334	-5	FL2A	M	40	0.31-7	188	72	FL4C	C	600	1.27-6	105	58
RJ2A	M	10	3.71-6	144	64	RK1B	C	630	3.55-6	334	-5	FL2A	M	50	7.36-7	254	75	FL4C	C	650	0.30-6	331	65
RJ2A	M	20	2.90-6	144	61	RK1B	C	660	3.25-6	311	11	FL2A	M	60	5.23-7	280	67	FL4C	C	700	5.83-6	326	80
RJ2A	M	40	2.08-6	140	57	RK2A	N	0	1.03-6	21	25	FL2A	M	70	6.31-7	206	55	FL4C	C	800	1.44-6	312	74
RJ2A	M	60	1.87-6	142	49	RK2A	M	5	7.20-6	8	14	FL2A	M	80	6.61-7	235	57	FL4C	C	900	3.20-6	307	71
RJ2A	M	80	1.72-6	141	44	RK2A	M	10	6.86-6	7	10	FL2A	M	90	5.47-7	220	38	FL4C	C	1000	4.19-6	289	62
RJ2A	M	100	1.44-6	131	70	RK2A	M	20	6.64-6	6	4	FL2A	M	100	4.50-7	233	41	FL4C	C	1100	1.61-6	297	60
RJ2A	M	140	1.71-6	144	35	RK2A	M	40	6.60-6	6	1	FL2A	M	120	4.04-7	252	14	FL4C	C	1200	1.56-6	311	43
RJ2A	M	180	1.72-6	145	46	RK2A	M	60	6.69-6	6	-2	FL2A	M	140	5.88-7	248	25	FL4C	C	1300	1.34-6	304	56
RJ2A	M	180	5.85-6	158	28	RK2A	M	80	6.58-6	6	-3	FL2A	M	160	2.08-7	252	46	FL4C	C	1400	1.23-6	297	53
RJ2A	M	180	5.85-6	158	28	RK2A	M	100	6.62-6	3	-4	FL2A	M	180	4.30-7	261	73	FL4C	C	1500	1.44-6	319	4
RJ2A	M	180	5.85-6	158	28	RK2A	M	140	5.17-6	4	-1	FL2B	N	0	0.44-6	176	82	FL4C	C	1600	0.45-6	58	75
RJ2A	M	180	6.46-6	160	27	RK2A	M	180	3.72-6	5	-22	FL2B	T	100	7.04-6	308	79	FL4C	C	1700	4.74-6	33	75
RJ2A	M	180	6.46-6	160	27	RK2A	M	180	3.72-6	5	-22	FL2B	T	215	6.51-6	15	40	FL4C	C	1800	3.25-6	35	73
RJ2A	M	180	6.46-6	160	27	RK2A	M	180	3.72-6	5	-22	FL2B	T	215	6.51-6	15	40	FL4C	C	1900	2.18-6	22	64
RJ2A	M	180	6.46-6	160	27	RK2A	M	180	3.72-6	5	-22	FL2B	T	215	6.51-6	15	40	FL4C	C	2000	2.08-6	15	59
RJ2A	M	180	6.46-6	160	27	RK2A	M	180	3.72-6	5	-22	FL2B	T	215	6.51-6	15	40	FL4C	C	2100	1.81-6	359	54
RJ2A	M	180	6.46-6	160	27	RK2A	M	180	3.72-6	5	-22	FL2B	T	215	6.51-6	15	40	FL4C	C	2200	1.66-6	346	31
RJ2A	M	180	6.46-6	160	27	RK2A	M	180	3.72-6	5	-22	FL2B	T	215	6.51-6	15	40	FL4C	C	2300	1.55-6	345	12
RJ2A	M	180	6.46-6	160	27	RK2A	M	180	3.72-6	5	-22	FL2B	T	215	6.51-6	15	40	FL4C	C	2400	1.41-6	346	10
RJ2A	M	180	6.46-6	160	27	RK2A	M	180	3.72-6	5	-22	FL2B	T	215	6.51-6	15	40	FL4C	C	2500	1.19-6	347	0
RJ2A	M	180	6.46-6	160	27	RK2A	M	180	3.72-6	5	-22	FL2B	T	215	6.51-6	15	40	FL4C	C	2600	1.07-6	346	-6
RJ2A	M	180	6.46-6	160	27	RK2A	M	180	3.72-6	5	-22	FL2B	T	215	6.51-6	15	40	FL4C	C	2700	1.07-6	346	-6
RJ2A	M	180	6.46-6	160	27	RK2A	M	180	3.72-6	5	-22	FL2B	T	215	6.51-6	15	40	FL4C	C	2800	1.07-6	346	-6
RJ2A	M	180	6.46-6	160	27	RK2A	M	180	3.72-6	5	-22	FL2B	T	215	6.51-6	15	40	FL4C	C	2900	1.07-6	346	-6
RJ2A	M	180	6.46-6	160	27	RK2A	M	180	3.72-6	5	-22	FL2B	T	215	6.51-6	15	40	FL4C	C	3000	1.07-6	346	-6
RJ2A	M	180	6.46-6	160	27	RK2A	M	180	3.72-6	5	-22	FL2B	T	215	6.51-6	15	40	FL4C	C	3100	1.07-6	346	-6
RJ2A	M	180	6.46-6	160	27	RK2A	M	180	3.72-6	5	-22	FL2B	T	215	6.51-6	15	40	FL4C	C	3200	1.07-6	346	-6
RJ2A	M	180	6.46-6	160	27	RK2A	M	180	3.72-6	5	-22	FL2B	T	215	6.51-6	15	40	FL4C	C	3300	1.07-6	346	-6
RJ2A	M	180	6.46-6	160	27	RK2A	M	180	3.72-6	5	-22	FL2B	T	215	6.51-6	15	40	FL4C	C	3400	1.07-6	346	-6
RJ2A	M	180	6.46-6	160	27	RK2A	M	180	3.72-6	5	-22	FL2B	T	215	6.51-6	15	40	FL4C	C	3500	1.07-6	346	-6
RJ2A	M	180	6.46-6	160	27	RK2A	M	180	3.72-6	5	-22	FL2B	T	215	6.51-6	15	40	FL4C	C	3600	1.07-6	346	-6
RJ2A	M	180	6.46-6	160	27	RK2A	M	180	3.														

SPEC	TREAT	J	D	I	SPEC	TREAT	J	D	I	SPEC	TREAT	J	D	I	SPEC	TREAT	J	D	I
CA3A	C 130	3.82-7	323	23	CA3B	N	C 1.72-5	117	72	CC6A	M	5 1.02-5	150	73	CE3A	T	600 3.70-5	261	45
CA3B	C 150	1.44-6	218	19	CA3B	M	40 5.89-6	160	27	CC6A	M	10 2.30-6	151	71	CE3A	T	600 5.71-5	345	74
CA3B	N	C 1.8A-5	73	59	CA3B	M	40 5.95-6	159	22	CC6A	M	20 9.73-6	160	64	CE3A	T	600 5.40-5	304	40
CA3B	M	5 6.58-6	150	78	CA3B	M	40 5.74-6	158	24	CC6A	M	40 7.64-6	157	64	CE3A	T	600 5.40-5	304	40
CA3B	M	10 3.97-6	337	64	CA4A	N	0 9.12-6	158	54	CC6A	M	40 7.64-6	157	64	CE4A	N	0 1.27-5	118	54
CA3B	M	20 2.54-6	336	44	CA4A	M	40 3.00-6	85	12	CC6A	M	60 7.21-6	157	67	CE4A	C	150 1.30-5	135	51
CA3B	M	40 1.80-6	330	21	CA4A	M	40 3.01-6	84	13	CC6A	M	80 7.17-6	156	64	CE4A	C	200 1.27-5	136	46
CA3B	M	60 2.19-6	322	4	CA4A	M	40 3.23-6	84	4	CC6A	M	100 7.81-6	156	65	CE4A	C	300 1.13-5	137	44
CA3B	M	80 0.01-6	336	-4	CA4B	N	0 6.80-6	36	64	CC6A	M	140 6.23-6	154	65	CE4A	C	400 8.50-6	140	41
CA3B	M	100 1.99-6	342	-4	CA4B	C	500 1.69-5	91	17	CC6B	N	0 1.50-5	153	70	CE4A	C	500 3.35-6	141	30
CA3B	M	140 2.43-6	349	-1	CA4B	C	500 1.72-6	96	16	CC6B	C	500 4.14-6	162	63	CE4A	C	600 7.01-6	11	4
CA3B	M	180 2.18-6	330	-15	CA4B	C	600 1.31-6	93	2	CC6B	C	500 3.62-6	155	64	CE4A	C	650 7.55-6	172	-82
CA3B	N	0 2.64-5	239	74	CA4B	C	650 1.02-6	102	40	CC6B	C	600 2.28-6	162	62	CE4B	N	0 1.73-5	136	60
CA3B	C	200 3.95-6	335	25	CB1A	N	0 7.23-6	121	77	CC6B	C	630 3.07-6	114	47	CE4B	T	100 1.34-5	139	58
CA3B	C	300 3.29-6	341	1	CB1A	M	5 6.71-6	141	60	CC6B	C	660 1.59-5	34	-2	CE4B	T	215 1.30-5	125	62
CA3B	C	400 3.35-6	343	-11	CB1A	M	10 6.03-6	145	57	CD1A	N	0 1.57-5	127	64	CE4B	T	306 1.04-5	130	57
CA3B	C	450 3.35-6	342	-18	CB1A	M	20 5.56-6	144	52	CD1A	M	5 1.53-5	121	57	CE4B	T	409 8.42-6	132	59
CA3B	C	500 3.45-6	344	-1	CB1A	M	40 5.24-6	141	48	CD1A	M	10 1.37-5	122	56	CE4B	T	505 6.25-6	119	54
CA3B	C	550 3.75-6	341	-24	CB1A	M	60 5.02-6	140	46	CD1A	M	20 1.17-5	121	55	CE4B	T	547 5.50-6	150	56
CA3B	C	600 4.02-6	340	-29	CB1A	M	80 4.69-6	144	43	CD1A	M	40 1.02-5	118	54	CE4B	T	600 6.30-5	114	79
CA3B	C	650 3.67-6	345	-24	CB1A	M	100 4.82-6	141	43	CD1A	M	60 9.92-6	116	55	CE4B	T	600 6.00-5	92	74
CA3B	C	700 2.60-6	339	-25	CB1A	M	140 4.53-6	137	41	CD1A	M	80 9.52-6	123	54	CE4B	T	600 4.76-5	40	72
CA3B	C	750 6.54-7	56	28	CB1A	M	180 3.45-6	131	43	CD1A	M	100 9.35-6	122	53	CE5A	N	0 1.22-5	123	42
CA3B	C	800 1.97-5	252	-17	CB2A	N	0 1.68-5	174	79	CD1A	M	140 8.69-6	176	57	CE5A	M	5 1.04-5	133	43
CA3B	C	850 2.07-6	303	-17	CB2A	M	40 6.10-6	158	63	CD1A	M	180 8.06-6	123	51	CE5A	M	10 9.03-6	136	39
CA3B	C	900 2.64-6	305	-22	CB2A	M	60 5.65-6	153	59	CD1B	N	0 1.45-5	129	62	CE5A	M	20 7.75-6	136	37
CA3B	C	950 2.66-6	307	-24	CB2A	M	80 4.68-6	146	45	CD1B	C	500 3.67-6	121	43	CE5A	M	30 7.15-6	134	37
CA3B	C	1000 2.42-6	310	-26	CB2A	M	100 5.40-6	156	58	CD1B	C	550 3.01-6	116	45	CE5A	M	40 6.60-6	130	32
CA3B	C	1050 2.93-6	332	-21	CB2A	M	140 5.30-6	158	57	CD1B	C	600 6.11-6	340	15	CE5A	M	60 7.05-6	140	39
CA3B	N	0 3.30-5	142	40	CB2A	M	180 4.51-6	160	56	CD1B	C	650 1.76-5	47	24	CE5A	M	80 6.97-6	134	42
CA3B	M	5 9.54-6	148	75	CB3A	N	0 1.60-5	255	73	CD2A	N	0 1.40-5	102	61	CE5A	M	100 6.93-6	138	45
CA3B	M	10 9.29-6	149	76	CB3A	M	40 4.03-6	194	73	CD2A	M	40 8.84-6	110	50	CE5A	M	140 8.80-6	195	53
CA3B	M	20 9.24-6	227	70	CB3A	M	60 4.50-6	200	71	CD2A	M	60 8.48-6	106	50	CE5A	M	180 6.21-6	142	46
CA3B	M	40 1.73-6	240	55	CB3A	M	80 4.63-6	180	73	CD2A	M	80 9.20-6	115	51	CE5B	N	0 1.93-5	133	54
CA3B	M	60 1.40-6	265	59	CB3B	N	0 1.32-5	343	68	CD2B	N	0 1.74-5	119	66	CE5B	T	100 1.45-5	121	57
CA3B	M	80 1.25-6	262	29	CB3B	C	500 4.02-6	162	68	CD2B	C	500 4.53-6	111	50	CE5B	T	215 1.20-5	124	53
CA3B	M	100 1.10-6	262	40	CB3B	C	550 3.91-6	153	67	CD2B	C	550 3.40-6	100	61	CE5B	T	306 9.27-6	134	46
CA3B	M	140 6.75-7	301	18	CB3B	C	600 3.53-6	171	63	CD2B	C	600 1.40-6	166	50	CE5B	T	409 7.70-6	138	50
CA3B	M	180 2.26-7	339	36	CB3B	C	650 3.00-6	180	63	CD2B	C	630 3.54-6	163	50	CE5B	T	505 5.09-6	110	67
CA3B	N	0 4.43-5	137	41	CB4A	N	0 0.60-5	332	70	CD2B	C	660 8.79-6	125	26	CE5B	T	547 3.31-5	67	50
CA3B	M	5 9.07-6	154	75	CB4A	M	40 4.22-6	126	64	CD3A	N	0 1.64-5	105	58	CE5B	T	600 7.14-5	164	81
CA3B	M	10 4.80-6	243	73	CB4A	M	60 4.02-6	120	60	CD3A	M	40 8.85-6	120	57	CE5B	T	601 9.07-5	195	80
CA3B	M	20 3.07-6	273	56	CB4A	M	80 3.84-6	129	60	CD3A	M	60 9.24-6	117	57	CE5B	T	602 9.02-5	60	76
CA3B	M	40 2.60-6	278	24	CB4B	N	0 9.70-6	208	87	CD3A	M	80 8.62-6	121	59	CE6A	N	0 1.40-5	131	52
CA3B	M	60 2.31-6	287	11	CB4B	C	500 3.75-6	123	63	CD4A	N	0 1.26-5	121	61	CE6A	T	100 1.52-5	127	52
CA3B	M	80 2.48-6	286	5	CB4B	C	550 3.60-6	126	59	CD4A	M	40 7.33-6	131	62	CE6A	T	215 1.32-5	130	50
CA3B	M	100 2.77-6	290	3	CB4B	C	600 3.53-6	130	54	CD4A	M	60 8.16-6	148	69	CE6A	T	306 1.03-5	134	49
CA3B	M	140 2.75-6	236	-2	CB4B	C	630 3.72-6	123	47	CD4A	M	80 6.64-6	134	65	CE6A	T	409 8.32-6	125	46
CA3B	M	180 2.60-6	201	-10	CB4B	C	660 3.71-6	131	50	CD4B	N	0 1.21-5	123	73	CE6A	T	505 5.94-6	120	60
CA3B	N	0 2.75-5	165	-12	CB5B	N	0 6.98-6	347	81	CD4B	C	500 2.77-6	123	71	CE6A	T	547 8.80-6	315	52
CA3B	C	500 5.57-7	297	12	CB5B	C	500 2.14-6	140	50	CD4B	C	550 2.56-6	96	50	CE6A	T	600 5.50-5	340	47
CA3B	C	550 8.45-7	311	-20	CB5B	C	550 2.13-6	143	43	CD4B	C	600 1.23-6	283	47	CE6A	T	601 7.84-5	354	64
CA3B	C	600 1.51-6	313	-31	CB5B	C	600 2.13-6	156	43	CD4B	C	630 1.18-5	312	2	CE6A	T	602 7.57-5	326	75
CA3B	C	630 1.33-6	316	-40	CB5B	C	630 2.23-6	159	43	CD4B	C	660 1.57-5	114	13	CE6B	N	0 1.01-5	134	56
CA3B	C	660 1.35-6	314	-39	CB5B	C	660 2.52-6	173	42	CD5B	N	0 1.63-5	134	67	CE6B	M	5 1.47-5	134	54
CA4A	N	0 2.60-5	23	74	CB5B	N	0 5.88-6	155	64	CD5B	C	500 4.52-6	140	55	CE6B	M	10 1.34-5	135	52
CA4A	M	5 7.00-6	312	83	CB5B	C	550 2.80-6	135	65	CD5B	C	550 3.03-6	145	63	CE6B	M	20 1.17-5	136	51
CA4A	M	10 5.25-6	257	70	CB5B	C	600 2.78-6	135	63	CD5B	C	600 2.94-6	250	36	CE6B	M	30 1.06-5	136	48
CA4A	M	20 7.00-6	267	56	CB5B	C	630 2.65-6	136	16	CD5B	C	630 9.08-7	12	54	CE6B	M	40 1.11-5	131	50
CA4A	M	40 2.44-6	307	71	CB5B	C	660 2.64-6	132	21	CD5B	C	660 4.98-6	111	30	CE6B	M	60 9.40-6	134	47
CA4A	M	60 2.15-6	312	25	CB5B	C	660 2.10-6	135	12	CE1A	N	0 1.17-5	119	54	CE6B	M	80 9.31-6	138	46
CA4A	M	80 4.04-6	293	-23	CE1A	N	0 1.60-5	201	30	CE1A	M	5 1.20-5	120	55	CE6B	M	100 9.37-6	136	50
CA4A	M	100 3.77-6	304	0	CE1A	M	5 1.47-5	162	74	CE1A	M	10 1.08-5	122	53	CE6B	M	140 1.00-5	147	55
CA4A	M	140 2.00-6	104	-3	CE1A	M	10 1.34-5	144	72	CE1A	M	20 9.41-6	124	50	CE6B	M	180 8.78-6	142	44
CA4A	M	180 9.30-7	10	-38	CE1A	M	20 1.17-5	195	71	CE1A	M	40 9.37-6	125	52	CE6B	M	240 9.03-6	158	47
CA4B	N	0 2.31-5	137	-5	CE1A	M	40 1.03-5	199	70	CE1A	M	60 7.73-6	124	63	CE6B	M	300 4.15-6	145	38
CA4B	C	500 2.56-6	214	-11	CE1A	M	60 9.60-6	201	70	CE1A	M	80 7.49-6	127	65	CE6B	M	400 3.38-6	138	41
CA4B	C	550 2.00-6	212	-16	CE1A	M	80 9.23-6	201	70	CE1A	M	100 7.11-6	128	52	CE6B	M	600 2.07-6	137	45
CA4B	C	600 3.51-6	213	-25	CE2A	N	0 1.84-5	131	31	CE1A	M	140 7.14-6	130	51	CE6B	M	800 5.38-6	82	39
CA4B	C	630 3.31-6	214	-26	CE2A	M	40 9.10-6	192	75	CE1A	M	150 5.03-6	122	40	CE7A	N	0 2.31-5	120	60
CA4B	C	660 2.01-6	218</																

SPEC	TREAT	J	D	I	SPEC	TREAT	J	D	I	SPEC	TREAT	J	D	I	SPEC	TREAT	J	D	I
CF3B	C 450	4.21-6	143	44	CG6F	N 0	1.70-6	141	75	CH1A	N 0	1.23-6	158	56	CJ3B	C 400	4.41-6	140	35
CF3B	C 500	2.17-6	139	44	CG6F	C 500	2.21-6	127	45	CH1A	M 5	1.06-6	133	59	CJ3B	C 450	7.27-6	147	35
CF3B	C 530	6.72-7	110	44	CG6F	C 550	1.51-6	127	45	CH1A	M 10	9.43-6	138	46	CJ3B	C 500	7.41-6	147	35
CF3B	C 600	4.40-7	61	16	CG6F	C 600	6.30-7	86	26	CH1A	M 20	8.49-6	140	53	CJ3B	C 550	4.16-6	147	16
CF4A	N 0	2.72-6	179	51	CG6F	C 650	1.70-6	42	3	CH1A	M 30	4.10-6	130	50	CJ3B	C 600	4.32-6	147	16
CF4A	M 40	1.41-6	158	59	CH1A	N 0	1.02-6	153	59	CH1A	M 40	7.78-6	141	48	CJ3B	C 650	4.32-6	147	16
CF4A	M 60	1.77-6	154	67	CH1A	T 100	1.67-6	123	34	CH1A	M 50	7.36-6	136	50	CJ3B	C 700	6.42-6	140	1
CF4A	M 80	1.25-6	155	70	CH1A	T 215	1.64-6	155	49	CH1A	M 60	7.20-6	140	47	CJ4A	N 0	1.57-6	106	56
CF4A	M 90	1.65-6	131	36	CH1A	T 306	1.30-6	150	46	CH1A	M 70	7.11-6	142	43	CJ4A	M 0	1.73-6	75	67
CF4A	A 194	5.77-6	107	12	CH1A	T 405	5.41-6	157	56	CH1A	M 80	7.23-6	139	47	CJ4A	M 10	6.41-6	147	64
CF4A	C 500	1.10-6	114	16	CH1A	T 505	4.19-6	125	20	CH1A	M 90	7.20-6	141	49	CJ4A	M 30	6.40-6	77	60
CF4A	C 550	7.06-6	116	21	CH1A	T 547	3.33-6	145	25	CH1A	M 100	7.00-6	142	43	CJ4A	M 40	7.27-6	77	6
CF4A	C 600	2.15-6	138	43	CH1A	T 600	3.07-6	141	27	CH1A	M 120	6.97-6	140	46	CJ4A	M 60	7.27-6	77	6
CF4A	C 650	1.68-6	134	51	CH1A	T 650	1.26-6	175	47	CH1A	M 140	6.16-6	141	49	CJ4A	M 80	7.07-6	76	3
CF4A	C 700	5.82-7	149	40	CH1F	N 0	1.40-6	178	44	CH1A	M 160	6.36-6	142	47	CJ4A	M 100	7.07-6	76	3
CF4A	M 0	2.44-6	144	61	CH1F	N 0	1.74-6	144	62	CH1A	M 180	6.27-6	147	48	CJ4A	M 120	7.07-6	76	3
CF4A	C 100	1.78-6	153	53	CH1F	M 5	1.25-6	138	65	CH1F	N 0	1.30-6	107	57	CJ4A	M 140	6.47-6	77	6
CF4A	C 300	1.46-6	154	52	CH1F	M 10	1.01-6	138	63	CH1F	C 500	6.71-6	176	47	CJ4A	M 160	6.47-6	77	6
CF4A	C 400	1.11-6	151	53	CH1F	M 20	7.86-6	139	57	CH1F	C 550	2.31-6	149	52	CJ4A	C 600	5.40-6	77	67
CF4A	C 450	9.01-6	151	53	CH1F	M 30	6.08-6	143	56	CH1F	C 600	1.18-6	128	68	CJ4A	C 650	4.47-6	73	67
CF4A	C 500	6.52-6	150	47	CH1F	M 40	6.03-6	142	54	CH1F	C 650	1.00-6	260	64	CJ4A	N 0	2.11-6	76	6
CF4A	C 550	4.04-6	140	48	CH1F	M 60	5.20-6	132	52	CH1F	N 0	9.39-6	124	63	CJ4A	C 500	6.44-6	73	68
CF4A	C 600	2.06-6	152	44	CH1F	M 80	5.10-6	142	50	CH1F	M 40	4.21-6	131	64	CJ4A	C 550	5.22-6	71	6
CF4A	C 650	5.91-7	220	23	CH1F	M 100	4.65-6	134	48	CH1F	M 60	3.94-6	147	60	CJ4A	C 600	5.22-6	71	6
CF4A	C 730	9.13-7	156	61	CH1F	M 140	4.56-6	144	45	CH1F	M 80	3.75-6	146	61	CJ4A	C 650	4.75-6	70	21
CF5A	N 0	3.20-6	157	60	CH1F	M 180	4.11-6	138	44	CH1F	N 0	9.43-6	145	50	CK1A	N 0	1.20-6	127	76
CF5A	M 40	1.30-6	143	52	CH2A	N 0	1.65-6	131	74	CH1F	C 500	1.48-6	149	77	CK1A	N 0	1.18-6	134	56
CF5A	M 60	1.34-6	145	47	CH2A	M 5	1.12-6	138	70	CH1F	C 550	8.60-7	169	84	CK1A	M 0	1.43-6	132	46
CF5A	M 80	1.47-6	146	47	CH2A	M 10	9.33-6	142	67	CH1F	C 600	4.20-7	312	74	CK1A	M 10	7.22-6	122	46
CF5A	C 550	4.60-6	128	26	CH2A	M 20	7.96-6	145	64	CH1F	C 650	3.47-7	324	74	CK1A	M 20	7.47-6	124	41
CF5A	C 600	2.33-6	148	39	CH2A	M 30	6.40-6	142	61	CH1F	C 700	1.09-6	352	5	CK1A	M 40	7.11-6	121	40
CF5A	C 650	7.04-6	124	33	CH2A	M 40	6.27-6	145	62	CH1F	C 750	0.871-6	251	55	CK1A	M 60	6.44-6	124	37
CF5A	N 0	2.70-6	147	52	CH2A	M 60	5.89-6	146	57	CH1F	C 800	5.23-6	154	63	CK1A	M 80	6.21-6	121	36
CF5B	C 500	1.57-6	149	44	CH2A	M 80	5.38-6	137	60	CH1F	C 850	4.84-6	152	55	CK1F	N 0	1.14-6	127	35
CF5B	C 550	4.41-6	149	35	CH2A	M 100	5.15-6	143	55	CH1F	C 900	4.50-6	156	57	CK1B	C 500	6.47-6	132	26
CF5B	C 600	2.41-6	152	35	CH2A	M 140	5.20-6	146	53	CH1F	C 950	1.38-6	127	61	CK1B	C 550	6.15-6	131	24
CF5B	C 650	7.92-7	153	31	CH2A	M 180	4.72-6	144	48	CH1F	C 1000	2.22-6	181	74	CK1B	C 600	5.63-6	120	23
CF5B	C 700	1.03-6	186	43	CH2F	N 0	2.08-6	129	72	CH1F	C 1050	1.38-6	178	75	CK1B	C 650	4.46-6	130	24
CG1A	N 0	2.25-6	122	50	CH2F	T 100	1.98-6	159	55	CH1F	C 1100	4.02-7	280	61	CK1B	C 700	4.37-6	120	29
CG1A	M 5	1.54-6	136	51	CH2F	T 215	1.70-6	146	65	CH1F	C 1150	0.87-7	307	62	CK2A	N 0	5.50-6	106	44
CG1A	M 10	1.42-6	137	48	CH2F	T 306	1.16-6	161	59	CH1F	C 1200	4.02-7	206	14	CK2A	M 40	6.57-6	120	40
CG1A	M 20	1.30-6	136	46	CH2F	T 405	9.95-6	173	67	CH1F	C 1250	1.48-6	35	56	CK2A	M 60	6.37-6	123	36
CG1A	M 30	1.10-6	137	44	CH2F	T 505	3.66-6	121	54	CH1F	C 1300	4.43-6	147	60	CK2A	M 80	6.44-6	122	77
CG1A	M 40	1.12-6	137	42	CH2F	T 547	3.25-6	130	37	CH1F	C 1350	3.43-6	167	62	CK2B	N 0	1.24-6	121	40
CG1A	M 60	1.14-6	135	42	CH2F	T 600	3.41-6	181	50	CH1F	C 1400	3.12-6	151	68	CK2B	C 500	6.02-6	121	37
CG1A	M 80	1.10-6	136	41	CH2F	T 650	1.14-6	207	65	CH1F	C 1450	1.12-6	109	59	CK2B	C 550	5.53-6	120	34
CG1A	M 100	1.07-6	135	41	CH2F	T 700	1.02-6	170	61	CH1F	C 1500	2.15-6	124	81	CK2B	C 600	5.03-6	120	31
CG1A	M 120	1.03-6	136	39	CH2F	N 0	2.37-6	125	67	CH1F	C 1550	1.31-6	165	84	CK2B	C 650	4.52-6	116	30
CG1B	N 0	2.24-6	120	56	CH3A	M 5	1.40-6	124	63	CH1F	C 1600	6.94-7	321	61	CK2B	C 700	4.07-6	119	32
CG1B	C 500	1.48-6	138	67	CH3A	M 10	1.16-6	138	60	CH1F	C 1650	6.47-7	290	38	CK3A	N 0	1.20-6	117	63
CG1B	C 550	1.23-6	137	44	CH3A	M 20	9.41-6	140	55	CH1F	C 1700	5.92-7	323	31	CK3A	M 40	7.34-6	120	47
CG1B	C 600	4.51-6	134	40	CH3A	M 30	9.28-6	137	52	CH1F	C 1750	1.00-6	127	55	CK3A	M 60	7.13-6	124	44
CG1B	C 650	6.40-6	135	40	CH3A	M 40	7.02-6	131	50	CH1F	C 1800	1.03-6	80	34	CK3A	M 80	7.10-6	120	43
CG1B	C 700	6.40-6	136	37	CH3A	M 60	6.75-6	127	47	CH1F	C 1850	6.00-6	86	34	CK3B	N 0	1.17-6	120	67
CG1B	C 750	3.36-6	123	34	CH3A	M 80	6.12-6	129	44	CH1F	C 1900	4.14-6	84	30	CK3B	C 500	6.71-6	120	77
CG1B	C 800	1.07-6	120	35	CH3A	M 100	6.06-6	124	40	CH1F	C 1950	7.60-6	84	27	CK3B	C 550	4.01-6	120	76
CG1B	C 850	2.66-7	177	32	CH3A	M 140	6.10-6	125	40	CH1F	C 2000	7.71-6	81	24	CK3B	C 600	3.48-6	120	75
CG1B	C 900	1.55-7	120	36	CH3A	M 180	5.74-6	121	41	CH1F	C 2050	1.70-6	1	25	CK3B	C 650	1.70-6	121	75
CG2A	M 0	1.04-6	146	45	CH3A	M 200	1.75-6	121	59	CH1F	C 2100	1.70-6	79	1	CK3B	C 700	1.51-6	120	77
CG2A	M 10	1.03-6	148	47	CH3A	M 300	1.70-6	121	59	CH1F	C 2150	1.70-6	79	1	CK3B	C 750	1.04-6	120	76
CG2A	M 20	1.78-6	140	41	CH3A	M 400	1.10-6	174	59	CH1F	C 2200	6.16-6	7	27	CK3B	C 800	6.44-6	120	74
CG2A	M 30	1.61-6	139	46	CH3A	M 500	1.07-6	173	55	CH1F	C 2250	5.11-6	71	5	CK3B	C 850	6.44-6	120	74
CG2A	M 40	1.47-6	139	43	CH3A	M 600	9.24-6	121	57	CH1F	C 2300	4.03-6	77	8	CK3B	C 900	6.44-6	120	74
CG2A	M 60	1.37-6	138	45	CH3F	N 0	3.10-6	142	76	CH1F	C 2350	4.84-6	75	10	CK3B	C 950	7.27-6	124	32
CG2A	M 80	1.77-6	120	43	CH3F	T 100	1.08-6	170	50	CH1F	C 2400	1.73-6	75	44	CK3B	C 1000	7.05-6	124	31
CG2A	M 100	1.35-6	130	44	CH3F	T 215	1.70-6	174	66	CH1F	C 2450	7.67-6	64	15	CK3B	C 1050	6.47-6	124	30
CG2A	M 120	1.30-6	130	42	CH3F	T 306	1.11-6	171	43	CH1F	C 2500	2.04-6	80	26	CK3B	C 1100	6.47-6	124	30
CG2A	M 140	1.11-6	143	47	CH3F	T 405	1.11-6	170	42	CH1F	C 2550	2.74-6	82	19	CK3B	C 1150	7.27-6	124	30
CG2A	M 160	2.54-6	132	51	CH3F	T 505	4.15-6	140	44	CH1F	C 2600	2.79-6	84	15	CK3B	C 1200	7.27-6	124	30
CG2A	C 500	4.58-6	139	41	CH3F	T 547	3.06-6	128	37	CH1F	C 2650	1.44-6	267	14	CK3B	C 1250			

SPFC	TREAT	J	D	I	SPFC	TREAT	J	D	I	SPFC	TREAT	J	D	I	SPFC	TREAT	J	D	I				
CL4A	M	40	7.14-6	126	34	CN4A	C	600	1.01-6	106	36	CP4A	M	60	5.1-6	156	60	CR2A	C	600	1.12-6	112	36
CL4A	M	60	7.13-6	123	34	CN4B	C	600	9.41-7	106	20	CP4A	M	80	5.1-6	156	60	CR2A	C	630	7.12-6	7	36
CL4A	M	80	6.70-6	124	31	CN4C	C	600	1.24-6	106	2	CP4A	N	0	1.1-6	100	60	CR2A	C	630	1.12-6	1.1	36
CL4A	C	500	4.40-6	123	14	CN4A	N	0	1.08-6	46	66	CP4B	C	500	4.41-6	149	53	CR3A	N	0	1.04-6	187	52
CL4A	C	500	4.66-6	122	15	CN4A	C	500	1.75-6	151	66	CP4B	C	580	3.34-6	152	46	CR3A	M	5	1.02-6	149	52
CL4A	C	550	3.84-6	123	17	CN4A	C	500	1.18-6	153	67	CP4B	C	600	2.22-6	150	43	CR3A	M	17	8.49-6	140	52
CL4A	N	0	1.35-6	124	52	CN4A	C	600	6.47-7	269	59	CP4B	C	650	1.8-6	147	42	CR3A	M	20	7.38-6	136	52
CL4A	C	600	5.20-6	126	23	CN4A	C	600	8.06-7	284	40	CP4B	C	660	1.7-6	145	47	CR3A	N	40	8.09-6	130	56
CL4P	C	50	5.87-6	124	23	CN4A	C	600	7.72-7	252	15	CP5A	N	0	1.54-6	168	48	CR3A	M	60	5.45-6	127	51
CL4B	C	65	4.13-6	122	15	CN4B	N	0	9.86-6	142	66	CP5A	M	40	5.25-6	145	41	CR3A	N	70	5.05-6	124	53
CL4B	C	660	3.04-6	121	26	CN4P	M	40	3.60-6	149	65	CP5A	M	60	5.25-6	145	53	CR4A	N	0	2.13-6	149	57
CM1A	N	0	6.34-6	141	25	CN4B	M	60	3.25-6	129	62	CP5A	M	80	4.83-6	148	53	CR4A	M	40	6.13-6	135	60
CM1A	M	5	6.04-6	135	55	CN4P	M	80	3.26-6	144	62	CP5A	M	100	4.47-6	152	52	CR4A	M	60	5.51-6	137	58
CM1A	M	10	5.42-6	136	55	CM17	N	0	1.26-6	224	52	CP5A	M	140	4.40-6	148	52	CR4A	M	80	5.33-6	136	58
CM1A	M	20	4.96-6	136	50	CM1A	M	5	6.51-6	268	75	CP5A	M	180	3.86-6	146	49	CR4B	N	0	1.87-6	114	48
CM1A	M	40	4.27-6	136	44	CM1A	M	10	5.29-6	265	70	CP6B	N	0	1.89-6	55	40	CR4B	C	500	3.61-6	137	56
CM1A	M	60	3.84-6	134	41	CM1A	M	20	4.12-6	268	60	CP6B	C	500	3.54-6	137	45	CR4B	C	550	2.33-6	126	52
CM1A	M	80	3.78-6	132	47	CM1A	M	40	3.64-6	247	51	CP6B	C	550	2.88-6	136	47	CR4B	C	600	1.40-6	117	61
CM1A	C	550	1.91-6	137	34	CM1A	M	60	2.92-6	291	40	CP6B	C	600	1.35-6	135	39	CR4B	C	650	7.6-6	137	62
CM1A	C	600	1.70-6	129	31	CM1A	M	90	2.58-6	274	31	CP6B	C	630	1.70-6	134	38	CR4B	N	0	2.45-6	66	62
CM1A	C	650	1.33-6	115	28	CM1A	M	100	2.65-6	320	64	CP6B	C	660	2.37-6	171	5	CR4B	C	660	7.50-6	104	41
CM1B	N	0	9.04-6	113	51	CM1A	M	140	3.62-6	303	35	CP7B	N	0	2.17-6	140	57	CR4B	C	690	3.44-6	96	40
CM1B	C	500	3.29-6	128	37	CM1A	M	180	6.62-6	1	-19	CP7B	C	600	4.1-6	129	53	CR4B	C	690	2.62-6	96	38
CM1B	C	550	2.31-6	127	37	CM1P	N	0	1.31-6	211	77	CP7B	C	550	2.74-6	130	47	CR4B	C	630	2.39-6	90	34
CM1B	C	625	1.99-6	127	28	CM1P	C	500	3.85-6	250	2	CP7B	C	600	1.69-6	132	41	CR4B	C	660	1.80-6	143	20
CM1P	C	640	1.65-6	124	24	CM1P	C	600	4.1-6	273	-3	CP7B	C	630	1.55-6	132	45	CR4B	N	0	7.51-6	146	15
CM2A	N	0	9.73-6	134	51	CM1P	C	650	4.63-6	265	-1	CP7B	C	660	1.58-6	232	75	CR4B	M	40	5.15-6	126	57
CM2A	M	40	5.98-6	125	45	CM2A	N	0	8.67-6	24	66	CG1A	N	0	8.14-6	58	4	CR4B	M	60	5.12-6	126	57
CM2A	M	60	5.91-6	127	45	CM2A	C	500	3.43-6	288	3	CG1A	M	5	3.97-6	58	72	CR4B	M	80	4.99-6	127	51
CM2A	M	80	5.79-6	127	44	CM2A	C	550	3.67-6	280	-5	CG1A	M	10	2.40-6	111	75	CR4B	M	90	1.32-6	79	15
CM2A	C	550	2.82-6	110	29	CM2A	C	600	3.89-6	260	-11	CG1A	M	20	1.75-6	124	71	CR4B	C	500	2.72-6	111	37
CM2A	C	600	2.63-6	122	28	CM2A	C	600	3.67-6	292	-15	CG1A	M	40	1.12-6	120	79	CR4B	C	550	2.40-6	108	37
CM2A	C	650	2.27-6	123	26	CM2A	C	650	4.06-6	251	-17	CG1A	M	60	6.81-6	124	79	CR4B	C	600	1.79-6	102	47
CM2B	N	0	1.08-6	101	56	CM2B	N	0	4.11-6	356	43	CG1A	M	80	9.08-6	149	67	CR4B	C	620	1.98-6	104	34
CM2B	C	500	3.88-6	128	34	CM2B	M	5	5.15-6	336	60	CG1A	M	100	4.36-6	120	67	CR4B	C	640	2.44-6	158	30
CM2B	C	550	3.00-6	123	36	CM2B	M	10	4.38-6	295	54	CG1A	M	140	4.07-6	149	63	CR4B	N	0	1.18-6	116	67
CM2B	C	625	2.31-6	127	27	CM2B	M	20	3.55-6	291	51	CG1A	M	180	2.04-6	205	63	CR4B	C	500	3.32-6	113	46
CM2B	C	640	1.78-6	131	24	CM2B	M	40	3.04-6	284	40	CG1B	N	0	9.66-6	66	52	CR4B	C	550	2.70-6	110	40
CM3A	N	0	1.33-6	150	65	CM2B	M	60	2.73-6	251	34	CG1B	C	500	4.67-6	239	55	CR4B	C	600	1.94-6	104	36
CM3A	M	40	6.13-6	146	51	CM2B	M	80	2.91-6	285	32	CG1B	C	550	4.66-6	272	0	CR4B	C	630	1.73-6	102	40
CM3A	M	60	5.84-6	135	48	CM2B	M	100	2.69-6	276	27	CG1B	C	600	7.16-6	277	-20	CR4B	C	660	1.67-6	98	37
CM3A	M	80	5.74-6	144	49	CM2B	M	140	2.50-6	284	15	CG1B	C	650	9.14-6	252	-7	CS1A	C	550	9.68-6	231	25
CM3A	C	550	2.66-6	143	28	CM2B	M	180	3.40-6	297	27	CG2A	N	0	4.04-6	102	7	CS1A	C	600	6.04-6	240	22
CM3B	C	600	2.20-6	142	28	CM2C	C	550	2.64-6	297	-9	CG2A	M	5	4.12-6	125	56	CS1A	C	650	7.37-6	240	-4
CM3A	C	650	1.97-6	144	15	CM2C	C	600	3.65-6	268	-13	CG2A	M	10	1.67-6	139	54	CS1B	N	0	1.06-6	154	94
CM3B	N	0	1.15-6	101	68	CM2C	C	650	4.21-6	263	-12	CG2A	M	20	2.88-6	146	48	CS1B	M	5	5.50-6	60	67
CM3B	C	500	4.83-6	138	30	CM3A	N	0	1.15-6	22	73	CG2A	M	40	2.53-6	151	45	CS1B	M	10	4.14-6	133	64
CM3B	C	550	4.11-6	141	33	CM3A	C	200	5.02-6	287	61	CG2A	M	60	2.41-6	154	40	CS1B	M	20	3.18-6	145	50
CM3B	C	600	3.61-6	142	25	CM3A	C	220	4.42-6	293	54	CG2A	M	80	2.28-6	151	35	CS1B	M	40	2.17-6	145	77
CM3B	C	650	1.77-6	152	20	CM3A	C	400	3.71-6	294	45	CG2A	M	100	2.27-6	151	35	CS1B	M	60	1.97-6	147	78
CM4A	N	0	1.05-6	113	29	CM3A	C	450	3.55-6	289	32	CG2A	M	140	4.1-6	274	-1	CS1B	M	80	1.81-6	136	77
CM4A	M	40	8.26-6	130	35	CM3A	C	500	3.60-6	292	22	CG2A	M	180	2.44-6	274	48	CS1B	M	100	1.64-6	150	76
CM4A	M	60	7.70-6	140	33	CM3A	C	550	3.64-6	296	10	CG2B	N	0	1.1-6	111	40	CS1B	M	140	1.47-6	137	75
CM4A	M	80	7.2-6	135	25	CM3A	C	600	4.00-6	299	-1	CG2B	C	500	1.04-6	230	-10	CS1B	M	160	1.30-6	120	79
CM4A	N	0	5.78-6	129	44	CM3A	C	650	4.19-6	301	2	CG2B	C	550	1.7-6	247	-23	CS2A	N	0	2.47-6	214	81
CM4A	A	1P4	3.02-6	123	3	CM3A	C	730	1.18-6	100	62	CG2B	C	600	1.78-6	258	-33	CS2A	M	40	4.35-6	142	56
CM4A	C	500	3.19-6	129	10	CM3B	N	0	5.63-6	115	75	CG2B	C	630	2.12-6	258	-20	CS2A	M	60	4.13-6	136	51
CM4A	C	550	7.11-6	121	17	CM3B	M	5	5.16-6	277	77	CG2B	C	660	2.57-6	242	-23	CS2A	M	80	3.59-6	143	50
CM4A	C	600	4.90-6	132	18	CM3B	M	10	5.10-6	277	69	CG3A	N	0	2.13-6	71	64	CS2A	C	550	1.45-6	158	17
CM4A	C	625	4.29-6	134	15	CM3B	M	20	3.68-6	290	61	CG3A	C	500	8.74-6	230	40	CS2A	C	600	1.11-6	145	16
CM4A	C	640	4.06-6	134	17	CM3B	M	40	2.65-6	289	49	CG3A	C	550	4.71-6	191	37	CS2A	C	650	1.06-6	146	5
CM4A	N	0	1.42-6	136	3	CM3B	M	60	2.65-6	290	35	CG3A	C	600	3.61-6	191	35	CS2B	N	0	9.08-6	81	60
CM4B	C	200	3.41-6	141	40	CM3B	M	80	2.78-6	286	23	CG3A	C	650	3.24-6	94	31	CS2B	C	500	8.13-6	138	54
CM4B	C	200	4.46-6	142	45	CM3B	M	100	2.88-6	281	35	CG3B	N	0	1.45-6	75	28	CS2B	C	550	5.93-6	134	54
CM4B	C	400	7.67-6	163	71	CM3B	M	140															

SPEC	TREAT	J	D	I	SPEC	TREAT	J	D	I	SPEC	TREAT	J	D	I	SPEC	TREAT	J	D	I				
CS59	C 400	4.32-6	122	50	CU4A	C 600	6.26-6	327	-22	CW2C	C 500	4.11-6	121	37	CX2R	N	0	2.00-6	125	62			
CS59	C 450	3.60-6	122	41	CU4A	C 600	6.08-6	328	-22	CW2C	C 551	3.48-6	118	41	CX2B	C 500	3.20-6	145	63				
CS59	C 500	2.84-6	117	23	CU4B	N	0	5.36-6	85	53	CW2C	C 600	2.84-6	115	-2	CX2P	C 550	2.32-6	139	65			
CS59	C 550	2.12-6	117	23	CU4B	C 500	5.03-6	327	-15	CW2C	C 650	2.65-6	108	15	CX2P	C 600	1.29-6	145	66				
CS59	C 600	1.51-6	117	7	CU4B	C 550	6.02-6	326	-13	CW3A	N	0	7.26-6	320	65	CX2B	C 630	5.71-7	161	67			
CS59	C 650	1.27-6	104	-13	CU4B	C 600	6.15-6	326	-18	CW3A	C 100	3.16-6	107	63	CX2B	C 650	1.58-6	202	68				
CS59	C 700	1.30-6	164	11	CU4B	C 650	5.67-6	325	-17	CW3A	C 100	2.80-6	112	60	CX3A	N	0	2.57-6	170	73			
CT1A	N	0	1.00-6	62	15	CU4B	C 700	6.12-6	326	-18	CW3A	C 200	2.39-6	116	51	CX3A	M	40	6.81-6	155	73		
CT1A	C 500	1.50-6	149	33	CU4A	N	0	1.16-6	60	73	CW3A	C 400	1.96-6	112	44	CX3A	M	60	6.43-6	146	73		
CT1A	C 550	1.74-6	151	35	CU4A	C 500	3.37-6	130	54	CW3A	C 500	1.60-6	117	37	CX3A	M	80	6.36-6	150	73			
CT1A	C 600	1.14-6	156	10	CU4A	C 550	2.66-6	122	46	CW3A	C 600	1.19-6	107	13	CX3B	N	0	1.40-6	93	76			
CT1A	C 650	1.01-6	160	4	CU4A	C 600	2.21-6	133	48	CW3B	N	0	2.00-6	114	75	CX3B	C 500	3.03-6	151	73			
CT1A	C 650	1.16-6	176	-4	CU4A	C 650	1.91-6	125	43	CW3B	M	5	9.55-6	127	64	CX3B	C 550	2.10-6	144	75			
CT2A	N	0	7.57-6	158	78	CU4A	N	0	4.51-6	74	46	CW3B	M	10	7.92-6	132	55	CX3B	C 600	1.34-6	153	69	
CT2A	M	40	2.04-6	151	74	CU4A	M	5	4.64-6	122	71	CW3B	M	20	6.85-6	134	51	CX3B	C 630	1.03-6	164	60	
CT2A	M	60	1.66-6	160	60	CU4A	M	10	4.22-6	127	68	CW3B	M	30	6.31-6	134	46	CX3B	C 660	1.61-6	167	29	
CT2A	M	80	1.67-6	157	62	CU4A	M	20	3.69-6	127	63	CW3B	M	40	6.20-6	133	47	CX4A	N	0	1.86-6	153	50
CT2A	N	0	1.62-6	62	61	CU4A	M	40	3.22-6	133	59	CW3B	M	60	5.76-6	134	40	CX4A	M	40	6.13-6	153	71
CT2B	C 500	2.38-6	136	31	CU4A	M	60	3.13-6	123	60	CW3B	M	80	5.31-6	135	39	CX4A	M	60	5.16-6	137	71	
CT2B	C 550	1.96-6	136	31	CU4A	M	80	3.05-6	124	59	CW3B	M	100	5.02-6	137	39	CX4A	M	80	5.40-6	134	67	
CT2B	C 600	1.70-6	139	26	CU4A	M	100	3.20-6	129	56	CW3B	M	140	5.58-6	134	34	CX4A	N	0	2.02-6	128	60	
CT2B	C 650	1.28-6	156	57	CU4A	M	140	2.99-6	129	59	CW3B	M	180	5.39-6	134	37	CX4P	C 500	3.37-7	141	71		
CT2P	C 650	1.41-6	177	20	CU4A	M	180	2.93-6	170	55	CW4A	N	0	1.89-6	107	80	CX4B	C 550	2.37-6	166	70		
CT3A	N	0	1.44-6	125	46	CU2A	N	0	1.28-6	128	35	CW4A	T	100	1.12-6	250	81	CX4P	C 600	1.45-6	164	71	
CT3A	M	5	7.60-6	124	67	CU2A	M	40	5.81-6	131	67	CW4A	T	215	8.01-6	12	76	CX4B	C 630	9.31-7	153	81	
CT3A	M	10	6.45-6	120	56	CU2A	M	60	5.39-6	135	54	CW4A	T	306	8.77-6	64	70	CX4B	C 660	5.26-7	755	68	
CT3A	M	20	5.42-6	130	56	CU2A	M	80	5.30-6	135	56	CW4A	T	409	6.42-6	12	63	CY1A	N	0	3.20-6	165	64
CT3A	M	40	4.42-6	130	47	CU3A	N	0	1.95-6	142	64	CW4A	T	505	2.60-6	107	63	CY1A	M	40	6.01-6	154	64
CT3A	M	60	4.47-6	129	46	CU3A	M	40	4.74-6	124	70	CW4A	T	647	2.33-6	128	55	CY1A	M	60	6.81-6	165	64
CT3A	M	80	4.37-6	131	45	CU3A	M	60	4.71-6	120	55	CW4A	T	650	2.46-6	75	63	CY1A	M	80	6.83-6	161	66
CT3A	N	0	1.09-6	67	55	CU3A	M	80	4.51-6	120	55	CW4A	T	650	1.94-6	161	64	CY1A	C	550	4.44-6	115	40
CT3B	C 500	3.72-6	136	2	CU3A	M	100	4.15-6	125	54	CW4A	T	755	4.26-6	355	53	CY1A	C	600	1.07-6	250	71	
CT3B	C 550	2.70-6	133	21	CU3A	M	120	3.60-6	132	51	CW4B	N	0	2.01-6	94	68	CY1A	C	650	1.26-6	327	65	
CT3B	C 600	2.02-6	150	17	CU3B	C 500	2.45-6	130	49	CW4B	M	5	8.24-6	94	66	CY1B	N	0	3.42-6	66	74		
CT3B	C 650	2.20-6	135	11	CU3B	C 600	2.17-6	125	41	CW4B	M	10	6.30-6	101	62	CY1P	C	500	9.90-6	133	72		
CT4A	N	0	1.60-6	115	58	CU3B	C 650	1.60-6	124	43	CW4B	M	20	5.14-6	116	55	CY1P	C	550	6.03-6	129	72	
CT4A	M	40	4.43-6	125	45	CU3B	C 700	1.71-6	123	43	CW4B	M	30	4.60-6	112	46	CY1P	C	600	1.13-6	310	75	
CT4A	M	60	4.09-6	125	46	CU3B	N	0	1.76-6	127	40	CW4B	M	40	4.31-6	111	44	CY1P	C	630	1.62-6	321	35
CT4A	M	80	3.85-6	132	47	CU3B	M	40	5.65-6	125	52	CW4B	M	60	3.96-6	112	39	CY1P	C	660	1.23-6	341	17
CT4A	N	0	1.78-6	67	73	CU4A	M	60	5.21-6	131	47	CW4B	M	80	4.02-6	110	30	CY2A	N	0	3.56-6	159	68
CT4B	C 500	3.50-6	129	25	CU4A	M	80	5.21-6	125	47	CW4B	M	100	3.94-6	112	40	CY2A	M	5	2.42-6	153	77	
CT4B	C 550	3.12-6	131	25	CU4A	M	100	5.60-6	126	37	CW4B	M	140	3.92-6	111	37	CY2A	M	10	1.37-6	156	75	
CT4B	C 600	2.70-6	134	24	CU4A	M	120	4.58-6	125	33	CW4B	M	180	3.63-6	112	37	CY2A	M	20	1.34-6	150	71	
CT4B	C 650	2.53-6	134	21	CU4A	M	140	4.54-6	127	33	CW4C	N	0	2.15-6	40	63	CY2A	M	40	9.32-6	164	66	
CT4B	C 650	2.27-6	139	1	CU4A	M	160	4.07-6	131	29	CW4C	C 152	7.14-6	114	63	CY2A	M	60	7.70-6	167	69		
CT4B	N	0	6.73-6	60	67	CU4A	M	180	4.28-6	130	29	CW4C	C 200	6.94-6	120	60	CY2A	M	80	7.32-6	136	70	
CT5A	M	40	2.12-6	129	67	CU4A	M	200	4.07-6	131	34	CW4C	C 300	5.40-6	121	52	CY2A	M	100	6.92-6	135	77	
CT5A	M	60	1.80-6	130	64	CU4A	M	220	3.60-6	125	44	CW4C	C 400	5.34-6	125	48	CY2A	M	140	6.43-6	136	66	
CT5A	M	80	1.98-6	133	51	CU4A	M	240	3.30-6	156	54	CW4C	C 500	4.72-6	123	43	CY2A	M	160	7.32-6	137	66	
CU1A	N	0	1.81-5	218	-2	CU4A	M	260	1.73-6	158	46	CW4C	C 551	3.74-6	122	41	CY2B	N	0	3.41-5	104	77	
CU1A	N	50	7.47-6	224	24	CU4A	M	280	1.37-6	155	38	CW4C	C 600	3.34-6	114	28	CY2B	C	500	8.68-6	161	77	
CU1A	N	100	6.41-6	252	12	CU4A	M	300	1.24-6	170	32	CW4C	C 650	1.99-6	52	-34	CY2B	C	550	5.93-6	146	76	
CU1A	M	20	6.13-6	251	0	CU4A	M	320	1.24-6	182	24	CW5A	N	0	2.42-6	90	64	CY2B	C	600	1.63-6	316	66
CU1A	M	40	6.07-6	290	-5	CU1A	N	0	1.15-6	104	14	CW5A	T	100	1.92-6	39	63	CY2B	C	650	1.17-6	341	66
CU1A	M	60	5.74-6	291	-14	CU1A	M	0	1.44-6	84	52	CW5A	T	215	7.57-6	202	75	CY3A	N	0	2.85-6	151	66
CU1A	M	80	5.93-6	291	-18	CU1A	M	10	1.64-6	83	41	CW5A	T	306	8.10-6	164	64	CY3A	M	40	6.25-6	150	71
CU1A	M	100	6.45-6	223	-19	CU1A	T	100	1.68-6	94	40	CW5A	T	409	9.22-6	119	60	CY3A	M	60	5.05-6	116	70
CU1A	M	120	6.03-6	233	-12	CU1A	T	215	9.63-6	36	40	CW5A	T	505	4.50-6	126	44	CY3A	M	80	6.67-6	138	67
CU1A	M	140	5.96-6	221	-10	CU1A	T	306	6.22-6	117	44	CW5A	T	647	3.51-6	111	43	CY3A	C	550	1.20-6	156	66
CU1A	M	160	6.11-6	319	-47	CU1A	T	409	6.11-6	93	33	CW5A	T	650	3.94-6	110	43	CY3A	C	600	4.92-6	127	61
CU1A	M	180	4.54-6	301	-1	CU1A	T	505	2.83-6	120	23	CW5A	T	650	4.04-6	107	43	CY3A	C	650	1.05-6	277	66
CU1B	C 500	4.54-6	302	-11	CU1A	T	647	2.44-6	113	22	CW5A	T	755	4.20-6	183	61	CY3B	N	0	2.16-6	77	77	
CU1B	C 550	4.76-6	301	-24	CU1A	T	755	3.50-6	94	12	CW5A	T	755	5.14-6	147	54	CY3B	C	500	8.47-6	151	76	
CU1B	C 600	4.77-6	303	-27	CU1A	T	850	6.77-6	62	0	CW5A	N	0	1.60-6	120	50	CY3B	C	550	5.21-6	127	68	
CU1B	C 650	5.06-6	304	-31	CU1A	T	950	5.01-6	73	24	CW5B	M	5	5.10-6	64	60	CY3B	C	600	1.50-6	127	62	
CU1B	C 650	5.32-6	303	-35	CU1A	T	1050	5.34-6	61	-21	CW5B	M	10	4.05-6	116	65	CY3B	C	630	1			

SPEC	TREAT	J	D	I	SPEC	TREAT	J	D	I	SPEC	TREAT	J	D	I	SPEC	TREAT	J	D	I				
C22A	N	0	5.18-6	17	52	D44A	M	140	3.30-6	157	75	DC1A	M	40	4.70-6	107	74	DD2B	N	0	2.86-6	141	79
C22A	N	0	5.03-6	21	56	D44A	M	140	2.46-6	140	40	DC1A	M	60	3.59-6	103	76	DD2B	C	150	1.71-6	137	77
C22A	N	0	5.31-6	17	52	D44A	M	140	2.02-6	127	-73	DC1A	M	80	3.78-6	84	83	DD2B	C	200	1.63-6	137	78
C22A	M	5	7.65-7	7	54	D44A	C	300	2.88-6	112	63	DC1A	M	100	3.61-6	57	74	DD2B	C	300	1.28-6	143	79
C22A	M	10	2.71-7	4	53	D44A	C	400	3.14-6	113	58	DC1A	M	140	3.78-6	113	63	DD2B	C	400	1.18-7	141	79
C22A	M	20	1.72-7	349	57	D44A	C	450	2.22-6	111	59	DC1A	M	180	2.46-6	96	59	DD2B	C	500	1.08-7	140	79
C22A	M	30	1.07-7	365	56	D44A	C	500	1.24-6	103	61	DC1B	N	0	2.28-6	331	58	DD2B	C	600	3.45-7	144	79
C22A	M	40	6.81-8	325	52	D44A	C	550	1.00-6	98	61	DC1B	C	150	8.79-6	49	82	DD3A	N	0	2.05-6	167	74
C22A	M	50	7.49-9	325	56	D44A	C	600	3.70-7	86	43	DC1B	C	200	7.82-6	75	81	DD3A	M	40	1.23-6	162	64
C22A	M	100	4.90-9	325	39	D44A	C	670	3.86-7	110	45	DC1B	C	300	6.05-6	109	72	DD3A	M	60	1.05-6	174	60
C22A	M	140	5.81-9	106	39	D44A	C	660	2.60-7	110	45	DC1B	C	400	5.86-6	104	76	DD3A	M	80	1.02-6	150	60
C22A	M	180	4.28-9	92	53	D45A	N	0	3.73-5	257	75	DC1B	C	500	1.02-6	106	66	DD3B	N	0	6.25-6	156	56
C22A	N	0	1.88-6	17	74	D45A	M	5	1.04-5	325	82	DC1B	C	600	3.27-7	17	34	DD3B	C	500	5.29-7	172	64
C22A	M	5	9.61-7	32	77	D45A	M	10	1.27-5	140	81	DC2A	N	0	2.35-6	37	59	DD3B	C	550	3.74-7	156	67
C22A	M	10	7.11-7	31	80	D45A	M	20	1.02-5	147	77	DC2A	N	0	2.06-6	43	63	DD3B	C	600	3.14-7	171	67
C22A	M	20	5.47-7	40	81	D45A	M	40	6.31-6	116	75	DC2A	M	10	9.76-6	95	82	DD3B	C	650	2.28-7	175	65
C22A	M	40	4.27-7	49	85	D45A	M	60	5.83-6	132	72	DC2A	M	10	9.33-6	107	82	DD3B	C	660	1.63-7	21	66
C22A	M	60	3.90-7	65	85	D45A	M	80	5.52-6	140	71	DC2A	M	20	7.23-6	115	80	DD4A	N	0	2.76-6	97	74
C22A	M	80	3.76-7	77	82	D45A	M	100	4.72-6	153	69	DC2A	M	20	7.02-6	125	77	DD4A	M	5	1.61-6	90	78
C22A	M	100	3.20-7	70	70	D45A	M	140	5.74-6	163	69	DC2A	M	40	4.93-6	150	79	DD4A	M	10	1.58-6	125	74
C22A	M	140	2.64-7	17	76	D45A	M	180	3.36-6	134	61	DC2A	M	40	4.06-6	166	79	DD4A	M	20	1.61-6	141	76
C22A	M	180	2.20-7	69	90	D45A	M	140	3.27-6	172	-25	DC2A	M	60	3.92-6	158	74	DD4A	M	20	1.30-6	142	74
C24A	N	0	1.45-6	321	70	D45A	C	350	4.34-6	127	59	DC2A	M	60	3.48-6	180	73	DD4A	M	40	1.24-6	142	66
C24A	M	5	4.40-7	357	70	D45A	C	400	2.96-6	123	53	DC2A	M	80	3.40-6	155	73	DD4A	M	50	1.18-6	137	71
C24A	M	10	3.27-7	1	74	D45A	C	450	4.11-6	120	53	DC2A	M	80	3.41-6	162	73	DD4A	M	60	1.07-6	147	72
C24A	M	20	1.68-7	14	76	D45A	C	500	1.67-6	137	54	DC2A	M	100	3.20-6	147	76	DD4A	M	70	1.08-6	147	71
C24A	M	40	5.08-8	21	76	D45A	C	550	1.10-6	141	55	DC2A	M	100	3.29-6	150	75	DD4A	M	80	1.00-6	146	65
C24A	M	60	7.33-8	55	78	D45A	C	600	3.95-7	169	19	DC2A	M	140	3.47-6	159	68	DD4A	M	90	1.00-6	146	71
C24A	M	80	6.80-8	7	74	D45A	C	670	3.24-6	154	40	DC2A	M	140	3.50-6	159	66	DD4A	M	100	9.13-7	146	71
C24A	M	100	7.48-8	345	82	D45A	C	700	1.14-5	30	72	DC2A	M	180	3.72-6	113	42	DD4A	M	120	9.69-7	150	65
C24A	M	140	1.05-8	35	-72	D45A	C	750	7.26-6	42	82	DC2A	M	180	3.53-6	118	43	DD4A	M	140	9.04-7	162	66
C24A	M	180	1.36-8	367	51	D45A	C	800	5.08-6	86	45	DC2B	N	0	1.64-5	106	55	DD4A	M	160	9.01-7	140	65
C24A	C	150	1.88-7	4	65	D45A	C	850	2.29-6	35	81	DC2B	C	300	7.41-6	134	75	DD4A	M	180	9.34-7	162	65
C24A	C	200	1.34-7	357	65	D45A	C	900	1.35-6	1	74	DC2B	C	400	4.65-6	135	71	DD4A	M	200	7.66-6	206	67
C24A	C	300	1.02-7	74	85	D45A	C	950	1.78-6	61	65	DC2B	C	450	4.90-6	132	72	DD4B	C	500	5.67-6	152	64
C24A	C	400	7.62-8	156	69	D45A	C	100	1.27-6	16	78	DC2B	C	500	2.53-6	124	63	DD4B	C	550	3.40-7	165	69
C24A	C	500	2.74-8	125	63	D45A	C	140	1.30-6	176	69	DC2B	C	550	1.49-6	127	70	DD4B	C	600	3.07-7	149	64
D21A	N	0	3.60-5	122	66	D45A	C	180	1.81-6	200	9	DC2B	C	600	4.38-7	204	70	DD4B	C	650	2.07-7	132	64
D21A	M	5	1.91-5	55	76	D45A	C	200	2.41-6	111	87	DC3A	N	0	1.41-5	353	60	DD4B	C	660	3.70-7	11	60
D21A	M	10	1.35-5	102	77	D45A	C	250	7.90-6	9	83	DC3A	N	0	1.63-5	366	64	DD4B	C	670	2.33-7	120	66
D21A	M	20	1.01-5	114	77	D45A	C	300	6.40-6	56	84	DC3A	M	10	8.46-6	31	83	DD4B	C	680	1.49-6	115	69
D21A	M	40	7.06-6	119	75	D45A	C	350	6.25-6	85	82	DC3A	M	10	8.73-6	32	86	DD4B	C	690	1.39-6	113	63
D21A	M	60	7.92-6	106	73	D45A	C	400	3.30-6	82	77	DC3A	M	20	6.15-6	102	86	DD4B	C	700	1.40-6	124	63
D21A	M	80	5.25-6	119	69	D45A	C	450	1.63-6	37	71	DC3A	M	20	6.30-6	137	86	DD4B	C	710	2.18-6	112	66
D21A	M	100	4.40-6	93	75	D45A	C	500	1.63-6	132	-81	DC3A	M	40	4.19-6	135	66	DD4B	C	720	2.18-6	112	66
D21A	M	140	4.40-6	122	42	D45A	C	550	1.50-5	101	13	DC3A	M	40	4.35-6	160	83	DD4B	C	730	4.71-6	125	62
D21A	M	180	4.40-6	119	69	D45A	C	600	7.80-6	134	78	DC3A	M	60	3.74-6	130	78	DD4B	C	740	2.31-6	122	63
D21A	M	200	2.11-5	2	81	D45A	C	650	5.18-6	140	70	DC3A	M	60	3.27-6	140	77	DD4B	C	750	4.86-6	156	66
D21A	C	300	4.70-6	61	61	D45A	C	700	5.10-6	144	72	DC3A	M	80	3.43-6	123	40	DD4B	C	760	3.07-6	258	80
D21A	C	400	3.15-6	67	63	D45A	C	750	2.39-6	130	60	DC3A	M	80	3.41-6	137	40	DD4B	C	770	1.68-6	57	64
D21A	C	450	4.65-6	120	71	D45A	C	800	1.16-6	134	76	DC3A	M	100	2.70-6	100	82	DD4B	C	780	1.54-6	103	64
D21A	C	500	2.63-6	66	63	D45A	C	850	2.53-7	231	10	DC3A	M	100	2.55-6	110	73	DD4B	C	790	1.75-6	107	62
D21A	C	550	1.23-6	65	63	D45A	C	900	2.01-7	242	-15	DC3A	M	140	2.55-6	130	74	DD4B	C	800	1.40-6	110	60
D21A	C	600	1.60-6	67	67	D45A	C	950	2.83-7	284	-7	DC3A	M	140	2.61-6	133	73	DD4B	C	810	1.14-6	111	69
D21A	C	650	1.44-6	67	67	D45A	C	1000	2.42-6	349	65	DC3A	M	180	3.49-6	284	73	DD4B	C	820	1.05-6	112	65
D21A	C	700	2.35-6	109	69	D45A	C	1050	1.77-6	314	59	DC3A	M	180	3.47-6	281	73	DD4B	C	830	1.05-6	116	66
D21A	N	0	7.20-5	43	81	D45A	C	1100	6.78-6	32	81	DC3B	N	0	1.31-5	320	40	DD4B	C	840	0.96-6	115	60
D21A	M	5	1.64-5	16	85	D45A	C	1150	6.19-6	81	85	DC3B	C	300	7.12-6	136	79	DD4B	C	850	0.86-6	116	60
D21A	M	10	1.37-5	18	83	D45A	C	1200	3.51-6	131	82	DC3B	C	400	4.10-6	130	74	DD4B	C	860	0.92-6	116	67
D21A	M	20	1.04-5	15	73	D45A	C	1250	2.70-6	111	75	DC3B	C	450	4.13-6	124	75	DD4B	C	870	0.85-6	116	61
D21A	M	30	1.12-6	14	71	D45A	C	1300	3.45-6	96	76	DC3B	C	500	4.10-6	119	75	DD4B	C	880	2.01-6	124	71
D21A	M	40	8.47-6	21	71	D45A	C	1350	3.28-6	88	75	DC3B	C	550	1.21-6	110	80	DD4B	C	890	4.40-6	121	69
D21A	M	50	1.25-6	16	72	D45A	C	1400	1.73-6	4	83	DC3B	C	600	1.44-6	107	84	DD4B	C	900	4.39-6	123	67
D21A	M	100	1.82-6	54	69	D45A	C	1450	2.41-6	52	69	DC4A	N	0	2.70-5	168	83	DD4B	C	910	1.85-6	124	69
D21A	M	140	5.37-6	92	82	D45A</																	

SPEC TRFAT	J	D	I	SPEC TRFAT	J	D	I	SPEC TRFAT	J	D	I	SPEC TRFAT	J	D	I					
FE1R	C	60	1.20-5	163	60	1.02-6	140	49	FA3A	N	0	2.12-5	353	43	FA4A	M	100	2.10-6	344	44
FE1A	N	0	2.40-5	136	60	1.02-6	140	50	FA3A	N	0	2.44-5	101	50	FA4A	M	140	2.20-6	4	50
FE2A	M	40	1.40-5	136	60	1.02-6	140	51	FA3A	M	20	4.56-6	18	42	FA4A	M	180	2.27-6	71	50
FE2A	M	60	1.20-5	137	50	1.02-6	140	52	FA3A	M	40	3.94-6	19	32	FA4A	N	0	1.43-4	151	34
FE2A	M	60	1.20-5	135	51	1.02-6	140	53	FA3A	M	60	3.42-6	27	30	FA4A	C	500	2.45-6	350	43
FE2A	M	100	1.27-5	144	52	1.02-6	140	54	FA3A	M	80	3.94-6	24	48	FA4A	C	550	1.38-6	350	40
FE2A	N	0	1.42-5	38	52	1.02-6	140	55	FA3A	M	100	3.65-6	27	32	FA4A	C	600	3.32-7	350	41
FE2A	C	500	4.70-6	128	50	1.02-6	140	56	FA3A	M	140	3.56-6	25	42	FA4A	C	630	3.35-7	350	40
FE2A	C	550	3.32-6	127	46	1.02-6	140	57	FA3A	M	180	3.44-6	46	70	FA4A	C	660	2.20-6	350	40
FE2A	C	600	1.37-6	126	39	1.02-6	140	58	FA3A	N	0	2.03-5	20	-2	FA4A	N	0	2.27-6	30	70
FE2A	C	630	1.27-6	157	25	1.02-6	140	59	FA3B	C	500	2.83-6	24	37	FA4A	M	5	1.74-4	61	72
FE2A	C	660	5.28-6	157	9	1.02-6	140	60	FA3B	C	550	2.46-6	21	33	FA4A	M	10	1.10-4	73	72
FE3A	N	0	2.43-5	131	60	1.02-6	140	61	FA3B	C	600	2.22-6	22	29	FA4A	M	20	5.70-5	69	71
FE3A	M	40	1.38-5	129	57	1.02-6	140	62	FA3B	C	630	2.21-6	26	23	FA4A	M	40	2.15-5	61	71
FE3A	M	60	1.33-5	140	56	1.02-6	140	63	FA3B	C	660	2.90-6	59	47	FA4A	M	60	2.44-6	66	70
FE3A	M	80	1.31-5	140	56	1.02-6	140	64	FA4A	N	0	2.44-5	5	56	FA4A	M	80	1.62-6	340	74
FE3A	M	100	1.26-5	144	57	1.02-6	140	65	FA4A	M	10	6.24-6	20	54	FA4A	M	100	2.26-6	139	27
FE3A	N	0	2.42-5	123	60	1.02-6	140	66	FA4A	M	20	5.26-6	22	55	FA4A	M	140	4.00-6	140	17
FE3A	C	500	5.42-6	128	51	1.02-6	140	67	FA4A	M	40	4.99-6	19	54	FA4A	M	160	2.50-6	109	7
FE3A	C	550	3.23-6	127	47	1.02-6	140	68	FA4A	M	60	4.27-6	27	54	FA4A	M	180	2.44-4	60	65
FE3A	C	600	1.41-6	117	43	1.02-6	140	69	FA4A	M	80	4.21-6	31	57	FA4A	M	200	5.24-6	91	67
FE3A	C	630	9.93-7	115	38	1.02-6	140	70	FA4A	M	100	4.49-6	18	57	FA4A	M	300	4.04-6	80	67
FE3A	C	660	1.85-6	26	11	1.02-6	140	71	FA4A	M	140	3.09-6	12	61	FA4A	M	600	6.95-7	74	70
FE4A	N	0	2.70-5	132	71	1.02-6	140	72	FA4A	M	180	3.04-6	347	52	FA4A	M	630	5.21-6	165	43
FE4A	M	40	1.30-5	132	53	1.02-6	140	73	FA4A	N	0	1.86-5	58	12	FA4A	N	0	2.77-4	32	-1
FE4A	M	60	1.28-5	135	50	1.02-6	140	74	FA4A	M	500	3.32-6	14	60	FA4A	M	5	1.97-4	43	59
FE4A	M	80	1.23-5	132	51	1.02-6	140	75	FA4A	M	550	2.94-6	17	60	FA4A	M	10	8.31-6	51	33
FE4A	M	100	1.18-5	134	52	1.02-6	140	76	FA4A	M	600	2.49-6	12	62	FA4A	M	20	2.50-6	62	67
FE4A	N	0	2.43-5	134	72	1.02-6	140	77	FA4A	M	630	2.16-6	18	58	FA4A	M	30	1.64-6	102	73
FE4A	C	500	4.20-6	121	51	1.02-6	140	78	FA4A	M	660	2.61-6	141	62	FA4A	M	40	1.63-6	50	70
FE4A	C	550	3.35-6	119	50	1.02-6	140	79	FA4A	M	5	1.89-5	346	52	FA4A	M	60	4.44-6	66	74
FE4A	C	600	1.32-6	105	45	1.02-6	140	80	FA4A	M	10	1.13-5	335	56	FA4A	M	70	3.70-6	70	73
FE4A	C	630	5.92-7	150	20	1.02-6	140	81	FA4A	M	20	7.57-6	330	55	FA4A	M	80	2.60-6	48	57
FE4A	C	660	2.30-6	310	20	1.02-6	140	82	FA4A	M	30	5.47-6	320	61	FA4A	M	90	2.40-6	136	62
FE5A	N	0	2.40-5	95	48	1.02-6	140	83	FA4A	M	40	4.97-6	327	58	FA4A	M	100	1.78-6	25	59
FE5A	M	40	1.95-5	119	57	1.02-6	140	84	FA4A	M	50	3.86-6	329	51	FA4A	M	120	1.56-6	173	63
FE5A	M	60	1.82-5	121	54	1.02-6	140	85	FA4A	M	60	2.97-6	332	55	FA4A	M	140	5.10-7	102	39
FE5A	M	80	1.60-5	123	51	1.02-6	140	86	FA4A	M	70	3.06-6	314	61	FA4A	M	160	1.74-6	244	-33
FE5A	M	100	1.52-5	125	48	1.02-6	140	87	FA4A	M	80	2.37-6	317	53	FA4A	M	180	2.13-6	232	-40
FE5A	M	120	1.40-5	125	44	1.02-6	140	88	FA4A	M	90	2.45-6	324	51	FA4A	M	200	3.17-4	43	58
FE5A	M	140	1.46-5	125	45	1.02-6	140	89	FA4A	M	100	2.58-6	316	50	FA4A	M	300	6.13-6	51	64
FE5A	M	160	1.38-5	123	42	1.02-6	140	90	FA4A	M	120	2.32-6	327	42	FA4A	M	600	5.47-6	57	66
FE5A	M	180	1.28-5	132	43	1.02-6	140	91	FA4A	M	140	1.54-6	344	48	FA4A	M	630	3.45-6	296	66
FE5A	N	0	2.91-5	110	72	1.02-6	140	92	FA4A	M	160	1.75-6	332	43	FA4A	M	660	3.24-6	63	50
FE5A	C	500	6.18-6	120	40	1.02-6	140	93	FA4A	M	180	2.14-6	328	70	FA4A	M	0	2.44-6	63	50
FE5A	C	550	4.21-6	124	47	1.02-6	140	94	FA4A	M	5	7.10-5	329	41	FA4A	M	10	2.00-4	62	57
FE5A	C	600	1.40-6	107	51	1.02-6	140	95	FA4A	M	500	6.25-6	337	62	FA4A	M	5	1.44-4	72	54
FE5A	C	630	1.24-6	63	22	1.02-6	140	96	FA4A	M	550	5.15-6	341	68	FA4A	M	10	0.33-6	85	54
FE5A	C	660	1.26-5	76	21	1.02-6	140	97	FA4A	M	600	2.95-6	356	66	FA4A	M	20	2.53-6	88	57
FE6A	N	0	1.72-5	144	65	1.02-6	140	98	FA4A	M	630	2.72-6	353	61	FA4A	M	40	2.50-6	273	-25
FE6A	C	500	4.59-6	122	50	1.02-6	140	99	FA4A	M	660	2.50-6	347	43	FA4A	M	60	6.20-6	174	-40
FE6A	C	550	3.38-6	124	49	1.02-6	140	100	FA4A	M	5	8.39-5	11	59	FA4A	M	80	5.64-6	210	36
FE6A	C	600	1.31-6	120	46	1.02-6	140	101	FA4A	M	10	8.42-6	334	55	FA4A	M	100	2.50-6	189	82
FE6A	C	630	1.00-6	243	22	1.02-6	140	102	FA4A	M	20	5.45-6	334	55	FA4A	M	140	4.70-6	264	40
FE6A	C	660	3.37-5	103	-12	1.02-6	140	103	FA4A	M	40	2.94-6	332	53	FA4A	M	180	6.02-6	50	-7
FE7A	N	0	2.67-5	90	45	1.02-6	140	104	FA4A	M	60	1.03-6	303	39	FA4A	M	300	9.28-6	50	56
FE7A	M	40	1.37-5	120	57	1.02-6	140	105	FA4A	M	80	1.61-6	30	60	FA4A	M	600	6.70-6	92	54
FE7A	M	60	1.30-5	120	55	1.02-6	140	106	FA4A	M	100	9.50-7	14	27	FA4A	M	630	4.18-6	63	32
FE7A	M	80	1.20-5	132	54	1.02-6	140	107	FA4A	M	120	1.62-6	322	2	FA4A	M	660	3.76-6	12	25
FE7A	M	100	1.17-5	128	54	1.02-6	140	108	FA4A	M	140	1.57-6	32	19	FA4A	M	0	4.15-4	58	67
FE7A	M	120	1.07-5	127	74	1.02-6	140	109	FA4A	M	5	7.42-5	9	56	FA4A	M	5	3.34-4	60	67
FE7A	M	140	1.00-5	124	45	1.02-6	140	110	FA4A	M	10	1.67-5	348	52	FA4A	M	10	2.44-4	71	67
FE7A	M	160	1.00-5	124	46	1.02-6	140	111	FA4A	M	20	9.09-6	337	54	FA4A	M	20	1.24-4	47	55
FE7A	M	180	1.00-5	115	36	1.02-6	140	112	FA4A	M	30	5.11-6	327	58	FA4A	M	40	5.46-6	58	47
FE7A	M	200	1.15-5	21	21	1.02-6	140	113	FA4A	M	40	3.45-6	324	58	FA4A	M	60	2.42-6	126	44
FE7A	M	220	1.20-5	123	70	1.02-6	140	114	FA4A	M	50	2.63-6	325	53	FA4A	M	80	1.22-5	81	-23
FE7A	M	240	1.15-5	121	56	1.02-6	140	115	FA4A	M	60	2.31-6	333	56	FA4A	M	100	1.22-6	321	-46
FE7A	M	260	1.05-5	125	54	1.02-6	140	116	FA4A	M	80	1.75-6	326	58	FA4A	M	140	2.13-6	170	-41
FE7A	M	280	1.07-5	123	53	1.02-6	140	117	FA4A	M	100	1.05-6	341	54	FA4A	M	180	4.56-6	56	67
FE7A	M	300	9.42-6	130	51	1.02-6	140	118	FA4A	M	120	1.18-6	310	61	FA4A	M	300	7.02-6	66	52
FE7A	M	320	1.35-5	127	60	1.02-6	140	119	FA4A	M	140	3.60-7	242	45	FA4A	M	600	5.11-6	64	59
FE7A	M	340	1.35-5	126	60	1.02-6	140	120	FA4A	M	160	1.62-6	322	2	FA4A	M	630	3.16-6	76	14
FE7A	M	360	1.35-5																	

SPEC	TREAT	J	D	I	SPEC	TREAT	J	D	I	SPEC	TREAT	J	D	I	SPEC	TREAT	J	D	I				
FD2R	N	0	1.56-5	356	74	MA1A	M	140	7.19-6	125	80	MF5A	N	0	6.27-6	60	75	MM2A	N	0	4.25-7	97	52
FD2R	C	500	2.73-6	127	69	MA1A	M	140	4.72-6	98	80	MF5B	N	0	2.41-6	75	73	MM2B	N	0	2.13-7	133	34
FD2R	C	550	2.43-6	138	71	MA1B	N	0	9.62-6	122	80	MG1A	N	0	2.62-7	20	55	MM3A	N	0	2.24-7	84	50
FD2R	C	600	1.97-6	137	68	MA2A	N	0	8.27-6	148	72	MG1A	N	0	2.52-7	19	55	MM3B	N	0	1.56-7	83	-5
FD2R	C	630	1.76-6	150	69	MA2B	N	0	1.09-5	124	72	MG1A	M	5	2.28-7	24	52	MM4A	N	0	2.79-7	129	-6
FD2R	C	660	1.78-6	121	54	MA3A	N	0	8.89-6	164	62	MG1A	M	10	1.96-7	27	48	MM4B	N	0	3.39-7	127	-77
FD3A	N	0	1.21-5	44	60	MA3B	N	0	1.06-5	154	68	MG1A	M	20	1.60-7	30	35	MM5A	N	0	2.39-7	107	-7
FD3A	M	5	4.41-6	74	68	MA4A	N	0	1.47-5	164	77	MG1A	M	40	1.18-7	60	29	MM1A	N	0	2.01-7	336	-5
FD3A	M	10	3.08-6	91	69	MA4B	N	0	1.23-5	166	80	MG1A	M	80	1.24-7	65	6	MM1A	N	0	2.88-7	11	-11
FD3A	M	20	2.50-6	102	68	MA5A	N	0	6.17-6	217	51	MG1A	M	100	1.85-7	74	6	MM1A	M	5	1.15-7	P	-2P
FD3A	M	40	1.91-6	108	62	MA5B	N	0	7.24-6	234	68	MG1A	M	140	1.71-7	60	9	MM1A	M	10	9.71-8	13	-34
FD3A	M	60	1.85-6	103	60	MB1A	N	0	2.60-6	152	48	MG1A	M	180	1.40-7	94	-8	MM1A	M	20	7.50-8	24	-29
FD3A	M	80	1.68-6	102	59	MB1B	N	0	2.11-6	156	46	MG1B	N	0	2.63-7	358	68	MM1A	M	40	9.87-8	29	-10
FD3A	M	100	1.57-6	145	56	MB1B	N	0	2.11-6	156	46	MG2A	N	0	2.14-7	5	62	MM1A	M	80	6.43-8	53	-53
FD3A	M	140	1.53-6	132	56	MB1B	M	5	2.17-6	157	45	MG2B	N	0	2.46-7	352	63	MM1A	M	120	6.25-8	17	-13
FD3A	M	180	1.17-6	155	31	MB1B	M	10	2.12-6	157	45	MG3A	N	0	1.57-7	357	59	MM1A	M	180	6.01-8	351	-24
FD3B	N	0	1.29-5	93	62	MB1B	M	20	2.01-6	157	44	MG3B	N	0	2.31-7	32	60	MM2A	N	0	1.40-7	22	-5
FD3B	C	500	1.66-6	106	64	MB1B	M	40	1.91-6	156	46	MG6A	N	0	1.35-7	348	55	MM2B	N	0	1.66-7	1	12
FD3B	C	550	1.47-6	104	63	MB1B	M	80	1.62-6	156	44	MG6B	N	0	2.44-7	341	59	MM3A	N	0	1.21-7	8	-7
FD3B	C	600	1.18-6	101	64	MB1B	M	100	1.33-6	155	47	MG7A	N	0	1.46-7	18	76	MM3B	N	0	2.01-7	18	-6
FD3B	C	630	1.02-6	103	66	MB1R	M	140	7.74-7	162	41	MG7B	N	0	1.72-7	24	71	MM4A	N	0	2.15-7	19	-5
FD3B	C	660	1.01-6	138	52	MB1R	M	180	5.61-7	155	44	MH1A	N	0	1.67-7	175	71	MM4B	N	0	2.56-7	20	-1
FD4A	N	0	1.54-5	63	88	MB2A	N	0	3.16-6	157	48	MH1A	N	0	1.69-7	189	72	MM5A	N	0	9.29-7	19	0
FD4A	M	5	5.72-6	93	74	MB2B	N	0	4.30-6	153	51	MH1A	M	5	1.57-7	172	63	MM5B	N	0	2.66-7	17	0
FD4A	M	10	4.29-6	114	73	MB3A	N	0	2.92-6	144	57	MH1A	M	10	1.59-7	164	54	MO1A	N	0	1.84-6	52	40
FD4A	M	20	3.52-6	127	72	MB3B	N	0	3.06-6	143	56	MH1A	M	20	1.53-7	166	59	MO1A	M	5	1.74-6	52	41
FD4A	M	40	3.06-6	130	69	MB4A	N	0	3.58-6	143	45	MH1A	M	40	1.54-7	148	67	MO1A	M	10	1.73-6	52	40
FD4A	M	60	2.71-6	134	67	MB4B	N	0	2.97-6	141	46	MH1A	M	80	1.22-7	163	63	MO1A	M	20	1.75-6	53	39
FD4A	M	80	2.48-6	130	70	MB5A	N	0	1.98-6	142	41	MH1A	M	120	9.44-8	201	59	MO1A	M	40	1.78-6	55	37
FD4A	M	100	2.36-6	144	63	MB5B	N	0	2.08-6	143	41	MH1A	M	180	9.67-8	166	36	MO1A	M	80	1.81-6	55	40
FD4A	M	140	2.33-6	137	69	MC1A	N	0	2.01-6	151	71	MH1B	N	0	5.97-7	340	77	MO1A	M	120	1.86-6	55	38
FD4A	M	180	1.88-6	164	66	MC1A	N	0	2.01-6	151	71	MH2A	N	0	6.52-7	353	71	MO1A	M	180	1.64-6	57	39
FD4A	N	0	1.52-5	74	56	MC1A	M	5	2.14-6	154	72	MH2B	N	0	7.61-7	356	74	MO1B	N	0	5.53-7	45	85
FD4B	C	500	2.00-6	122	65	MC1A	M	10	2.10-6	154	70	MH3A	N	0	1.01-7	8	41	MO2A	N	0	8.36-7	84	30
FD4B	C	550	1.74-6	128	67	MC1A	M	20	2.03-6	155	69	MH3B	N	0	2.63-7	359	69	MO2B	N	0	6.54-7	54	39
FD4B	C	600	1.27-6	143	68	MC1A	M	40	2.00-6	155	69	MH4A	N	0	8.09-7	352	75	MO3A	N	0	4.22-7	9	32
FD4B	C	630	1.14-6	125	68	MC1A	M	80	1.68-6	152	70	MH4B	N	0	5.29-7	346	77	MO3B	N	0	6.16-7	110	19
FD4B	C	660	1.06-6	122	63	MC1A	M	100	1.36-6	156	71	MH5A	N	0	5.38-7	346	73	MO4A	N	0	3.42-7	135	-13
FE1A	N	0	5.72-6	142	76	MC1A	M	140	9.16-7	156	69	MH5B	N	0	5.94-7	333	71	MO4B	N	0	2.77-7	92	-11
FE1A	M	5	2.50-6	160	46	MC1A	M	180	4.64-7	145	58	MJ1A	N	0	3.34-7	352	63	MO5A	N	0	1.76-6	49	36
FE1A	M	10	1.66-6	169	46	MC1B	N	0	1.99-6	152	67	MJ1A	N	0	3.22-7	358	63	MO5B	N	0	4.95-7	91	75
FE1A	M	20	1.14-6	170	44	MC2A	N	0	2.06-6	188	69	MJ1A	M	5	3.01-7	355	64	MO6A	N	0	6.92-6	61	48
FE1A	M	40	5.48-7	172	44	MC2R	N	0	2.53-6	200	65	MJ1A	M	10	2.67-7	358	63	MO6B	N	0	1.77-2	38	19
FE1A	M	60	3.11-7	175	38	MC3A	N	0	2.01-6	193	60	MJ1A	M	20	2.95-7	351	66	MP1A	N	0	2.62-6	69	92
FE1A	M	80	1.94-7	167	43	MC3B	N	0	1.76-6	202	58	MJ1A	M	40	2.76-7	347	71	MP1A	M	5	2.53-6	63	84
FE1A	M	100	2.42-7	179	68	MC4A	N	0	1.17-6	197	61	MJ1A	M	80	2.30-7	344	65	MP1A	M	10	2.51-6	60	84
FE1A	M	140	2.64-7	250	80	MC4B	N	0	1.40-6	187	54	MJ1A	M	120	2.04-7	348	56	MP1A	M	20	2.52-6	57	84
FE1A	M	180	3.15-7	124	65	MC5A	N	0	1.28-6	193	52	MJ1A	M	180	2.84-7	332	62	MP1A	M	40	2.46-6	53	84
FE1B	N	0	7.17-6	135	55	MC5C	N	0	1.86-6	206	58	MJ1B	N	0	1.06-6	345	59	MP1A	M	80	2.30-6	36	86
FE1B	C	500	4.54-7	162	28	MD1A	N	0	1.47-7	12	41	MJ2A	N	0	3.51-7	325	61	MP1A	M	120	1.86-6	65	84
FE1B	C	550	2.20-7	158	28	MD1A	N	0	1.47-7	12	41	MJ2B	N	0	7.81-7	345	62	MP1A	M	180	1.18-6	66	80
FE1B	C	600	3.21-8	173	21	MD1A	M	5	1.21-7	3	36	MJ3A	N	0	6.31-7	329	66	MP1B	N	0	2.40-6	54	82
FE2A	N	0	8.64-6	160	53	MD1A	M	10	1.59-7	1	7	MJ3B	N	0	1.15-6	331	64	MP2A	N	0	2.27-6	78	77
FE2A	M	5	3.86-6	163	52	MD1A	M	20	1.22-7	31	5	MJ4A	N	0	2.99-7	290	58	MP2B	N	0	2.72-6	68	78
FE2A	M	10	2.47-6	169	49	MD1A	M	40	9.95-8	15	-13	MJ4B	N	0	2.82-7	287	63	MP3A	N	0	8.99-7	90	64
FE2A	M	20	1.63-6	172	46	MD1A	M	80	1.21-7	344	-24	MK1A	N	0	8.65-8	104	15	MP3B	N	0	8.89-7	86	82
FE2A	M	40	7.07-7	178	44	MD1A	M	100	6.06-8	300	2	MK1A	N	0	9.96-8	104	14	MP4A	N	0	1.08-6	112	70
FE2A	M	60	4.75-7	181	36	MD1A	M	140	6.96-8	318	0	MK1A	M	5	7.77-8	115	18	MP4B	N	0	1.29-6	122	69
FE2A	M	80	3.09-7	180	53	MD1A	M	180	6.06-8	317	39	MK1A	M	10	6.54-8	122	15	MP5A	N	0	4.19-6	128	71
FE2A	M	100	5.05-7	195	28	MD1C	N	0	1.72-7	56	65	MK1A	M	20	5.61-8	114	25	MP5B	N	0	2.03-6	120	63
FE2A	M	140	4.45-7	35	-62	MD2A	N	0	6.80-8	169	22	MK1A	M	40	6.62-8	109	45						
FE2A	M	180	9.77-7	52	-9	MD2B	N	0	1.67-7	347	-74	MK1A	M	80	6.83-8	108	42						
FE2R	N	0	7.77-6	149	51	MD3A	N	0	2.06-7	39	77	MK1A	M	120	8.02-8	147	83						
FE2R	C	500	7.19-7	150	21	MD3B	N	0	2.52-7	261	73	MK1A	M	180	9.57-8	111	17						
FE2R	C	550	4.30-7	150	21	MD4A	N	0	2.04-7	241	53	MK1B	N	0	1.26-6	92	24						
FE2R	C	600	5.45-8	78	49	MD4B	N	0	1.56-7	18	64	MK2A	N	0	1.44-7	94	33						
FE3A	N	0	9.45-6	146	49	MD5B	N	0															

APPENDIX 3

Useful Conversions Between SI Units and EMU

<u>Quantity</u>	<u>SI unit</u>	<u>CGS emu</u>
Charge Q	Coulomb, C	10^{-1}
Current, I	Ampere, A	10^{-1}
Electric Dipole moment, p	C-m	10
Potential Diff, V	Volt, V	10^8
Electric Field strength, E	V/m	10^6
Capacitance, C	Farad, F	10^{-9}
Resistance, R	Ohm, Ω	10^9
Resistivity, ρ	Ω -m	10^{11}
Conductance, G	Siemens, S	10^{-9}
Conductivity, σ	$\Omega^{-1} \text{m}^{-1}$	10^{-11}
Polarization, P	C/m^2	10^{-5}
Displacement, D	C/m^2	$4\pi \times 10^{-5}$
Magnetic Dipole moment, m	A-m^2	10^3
Magnetic Pole strength, P	A-m	10

APPENDIX 3

Continued

Useful Conversions Between SI Units and EMU

<u>Quantity</u>	<u>SI unit</u>	<u>CGS emu</u>
Magnetic Flux density, B	Weber/m ² , Wb/m ² , Tesla, T	10 ⁴ gauss
Magnetic Field strength, H	A/m	$4\pi \times 10^{-3}$ oersted
Magnetic Flux, ϕ	Weber, Wb	10 ⁸ maxwell
Inductance, L	Henry, H	10 ⁹
Magnetization, M	A/m	10 ⁻³
Magnetic Polarization, I	Wb/m ²	10 ⁴ /4 π
Magnetomotive Force, \mathcal{H}	A	4 π /10
Reluctance, \mathcal{R}	A/Wb or H ⁻¹	4 $\pi \times 10^{-9}$

One SI unit has the value in emu given in column 3

$$\mu_0, \text{ Permeability of free space, } = 4\pi \times 10^{-7} \text{ H/m}$$

$$\epsilon_0, \text{ Permittivity of free space, } = 8.84 \times 10^{-12} \text{ F/m}$$

A conversion factor useful in geomagnetism is $\ln T = 1\gamma$

APPENDIX 4

Attitude of Strata at Sampling SitesGreat Slave Supergroup

<u>Site</u>	<u>Strike</u>	<u>Dip</u>	<u>V (cm)</u>	<u>H (cm)</u>
AA	282	14	0	800
AB	280	13	0	530
AC	280	13	0	350
AD	277	12	0	422
AE	286	17	10	344
BA	307	18	50	285
BB	288	15	50	570
BC	251	17	0	315
BD	297	20	40	545
BE	285	22	25	180
BF	245	14	0	770
BG	318	12	0	83
BH	3	18	0	302
BI	0	16	0	955
BJ	346	15	60	494
BK	2	12	47	164
BL	4	14	0	407
BM	14	13	0	275
BN	27	11	0	290
CA	294	7	0	173
CB	239	21	58	1745
CC	263	7	26	743
CD	330	13	0	627
CE	6	14	0	669

APPENDIX 4

Continued

<u>Site</u>	<u>Strike</u>	<u>Dip</u>	<u>V (cm)</u>	<u>H (cm)</u>
CF	11	14	0	525
CG	23	20	10	479
CH	16	17	40	284
CI	354	15	0	471
CJ	338	32	0	100
CK	318	13	12	157
CL	332	18	0	180
CM	334	14	0 (55)	400
CN	330	15	0 (30)	235
CO	337	16	10	426
CP	334	13	0	200
CQ	347	20	See Fig. 4.3.3g	
CR	338	14	0	206
CS	336	15	0	227
CT	332	16	0	438
CU	302	10	12	105
CV	304	10	8	95
CW	305	14	5	166
CX	315	12	0	257
CY	303	12	0	230
CZ	278	20	-	-
DA	278	20	-	467
DB	278	20	0	420
DC	278	20	28	345
DD	292	13	0	338

APPENDIX 4

Continued

<u>Site</u>	<u>Strike</u>	<u>Dip</u>	<u>V (cm)</u>	<u>H (cm)</u>
EA	353	18	0	299
EB	353	18	0	107
EC	353	18	0	107
ED	1	22	12	113
EE	1	22	0	30
FA	270	37	10	20
FB	270	37	0	552
FC	319	22	0	780
FD	319	22	0	500
FE	58	38	0	894

Strike measured in degrees east of true north.
Dip direction clockwise from strike. Dip is
measured in degrees below the horizontal.

V and H are the vertical and horizontal spreads
within the site.

Mount Clark Formation

Sites ordered in increasing age within each section.

<u>Site</u>	<u>Strike</u>	<u>Dip</u>	
MA	117	25	} Cap Mountain Section
MB	119	31	
MC	109	36	
ME	122	28	
MD	115	26	
MF	121	29	

B30043